UNCLASSIFIED

AD 258 462

Reproduced
by the

ARMED SERVICES TECHNICAL INFORMATION AGENCY
ARLINGTON HALL STATION
ARLINGTON VIRGINIA

UNCLASSIFIED

Best Available Copy

NOTICE: When government or other drawings, specifications or other data are used for any purpose other than in connection with a definitely related government procurement operation, the U. S. Government thereby incurs no responsibility, nor any obligation whatsoever; and the fact that the Government may have formulated, furnished, or in any way supplied the said drawings, specifications, or other data is not to be regarded by implication or otherwise as in any manner licensing the holder or any other person or corporation, or conveying any rights or permission to manufacture, use or sell any patented invention that may in any way be related thereto.

Best Available Copy

MCL - [illegible]

TECHNICAL DOCUMENTS LIAISON OFFICE
UNEDITED ROUGH DRAFT TRANSLATION

CATALOGED BY ASTIA
AS AD No. 258462

[illegible]

ASTIA
JUN 21 1961

61-3-5

XEROX

[illegible]

Date [illegible] 19[illegible]

Best Available Copy

Best
Available
Copy

MCL - [illegible]

TECHNICAL DOCUMENTS LIAISON OFFICE
UNEDITED ROUGH DRAFT TRANSLATION

[illegible]

Date [illegible] 19 [illegible]

Best Available Copy

[illegible], A. I. KARAYEV

[illegible]

[illegible]

[illegible] Office

[illegible], 1954

Foreign Pages: 2-37
120-360

Best Available Copy

TABLE OF CONTENTS

PAGE

. . . . . .

. 94

. 96

. 97

. 113

. 115

. 135

Best Available Copy

The book contains concise information (based on foreign sources) on the properties of liquid metals used as coolants in nuclear reactors.

The topics discussed are: heat transfer (in the liquid phase or during boiling and condensation); the interaction of liquid metals with structural materials; methods for removing impurities from liquid metals; and the peculiarities of design and operation of systems with liquid-metal coolants.

The introduction deals with the requirements to be met by heat-transfer media used in nuclear reactors and with ways of raising the efficiency of atomic power plants employing liquid-metal coolants.

The concluding sections of the book contain a brief survey of some domestic research work on liquid metals.

The book is intended for engineers and technicians in plants and design organizations, including those in the ship-building industry, as well as for students in power engineering and marine engineering institutes and technical schools.

FROM THE AUTHORS

Liquid-metal coolants find ever increasing application in the field of nuclear engineering.

Numerous articles have been published in foreign periodicals and monographs, dealing with studies of the properties of liquid-metal coolants and of their use in nuclear reactors. Many of these foreign research papers will remain unknown to the Soviet reader.

In compiling this monograph, the authors intended to give a brief account of the results of the most important foreign research conducted in the main fields of application of liquid-metal coolants in nuclear engineering (parts I and II).

A considerable portion of the foreign research data on liquid metals can be found in the Liquid Metals Handbook, published in the USA. However this monograph

cites no reference for physical constants and other quantities, they have been taken from this particular handbook.

The introduction provides a brief survey of the present state of nuclear engineering and discusses the advantages and shortcomings of the liquid-metal coolants as compared with other heat-transfer media used in nuclear power plants.

Part III contains a brief survey of some Soviet research in the field of liquid-metal coolants. A full account of the domestic research in this field would require a special monograph.

The authors wish to express their gratitude to Professors, Doctors of Technical Sciences, A. F. Alabyshev and A. V. Al'kir ich, for their valuable advice upon reading the manuscript, as well as to N. N. Yevdokimova for technical assistance in preparing the illustrations.

The authors would appreciate all critical remarks and suggestions which may prove useful for further improvement of their book.

The Most Important Liquid-Metal Coolants

Metal	Properties						
	Atomic weight	Atomic number	Melting point, °C	Boiling point, °C (p = 1 atmo abs)	Thermal conductivity at 400°C, kcal/m hr °C	Specific heat at 400°C, kcal/kg °C	Specific gravity at 400°C, kg/m³
Sodium, Na	22.997	11	97.8	883	61.3	0.3055	854
Potassium, K	39.096	19	63.7	760	34.4	0.1826	747
Sodium-potassium alloy (eutectic), Na-K(77% K)	-	-	-12.3	784	22.9	0.210	775
Lithium, Li	6.940	3	186	1317	32.4	1.0	790
Gallium, Ga	69.72	31	29.8	1983	25.2	0.082	5845
Mercury, Hg	200.61	80	-38.87	357	10.9	0.0324	12640
Tin, Sn	118.70	50	231.9	2270	28.4	0.0580	6835
Lead, Pb	207.21	82	327.4	1737	19.7	0.0370	10510
Bismuth, Bi	209.00	83	271.0	1477	13.3	0.0354	9910
Lead-bismuth alloy (eutectic), Pb-Bi (56.5% Bi)	-	-	125	1670	9.74	0.035	10180

Introduction

Technological progress in nuclear engineering depends on the reliable performance and the efficiency of reactors and power systems. The performance and efficiency characteristics of atomic power equipment are determined to a considerable extent by the choice of coolant, which influences the design of the reactor and the power system and effects their technological and economic indices.

An ideal coolant must have high specific heat and thermal conductivity, low viscosity, and negligible neutron capture cross section; it must be chemically stable in the operating temperature range when acted upon by neutron fields, and the resulting radioactivity must be weak and of short duration. The coolant must be chemically inactive with respect to the reactor vessel and to the fissile material or the sheathing of the heat-generating units; the coolant should not be a material which is scarce.

None of the coolants presently used meets all these requirements. In designing an atomic reactor, it becomes necessary to compromise by selecting the coolant on the basis of the particular advantages it [illegible] to offer.

For example, in selecting water for the coolant and neutron moderator in a water-moderated water-cooled reactor, one is influenced by the relative compactness of the reactor, by the unlimited availability of water and its low cost, even including the cost of chemical desalting, and by the favorable heat-transfer characteristics.

At the same time, the drawbacks of water as a coolant agent reduce the technological and economic value of the set-up. Due to the low boiling point of water, a pressure of about 100 atmospheres must be maintained in the vessel even at the moderate temperature of the coolant at the reactor output (about 300°C). The low temperature of water leaving the reactor leads to low pressure and temperature of the steam produced by the steam generator, and as a result to low efficiency for

NSL-554/102

the unit.

The high water pressure requires increasing the thickness of the reactor vessel, and results in increased weight, which is undesirable in propulsion power plants. A rupture in the vessel of such a reactor has serious consequences, as large amounts of active water turn into steam, which subsequently condenses over extensive areas. This danger is considerably greater in the case of homogeneous reactors, where the aqueous fuel solution carries fission products.

Radiolytic dissociation of water followed by recombination of hydrogen and oxygen molecules requires provisions for removal of the explosive mixture. The corrosive properties of water make it necessary to line the reactor vessel with stainless steel.

As coolants, organic compounds have a number of advantages over water: a higher boiling point at atmospheric pressure and relatively low vapor pressure at 300-350°C, which lowers the requirements for the reactor vessel. Due to irradiation in the radioactive core, however, organic coolants undergo polymerization followed by changes in some of their physical properties, and at higher temperatures these compounds undergo thermal dissociation. Removal of polymerization products requires additional facilities, which complicate operation of the unit.

The liquid-metal coolants have a high boiling point even at atmospheric pressure. Thus the boiling point of sodium is 883°C. This makes it possible, in the secondary circuit of the atomic reactor, to obtain high-temperature high-pressure steam or high-temperature gas under appropriate pressure. As a result, both steam-turbine and gas-turbine nuclear power plants with liquid-metal cooled reactors can have high efficiency.

At the present time, liquid metals appear to be the only possible coolants for fast-neutron reactors, as the use of gases is excluded due to the impossibility of obtaining sufficiently intensive heat removal from a volume or surface, and the use of water is not possible due to its moderating action.

At the same time, the liquid metals have their drawbacks; they interact chemically with water; sodium and potassium are inflammable; mercury is toxic and has a high thermal-neutron capture cross section; it requires a large amount of energy to circulate lead and bismuth; and so forth.

Selection of corrosion-resistant structural materials and protection of the coolant from oxidation are the most important engineering problems encountered in designing liquid-metal systems.

As will be shown below, the most promising coolants for increasing the efficiency of atomic reactors are liquid metals and alloys. This permits overlooking the shortcomings of liquid-metal coolants. The liquid-metal coolants can be used to especial advantage in fast and intermediate neutron units as well as in liquid-metal-fuel reactors.

The following brief survey of the development trends in atomic power engineering and of the layouts and designs of stationary and propulsion nuclear power plants serves to demonstrate the importance and the technological and economic advantages, as well as specific drawbacks, of reactors employing liquid-metal coolants.

1. Atomic Electric-power Stations

Construction Planning. By the year 2000, the world output of electric power is expected to increase 4 to 5 times above the level of 1955, when electric-power output reached 1,500 billion kw-hrs. The production of 6,000 billion kw-hrs a year will require a yearly consumption of about 2,200 million tons of reference fuel.

Even at present, in most countries expansion of electric-power production is limited by an inadequate rate of mine development and by too slow an increase in coal output. The world resources of organic fuel are limited and amount, in tons of reference fuel, to:

Coal ..... $2.6 \cdot 10^{12}$

Oil ..... $0.27 \cdot 10^{12}$

Natural gas ..... $0.02 \cdot 10^{12}$

TOTAL $2.89 \cdot 10^{12}$

The resources of nuclear fuel are estimated, in terms of reference fuel (in tons), at:

Uranium ..... $61.5 \cdot 10^{12}$

Thorium ..... $2.5 \cdot 10^{12}$

TOTAL $64 \cdot 10^{12}$

Thus, the reserves of nuclear fuel exceed those of organic fuel by 22 times. Present-day types of reactors do not permit a high degree of uranium burnup and can utilize only a small portion of the heat equivalent of the available uranium and thorium. Only after the mastering of controlled thermonuclear reactors will power resources become unlimited. Give the above-mentioned difficulties of increasing the output of organic fuel, however, nuclear fuel is, for the time being, the sole means of boosting the output of electric power in a number of countries. One of these countries is Britain, where it is planned to raise the output of atomic electric-power stations to 6 million kw by 1965, and to 35 million kw by 1975.

The pioneer in the construction of atomic electric-power stations is the USSR, where the first 5000-kw atomic electric-power station in the world has been in successful operation since June, 1954.

At the World Symposium on Power Resources in Belgrade (in 1957), the Soviet delegation reported on the plans for development of atomic power in the Soviet Union. The power resources of the USSR are estimated in billions of tons of reference fuel as follows:

Coal 197.4

Peat 22.8

Shale 5.75

TOTAL 225.95

Including the available power of large rivers, the total power resources amount to 625.95 billion tons of reference fuel, not considering the reserves of oil and natural gas.

The atomic electric-power stations which we plan to construct in the near future will be equipped with reactors producing up to 200-210 thousand kw of electric power. Thus, one of the electric power stations under construction will have two 210 thousand-kw reactors, each providing heat for the operation of three 70 thousand-kw steam turbines. Another electric-power station will have two reactors for the operation of steam turbines with total power output of 400 thousand kw. We plan to construct four experimental reactors of 5 to 50 thousand-kw capacity.

Operation of these large atomic electric-power stations and experimental reactors will provide a basis for selecting the most reliable and economical types of reactor power plants for further development of atomic power in the USSR.

The cost of one kilowatt-hour of electric energy will be lower at the atomic electric-power stations than at stations using coal.

At the present time, the first section of the two-reactor Calder Hall station producing 92 thousand kw is in operation in Great Britain.

Even larger electric-power stations are being built. Construction of two 500 thousand-kw atomic electric-power stations has recently been approved.

At Dounreay (Scotland), construction is now being completed on an atomic electric-power station with an experimental fast-neutron reactor having a 60 thousand-kw heat output. The coolant is sodium with a small amount of potassium added to reduce the solidification temperature. The core of the reactor is 0.6 m in diameter and 0.6 m high. Twenty parallel loops of the primary-circuit heat exchanger remove heat from the core, and four other loops from the blanket. From

the coolant of the secondary circuit (Na or NaK), heat is transferred to a steam generator feeding a turbine. The high temperature of the sodium maintains an efficient superheated-steam cycle.

In fast-neutron reactors with a small core, high heat-transfer efficiency is necessary. A reactor of this type does not require a large excess reactivity (1 to 1.5% as against 9 to 10% in water-moderated reactors). There exists a danger that the reactor may explode in the event of a cooling system malfunction permitting molten uranium to accumulate in the vessel in an amount exceeding the critical mass. To prevent danger from sodium leaks, the reactor unit is contained inside a steel sphere.

According to British sources, the production cost of one kilowatt-hour delivered by atomic electric power stations is comprised of the following items:

Depreciation cost (5% for 20 years)		0.37 pence/kilowatt-hour
Cost of the initial uranium charge		0.06 "
Expenditures for replacement of burntup uranium (2,000 pounds sterling/kilogram)		0.24 "
Operating expenses		0.06 "
	TOTAL	0.73 pence/kilowatt-hour
Proceeds from plutonium bred		0.07 "
	Net Cost	0.66 pence/kilowatt-hour

At coal-fired electric-power stations in Britain, the production cost of one kilowatt-hour is close to 0.7 pence.

It is expected that the cost of 1 kw-hr at coal-fired electric-power stations will keep increasing and will reach: in 1970, 0.67 pence; in 1980, 0.73 pence; in 1990, 0.84 pence.

Conversely, the production cost of 1 kw-hr at atomic electric-power stations will fall from year to year:

nel/554

Component costs of 1 kw-hr (in pence)	Year			
	1960	1970	1980	1990
Depreciation cost	0.37	0.30	0.26	0.22
Cost of uranium charge	0.06	0.04	0.03	0.02
Expenditures for replacement of burntup uranium	0.24	0.13	0.08	0.06
Operating expenses	0.06	0.05	0.04	0.03
TOTAL	0.73	0.52	0.41	0.33
Proceeds from plutonium bred	-0.07	-0.05	-0.03	-0.01
Net Cost	0.66	0.47	0.38	0.32

The above reduction in kw-hr cost at atomic electric power stations will be achieved by reducing the cost of equipment and of uranium.

In the USA, construction of atomic electric-power stations is expected to reach a total of 1 million kilowatts by 1962, from 3 to 4 million kilowatts by 1965, and from 50 to 75 million kilowatts by 1975; this is to be achieved by putting in service 8 to 12 million kilowatts every year. The first USA atomic electric-power station, the 60 thousand-kw station at Shippingport, was put into service in 1958. Its reactor had reached criticality in December, 1957.

In France, atomic electric-power stations will produce 15-35% of the electric power by 1975. The first atomic electric-power station, at Marcoule, will have an output of 30 thousand kw, and the second, at Veine, an output of 60 thousand kw. Later on, one atomic electric-power station will be placed in service each year, and the capacity of these stations will be gradually increased.

mel/554

In the Federal Republic of Germany, 3 to 4 atomic electric-power stations with a total 500 thousand-kw capacity are to be built by 1965.

In Sweden, two atomic electric-power stations, "Adam", with a 60 thousand-kw heat output, and "Eve", with a 100 thousand-kw output of electric power, are to be constructed by 1960. The output of the atomic electric-power stations is expected to reach 800 to 1,000 thousand kw by 1965, 3 to 6 million kw by 1970, and 6 to 12 million kw by 1975. The cost of electric power at the atomic stations will be half as much as at the coal-plants and will be equal to that at hydraulic electric-power stations.

Norway, Finland, and Denmark, together with Sweden, plan to build atomic electric-power stations. In Norway and Finland, reactors will be built to produce steam for industrial purposes.

In Belgium, it is planned to construct in 1962-1967 four atomic electric-power stations with a combined output of 500-600 thousand kw; these stations will produce 15% of the total output of electric power.

In Switzerland, Spain, and other European countries, plans are also being made for construction of atomic electric-power stations.

In Britain, Japan has ordered equipment for a Calder Hall-type atomic electric-power station with a 140 thousand-kw capacity and in the USA, equipment for a Shippingport-type station with a 134 thousand-kw capacity. Reactor designs of domestic type are under development. By 1965, the output of atomic electric-power stations is expected to reach 450 thousand kw.

In Canada, plans are being made to put into operation an atomic electric-power station with a 10-20 thousand-kw capacity, which is later to be increased to 100 thousand kw. By 1975, the atomic electric-power stations are expected to produce 15% of the total output of electric power.

Equipment of Atomic Electric Power Stations. The Atomic Electric-power Station of the Academy of Sciences of the USSR is equipped with a thermal uranium-

mr1/554

graphite reactor which is water-cooled under a pressure of 100 atmos abs. The heat exchangers produce steam compressed to 12.5 atmos abs at 260°C. The fuel used is uranium enriched to 5% U^{235}.

In September, 1958, operation began of the first section of the second Soviet atomic electric-power station, with a capacity of 100 Mw. Its full capacity will be 600 Mw, which means that this will be the largest of the atomic electric-power stations presently under construction throughout the world. The station is equipped with thermal graphite-moderated water-cooled reactors.

The 420-Mw electric-power station under construction will be equipped with two reactors with an electric output of 210 Mw each. A heat flow diagram of one of the units of the electric-power station is shown in Fig. 1. The heat output of the reactor is 760 Mw. Water is passed through the reactor at a rate of 31,500 m^3/hr under a pressure of 105 atmos abs at an inlet temperature of 250°C and an outlet temperature of 275°C. The water is delivered by six circulating pumps of the glandless type.

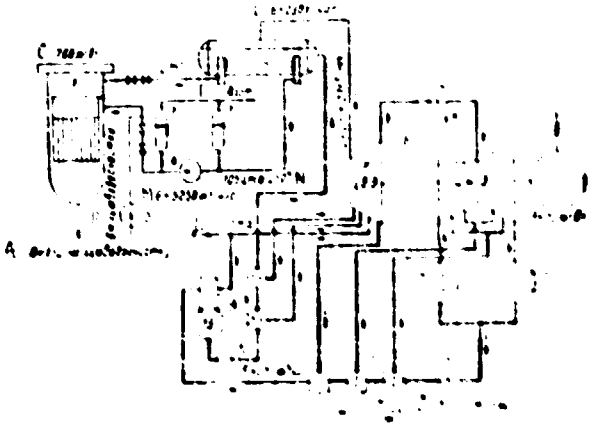

Fig. 1. Heat flow diagram of a 210-Mw unit of the 420-Mw atomic electric-power station.

1- reactor; 2- steam generator; 3- volume compensator; 4- circulating pump; 5- adding pump; 6- steam turbine; 7- moisture separator; 8- steam for the feed water heater; 9- condenser; 10- condensate pump; 11- regenerative heaters; 12- feed pump; 13- deaerator.

A- To water purifier; B- from water purifier; C- 760 Mw; D- nitrogen; E- 6 x 290 tons/hr; F- 29 atmos abs at 231°C; G- high-pressure cycle; H- low-pressure cycle; I- 3 x 70 Mw; J- 6 x 300 m^3/hr; K- 6 x 250 m^3/hr; L- 3.5 atmos abs; M- 6 x 5250 m^3/hr; N- 105 atmos abs at 250°C.

mel/554

From each of the reactors, water heated to 275°C is delivered to six steam generators, each of which produces dry saturated steam compressed to 32 atmos abs at 239°C at a rate of 230 tons per hour. The steam generators are of the horizontal type with U-shaped tubes. Each two steam generators supply steam for a two-casing 70-Mw turbine with intermediate steam separation between the high-pressure and the low-pressure sections.

A cross section of the reactor of this station is shown in Fig. 2. The uranium dioxide heat-generating elements are located within a core 3 m in diameter and 2.5 m high. The replacement basket houses 349 hexahedral fuel tubes arranged in a triangular lattice with 147-mm spacing. The 3.2-m long tubes are made from 2-mm thick zirconium tubing; the hexahedron is inscribed in a circle 165 mm in diameter.

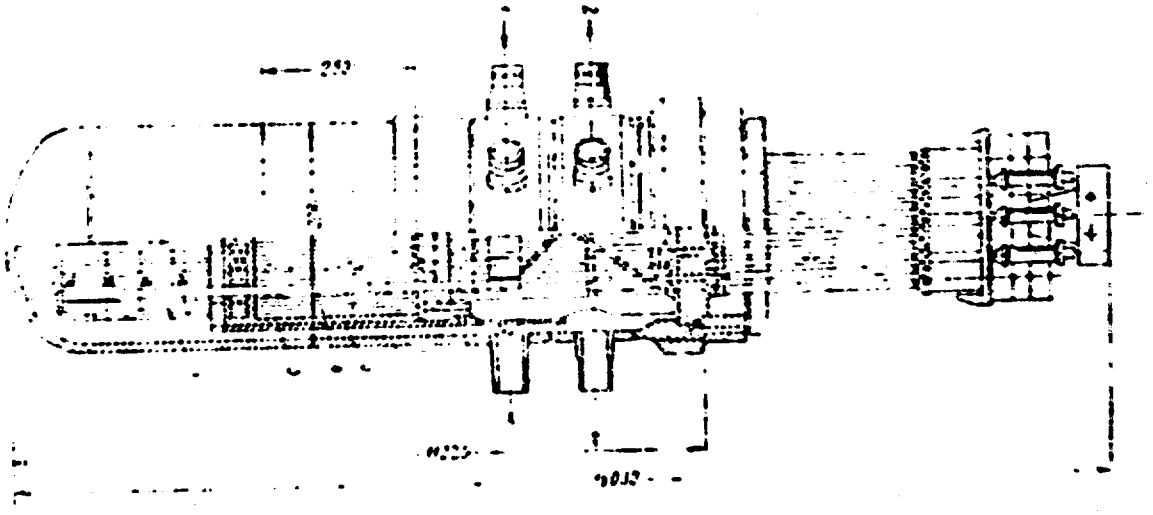

Fig. 2. Pressurized-water reactor.

1- water inlet; 2- water outlet; 3- replacement basket; 4- fuel element tubes; 5- core hollow; 6- compensating tubes.

mc1/554

The reactor vessel is 3.8 m in diameter and about 19 m high, and is 100 mm thick in its lower section and 180 mm thick in its upper section, which is covered with a removable flat lid. The vessel is made of medium-temperature steel with a yield point of 50 kg/mm^2 at 325°C. The weight of the vessel without the lid is 170 tons; the total weight of the dry reactor is 420 tons.

The uranium charge consists of 17 tons of natural uranium dioxide and 23 tons of uranium dioxide enriched to 1.5%. The vessel is protected from the action of neutrons by a steel shield 40 to 90 mm thick and a layer of water 200 mm thick.

The reactor is controlled by shim tubes containing a neutron-absorbing material. There are six scram tubes and two automatic control rods.

Steam enters the turbine under a pressure of 29 atmos abs and, before entering the low-pressure cycle at 2.2 atmos abs, is dessicated in a louver-type separator.

The over-all efficiency of the station is 27.5%. The operating electric-power consumption is 7.45%. The station is expected to be put into service in 1960.

A second large atomic electric-power station (400 Mw) will have a uranium-graphite reactor. Water heated in the reactor will transfer heat in a steam generator producing steam at a pressure of 90 atmos abs. Subsequently, the steam will be superheated to 500°C in special channels within the reactor. The station will be equipped with 100-Mw turbines set to operate at 500°C on standard steam under a pressure of 90 atmos abs. The fuel charge will consist of 185 tons of uranium enriched to 1.2%.

Construction is also planned for four experimental reactors including a boiling reactor with a 300-Mw heat output, supplying steam for a 50-Mw turbine.

A projected graphite-moderated liquid-sodium-cooled reactor will have a 150 to 180-Mw heat output. The heat exchanger of the tertiary circuit supplies steam under 100 atmos abs at 500-510°C, which is delivered to a 50-Mw turbine.

mcl/554

Another experimental reactor will have a 200-Mw heat output and will operate in conjunction with breeding of Pu^{239} from U^{238}. The steam will be used for a [illegible] turbine. The coolant is sodium. The heat exchanger will produce steam at 500°C under a pressure of 90 atmos abs.

The fourth reactor is of the homogeneous type. Heavy water will serve as moderator, and a heavy-water solution of uranium salts or a suspension of uranium and thorium powders will be used for fuel. Th^{232} will be used for breeding U^{233}. The heat output of the reactor will lie between 25 and 35 Mw.

The first British atomic electric-power station, Calder Hall, uses graphite-moderated CO_2-cooled uranium reactors with a heat output of 180 Mw.

The graphite stacking of the reactor is built in the shape of a 24-face prism 11.9 m across, 8.23 m high, and weighing 1,146 tons. It accommodates 1,696 vertical fuel channels in groups of sixteen. The graphite stack is placed within a steel jacket with holes through which takes place circulation of 0.5% of the CO_2 used in the cooling of the steel case.

Fuel rods of natural uranium, 1,020 mm long and 29.2 mm in diameter, are sheathed in magnesium-alloy casings provided with transverse fins to facilitate heat exchange. The thermal shield, consisting of steel plates, is 102 mm thick; the biological shield, made of concrete, is 2.14 m thick.

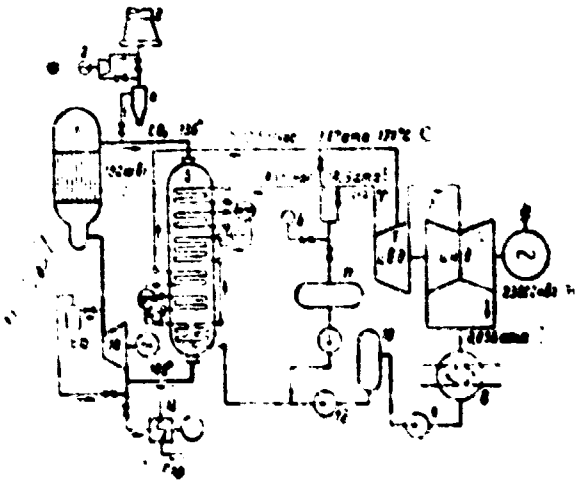

Fig. 3. Heat flow diagram of the Calder Hall Atomic Electric Power Station.

1- reactor; 2- CO_2 exhauster; 3- CO_2 exhaust pipe; 4- filter for the CO_2 exhaust during shutdown; 5- heat exchanger; 6- relief valve; 7- turbine generator; 8- condenser; 9- condensate pump; 10- deaerator; 11- standby condenser; 12- feed pump; 13- liquid-CO_2 tank and vaporiser; 14- CO_2 blower; 15- filter traps for radioactive matter.

A- 180 MW; B- 13.5 tons/hr; C- 3.67 atmos abs at 171°C; D- 45 tons/hr; E- 14.3 atmos abs at 313°C; F- high-pressure cycle; G- low-pressure cycle; H- 43,000 hp; I- 0.055 atmos abs; J- steam.

The heat-flow diagram of the Calder Hall atomic electric-power station is shown in Fig. 3.

Carbon dioxide is delivered to the reactor with the aid of four gas blowers with a capacity of 227 kg/sec, operated through a 1,542-hp drive. The blower shaft is sealed by a floating ring contacting the butt surface of a sleeve on the drive shaft; the contact surface is continuously oiled.

From the reactor, the CO_2 gas is delivered to four heat exchangers encased in housings 23.6 m high with an inner diameter of 5.28 m. Each housing encloses steam generators with capacities of 45 tons/hr at 14.3 atmos abs and 313°C, and 13.5 tons/hr at 3.67 atmos abs and 171°C.

Each steam-generator pair supplies a 45-Mw turbine. In the high-pressure section, the 14.3-atmos abs steam is worked down to 3.67 atmos abs and mixed with steam from the low-pressure steam generator; it subsequently passes through the last stages of the high-pressure section and through the double-flow low-pressure section.

The net efficiency of the station is 21-22%; by employing regeneration, it can be increased to 25-26%.

Larger atomic electric-power stations in Britain are also planned; they are to be equipped with graphite-moderated gas-cooled natural-uranium reactors.

Basic Specifications of British Atomic Electric-power Stations

Equipped with Graphite-moderated Gas-cooled Reactors

Station	Number of reactors	Turbine generating capacity, Mw	Uranium charge per reactor, tons	CO_2 pressure, kg/cm^2	Total capacity, Mw	Year of completion
Calder Hall	4	8 x 23	130	7	184	1958
Berkeley	2	4 x 80	240	8.8	320	1960
Bradwell	2	6 x 52	250	10.6	312	1960
Hunterston	2	6 x 60	251	10.6	360	1961
Hinkley Point	2	6 x 93.5	300 - 400	12 - 12.5	560	1962

The reactor of the Bradwell electric-power station has a 525-Mw heat-generating capacity. Its core is 15.2 m in diameter and 9.15 m high, and contains 3,000 channels, which accommodate magnesium-alloy-sheathed uranium rods about 25 mm in diameter. The maximum temperature on the surface of the fuel rods is 425°C; the maximum temperature of the CO_2 gas is 380°C. The circulation of the carbon dioxide is maintained by six gas blowers. Each of the blowers is operated by a 3,000-hp drive.

The graphite stacking is contained in a 76-mm thick steel sphere 21.4 m in diameter. The core weighs 2,000 tons.

The biological shield (concrete) is 2.75 m thick. The rated uranium burnup is 3,000 Mw. days/tons.

The reactor of the Hinkley Point electric-power station (Fig. 4) is designed for a heat output of 900 Mw. The graphite stacking is shaped into a 24-face

prism. The diameter of the containing sphere is 20.5 m; the thickness, 76 mm; and the weight, 1,700 tons. From the reactor, heat is transported by carbon dioxide to six steam generators of the dual-pressure type. The blowers are operated by 20-30-Mw drives.

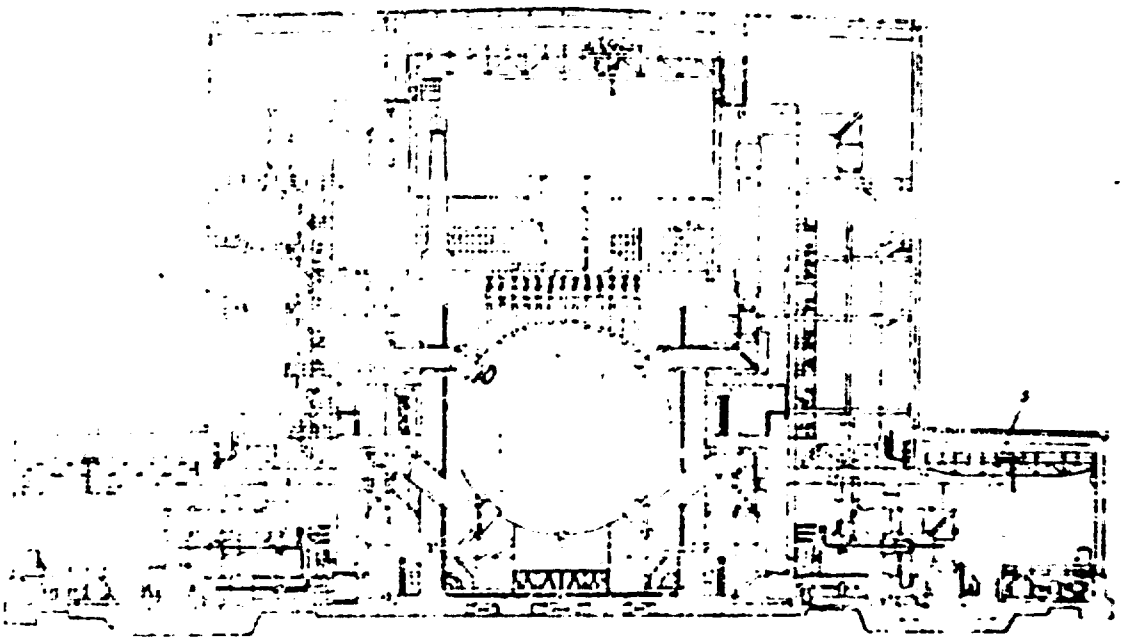

Fig. 4. Cross section of the reactor room of the Hinkley Point atomic electric-power station.
1- reactor vessel; 2- tubes for fuel elements and for control rods; 3- high-pressure drum of the steam generator; 4- low-pressure drum of the steam generator; 5- gas blower.

The efficiency of the Hinkley Point electric-power station is 26%; the installation cost, 120 pounds sterling per kilowatt; and the cost of 1 kilowatt-

kour, 0.65 pence.

Subsequent electric-power stations will be using beryllium-sheathed fuel rods, which will permit raising the temperature of the gas leaving the reactor. An experimental reactor is presently being designed which will use thorium and uranium-233 as a fuel.

The reactor of the first USA atomic electric-power plant at Shippingport has a design similar to that of the Soviet reactor shown in Fig. 2. The heat-generating capacity of the American reactor is 231 Mw, and the turbine output is 60 Mw. Water is circulated under a pressure of 140 atmos abs and has an inlet temperature of 264°C and an outlet temperature of 283°C. A water flow of 14,000 m^3/hr is maintained by four circulating pumps, each with 1,200-kw drives.

The reactor vessel, 9.5 m high and 2.75 m in diameter, is made of carbon steel 216 mm thick, and weighs 230 tons. To prevent corrosion, the vessel is lined with sheets of stainless steel 6.3 mm thick. On the outside, the vessel is heat-insulated with pressed glass fiber 100 mm thick.

The cylinder-shaped core has a height and a diameter of 1.83 m. The heat-generating units are placed inside a thin-walled stainless steel cylinder 2.4 m in diameter supported by a steel grid. The thick-walled outer vessel is protected from radiation by two concentric steel screens.

Some of the fuel units used are in the form of 2-mm thick vertical parallel zirconium-uranium-alloy plates spaced 2 mm apart and installed in square zirconium boxes. Uranium is enriched more than 50%. Each four boxes are welded into a section so that the spaces between them form a cross in which a cross-shaped hafnium control rod can slide. The amount of U^{235} in these units is 52 kg.

The rest of the fuel units consist of zirconium tubes with a diameter of 10.5 mm and a wall thickness of 0.7 mm, filled with natural uranium oxide to a total amount of 11 tons. Bundles of 100 tubes are welded to square-shaped zirconium plates, forming a section 250 mm high. Along the 1.83-m height of the

core, these sections are stacked by sevens between the top and the bottom grids.

The four heat exchangers produce 447 tons/hr of saturated steam at 40 atmos abs and 254°C. In the high-pressure cycle of the turbine, this steam expands to 3.16 atmos abs, acquiring a moisture content of 11.6%. The moisture is removed by a centrifugal separator; from there the steam enters the low-pressure cycle with a 1% moisture content. Upon the expansion in the low-pressure cycle to 0.05 atmos abs, the steam has an ultimate moisture content of 12-13%.

The rated efficiency of the Shippingport station is 26.5% without regeneration and 29.5% with regeneration.

The estimated construction cost of the station is 180 dollars/kw; the cost of 1 kw-hr is 0.4 cent.

The second atomic electric-power station under construction in the USA at Indiana Point (sic) will have a capacity of 236 Mw, of which only 140 Mw are produced from nuclear fuel, and the remaining 96 Mw in an oil-fired steam superheater. The reactor at this station is of the same type as at Shippingport.

The heat exchangers produce 860 tons/hr of saturated steam at 29.4 atmos abs and 232°C, which is subsequently superheated to 535°C; the efficiency of the station is 31.8%.

Such mixing of nuclear and organic fuel is not a fortunate solution. A more advanced approach is to be found at the Soviet electric-power station discussed above, where steam is superheated in the reactor channels.

The above examples show that pressurized-water reactors make possible station efficiency of 25 to 26%. By superheating the steam in some of the reactor channels, the efficiency can be raised to 28-30%. Reactors cooled by high-boiling liquids promise to raise the efficiency of atomic electric-power plants still further, since the vessel need not sustain pressures of 100-150 atmos abs when the coolant temperature reaches 400°C or above at the outlet. Among such high-temperature liquids are molten metals, metal alloys (sodium, sodium-potassium, lead-

bismuth, mercury), or organic compounds (diphenyl, diphenyl oxide, and the terphenyls).

The physical properties of some organic coolants are given in the following table.

Physical properties	Coolants				
	Diphenyl	Terphenyl isomer mixture	O-Terphenyl	M-Terphenyl	P-Terphenyl
Melting point, °C	69	60-145	50-55	75-85	200-215
Boiling point, °C	255	364-418	330-344	368-378	381-388
Vapor pressure, atmos abs					
at 325°C	3.7	0.4	0.8	0.4	0.3
at 425°C	15	2	3.4	2.0	1.5

An experimental 45-kw thermal and 12.5-kw electrical reactor is under construction in the USA; it will use diphenyl both as moderator and as coolant. The core of this reactor is 2 m high and 1.4 m in diameter and accomodates 138 packages of fuel elements of square cross section. A package contains 10 aluminum-clad uranium plates. The uranium is enriched to 1.8%.

The diphenyl is contained in a thin-walled tank. A 150-mm thick sheet of carbon steel is installed around the core, serving as shielding from thermal neutrons. The maximum temperature on the surface of the fuel elements is 339°C and at the center, 482°C. The reactor has a rated uranium burnup of 3,000-4,000 kw-days/ton.

The diphenyl circulates at a rate of 3,000 tons/hr, passing down the core channels under a pressure of 3.5 atmos abs, reaching a temperature of 325°C, and subsequently transporting the heat to two heat exchangers, each of which produces 37 tons/hr of steam under 29 atmos abs at 280°C.

With these steam characteristics, the efficiency of this station is about the same as that of the Shippingport station (with a reactor cooled by water under a pressure of 140 atmos abs).

Organic coolants make it possible to achieve a somewhat higher efficiency than when water is used. Their main advantage, however, consists in their low pressure at a higher outlet temperature than occurs in water-cooled reactors; this reduces the required thickness and weight of the reactor vessel. A disadvantage of the organic coolants lies in their low heat resistance. With a majority of organic compounds, heating above 350-400°C leads to intensive thermal decomposition whose products (resins) impede heat exchange and can clog the fuel channels. Special facilities for the removal of polymerization products (high-molecular-weight compounds) mean more complex procedures and more costly equipment.

In the USA, production has been started of an organic moderator, isopropyldiphenyl. An experimental reactor employs a solid moderator, polyethylene. Composites of lead and polyethylene are used for shielding in some shipboard reactors.

More promising are the liquid-metal heat transfer agents, especially sodium, potassium, and their alloys. The disadvantages of these metals are: explosion hazard, fire hazard, the possibility that chemical reaction products may form, and the need for heating the circulation circuit, since Na and K solidify at room temperature.

Bismuth and lead-bismuth alloys present no explosion or fire hazard, but they require more energy for circulation and lead to greater erosion of the

circulation circuit.

Experimental graphite-moderated sodium-cooled reactors are under construction in some countries. Compared with gas, sodium permits a higher heat yield per weight unit of uranium. Liquid sodium reacts with graphite and impairs its moderating properties. Graphite is, therefore, protected from contact with sodium by metal (e.g., zirconium) casings with low neutron absorption. The presence of such casings in the core affects the neutron balance unfavorably, and makes it necessary to use enriched uranium. This is the disadvantage of the sodium-cooled reactor as compared with a gas-cooled type.

In April, 1957, an experimental graphite-moderated sodium-cooled reactor was put into service in the USA; it has a heat output of 20,000 kw and was designed to serve as a prototype of a high-capacity power reactor. Its core and reflector are contained in a steel vessel 3.8 m high and 3.36 m in diameter. The graphite moderator consists of 119 hexahedral columns arranged in a triangular lattice with 283-mm spacing. The prisms are 3.05 m high, which includes 1.83 m extending into the core and 0.61 m extending into the end reflectors. For protection from the action of sodium, the graphite prisms are placed in 0.84-mm thick zirconium casings. Each column contains a centrally located zirconium tube with an inner diameter of 67 mm and a wall thickness of 0.84 mm. Heat-generating units 1.83 m high are placed inside zirconium tubes; they consist of clusters of 7 elements, each containing an assembly of 150-mm long slugs. The uranium slugs, 19 mm in diameter, are contained in 0.25-mm thick stainless-steel tubes. The slugs are thermally bonded by a Na-K alloy filling the 0.25-mm annular gap between the slug and the tube. The ends of the tubes are filled with helium, compensating for the thermal expansion of the Na-K alloy.

The fuel rods of a unit are separated by spiral spacers made of stainless wire.

Sodium circulates upward inside the zirconium tubes, where it washes the fuel rods and is heated from 260 to 516°C. The temperature in the center of the fuel rods should not exceed 650°C. The enrichment of the uranium with U^{235} isotope is about 3%. The sodium also cools the casings of the graphite columns. Reactivity is controlled with the aid of four rods containing a boron-nickel alloy.

The use of sodium-cooled graphite-moderated reactors will be justified only if the cost of the graphite-moderated sodium-cooled reactor is considerably below that of gas-cooled reactors.

Plans have been announced to build a reactor with heavy water as a moderator and sodium as coolant. In such a reactor, sodium must be prevented from making contact with the heavy water.

The idea of a liquid-metal fueled reactor is worth investigating. A diagram of a 210-Mw plant with such a reactor is shown in Fig. 5. The core consists of a graphite vessel containing a graphite cylinder 1.524 m in height and in diameter, having vertical channels 51 mm in diameter arranged in a triangular lattice spaced at 69-mm intervals. A uranium-bismuth alloy is circulated through the core channels. The alloy circulates at a rate of 80,500 tons/hr; the inlet temperature of the alloy is 400°C, its outlet temperature, 550°C. 500 Mw of heat is generated in the core.

The graphite vessel of the core is contained in a steel vessel 4.6 m high and 3.7 m in diameter. The annular gap between the outer vessel and the core vessel is filled with graphite rods 80 mm in diameter and 110 mm apart. Between the rods of the blanket, a Th_3Bi_5 suspension in molten bismuth, Bi, is circulated. The alloy circulates at 8,050 tons/hr. The heat-generating capacity of the blanket is 50 Mw; the total heat-generating capacity of the reactor is 550 Mw.

There are plans to use reactors of this type for propulsion purposes, but with the blanket replaced by a graphite reflector.

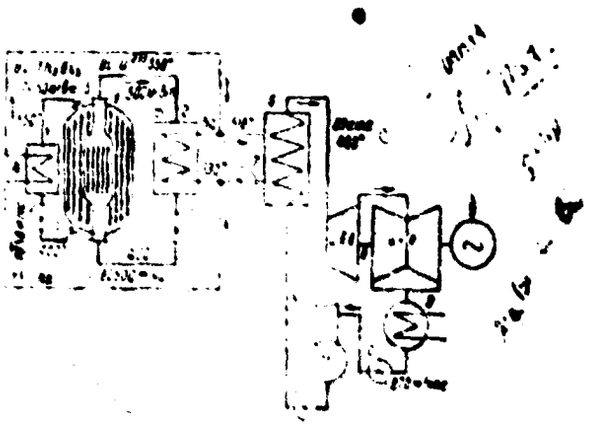

Fig. 5. Heat-flow diagram of electric-power station with a liquid-metal fueled reactor.

1- reactor; 2- core heat exchanger; 3- core circulating pump; 4- blanket heat exchanger; 5- blanket circulating pump; 6- steam generator; 7- intermediate circuit circulating pump; 8- steam turbine; 9- condenser; 10- condensate pump; 11- deaerator; 12- feed pump.

A- 50 Mw; B- 500 Mw; C- 89 atmos abs at 480°C;

D- high-pressure cycle; E- low-pressure cycle;

F- 870 tons/hr; G- 80,500 (sic) tons/hr; H- 8,050 tons/hr.

The coolant in the core and blanket heats the sodium in the heat exchangers of the intermediate circuit. Subsequently the sodium exchanges heat in the steam

generator, which produces 870 tons/hr of steam at 89 atmos abs and 480°C. This steam operates a 210-Mw two-cylinder turbine. The efficiency of the plant is about 33%. The installation cost is estimated at 238 dollars per kilowatt, and the cost of 1 kilowatt-hour at 0.78 cent. In a reactor of this type, the temperature of the alloy can reach 600°C and more, which, where sodium is used in the intermediate circuit, permits raising the efficiency to 35-38%.

Fig. 6 shows diagrams of plants using liquid-metal-cooled reactors.

If, in the intermediate circuit, mercury is used (Fig. 6b) instead of the sodium-potassium alloy (Fig. 6a), then it is possible to obtain mercury vapor under a pressure of 10-15 atmos abs at a temperature of 515-550°C. Upon leaving the mercury vapor turbine, the mercury vapor can exchange its latent heat of vaporization in a condenser and generate steam under a pressure of about 30 atmos abs, which will operate a conventional steam turbine.

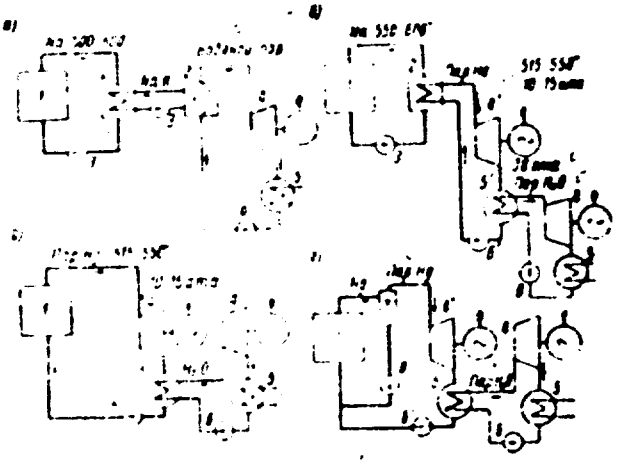

Fig. 6. Heat-flow diagrams of plants with liquid-metal-cooled reactors:

a- three-circuit plant with a conventional steam cycle; b- three-circuit plant with two-stage mercury-water cycle; c- two-circuit plant with a boiling-mercury reactor and a two-stage cycle; d- two-circuit plant with a liquid-mercury cooled reactor and a two-stage cycle.

1- reactor; 2 and 2'- heat exchangers; 3 and 3'- circulating pumps; 4 and 4'- steam and mercury-vapor turbines; 5 and 5'- steam and mercury-vapor condensers; 6 and 6'- condensate pumps; 7- separator-expander; 8- circulating pump.

A- Steam; B- b); C- Hg vapor; D- 10-15 atmos abs; E- 30 atmos abs; F- H_2O steam; G- c); H- d).

Such a two-stage power-generating system will have an efficiency of 40% at a mercury-vapor temperature of 500°C, and 45% at 550°C.

The use of mercury in the intermediate circuit will not only increase the efficiency of the system but will also simplify it, since there will be no need for heating the intermediate circuit, as mercury solidifies at minus 39°C.

Mercury was used as a coolant in the first Canadian thermal-neutron reactor.

The large neutron capture cross section of mercury is an obstacle to its use in thermal reactors. If an economical way could be found to remove the Hg^{200} and Hg^{201} isotopes from mercury, the cross section for slow-neutron capture would be reduced sixfold.

In fast-neutron reactors, mercury can be used to remove heat directly from the fuel elements, since, with respect to fast neutrons, mercury has a total cross section for neutron capture of the same order as lead and bismuth (Fig. 7). The top curves are those for thermal neutrons; the bottom ones, for fast neutrons.

Fig. 7. Total neutron-capture cross sections of liquid metals as functions of neutron energy.
A- Total neutron cross section, barns; E- neutron energy, ev (for fast neutrons, Mev).

At the Second International Conference on Peaceful Uses of Atomic Energy in 1958, the Soviet delegation announced that operation of an experimental fast reactor employing mercury as a coolant had begun recently.

The simplest and most economical layout with a fast reactor may be the layout shown in Fig. 6e. Here, generation of mercury vapor takes place in the channels of the fuel elements. This once-through layout for mercury vapor generator has not yet been tested under semi-industrial or industrial conditions. A more reliable but somewhat less economical layout is shown in Fig. 6d, where multiple forced circulation of mercury under overpressure takes place in the reactor. The mercury vapor is generated in an expander-type separator. This type of mercury vapor generator has been tested under semi-industrial conditions.

When the surface temperature of the heat-generating elements is on the order of 650°C, the two-stage mercury- and water-cooled plant can reach an efficiency of 50%, which is not possible with other liquid-metal coolants. In the case of gas-cooled reactors, an efficiency of 23-26% could be reached, given a fuel element surface temperature of 400°C. With the use of metal jackets, which permit temperatures as high as 600-650°C, the efficiency of gas-cooled plants can be increased to 30-35%. With hollow ceramic fuel elements, the operating temperature is expected to increase to 800°C.

With uranium or thorium carbide fuel elements in ceramic or graphite casings, a gas (carbon dioxide, helium, hydrogen) can be heated to 750-1,000°C. At such temperatures, gas turbines can be used with very high efficiency. Design studies have shown that, at gas temperatures of about 750°C, it is possible to operate closed-cycle gas turbine units with an output of 100 to 300 kw and an efficiency of 40-42%. At higher temperatures, both the output and the efficiency of gas turbine plants will be even higher.

Thus, of all reactor types feasible in the near future, the most economical will be the gas-cooled or liquid-metal-cooled reactors.

2. Mobile and Transportable Units

For desert, polar, and mountain areas where fuel delivery is difficult, atomic power units are the most reliable and convenient source of electric energy. The first 2,000-kw electric-power station of this type has been built in the Soviet Union.

In the USA, low-capacity transportable atomic electric-power plants are being designed for use by the army and at naval and aviation bases. The first experimental 2,000-kw army power reactor for transportable electric power stations (Fig. 8) was put in service in April, 1957. The reactor has a 10,000-kw heat

output and is cooled with 85 atmos abs pressurized water at a temperature of 220°C at the inlet and of 230°C at the outlet. The water circulates at a rate of 750 tons/hr. The steel housing of the reactor is lined on the inside with concrete 0.6 m thick. The core accommodates 40 fuel elements of 42 x 42-mm cross section. The core is contained in a steel tank 1.22 m in diameter with an iron-and-water shielding 1.2 m thick.

The thickness of the concrete biological shield of the reactor is 2.85 m. The steam generator consists of a vertical cylindrical vessel accommodating U-shaped bundles of tubes for circulating the water which cools the reactor. About 10 tons/hr of steam at 13.6 atmos abs and 207°C is generated between the tubes. The back pressure of the turbine is 0.07 atmos abs.

The rated efficiency of the electric-power plant is 15%; the installed cost is 436 dollars per kilowatt; and the cost of 1 kw-hr is about 5 cents.

The fuel used is highly enriched uranium in stainless-steel jackets. One charge requires 25 kg of uranium.

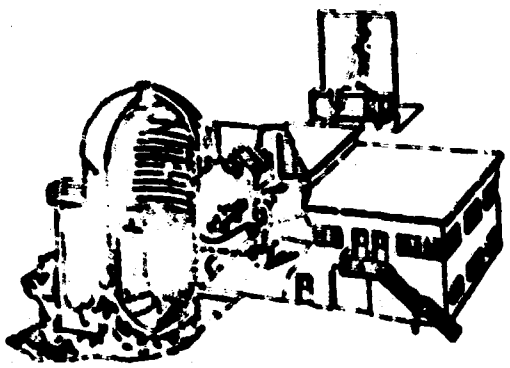

Fig. 8. Transportable 2,000-kw atomic electric-power station (Fort Belvoir).

The total weight of the reactor, steam generator, and auxiliary equipment is 1,300 tons; the reactor without the concrete shield weighs 560 tons. Efforts are being made to obtain a 25-ton figure to make transportation by air possible.

Lighter models of transportable army power reactors of the boiling, gas-cooled, and liquid-metal-fueled types are presently being developed.

In Britain, mass production is being set up for small-size pressurized-water atomic reactors which can be used for 10-20-Mw electric-power stations. The cost of a 10-Mw unit is 150 pounds sterling per kilowatt. The cost of electric power is expected to be 1-1.5 pence/kw-hr. The uranium charge is 0.5-3.5 tons; the uranium is enriched to 4-12%.

Information is available regarding plans for construction of trains with portable atomic power units.

It has been reported in press that, in the USSR, low-capacity wheeled mobile atomic electric-power stations have been developed for transportation on highways. These units can be used in areas where virgin land is being developed, at construction sites, and so on.

In the USA, plans are made for an atomic truck train to be used in Alaska. It will consist of 4 to 5 trailers, each 8 m long.

3. Atomic Prime Movers for Locomotives, Automobiles, and Aircraft

In various countries, plans have been under development for reactors and power units to be used in locomotives, automobiles, and aircraft, but no really feasible projects have yet been announced.

In the USA, a reactor design for a 6,900-hp locomotive with a steam turbine was under consideration. The weight of the locomotive was set at 500 tons; the weight of the atomic power unit, at 100 tons, i.e., at 20% of the weight of the locomotive.

In another project for a locomotive with an 8,000-hp steam turbine, the weight of the reactor with shield came to 181 tons. The 30-Mw heat-generating homogeneous reactor is situated in a vessel 0.305 x 0.915 x 0.915 mm (sic) in size. The shield is 1.22 m thick. The core consists of 10,000 stainless steel tubes for the circulation of the water coolant, with the space between the tubes filled with 176 kg of a uranyl sulfate solution containing 9 kg of uranium-235. The lower portion of the vessel houses the circulating pump for the uranyl sulfate solution. Water also serves as a neutron moderator and reflector. Cadmium rods are used for control.

Upon leaving the tube assembly, the water passes through a separator yielding steam at 17.5 atmos abs and 204°C. Through a reducer, the turbine is connected with 4 electric generators supplying 12 traction motors on the axles of the locomotive. The turbine condenser is water-cooled, the circulating water being cooled in radiators on the trailer section.

The daily uranium-235 consumption is 37 grams. Twice a year, the reactor is scheduled for refueling. The planned cost of the locomotive is 1.2 million dollars.

Plans have been completed for a gas-cooled reactor for a 3,000-hp gas turbine locomotive. The heat output of the enriched-uranium reactor is 15,000 hp. With the gas entering the turbine at 700°C, the efficiency at the turbine shaft is 20%. Allowing for the efficiency of the electrical transmission, the efficiency at the wheel's rim came to 16%. The locomotive is 20.7 m long and 3.2 m wide, and weighs 174 tons. The cost of operation came out higher than that of a diesel-electric locomotive. The cost of a locomotive in lot production is estimated at 1 million dollars. The shield of the reactor weighs 38.5 tons. The reactor in question is of the single-circuit air-cooled type.

In West Germany, design of a 5,900-hp atomic locomotive has been completed. The reactor is helium-cooled. The locomotive is driven by a double-shaft gas-

turbine unit with an efficiency of about 15%. The weight of the eight-axle locomotive with an electrical transmission is 175 tons; the length, 35 m; the cost, 2 million marks. The mileage cost is lower than that of a steam locomotive, but higher than that of a diesel locomotive.

In Japan, construction of a 3,000-hp atomic locomotive is planned. Its length will be 30 m; weight, 179 tons; and speed, 90 km/hr. It is lithium-cooled and beryllium-moderated. It can operate on one uranium charge for 8 months, which corresponds to a run of 155 thousand km.

Attempts to design an atomic engine for the automobile so far have not yielded any positive results. Thus, for a truck with 1.5-ton load capacity, the weight of a 100-hp atomic engine came to 50 tons. When in the future it becomes possible to design light-weight biological shielding, the problem of an atomic engine for heavy automobiles and buses will be solved.

Design work on atomic engines for aircraft is being done in various countries. The most likely approaches seem to be turbojet or turboprop engines, although the latter may prove too heavy. Ramjet engines may be possibly used after reactors are created with high surface temperatures at the fuel elements. The chances of utilizing steam-turbine engines still are obscure.

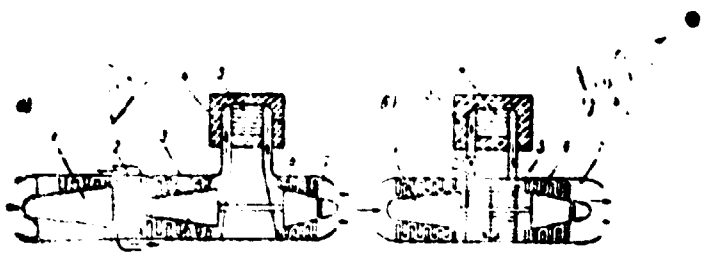

Fig. 9. Diagrams of turbojet motors with atomic reactors:

а- gas-cooled.

1- low-pressure compressor; 2- intermediary cooler; 3- high-pressure compressor; 4- biological shield, 5- reactor; 6- turbine; 7- jet duct.

б- liquid-metal cooled.

1- compressor; 2- circulating pump; 3- biological shield; 4- reactor; 5- heat exchanger; 6- turbine; 7- jet duct.

Fig. 9 shows two variants of a turbojet engine for aircraft. The first type provides for an air-cooled reactor with intermediate cooling of the air during compression. In the second type, the reactor is cooled by a liquid metal which transfers heat to the air in a heat exchanger.

With air entering the turbine at 800°C and a flight speed two or three times the speed of sound, the weight of the power plant comes to 1-1.5 kilograms per kilogram of thrust, bringing the total weight of the aircraft to between 80 and 120 tons. The reactor is to be located near the center of gravity of the airplane. The fuselage may be rather long, to keep the crew as far away as possible

from the reactor. The engine will be situated as close as possible to the reactor. If the aircraft is of a "flying-wing" design, the reactor may be situated at one end, and the crew at the other.

Runways to accommodate heavy atomic airplanes must be extremely strong. Seaplanes are more convenient in the sense that there is less danger of radioactive contamination in case of a crash, and that no runway is required.

The weight of the biological shield of an aircraft reactor is estimated to be between 10 and 45 tons. The weight of the reactor, the shield, and the turbojet engine constitutes about half the weight of the equipped airplane.

Efforts are being made to develop light-weight biological shielding for reactors. A shield of boron carbide with aluminum ("boral") is 100 times as effective as a heavy aggregate shield. A layer of "boral" 6 mm thick gives better protection from high-energy neutrons than a 0.6-m layer of concrete.

Another light-weight neutron-attenuating material is offered by polymerized acrylic plastics containing not less than 0.1 g of boron per cm^2 of surface. Combinations alternating steel sheets, wood fiberboard, and cellulose acetate with boron are also considered to be possible light-weight shielding from fast and thermal neutrons. A light-weight shielding has also been proposed in the form of matrices of a flexible metal (aluminum, zirconium) filled with a refractory material, boron oxide or boron carbide. The matrix is pressed in, by rolling, between sheets of aluminum or stainless steel casing. The boron content of a filled matrix is 35-50%. A 7-cm thick shield of this kind gives sufficient protection from thermal neutrons. The reliability of these cats is still unsettled.

Fuel elements of carbides with low uranium content are most promising for high-temperature aircraft reactors. For cladding uranium oxide elements, high-melting metals can be used, e.g., niobium, tungsten, molybdenum silicide.

A homogeneous reactor has been designed with a core of an alloy of enriched uranium with beryllium, which acts as a moderator. In another experimental

reactor, a ceramic fuel is dispersed throughout the graphite moderator. A thermal aircraft reactor has also been designed to operate on a solution of uranium in bismuth. It is a graphite-moderated heterogeneous reactor.

Land-based prototypes of aircraft reactors have been tested in the USA since 1951. In 1954, a 2.5-MW experimental reactor reached criticality. It uses a uranium tetrafluoride concentrate as fuel. The reactor is 0.9 m high.

American experts believe that the first atomic-powered aircraft flights will occur in 1960.

4. Marine Power Plants

The relatively low efficiency of conventional marine power plants necessitates fuel stocks which take up about one third of a ship's tonnage. This limits the possibility of further improvement in cruising speed and self-sufficiency of vessels at sea. Complicating plant design in order to increase efficiency results in reduced fuel consumption but, at the same time, leads as a rule to an increase in the weight of the power plant as well.

Nuclear fuel solves the problem of increasing the speed and self-sufficiency of seagoing vessels as well as the problem of reducing transportation costs.

The world's first atomic-powered sea vessel in peaceful use is the Soviet icebreaker "Lenin," intended for operation in the Arctic. Its displacement is 16,000 tons; cruising speed, about 18 knots; plant capacity, 44,000 hp. The length of the vessel is 134 m; the beam, 27.6 m; and the freeboard, 16.1 m.

The icebreaker is equipped with three water-moderated water-cooled reactors, one of which is a spare. The biological shield is of the composite type and consists of layers of water, iron, and concrete aggregates. The uranium charge is sufficient for several years of navigation.

For tankers and freighters as well as for ocean liners, the use of atomic

power plants is very promising as far as further improvement in speed and self-sufficiency is concerned.

Research carried out at the Institute of Complex Transportation Problems of the Academy of Sciences of the USSR showed that transportation costs in the case of a tanker with a nuclear-fueled gas turbine power plant and a cruising speed of 18-20 knots are only one third of those in the case of an oil-fired tanker. The comparison was made between tankers of a load capacity of 25,000 tons equipped with steam-turbine power plants operating on oil and on nuclear fuel, as well as tankers of 32,000 tons capacity equipped with gas-turbine power plants.

On January 21, 1954, the first atomic-powered submarine "Nautilus" was launched in the USA. Its displacement is 2,980 tons when surfaced and 3,180 tons when submerged; its length is 91.5 m; diameter of the rigid hull, 8.5 m; and maximum submersion depth, 230 m. The nuclear fuel charge is sufficient for submerged travel over 30,000 miles at a cruising speed of 20 knots. According to official sources, the submerged speed of "Nautilus" is around 20 knots. The power capacity of the double-shaft steam-turbine plant is about 20,000 hp. The submarine is equipped with an emergency diesel-electric plant of the accumulator type and with special apparatus for extraction of oxygen from sea water for the purpose of regenerating the air in the compartments. The crew of the submarine consists of 101 men.

The cost of the submarine was between 55 and 75 million dollars, or about three times as much as the cost of a conventional submarine. The uranium consumption is about 1.5-2 kg/yr per 1,000 hp. The efficiency of the power plant is 20%.

The reactor of the "Nautilus" is of the thermal-neutron type with water as moderator and coolant (as in the reactor of Fig. 2). The water temperature at the outlet of the reactor reaches 260°C. This permits the steam generator to produce at a pressure of 18.5 atmos abs and a temperature of 215°C. The

zirconium-sheathed fuel elements of the reactor are made of a uranium-zirconium alloy. The uranium is enriched by about 40% with respect to the U^{235}. The diameter of the core is 2.7 m, the diameter of the reactor with shield is 4.5 m. The shielding consists of a layer of water and of lead plates with an organic filler. The uranium charge is about 20 tons. One charge can last 2 to 2.5 years. The control rods are made of hafnium. Starting the reactor and bringing it to full power takes about two hours.

The adjustment of the atomic power plant of the "Nautilus" took considerable time. By April, 1957, the submarine had made 56,000 miles on the initial uranium charge. In April, 1957, the core of the reactor was demounted and replaced by a new core, which was adjusted in July and August of the same year. There were cases of severe radiation exposure among the crew. This particular submarine is characterized by the considerable size and weight of its power plant, low efficiency, insufficient maneuverability, and a high noise level.

The second American submarine, the "Seawolf," was launched on July 21, 1955. Its displacement when submerged is 3,760 tons; its length, 99 m; and the diameter of its rigid hull, 9.2 m. The submarine was commissioned in 1957. The crew numbers about 100 men. The capacity of the steam-turbine power plant is 25,000-30,000 hp; the rated underwater cruising speed is 25 knots.

The "Seawolf" is equipped with a liquid-sodium-cooled intermediate reactor. This made it possible to attain steam characteristics of 36 atmos abs and 400°C, which corresponds to an efficiency of 25-27%.

To prevent radioactive contamination in case of an accident, the heat exchanger is designed on the "tube-in-a-tube" principle. The radioactive sodium circulates in the inner tube, and water flows around the outer tube. The annular gap between the tubes is filled with a sodium-potassium alloy; the Na-K pressure is maintained above the Na pressure, which prevents radioactive sodium from entering the water region.

High thermal stresses in the complex tube system and the corrosive action of sodium on steel led to the development of cracks at those points where the tubes are mounted into the tube adapters of the steam superheater and (to an extent) of the vaporizer. It became necessary to remove the superheater, which reduced the capacity of the power plant by 20%. Due to leakage in the heat exchanger of the primary circuit and to a tube breakage in the secondary circuit, a radioactive-sodium leak occurred. These accidents caused a number of fatal casualties.

The sodium-cooled reactor is to be dismounted and a reactor of the "Nautilus" type installed. This solution must be considered a rash one, as the sodium-cooled reactor of the "Seawolf" is technologically more advanced than the reactor on the "Nautilus."

The third submarine, "Skate," equipped with a water-moderated water-cooled reactor, was launched in May, 1957. Test runs of this submarine began in November, 1957.

Five more submarines with displacements of 3,000 tons each have been designed with speeds in excess of 30 knots. One of them, of the "Albacore" class, has a streamlined drop-shaped hull reminiscent of a whale's body. A hull of such a shape increases the maneuverability and speed of the vessel. Such submarines can be used for submarine chasing. The picket submarine "Triton" displacing 5,450 tons will have two reactors. The submarine "Halibut" with a displacement of 2,800 tons is intended for guided-missile launching. A prototype of a reactor for small-displacement submarines reached criticality in December, 1956.

The USA is building the "Long Beach," a light cruiser of the "Boston" class, with a displacement of 14,000 tons and a length of 210 m, intended for launching of guided missiles. It will be equipped with two pressurized-water reactors. Plans are being initiated for construction of a ship with a displacement of

85,000 tons, equipped with eight reactors, and having a speed of 33 knots. Its power plant will be of the four-shaft type; each shaft will be served by two reactors and two turbines.

From 1960 on, all new military ships will be designed with atomic engines only.

Work has begun on designing liners and freighters with atomic power plants. Organic-moderated reactors, gas-cooled reactors with gas-turbine power plants employing helium, graphite-moderated reactors with a gas-turbine power plant, and a boiling reactor are being developed. In the USA, construction of the first atomic-powered freight-passenger ship has been approved; it is designed to carry 100 passengers and 12,000 tons of freight. The reactor is of the pressurized-water type; the capacity of the power plant, 20,000 hp; the speed, 21 knots; the length of the ship, 166 m.

A tanker with a load capacity of about 30,000 tons, a power plant capacity of 16,000 hp, and a speed of 18.6 knots consumes, on a 8,500-mile cruise, 3,000 tons of oil. A tanker is being planned having a load capacity of 38,000 tons and a length of 212 m, equipped with a gas-cooled reactor. The fuel will be slightly enriched uranium. The gas temperature at the turbine inlet will be 700°C. It is emphasized that the gas-turbine plant will perform with high efficiency under all loads. The cost of a run of the atomic-powered tanker will not exceed that of an oil-fired one. In another project, a tanker displacing 50,000 tons will be 205 m long with a 30-m beam and have a load capacity of 36,000 tons. A 30,000 hp steam-turbine plant will operate on saturated steam under a pressure of 34 atmos abs and maintain a cruising speed of 19 knots. According to a preliminary estimate, the cost of such an atomic-powered tanker will be 50% above the cost of a conventional tanker. The cost of the atomic power plant proper is 2.5 to 3 times higher than that of an oil-fired plant. The atomic-powered ship, however, can carry 10% more payload than a conventional

tanker of the same displacement.

Data have been made public on a 22,000-hp atomic steam-turbine plant for use on tankers.

The plant is powered by a water-moderated water-cooled reactor with a 85-Mw heat output. Its core consists of 32 heat-generating elements about 2.3 m high, arranged in a lattice 1.67 m in diameter. Each heat-generating element contains 200 stainless steel-sheathed uranium dioxide rods 12.7 mm in diameter. The core is surrounded by an annular water reflector in which the steel plates of the thermal shielding are situated. The reflector is 0.38 m thick. The carbon-steel reactor vessel is 2.5 m in diameter and is lined with stainless steel. The vessel is enclosed in a stainless-steel hull 76 mm thick.

Water enters the reactor under a pressure of 122 atmos abs at a temperature of 243°C and is heated in the core to 258°C. Four circulating pumps deliver it to two steam generators. The electric motors of the pumps have an auxiliary winding fed from a reserve current source. The steam generators use natural circulation.

The total maximum output of the high- and low-pressure turbines is 22,000 hp. The two turbines are connected with the propeller shaft through a two-stage gear transmission.

The steam pressure at the turbine inlet is 29 atmos abs; the condenser vacuum is 71 mm Hg.

Two 750-kw diesel generators are included in the equipment. In case of failure of the reactor, the ship can be kept underway using a 750-hp electric motor.

The planned service life of one uranium charge is about 3 years.

The maximum speed of fast ocean liners increased from 26 knots in 1934 to 35 knots in 1952. The ocean liner "United States" with a displacement of 45,000 tons and a 175,000-hp power plant has a cruising speed of 35.5 knots. Its oil

consumption amounts to 50 tons/hr. Consideration is being given to construction of a liner displacing 53,000 tons, 300-m long, capable of carrying 2,000 passengers. Its atomic power plant will make possible a speed in excess of 36 knots.

In Britain, orders have been placed for the construction of the first atomic-powered submarine and tanker. The submarine will be equipped with a pressurized-water reactor. The launching is expected in 1959. Development work is being done on an organic-moderated reactor for another submarine. The power plant will be of the steam-gas type or have a special gas turbine. Work is also going on with a gas-cooled reactor of the Calder Hall type, having an electric output of 16,000-24,000 hp.

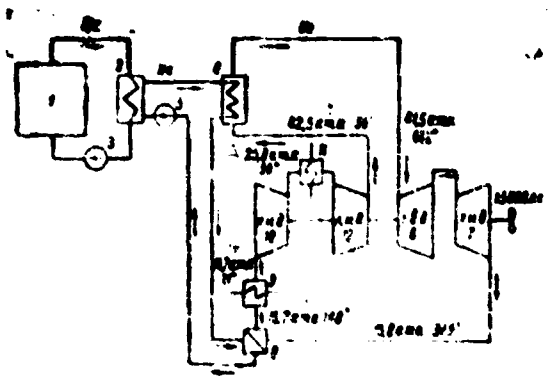

Fig. 10. Diagram of an atomic-fueled marine gas-turbine power plant.

1- reactor; 2- primary-circuit heat exchanger; 3- primary-circuit circulating pump; 4- intermediate-circuit heat exchanger; 5- intermediate-circuit circulating pump; 6- high-pressure turbine; 7- low-pressure turbine; 8- regenerator; 9- gas cooler; 10- low-pressure compressor; 11- intermediate cooler; 12- high-pressure compressor.

A- 25.8 atmos abs at 96°C; B- 42.5 atmos abs at 96°C; C- 41.5 atmos abs at 662°C; D- 15,000 hp; E- 15.8 atmos abs at 389°C; F- 15.7 atmos abs at 140°C; G- 15.7 atmos abs at 21°C.

A 15,000-hp marine atomic gas-turbine power plant was designed in Britain. Its layout is shown in Fig. 10. The reactor is cooled with liquid sodium. In

another design, for a 17,500-hp marine gas-turbine power plant, the reactor planned is to be cooled with helium at an outlet temperature of 870°C. In the secondary circuit, the maximum helium temperature will be 760°C. The rated efficiency of the plant is 42%. Sodium is a fire hazard and has an induced radioactivity requiring more biological shielding than in the case of gas or water. For gas-turbine power plants, gas-cooled reactors are more promising. In fast and intermediate reactors, however, the physical advantages of sodium may compensate for its shortcomings.

For a tanker displacing 80,000 tons, with a speed of 25 to 30 knots, both organic and liquid-metal cooled reactors have been considered. It was found that the organic-cooled organic-moderated reactor was 20-25% cheaper than the liquid-metal type, but the efficiency of the liquid-metal cooled reactor was higher.

The Esher-Wiss* Company designed a 20,000-hp gas-turbine atomic power plant for a tanker; its heat flow diagram is shown in Fig. 11. The compressor group is driven by a high-pressure turbine of the axial-flow type. Two low-pressure radial-flow turbines (one of them shown in the diagram) are connected with the propeller shaft through a reducer. Through the reducer, the propeller shaft can also be driven by a reserve steam turbine operated by superheated steam. For a starting engine, another steam turbine is used. The fan of the afterheat-removal system of the reactor is also steam driven.

---

* Translator's Note: Transliteration - original spelling not available.

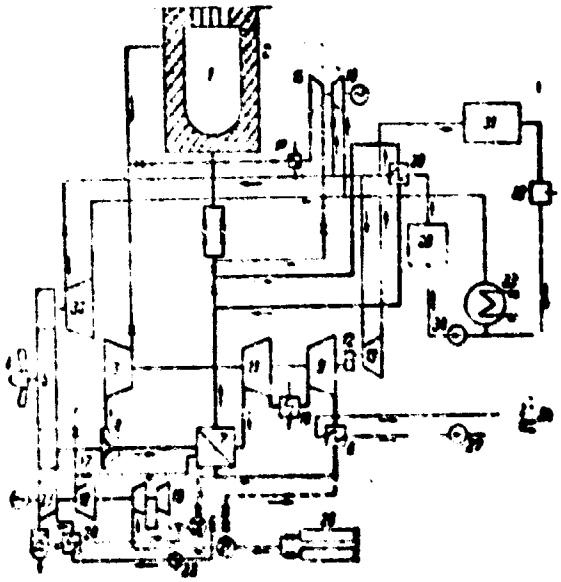

(See following page for legend of picture)

Fig. 11. Diagram of a 20,000-hp atomic gas-turbine power plant for use on a tanker.

1- reactor; 2- primary shield; 3- high-pressure axial-flow gas turbine; 4- low-pressure radial-flow gas turbine; 5- reducer; 6- propeller; 7- regenerator; 8- final gas cooler; 9- low-pressure compressor; 10- intermediate gas cooler; 11- high-pressure compressor; 12- starting turbine reducer; 13- starting steam turbine; 14- gas cooler of the afterheat removal system; 15- fan of the afterheat removal system; 16- steam drive for the fan; 17- bypass reduction unit; 18- auxiliary gas turbine; 19- compressors; 20- low-pressure accumulator; 21- high-pressure accumulator; 22- gas cooler; 23- turbine-type expander; 24- heat exchanger; 25- xenon filter and separator; 26- nitrogen-adding cylinders; 27- outboard water pump; 28- steam boiler; 29- steam superheater; 30- reserve steam turbine; 31- freight-tank heating system; 32- auxiliary condensing unit; 33- reserve turbine condenser; 34- condensate pump; 35- hot water for tank flushing.

Reversing can be accomplished with the aid of a variable pitch propeller or by using reversible radial-flow turbines.

The coolant used in this power plant is nitrogen. Its optimum parameters were calculated as follows: the pressure increase ratio in the gas-turbine cycle is between 4 and 5; the gas pressure (p) lies between 20 and 60 kg/cm^2;

and the starting gas temperature is 675-750°C. A plant with a higher pressure increase ratio would be more expensive and less reliable. The gaseous fission products (xenon) are trapped by diverting a portion of the nitrogen flow from the gas-turbine cycle into a turbine-type expander and a separator-type filter.

Cross-section and plan views of this gas-turbine plant are shown in Fig. 12.

In France, two atomic-powered submarines are planned. The first of these will be launched in 1960-1961. Its speed and maneuverability are below those of the "Nautilus." This submarine will be used for training purposes.

For 1961, construction of the liner "France" is planned, it will have a displacement of 55,000 tons and a speed of about 30 knots. Its boiler plant will later be replaced by a reactor power plant.

In West Germany, plans are being developed for an atomic-powered tanker with a load capacity of 22,000 tons and a length of 182 m. Its 10,000-hp steam-turbine plant is designed for a cruising speed of about 16 knots.

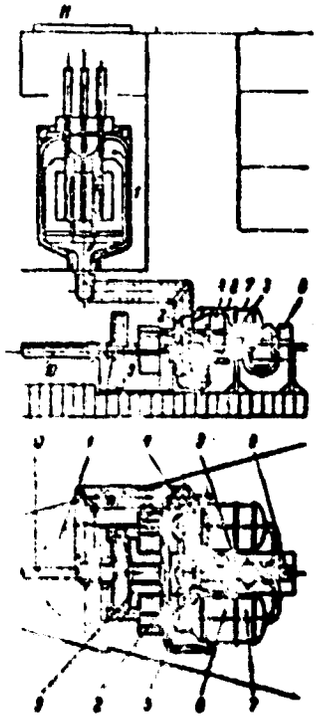

Fig. 12. Cross section and plan view of a 20,000-hp gas-turbine power plant for use on a tanker.
1- reactor; 2- high-pressure turbine; 3- low-pressure condenser; 4- high-pressure compressor with built-in cooler; 5- propulsion low-pressure gas turbine; 6- regenerator; 7- cooler; 8- starting turbine; 9- reducer; 10- propeller shaft; 11- removable plates for the extraction of reactor core.

A layout of the plant is shown in Fig. 13.

The reactor is of the thermal-neutron pressurized-water type. The fuel elements use enriched uranium; the uranium charge weighs 2,400 kg. The heat output of the reactor is 30.5 Mw, and it weighs 40 tons.

The core has a thermal shield 50-mm thick made of sheet stainless steel. The rigid hull of the reactor is 1.7 m in diameter and 5.6 m high; it is made of heat-resistant steel and lined with stainless steel. The water pressure in the circulation circuit is 160 atmos; the water temperature at the reactor inlet is 270°C and at the outlet, 290°C. The water flow is 1,020 tons per hour.

The entire reactor is shielded by a steel container 9.6 m in diameter and 12.6 m long, with walls 60 mm thick. To protect the reactor from jolts and shocks, a shock absorber is installed between the ship's hull and the container, consisting of steel sheets spaced at 500 mm with the interstices filled with oak boards. The biological shield is 1.1 m thick. It contains lead plates and an organic filler.

The atomic power plant for the tanker is expected to weigh 2,000 tons. An oil-fired boiler-type power plant for a tanker of this kind weighs 1,100 tons. The oil supply for a five-week run weighs 2,200 tons. Thus, the over-all weight of the plant with fuel supply amounts to 3,300 tons. Due to the lower weight of the atomic power plant, the payload of the tanker is increased.

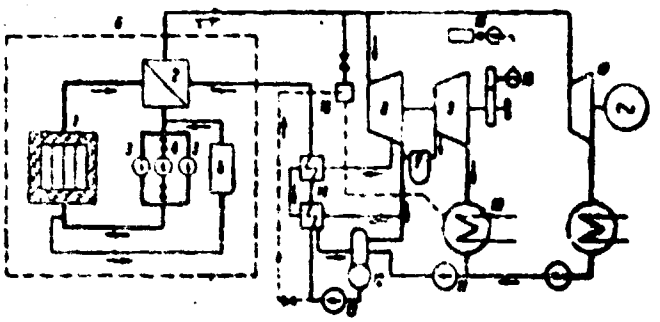

Fig. 13. Heat flow of a 10,000-hp gas-turbine power plant for use on a tanker.

1- reactor; 2- steam generator; 3- primary-circuit circulating pump; 4- standby circulating pump; 5- filter for trapping fission products; 6- container; 7- steam separator; 8- high-pressure turbine; 9- low-pressure turbine; 10- condenser; 11- condensate pump; 12- deaerator; 13- feed pump; 14- regenerator-type heaters; 15- electric motor; 16- diesel generator; 17- turbine generator; 18- reduction and cooling unit.

The two-cylinder turbine is designed to operate on saturated steam under a pressure of about 40 atmos abs. The separation of precipitating moisture is provided for between the cylinders. The efficiency of the plant is set at 28%. If oil is used to superheat the steam to 480°C, the efficiency can be increased

to 24%. An oil-fired boiler-type power plant has an efficiency of 25%.

In Sweden, construction of two atomic-powered ships with displacements of 45,000 tons is planned.

The Laval Company has designed a two-circuit marine atomic steam-turbine plant with a boiling reactor utilizing ordinary water.

The main feature of the boiling-water reactor -- its simplicity and the low weight of the lines between the reactor and the turbine -- is not put to advantage in this plant. The pressure in the vessel of a boiling-water reactor is lower than in a pressurized-water reactor. The wall thickness of the vessel and its weight are lower than in a water-cooled water-moderated reactor. The advantage of the boiling-water reactor is its capacity for self-regulation and its high operating stability under changeable conditions.

The steam-turbine plant has no peculiar features. An auxiliary oil-fired boiler is provided to supply the turbine generators and for heating. In case of reactor failure, the boiler can supply steam to a drive turbine, keeping the ship underway.

In Norway, construction is planned for an atomic-powered tanker with a displacement of 32,000 tons and a speed of 18 knots. The heat output of the reactor is 64 Mw; its weight is 1,000 tons. The moderator is D_2O; the coolant is H_2O; the uranium charge weighs 15 tons.

In Japan, design work is being done on a submarine tanker with a displacement of 30,000 tons, a length of 65 m, and a 21-m beam. The speed when submerged is 23 knots; the capacity of the power plant is 20,000-30,000 hp. A second tanker is being designed, for which data are not available.

The atomic power plants made possible the creation of a new type of seagoing passenger or freight vessel, capable of cruising both on and under the ocean surface.

By providing the hull of a submarine vessel with a very smooth outer surface

to 24%. An oil-fired boiler-type power plant has an efficiency of 25%.

In Sweden, construction of two atomic-powered ships with displacements of 45,000 tons is planned.

The Laval Company has designed a two-circuit marine atomic steam-turbine plant with a boiling reactor utilizing ordinary water.

The main feature of the boiling-water reactor -- its simplicity and the low weight of the lines between the reactor and the turbine -- is not put to advantage in this plant. The pressure in the vessel of a boiling-water reactor is lower than in a pressurized-water reactor. The wall thickness of the vessel and its weight are lower than in a water-cooled water-moderated reactor. The advantage of the boiling-water reactor is its capacity for self-regulation and its high operating stability under changeable conditions.

The steam-turbine plant has no peculiar features. An auxiliary oil-fired boiler is provided to supply the turbine generators and for heating. In case of reactor failure, the boiler can supply steam to a drive turbine, keeping the ship underway.

In Norway, construction is planned for an atomic-powered tanker with a displacement of 32,000 tons and a speed of 18 knots. The heat output of the reactor is 64 Mw; its weight is 1,000 tons. The moderator is D_2O; the coolant is H_2O; the uranium charge weighs 15 tons.

In Japan, design work is being done on a submarine tanker with a displacement of 30,000 tons, a length of 45 m, and a 21-m beam. The speed when submerged is 23 knots; the capacity of the power plant is 20,000-30,000 hp. A second tanker is being designed, for which data are not available.

The atomic power plants made possible the creation of a new type of seagoing passenger or freight vessel, capable of cruising both on and under the ocean surface.

By providing the hull of a submarine vessel with a very smooth outer surface

it is possible to reduce the hull resistance by 70%. It is thought possible to secure laminar flow of water about the vessel's hull through a special system of hydrodynamic control of the boundary layer.

This brief survey of the developments in the field of stationary and propulsion atomic power plants indicates that liquid-metal cooled reactors permit a plant efficiency of 25-35%, and in the case of a double mercury-water cycle, as high as 40-45%. Water- and organic-cooled reactors permit plant efficiency of 20-30%. The liquid-metal coolants can be matched only by the gaseous coolants, which permit an efficiency of up to 40%, although at a higher temperature than in the case of the liquid metals.

CHAPTER III

LIQUID METALS: HYDRAULICS AND HEAT TRANSFER

(GIDRAVLIKA I TEPLOOBMEN V ZHIDKIKH METALLAKH)

From the hydraulic viewpoint liquid metals do not differ from ordinary liquids. In particular, hydraulic resistance to the flow of metals in tubes, as tests have shown, can be calculated using the formulas for water, air, etc. With respect to heat transmission, liquid metals differ substantially from other fluids. Therefore empirical formulas used to calculate heat transfer for water, air, oil, and other media are not appropriate to the case in hand.

21. Hydraulics of a Liquid-metal Flow

In this section certain data which permit us to determine the hydraulic characteristics of a liquid-metal flow are given in a way convenient for calculations.

The diagram shown in Fig. 55 serves to determine the Reynolds number for a flow of sodium in a circular tube. The value of the correction factor (a) necessary to determine the Re for a flow of sodium-potassium alloys in a tube are also given there.

In like manner, pressure losses in a straight tube are found by using the diagram in Fig. 56.

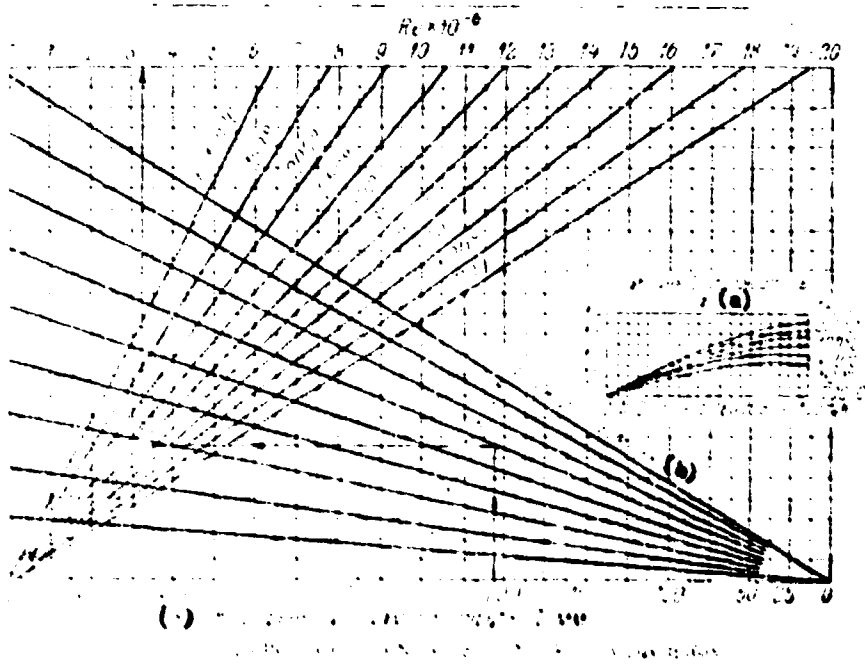

Fig. 55. Re for flows of Na and Na—K alloys in circular tubes.

(a) correction factor (b) velocity m/sec

(c) internal diameter of tube D mm

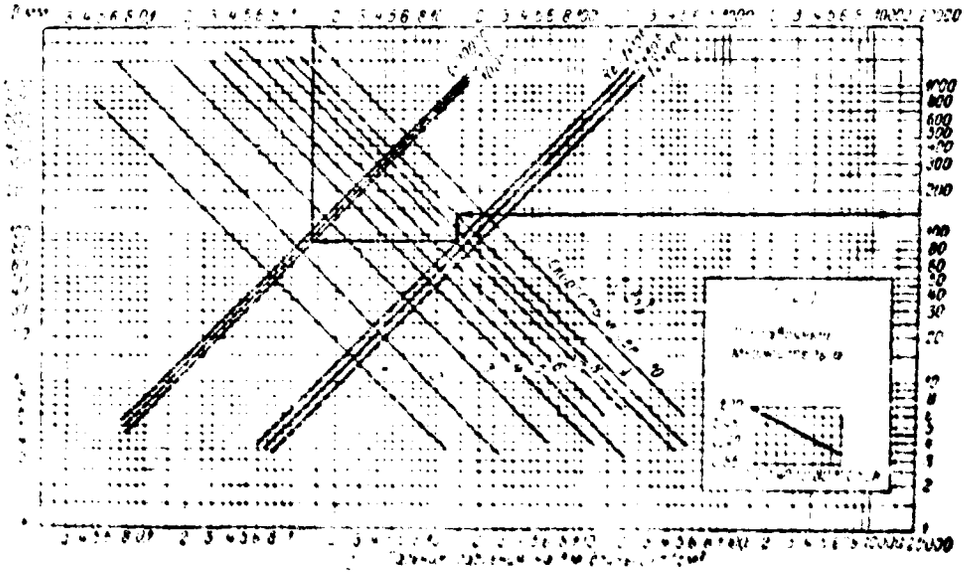

Fig. 56. Pressure losses in a straight tube for flows of Na and Na—K alloys.

(a) correction factor (b) velocity, m/sec

(c) pressure drop per 1 m length, kg/cm^2

From Figs. 57 and 58, the power required to pump sodium and sodium-potassium alloys through a section of straight horizontal tube of given length can be found; the graphs are constructed on the basis of the two preceding diagrams. If the tube slopes upward or downward, an appropriate modification in the pump power must be computed to compensate for the rise or fall in head. Head losses due to local resistance are determined in the usual manner and are also taken into account during the final determination of the power needed.

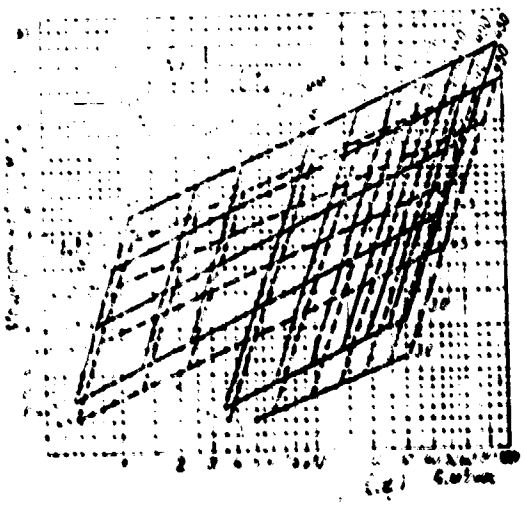

Fig. 57. Power required to pump Na.
(a) power per 10 running meters, h.p.
(b) velocity m/sec (c) diameter of tube, mm
(d) G, m^3/hr

The similarity in hydraulic characteristics of flows of liquid metals and water permits us to investigate the motion of metallic liquids by using models. From the data of Table 16, the temperature of the simulation water can be chosen so as to set the kinematic viscosity of the water equal to that of the alkali metals.

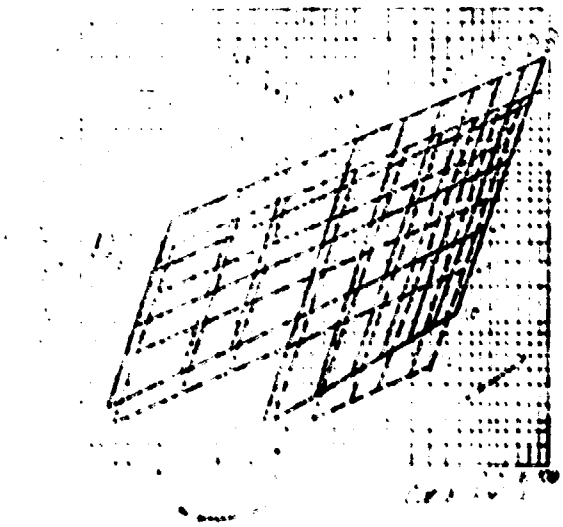

Fig. 58. Power necessary to pump a Na—K (44% K) alloy.
(a) power per 10 running meters, h.p.
(b) velocity m/sec (c) diameter of tube mm
(d) G/m^3 hr

TABLE 16

(A)

Equivalent Temperatures of Water

(B) Temperature of liquid metal t, °C	(C) Equivalent temperature of water θ, °C		
	(D) For Na	(E) For Na—K (56% K)	(F) For Na—K (78% K)

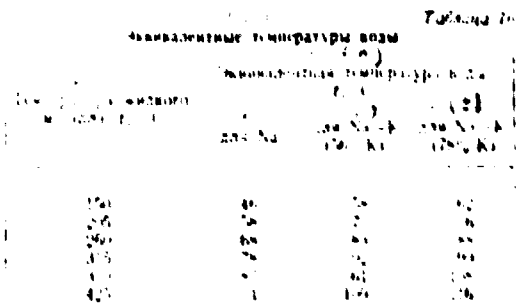

Velocities of liquid metals in circuits are usually low, since their heat-transfer properties are adequate even at low velocities. The use of higher velocities (more than 5 to 10 m/sec) is also unadvisable, because this will lessen the durability of structural materials.

The working pressure in liquid-metal circuits, is as a rule comparatively low. This is explained by the fact that liquid-metal heat-transfer media have a high boiling point and can be used over a wide range of temperatures without substantially increasing the pressure in the system. Therefore the maximum operating pressure in the system is determined by its hydraulic resistance and the entrance pressure required at the circulation pumps. The greater part of the resistance occurs in those sections where heat is supplied (reactor, heat exchanger, etc.). Because of the high rate of heat transmission, these sections are relatively short, which tends to reduce their hydraulic resistance.

Choice of optimum values for operating pressure and metal-flow velocity also depends on the conditions producing cavitation in those parts of the system where the pressure may equal the vapor pressure of the liquid at a given temperature, such as the pump intakes. It is advisable to feed inert gas under a pressure of approximately 1 atmos to those places which are considered dangerous from the viewpoint of cavitation.

In conclusion, let us introduce a number of nomographs (Figs. 59 through 64) which are useful in the rough evaluation of certain quantities characterizing a flow of liquid metals in tubes (mass and volume flow rates of the liquid pressure drop along a horizontal tube, and Reynolds number).

To find any unknown quantity, join two known points on the parallel scales of the given nomograph by a straight line; this will yield a solution where the calculation formula for the unknown parameter contains not more than two variables, or gives a point on an auxiliary scale where the calculation formula contains three or more variables. The point found should then be connected with a third

known point; then the point of intersection of a straight line with the scale where the unknown value is plotted will yield a final solution to the problem.

Example. A sodium-potassium alloy (56% K) flows through a tube of 15 mm diameter at 260° C with a velocity of 4.5 m/sec.

1. The pressure drop along a 6 m length of tube: by the nomograph of Fig. 62, $\Delta p = 0.56$ kg/cm^2; by calculation, $\Delta p = 0.546$ kg/cm^2.

2. Re number: by the nomograph of Fig. 64, Re = 200,000; by calculation, Re = 202,000.

3. Mass flow rate: by the nomograph of Fig. 61, G = 2,680 kg/hr; by calculation, G = 2,692 kg/hr.

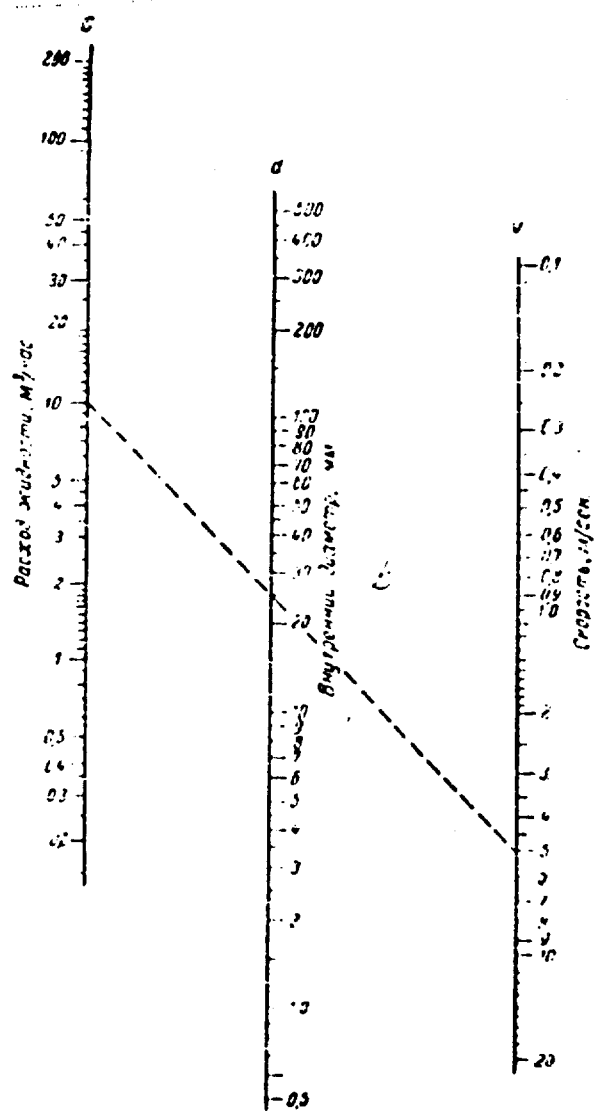

Fig. 59. The volume flow rate of liquid flowing in a circular tube.

(a) delivery of liquid, m^3 hr

(b) internal diameter, mm

(c) velocity, m/sec

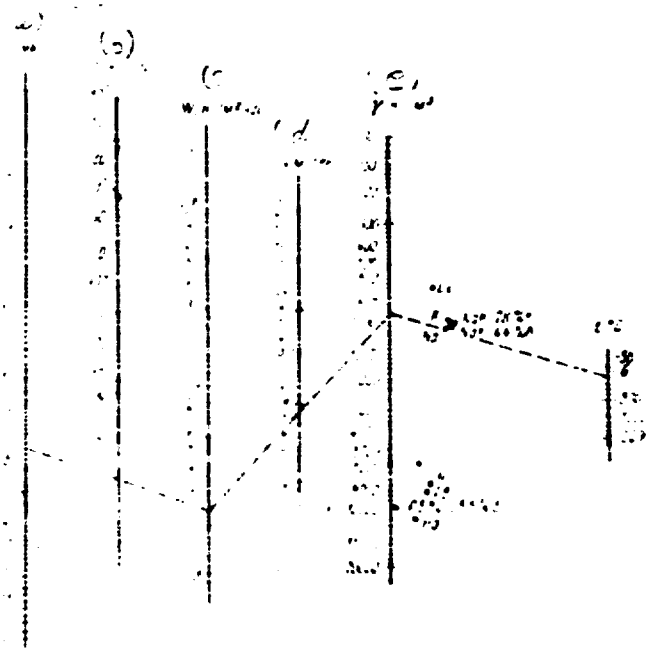

Fig. 60. Mass flow rate of liquid metals (Na, K, Na—K alloys, Li, Sn, Hg, Bi, Pb, and Pb—Bi alloy) flowing in a circular tube.
(a) D, mm (b) G, kg/hr (c) W, kg/m^2 hr (d) V, m/sec
(e) γ, kg/m^3

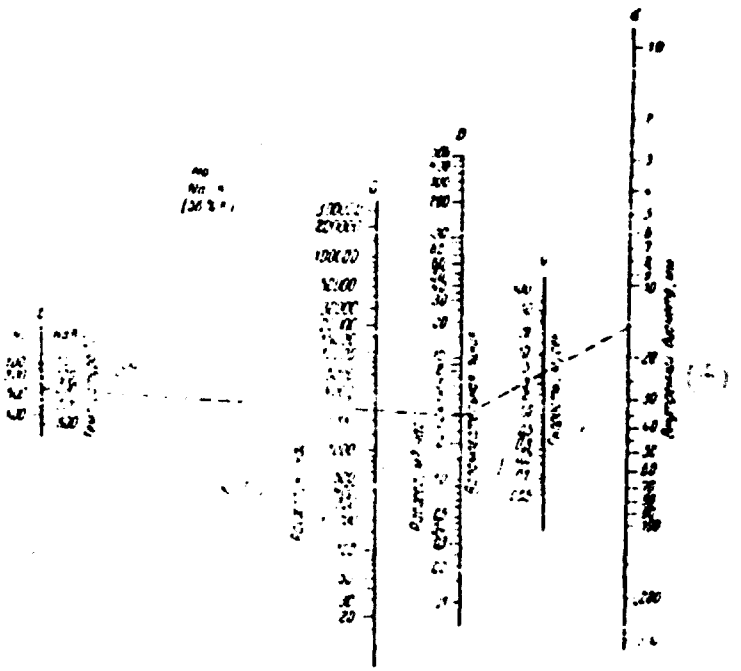

Fig. 61. Mass flow rate of Na and Na—K (56% K) alloy flowing in a circular tube.
(a) temperature, °C (b) output, kg/hr (c) output, m^3 hr (d) auxiliary line (e) velocity m/sec (f) internal diameter, mm

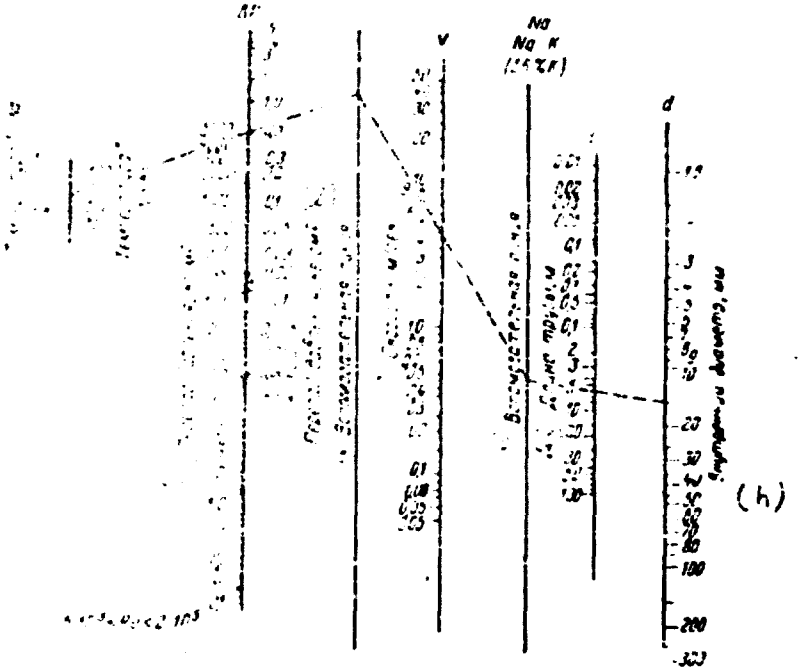

Fig. 62. Pressure losses for Na and a Na—K (56% K) alloy flowing in a circular tube.

(a) temperature, °C, Na (b) temperature °C, Na K

(c) pressure drop, kg/m^2 (d) pressure drop, kg/cm^2

(e) auxiliary line (f) velocity, m/sec

(g) length of pipe, m (h) internal diameter, mm

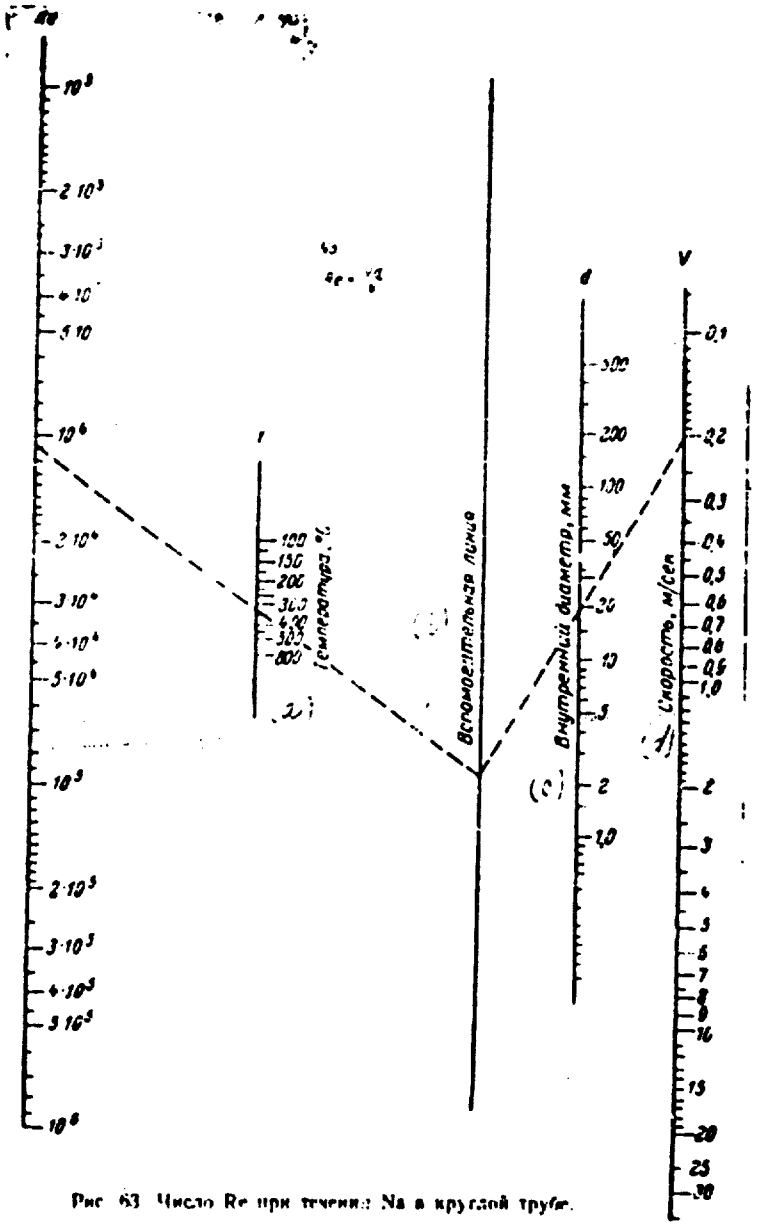

Рис. 63. Число Re при течении Na в круглой трубе.

Fig. 63. Re number for Na flowing in a circular tube.

(a) temperature, °C (b) auxiliary line

(c) internal diameter, mm (d) velocity, m/sec

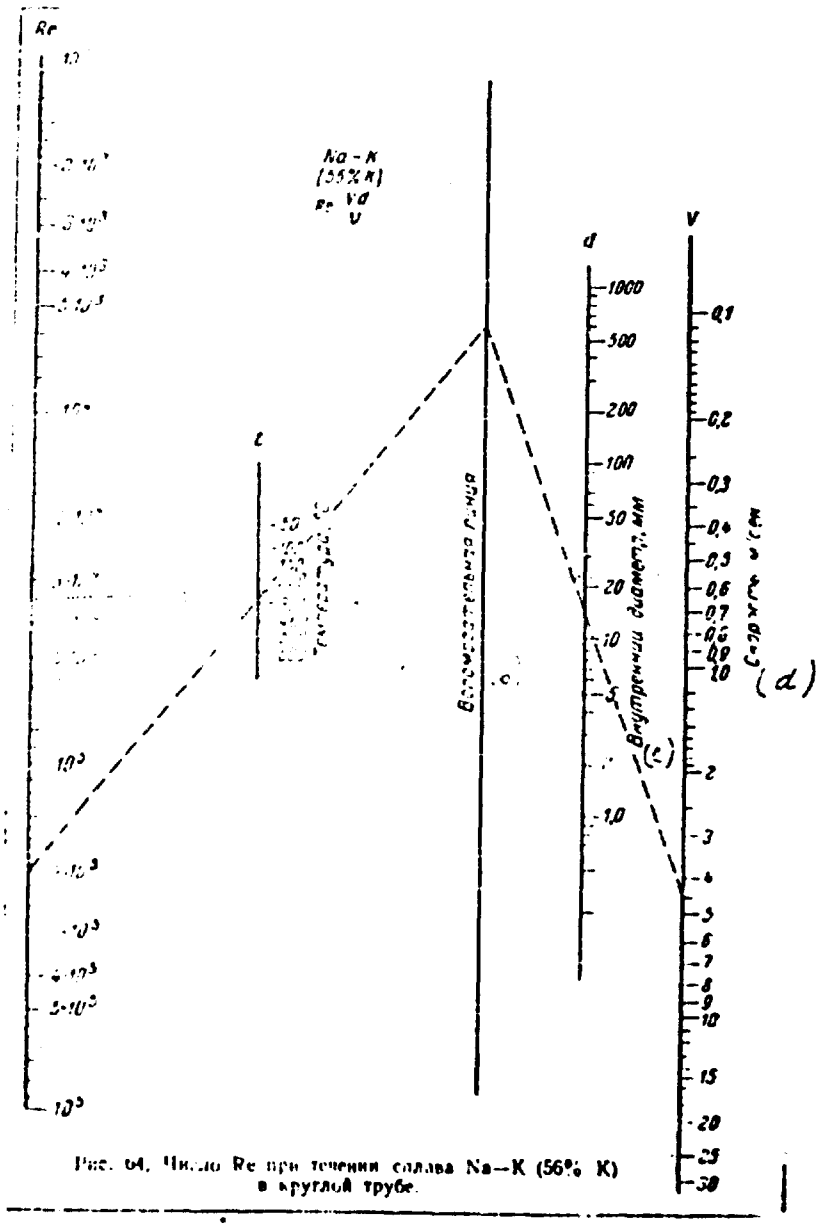

Рис. 64. Число Re при течении сплава Na—K (56% K) в круглой трубе.

Fig. 64. Re number for Na—K (56% K) alloy flowing in a circular tube.

(a) temperature, °C (b) auxiliary line

(c) internal diameter, mm (d) velocity, m/sec

22. Heat Transfer during Free Convection

It is known that in a gravitational field liquid volumes move relative to one another if their temperatures, and consequently their densities, are different. As a result of such movement, called natural or free convection, a transfer of heat from "hotter" areas of the liquid to "cooler" areas occurs.

In an atomic power installation, using a liquid metal as coolant, free convection is used to cool certain parts of the installation in the event of a forced shut-down of the pumps.

Free convection is characterized mathematically by an additional term in the equation for the amount of liquid motion. This term is expressed as follows:

$$(\rho - \rho_0) g_i \qquad (45)$$

Where ρ is the density of liquid kgf· sec^2/m^4;

g_i is the component of gravitational acceleration in the i, direction m/sec^2;

β is the coefficient of volumetric expansion of the liquid, 1/degree;

T is the temperature °K.

The index "0" designates certain initial values of parameters which can be selected according to the conditions of the heat-transfer process.

Analysis of the motion and energy equations indicates that free convection is characterized by the following dimensionless groups:

Gr $\frac{g_i \beta \Delta T l_0^3}{\nu^2}$ (число Грасгофа). GRASHOF NUMBER

Pr $\frac{\nu}{a}$ (число Прандтля). PRANDTL NUMBER

Where l is a line, taken as a defining dimension;

ν is the kinematic viscosity;

λ is the thermal conductivity of the liquid.

The dimensionless parameter

must also be introduced if heating due to internal friction in the liquid becomes substantial and the term $\frac{}{}$ becomes comparable with or greater than one.

For liquid metals the Prandtl number is small, and the effect of viscosity on heat transfer may be neglected. For example, for free convection in a large volume of liquid metal, the heat flow is proportional to the product $Gr \cdot Pr^2$, which does not depend on . However, for natural convection in a small volume bounded by walls, the effect of viscosity is noticeable and the rate of heat transfer must be expressed by the Gr and Pr numbers separately.

Results of experimental investigations confirm these conclusions.

Vertical plates and cylinders. Schmidt and Beckman obtained an accurate solution for free convection of air near a vertical plate (the case of laminar flow in a boundary layer), given that the temperature of the surface of the plate is constant. This solution was expanded into various Prandtl numbers by Latrakh. The result of his calculation is shown in Fig. 65; the physical constants entering into the Grashof, Nusselt, and Prandtl numbers are related to the temperature beyond the surface of the plate. The distributions of temperatures and velocities calculated for a Prandtl number equal to 0.01 are shown in Fig. 66. An analogous solution was obtained by Sperry and Gregg for a uniform distribution of heat-flow intensity over the height of the plate. In this case the heat-transfer coefficient α is approximately 10% higher than the value of α found for the condition $T_w = \text{const}$, where the Grashof number is determined by the constant

temperature T_w:

$$Gr = \frac{\rho g \beta (T_w - T_0)}{\nu^2}$$

The theoretical solutions shown in Figs. 65 and 66 were obtained for the condition that the local Grashof number does exceed 10^8, since when $Gr = 10^8$ the flow near the wall becomes turbulent.

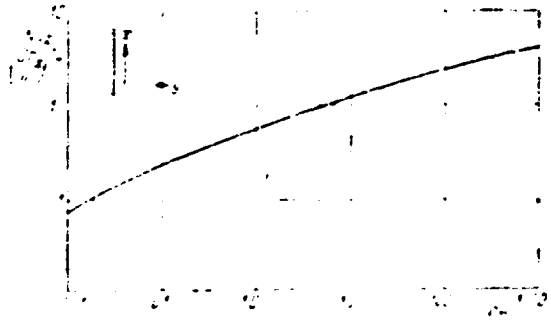

Fig. 65. Heat transfer for free laminar flow of a liquid along a vertical plate (Ostrakh solution).

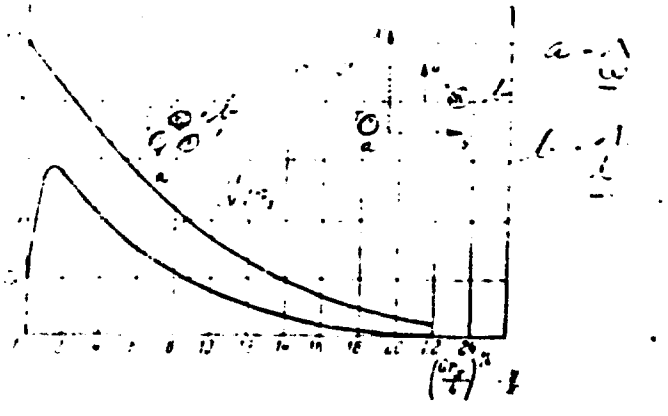

Fig. 66. Profiles of temperatures and velocities near the surface of a vertical plate for free laminar flow of a liquid metal.

Eckert and Jackson obtained the following equation for calculating heat transfer for turbulent flow of a liquid along a vertical plate, the temperature of which is constant:

$$\text{Nu}_x = \text{const}\,(\text{Gr}_x\text{Pr})^{0.47}\frac{1}{(1+0.494\,\text{Pr}^{0.67})^{0.4}} \qquad (46)$$

According to Formula (46) the heat flux on the surface is proportional to $\text{Pr}^{-0.67}$. In spite of the fact that this proportionality may not hold for low Prandtl numbers, Expression (46) can be used in practical computations. For a constant heat flow at the surface Equation (46) takes the form:

$$\text{Nu}_x = \text{const}\,(\text{Gr}_x\text{Pr}^{0.67})^{0.4}\frac{1}{(1+0.494\,\text{Pr}^{0.67})^{0.4}} \qquad (47)$$

The theoretical results obtained above can be used to calculate heat transfer for a vertical cylinder.

Horizontal plates and cylinders. Levy studied laminar and turbulent free flow near a horizontal surface. The curve of the heat-transfer coefficient for small Prandtl numbers, calculated by Levy as an average over the circumference of the cylinder, is shown on Fig. 67. A theoretical curve obtained by Hymen, Penilla, and Erlich, and experimental points for a number of liquid metals (Hg, Pb, Bi, eutectic of Pb—Bi, Na and Na—K alloy) are also shown on Fig. 67. If the flow near a surface is laminar, experimental data on heat transfer to liquid metals for cylinders of a diameter $\underline{d}$ ranging from 5 to 40 mm can be represented by the function:

$$\text{Nu}_d = 0.53\,(\text{Gr}_d\text{Pr})^{0.25}. \qquad (48)$$

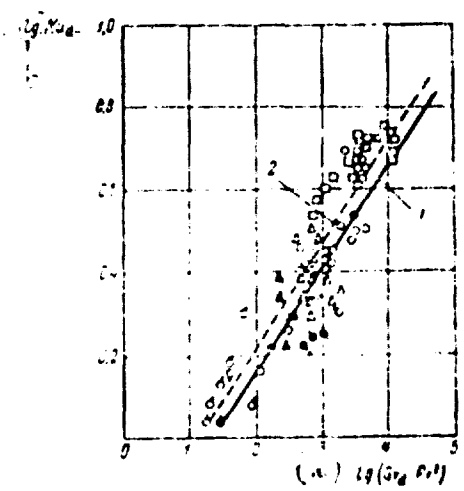

Fig. 67. Heat transfer for laminar free flow of a liquid metal near the surface of a horizontal cylinder.

(1) Levy solution; (2) solution of Hymen and others.

● — Pb—Bi; ◐ — Na; ◑ — Na—K; ◒ — Bi; △ — Pb; ▽ — Hg (experimental points of Hymen and others).

For horizontal plates, discussed above, the following expressions for laminar (49) and turbulent (50) flow were obtained by Mausteller and MacGoff:

$$Nu = 0.57 (Gr_A Pr)^{1/4} \frac{1}{(0.76 + Pr)^{1/4}} \qquad (49)$$

$$Nu = 0.13 Gr_A^{1/3} Pr^{1/3} \frac{1}{(1 + 0.61 Pr^{1/3})^{1/3}} \qquad (50)$$

There is no experimental data in the literature which can be compared with Formulas (49) and (50)

Vertical tubes or parallel plates. If free convection occurs inside a vertical tube or in the space between two vertical planes, theoretical analysis of heat transfer becomes difficult. It is evident that case a (Fig. 68) (two infinite vertical plates heated to a certain temperature) is the simplest from an analytic viewpoint. Ostrakh found an accurate solution for a laminar flow of liquid between plates with and without heat source between them, when the temperatures along the height of plate are constant, but not necessarily equal to one another.

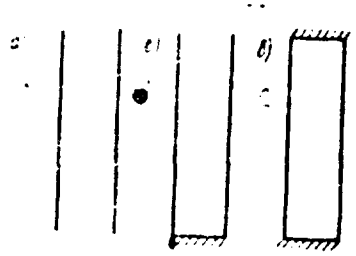

Fig. 68. Heat transfer diagram for parallel plates.

_____ Heating or cooling surface.

_____ Heat-insulated surface.
////////

The results of the calculation where the temperature of the surface is uniform is shown on Fig. 69. The various lines on the figure refer to various values of the parameter

where Q is the heat flow through unit volume between the plates, kcal/m^3 hr;

d is the distance between the plates, m;

λ is the thermal conductivity of the liquid, kcal/m· hr ^{o}C;

T_1 is the temperature of the plates, ^{o}C;

T_2 is the temperature of the liquid, ^{o}C.

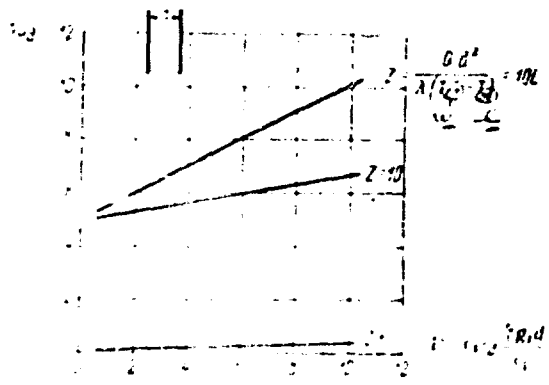

Fig. 69. Heat transfer for free laminar flow of a liquid between two vertical parallel plates having uniform temperature.

Ostrakh and Littkie found an analogous solution for the case where one plate is evenly heated and the other is evenly cooled from without. The results of the calculation are shown in Fig. 70, where the ordinate axis gives the ratio of the actual temperature drop between the plates to the drop which would exist under heat transfer by pure heat conduction.

Laytkhill and Levy solved the problem of convection heat transfer for the conditions prevailing when the space inside a tube or between plates is bounded on one side by a wall and the temperature of all walls is constant (case b, Fig. 68).

The results of the given studies can be used for approximate calculations of heat transfer in liquid metals.

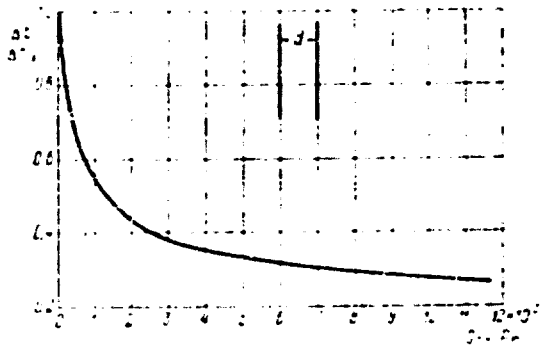

Fig. 70. Free laminar flow between two vertical parallel plates differing in temperatures.

The heat-transfer process is even more complicated for free convection in a space enclosed on all sides (Fig. 68c). Ostrakh obtained a solution to this problem for the case where heat sources are present and the temperature of the bounding surfaces is uniform at all points. The curve found by him is shown on Fig. 71.

At very small values of distance d, heat-transfer calculations can be based on the results of Timo's work on heat transfer in narrow annular slots, which will be discussed below.

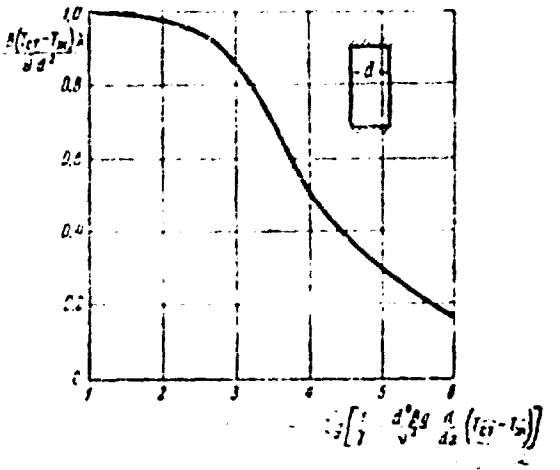

Fig. 71. Heat transfer for free convection of a liquid in a space enclosed on all sides.

Narrow annular slots, horizontal and vertical. Experimental research on free convection in liquid sodium, occurring inside a vertical annular slit, was conducted by a number of researchers (Timo, Mausteller and MacGoff, Paulidg). The lateral faces of the slit were heat-insulated, the metal was heated from below and cooled from above, and the hollow, in which the process of natural convection was developed, was enclosed on all sides.

The author's experimental data are shown in Table 17.

TABLE 17

(A)

Natural Convection in Narrow Vertical Annular Slots

(B)

Author

(C) Characteristic	(D) Symbol	(E) Tiwo	(F) Maustaller, MacGoff	(G) Mulidg

(H) Diameter, mm

(I) Height, mm

(J) Width of slot, mm

(K) Ratio $\frac{\delta}{D}$

(L) Minimum temperature above the slot, °C

(M) Maximum temperature below the slot, °C

(N) Temperature drop, °C

(O) Total heat flow due to free convection, kcal/hr

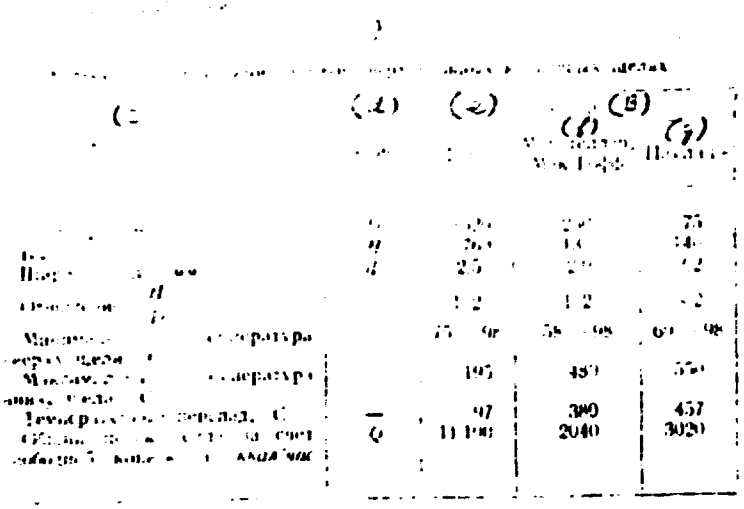

The results of these experiments can be represented by the following empirical formula:

(51)

where is the effective heat-transfer coefficient calculated for the total temperature difference, kcal/m^2 hr $^\circ$C;

is the diameter of the annular slot, m;

is the Grashof number calculated for the width of the slot (d).

When five horizontal baffles were installed at 25-mm intervals along the height of a 250-mm diameter annular slit, the total heat flow was found to be 25 times less than that for a slit without baffles.

Hanoman conducted measurements of heat transfer during natural convection in narrow vertical channels, using mercury, water, and oil as the working liquids.

In converting for sodium, his data can be represented by the formula:

(52)

where is the length of the heated section of the channel, m;

is the internal diameter of the channel, m.

These same data are shown in Fig. 72.

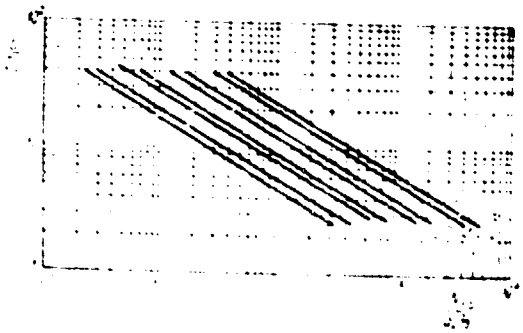

Fig. 72. Heat transfer in narrow vertical channels for natural convection of sodium.

Free convection in liquid-metal circuits. In cooling of atomic power plants, natural convection can be used together with forced convection; which type governs in a given process depends on the mode of operation. The average liquid flow velocity in circuits where natural and forced circulation exist is determined by solving simultaneously the hydraulic-pressure-balance equation and the heat-balance equation for the circulation loop. The way in which the heat-transfer coefficient depends on velocity will be determined by which type of motion (natural or forced) predominates.

Heat transfer for mixed motion of a liquid under the conditions of laminar flow in a short vertical tube at constant wall temperature was investigated theoretically by Martinelli and Boulter. As a result they obtained the following expression for the Nusselt number:

$$\mathrm{Nu}_D = 1.75 \left[\frac{\pi}{4} \mathrm{Re}_D \mathrm{Pr} \frac{D}{L} + 0.0572 \left(\mathrm{Re}_D \mathrm{Pr} \frac{D}{L} \right)^{3/2} \right]^{1/3}. \qquad (53)$$

where L is the length of the tube, m;

D is the diameter of the tube, m.

The "plus" sign in the radicand is selected when the natural and forced convections flow in the same direction; the "minus" sign when the directions of flow are opposed. Equation (53) is accurate if the velocity profile of the liquid is linear and if the intensity of heat transfer is determined mainly by the conditions of the process occurring near the tube walls. For liquid metals these assumptions are often inaccurate.

MacGoff and Maustellor studied heat transfer in the space between tubes of vertical single-and multitube heat exchangers not having interior baffles. An alloy of sodium and potassium (56% K) was used as the heat-transfer medium. Both forced and natural circulation of a liquid metal in the space between tubes were investigated. The corresponding experimental data are shown in Table 18.

TABLE 18

Cooling of Vertical Tube Banks in Heat Exchangers by a Sodium-potassium alloy

(A) Number of tubes

(B) Exterior diameter of tubes D, mm

(C) Length of tube l, mm

(D) Cross section of flow F, m^2

(E) Free convection

(F) Forced convection

(G)* Of 19 pipes, 2 were closed

TABLE 18

continued

Таблица 14

Оптимальные размеры [illegible] труб в теплообменниках сплавом натрий–калий

(2)	[illegible]			17*	7	19	1
	[illegible]			[illegible]	[illegible]	10	125
	[illegible]			95	11	95	722
	[illegible] F, м²			2.32 [illegible]	3.37 [illegible]	[illegible]	2.56 10
	Re_f	min		140	[illegible]	500	[illegible]
		max		7.4(0)	7.4 0	2(00)	20 (00)
		[illegible]		1.70(0)	2.25(0)	5 470	8 050
	Pe_f	min		5(00)	4 [illegible]	[illegible]	[illegible]
Вынужденная конвекция		max		12	21		
		min		34	68	20	170
	Nu_f	max		0.24	0.56	1.82	4.20
		min		0.62	1.30	1.40	7.10
	Re_f	max		2(00)	[illegible]	2 1(00)	15(00)
		min		2.7(0)	[illegible]	15(00)	120 (00)
	ε	max		3.5(0)	1.40(0)	11.25(0)	11 250
		min		16.1(0)	[illegible]	24.9(0)	15 700
	Pe_f	max		38	40	27	210
		min		3.20	16 [illegible]	[illegible]	1100
	Nu	max		[illegible]	[illegible]	1.20	6.50
		min		2.40	[illegible]	3.40	8.20

(2) [illegible] 0 мм [illegible]

Best Available Copy

Arrangement of tubes in the shells of the heat exchangers is shown schematically in Figure 73.

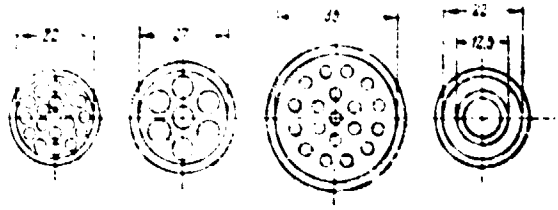

Fig. 73. Arrangement of tubes in the shells of heat exchangers investigated by MacGoff and Maustoller.

For multitube heat exchangers one general empirical formula was obtained for both free and forced convection

$$\left[\quad \right] \qquad (5A)$$

where D is the outside diameter of the tube;

F_1 is the cross-sectional area of the liquid-metal passage;

F_2 is the heat-exchange surface.

The experimental data on free convection for a single-tube heat exchanger do not conform to this function.

23. Heat Transfer during Forced Convection

By heat transfer under forced convection, we mean the exchange of heat between a solid surface and a pumped liquid in contact with it.

For a liquid flowing turbulently near any surface (for example, in a circular tube) the entire flow area can be arbitrarily divided into three parts:

Laminar sublayer, directly adjacent to the surface of the solid; in it the drag action of the wall shows up strongly; here the particles of the liquid move in an orderly manner and eddy currents are not formed spontaneously.

Turbulent nucleus core — the basic central area of the flow characterized by essentially disordered motion of liquid particles.

The intermediate or transition area located between the laminar sublayer and the turbulent nucleus.

The heat is transferred in a flow due both to the molecular heat conductivity of the liquid (λ) and to the turbulent mixing of volume (moles).

The intensity of the molecular heat transfer in a liquid can be characterized by its thermal diffusivity $a = \frac{\lambda}{c\rho}$. Analogously, the momentum transfer due to internal friction in a liquid is characterized by the kinematic viscosity $\nu = \frac{\mu}{\rho}$. The dimensionless ratio of these values is called the Prandtl number:

$$Pr = \frac{\nu}{a}$$

Conventional fluids (water and air) have Pr numbers of 0.7 through 200, while liquid metals are characterized by very low Pr values, ranging from 0.005 to 0.1 (Fig. 7a); this is associated with their high thermal conductivity (Fig. 7b). In contrast to nonmetallic liquids, where heat transfer in a flow is partially carried on by molecular transport, in liquid metals molecular exchange of heat can play a large role (even in the region of the turbulent core).

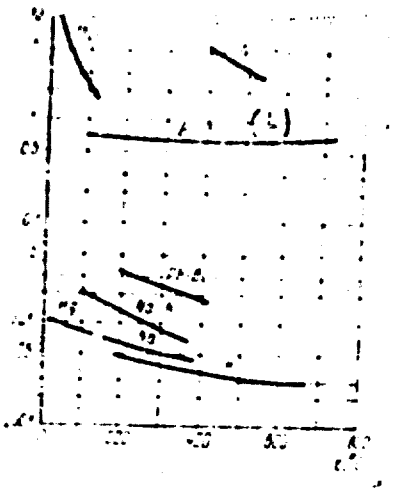

Fig. 74. Values of Pr numbers for various heat-transfer media.

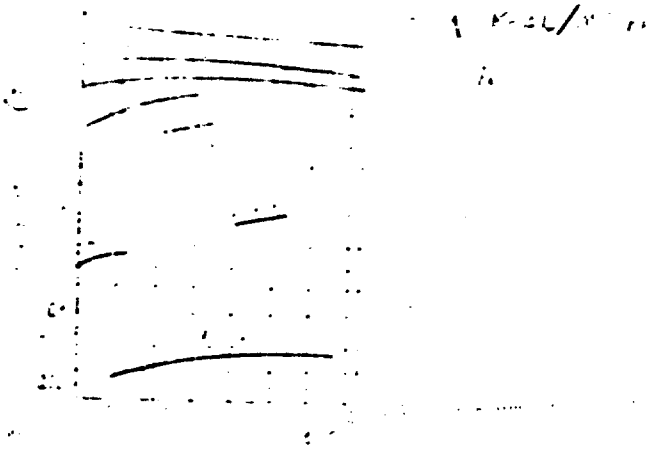

Fig. 75. Thermal conductivity of various heat-transfer media.

Best Available Copy

The role of the laminar sublayer in the total resistance to heat transfer in liquid metals is smaller than in conventional liquids, since in this case the sublayer is relatively thin (ν is small) and conducts heat well (λ is large). These concepts are illustrated in Fig. 76, where the distribution of temperatures in turbulent liquid flow is shown for various Pr numbers.

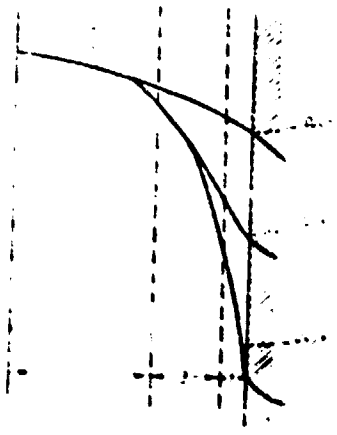

Fig. 76. Distribution of temperatures in turbulent flow of a liquid. (1) laminar sublayer; (2) turbulent core, (3) transition area.

In turbulent flow of liquid metals the ratio of the heat flow transferable by molecular heat conduction to the heat flow transferable due to turbulent mixing can be approximately evaluated in the following manner. At values of

$$\text{Pr} \ll 1,$$

where w is the velocity of the liquid;

l is a characteristic geometric quantity;

a is the thermal diffusivity of the liquid;

the mechanism of heat transfer by molecular heat conduction prevails. For Pe numbers on the order of 1,000 the role of the molecular and turbulence mechanisms of heat transfer is approximately the same, and only when Pe>50,000; i.e., at very high flow velocities in the core of the flow turbulent heat transfer prevails and the relative magnitude of the thermal resistance of the laminar sublayer strongly increases; this constitutes a large portion of the total resistance to heat transfer as it occurs for conventional liquids. Experimental data([47, 105]) completely confirm the specific character of the distribution of temperatures in the flow of a liquid metal.

From what has been said, it is clear that the formulas describing heat transfer in nonmetallic liquids cannot be used to calculate a heat-transfer coefficient in liquid metals.

Let us note one more peculiarity found during the study of heat transfer in liquid metals. Because in a number of cases the molten metals does not wet the heat-transfer surface, the contact of the liquid with the heated surface may not be completely satisfactory, which causes additional thermal resistance to heat transfer. Due to the poor liquid wall contact or because of the appearance on the layer separation surface of some impurities, oxides, etc., the thermal resistance can sharply diminish the heat-transfer coefficient α.

Turbulent flow of a liquid metal in a circular tube. The result of a theoretical solution of this problem, given a constant magnitude of heat flow along the tube wall [120] can be presented in the following form with a satisfactory degree of accuracy (Martinelli-Lyon formula):

$$\mathrm{Nu} = \ldots \quad (55)$$

where α is the heat-transfer coefficient, kcal/m^2·hr °C.

Seban and Shimazaki[148] solved the same problem for constant tube-wall temperature and obtained the equation

(56)

The accuracy of Equations (55) and (56) is confirmed by certain experiments conducted with sodium and a sodium-potassium alloy. Experimental data of Lyon, Werner, King, and Tidball on heat transfer to alkali metals are shown in Table 19 and Figs. 77 and 78.

TABLE 19

Conditions Under Which Certain Experiments on Heat Transfer to Sodium and to a Sodium-potassium Alloy Were Carried Out

Author	Type of experimental arrangement	Working liquid	Inside diameter of the tube	Wall material	Temperature range	Reynolds number range
Lyon	concentric tubes	52% Na—48% K alloy	11 and 18	nickel	105 to 125	15,000—90,000
Werner, King and Tidball	concentric tubes	56% Na—44% K alloy and 22% Na-78% K alloy	18	nickel	150 to 650	33,000—230,000 35,000—200,000

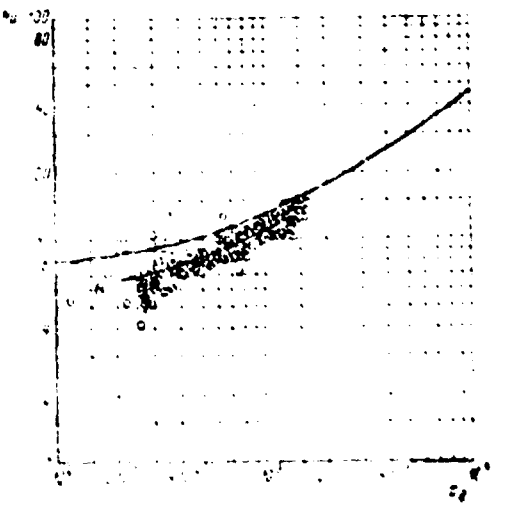

Fig. 77. Experimental data of Lyon on heat transfer for turbulent flow of Na–K (78% K) alloy in a circular tube. (1) Martinelli-Lyon solution.

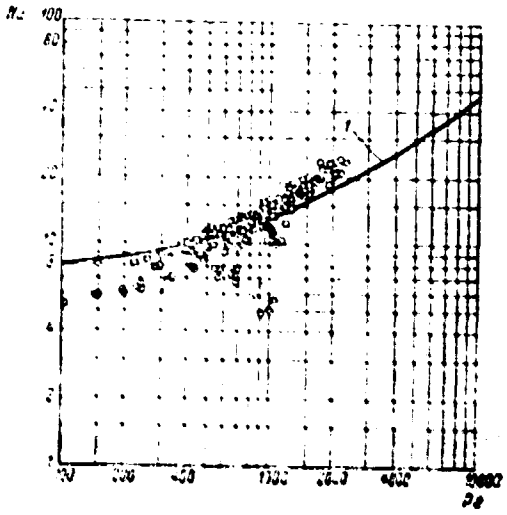

Fig. 78. Experimental data of Werner, King and Tidball on heat transfer for turbulent flow of Na–K alloy in a circular tube. (1) Martinelli-Lyon solution; ○ – alloy with 445 K; □ – alloy with 775 K.

Experimental data for other liquid metals (mercury, lead-bismuth alloy) deviate significantly from theory in that values of heat-transfer coefficients found experimentally are smaller, as a rule, than the theoretical coefficients. Let us examine the results of studies by certain authors.

Experiments on heat transfer to mercury [109] and to a eutectic bismuth-lead alloy [110] were conducted by Johnson, Hartnett, and Clabaugh. Under the conditions of turbulent liquid flow and for a constant heat flow along the tube wall, their heat-transfer coefficients were 25 to 35% lower than those calculated in accordance with the Martinelli-Lyon theory (Fig. 79). A diagram of the test set-up of Johnson et al is shown in Fig. 80. As these tests indicated, even a small amount of gas entrained by the liquid metal and circulating with it can strongly affect the intensity of heat transfer. In this case, the gas used was helium, sucked into the system from an expansion tank by a centrifugal pump (Fig. 80). The presence of the gas reduces the heat-transfer coefficient to the Pb—Bi alloy by approximately twice. After a baffle was installed in the lower section of the expansion tank so as to prevent formation of a funnel in the central section of the tank, capture of gas by the pump ceased. The heat-transfer coefficient to the alloy in the process section increased.

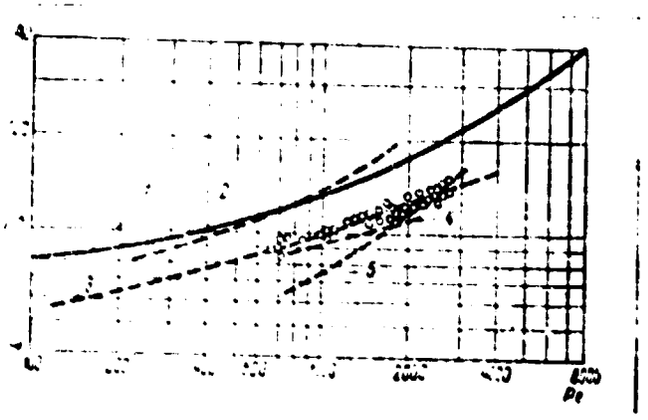

Fig. 79. Some experimental data on heat transfer to mercury and a Pb—Bi alloy for turbulent flow in tubes. (1) Martinelli-Lyon solution; (2) tests by Isakoff and Drew (mercury); (3) tests by Trefethen (mercury); (4) tests by Seban (eutectic Pb—Bi); (5) tests by Lubarsky (eutectic Pb—Bi); (6) tests by Johnson et al (eutectic Pb-Bi).

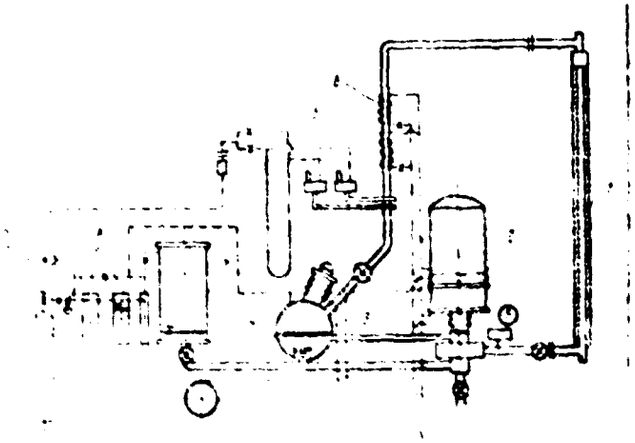

Fig. 80. Diagram of test setup of Johnson, Hartnett, and Clabaugh. (1) Process section; (2) pump; (3) tank; (4) baffle; (5) differential manometer; (6) cooler; (7) feeder tank; (8) gas purification; (9) manometer with a small separator.

Capture of gas by the pump is also undesirable because it increases the rate of oxidation of the liquid metal in the system. As was detected when the study in question was conducted, the accumulation of a noticeable amount of oxidizing metal (slag) in the tank was observed only before capture of the gas by the pump was eliminated.

Trefethen [114] conducted experiments on heat transfer to mercury. Stainless steel and copper were used as material for the tube; the copper surface was first washed with a mixture of solutions of hydrochloric acid (HCl) and mercurous chloride ($HgCl_2$), so that the surface was very wettable by the liquid metal. In the range of Peclet numbers of $100 < Pe < 2{,}000$ the intensity of heat transfer was the same on both surfaces and was 30% lower than the calculated Martinelli-Lyon curve.

A significant increase in the heat-transfer coefficient (by approximately twice) was detected in the experiments of Doody and Younger [67], who added small amounts of sodium (0.1% by weight, and less) to mercury. The authors attribute this phenomenon to an improvement of the wetting properties of the liquid metal, since in respect to mercury sodium is a surface-active element substantially reduces the surface tension of mercury. The experimental function $Nu = f(Pe)$, found by Doody and Younger in tests with added sodium, satisfactorily agrees with the data examined above (Johnson et al; Trefethen).

Data of Seban and Lubarsky on heat transfer to the eutectic alloy of bismuth and lead in general agree satisfactorily with Johnson's data in falling 30 to 50% below the calculated Martinelli-Lyon curve. Seban found that for an alloy flowing in tubes with a tin-coated interior the heat-transfer coefficient increases 25% in comparison with non-tin-coated tubes.

Translator's note: As the original text; according to the bibliography, Ref. 66 is meant.

A gradual decrease with time of the coefficient of heat transfer to mercury, α, was detected in the experiments of English and Barret [77]. The value of α for mercury flowing in a nickel tube is halved after operation of the apparatus for 35 hours, and in a tube of stainless steel, after 100 to 120 hours. This phenomenon can be explained by insufficient purity of the liquid metal, whose impurities gradually accumulated on the heat-transfer surface.

The contamination of the mercury was obviously enhanced by the lack of protection against atmospheric hydrogen.

A comparison of the results of the works mentioned is shown in Fig. 79.

In review article [119], Lubarsky and Kaufman offer the following empirical formula, which agrees with the data of the majority of foreign researchers on heat transfer during turbulent flow of liquid metals in tubes:

$$Nu = 0.625\,Pe^{0.4}. \qquad (57)$$

This formula is useful for calculating heat transfer beyond the region of thermal stabilization. For heat exchange within a stabilized region, see below. A result of experimental data used in arriving at Formula (57) is given in Fig. 81. The curve corresponding to the theoretical Martinelli-Lyon formula is also shown there. Practically all the data shown on the diagram were obtained through experiments with mercury and with the eutectic bismuth-lead alloy, in which constant heat flow conditions prevailed along the tube wall.

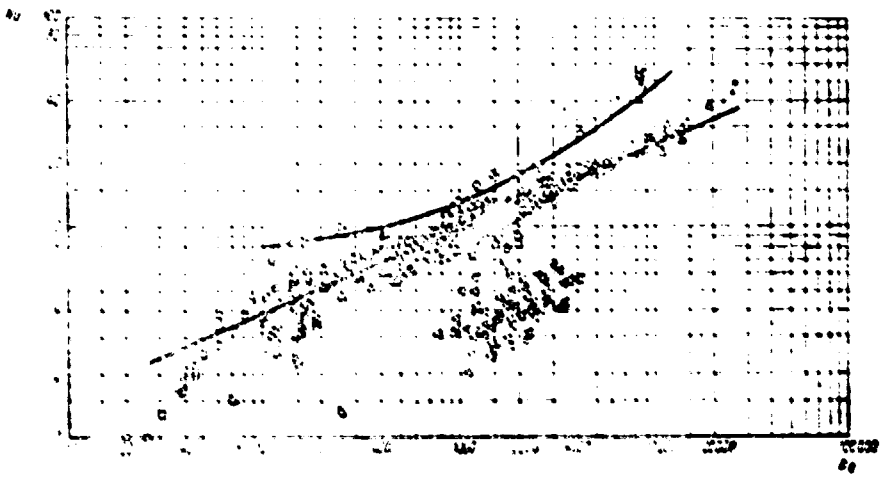

Fig. 61. Comparison of experimental data on heat transfer to liquid metals in tubes (constant heat flow along the tube wall).

Fig. 81. caption continued

(1) Martinelli-Lyon solution; (2) calculated by the formula $Nu = 0.625 \cdot Pe^{0.4}$; - Stromquist (mercury); , - Isakoff and Drew (mercury); ◇ - Johnson et al (mercury, eutectic Pb—Bi); - MacDonald and Quitention (sodium); - Elser (mercury); - Johnson et al (Hg, eutectic Pb—Bi, laminar flow); - Untermeyer (eutectic Pb—Bi); - Trefethen (mercury); - Seban (eutectic Pb—Bi); △ - English and Barret (mercury); - Untermeyer (eutectic Pb— Bi with added magnesium).

The various authors differ as to the effect on heat transfer of adding wetting agents* to mercury or a Pb—Bi alloy. In certain tests such a strong effect was found (Doody and Younger [66], mercury; Untermeyer, Pb—Bi alloy), and in other tests it was not detected at all (Johnson et al [109], mercury; Lubarsky, Pb—Bi alloy). Evidently this divergence is explained by a difference in the conditions of the tests conducted by various authors and primarily by the degree of purity of the liquid metal.

Turbulent flow of a liquid metal between two parallel planes heating from one side. For the condition of constant heat flow along a surface Seban [147] obtained the following theoretical formula

$$Nu = \frac{\alpha d_{eq}}{\lambda} = 5.8 + 0.021 Pe^{0.8}. \qquad (58)$$

* A steel surface can be wetted by mercury or a Pb—Bi alloy if a 0.1 to 0.2% of sodium or magnesium is added to the liquid metal.

where the Nu and Pe numbers are determined by the equivalent diameter of the channel which equals

$$d_{eq} = 2b$$

where b is the distance between the planes.

In Fig. 82 Seban's theoretical solution is compared with the experimental data of Sinis [19] for mercury flowing inside a channel of rectangular cross section with a high side ratio. Gradual formation of an oxide layer on the heat transfer surface was noticed by Sinis (carbon steel was used for the channel wall).

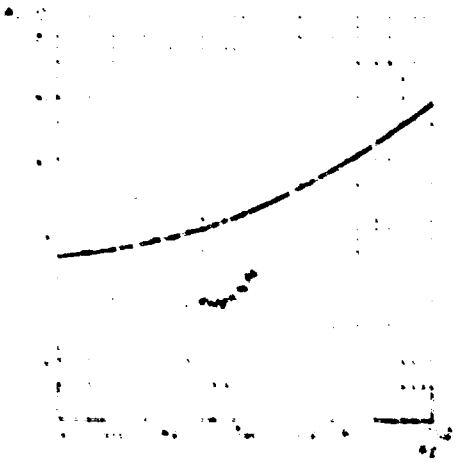

Fig. 82. Heat transfer to mercury flowing inside a slot channel.
(1) Seban solution.

Turbulent flow of a liquid metal between two parallel plates heating on both sides. A solution to the problem of the distribution of temperatures in a liquid flowing between plates was obtained by Seban [147], who found the form of the functions relating the Re and Pr numbers (Fig. 83) with the quantity $x = \frac{t_1 - t_2}{t_1 - t_0}$, where t_1 and t_2 are the temperatures corresponding to the first and second plates respectively, °C; t_0 is the average temperature of the liquid between the plates, °C.

Fig. 83. The distribution of temperatures in a liquid-metal flow between two parallel heated plates.

Let us assume that the coefficient of heat transfer from the wall to the liquid for single-sided heating equals α'. Then α' is determined by Formula (58). Since the values of x and α' are known, the values of the heat flows on each of the surfaces, q_1 and q_2, and also the values of the temperatures t_1, θ_1, θ_2, t_2 can be found by solving the following system of five algebraic equations:

$$\left.\begin{aligned} & \\ & \\ & \\ & \end{aligned}\right| \qquad (59)$$

Then the values of the heat-transfer coefficients for each of the plates equals:

$$\alpha_a = \alpha_b \frac{q_a}{q_b} \frac{t_a - t_m}{t_b - t_m}$$

Turbulent flow of a liquid metal across an annular slot. Let us denote by r_e and r_i the corresponding outside and inside radius of an annular space. If the ratio $\frac{r_e}{r_i}$ is approximately one, then the annular slot can be treated as a space between two parallel planes. In this case it is possible to use the formulas and methods for calculating heat exchange described above. However, when the ratio $\frac{r_e}{r_i} > 1.4$ a more accurate method of calculation is that proposed by Bailey. He obtained the formula:

$$Nu = Nu_3 \left(\frac{r_e}{r_i}\right)^{0.17} Pe^{0.30}, \qquad (60)$$

where

$$Nu_3 = \frac{1}{2}\left(\frac{1}{B} - 1\right)^2 \left[3 - 12B^2 - 4B^3 - 4(B+1)^2 \ln B\right]$$

$$B = \frac{r_e}{r_i}$$

The Nu and Pe numbers entering into Formula (60) are determined by the equivalent diameter which equals: $d_{eq} = 2(r_e - r_i)$.

Relation (60) can be represented in the following simplified form:

$$Nu = 0.75 \left(\frac{2r_e}{\lambda}\right)^{0.17} Pe^{0.30}. \qquad (61)$$

In this expression the coefficient of heat transfer, α_{TP}, is calculated from Formula (55) for a circular tube. Bailey's formula was confirmed for alkali metals by experiments of Werner, King, and Tidball, and of Lyon, Hall, and Jenkins [95].

The experimental data of Werner et al, and also of Lyon, are shown in Figs. 84 and 85.

Heat transfer from sodium to a sodium-potassium alloy was studied by Hall and Jenkins [95]. The test heat exchanger was so prepared that both the media exchanging heat flowed through the annular spaces between the tubes. It was discovered that even a small eccentricity of the heat exchanger tubes relative to one another produces a strong distortion of the temperature field in the liquid metal circulating in the annular space between the tubes; this in turn affects the intensity of heat exchange, particularly for high thermal stresses* at the heating surface (greater than $5 \cdot 10^5$ kcal/m^2 hr).

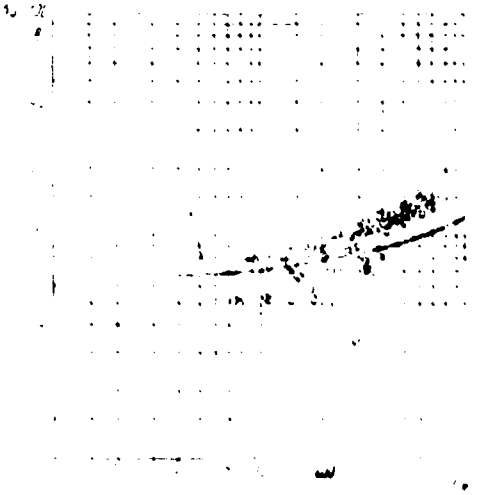

Fig. 84. Data of Werner, King, and Tidball on heat transfer to Na—K alloy flowing in an annular slot. (1) Bailey formula; ^ - 44% K alloy; □ - 78% K alloy.

* Translator's note. Russian original seems to use "thermal stresses" in error. The dimensions given suggest that "heat flux" was intended.

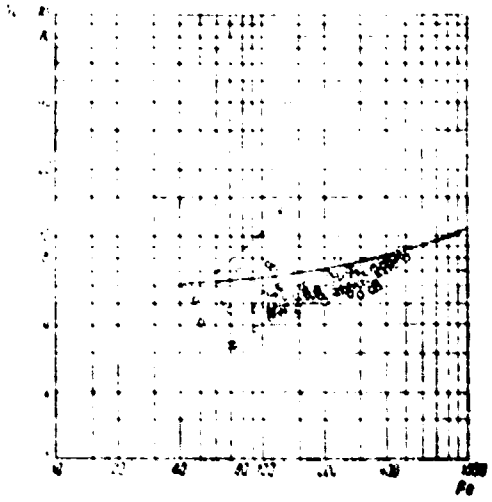

Fig. 85. Data of Lyon on heat transfer to Na—K alloy (42% K) flowing in an annular slot (1) Bailey formula.

These relations were confirmed by a theoretical analysis carried out by the authors.

Data on heat transfer to Na and Na— K in an annular space were obtained in tests by Hall and Jenkins, and are shown in Fig. 86. The transfer coefficient was determined through calculations based on measurements of the coefficient of heat transfer from the inside ring to the outside allowing for the thermal resistance of the tube wall*. The experimental points for the inside ring

---

* Carbon steel (for the Na test) and stainless steel (for the Na— K tests) were used for the tubes.

alone (inside radius r_i = 8.7 mm, outside radius r_o = 11.9 mm) are given in Fig. 86. As is clear from the graph, a satisfactory correspondence between Formula (61) and experiment was obtained, except for the area of small Peclet numbers (less than 100 to 150).

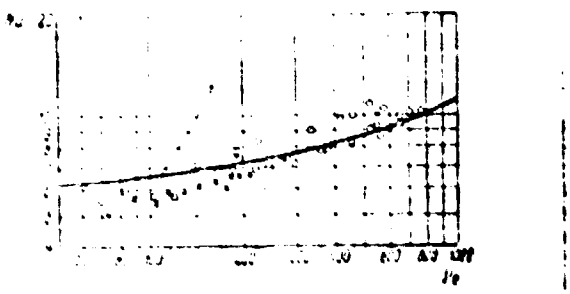

Fig. 86. Data of Hall and Jerkins on heat transfer for alkali metals flowing in annular slots. (1) Bailey formula: • - sodium-potassium alloy; x - sodium.

Turbulent flow of a liquid metal through noncircular channels. At present the methods developed for calculating heat transfer for a flow of liquid metals through noncircular channels are even less satisfactory, due to a number of difficulties originating in the course of theoretical and experimental investigations. In the first place, the hydrodynamics of turbulent flow in noncircular channels has not been adequately studied; secondly, the temperature and heat

flow along the perimeter of the channel is not constant and their distribution may be complex in character. For practical purposes it is most important to know the average heat-transfer coefficient for the entire channel, and also the maximum difference of temperature between the wall and the flowing liquid.

The problem of heat transfer to a liquid metal in noncircular channels was solved by Clayborn for a number of channel cross-section configurations (rectangle, triangle, and ellipse).

He made the following basic assumptions:

1. The distribution of the specific heat flow along the perimeter of the channel is uniform.

2. The velocity liquid flow at all points of the channel cross section is constant.

3. The heat is transferred only through molecular heat conduction. These assumptions are accurate for uniform supply (removal) of heat to (from) liquid metal moving turbulently in a channel at a comparatively small velocity (Pe 100).

Clayborn obtained the following values of Nu numbers and temperature differences (liquid-wall) for channels of various forms:

rectangle:

the maximum difference in temperature of the liquid and wall:

where q_l is the heat flow with respect to unit length of channel, kcal/m hr.

equilateral triangle:

a right isosceles triangle:

ε_{max} 0.2%.

The Nu numbers are determined by the equivalent diameter

$$d_e = \frac{4f}{\chi}$$

where f is the cross-sectional area of the channel;

χ is the perimeter of the channel.

The concept of the equivalent diameter can not always be applied with liquid metals. Actually, in a number of cases (flow in channels at comparatively small Re numbers, for example, when $Pe = 10^2$ to 10^3, or flow in closely spaced slots) where the zone of substantial temperature change near the wall is comparable with the channel width of the mechanism of heat transfer in the channel, in principle differs from the mechanism of heat exchange in a circular tube of equivalent diameter.

The intensity of heat exchange during the flow of a Na-K alloy in a rectangular channel of 12 X 1.5 mm cross section was determined by Tidball [162]. Investigations were conducted using a heat exchanger consisting of two rectangular channels separated by a thin (= 0.5 mm) wall of stainless steel.

The values of the heat-transfer coefficients, found from the coefficient of heat transmission, were close to the theoretical curve obtained for rectangular channels by Harrison and Meake [98]. The results of the experiments are shown in Fig. 87.

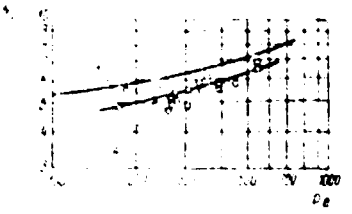

Fig. 87. Heat transfer for flow of Na—K alloy in a rectangular channel (1) Harrison and Menke formula; (2) experimental data of Tidball.

Heat transfer in the entrance section of a circular tube (turbulent flow). Formulas (55) and (57), given above, can be used to calculate heat transfer only for relatively long tubes, since the presence of a thermally stabilized section increases the heat-transfer coefficient in the entrance section of the tube.

According to the calculations of Deissler (Fig. 88) the average coefficient of heat transfer to liquid metal agrees with the heat-transfer coefficient beyond the thermally stabilized section for relative tube lengths of $l/d = 50$ or more. With short tubes it is necessary to calculate the heat-transfer coefficient with the entrance-section formulas.

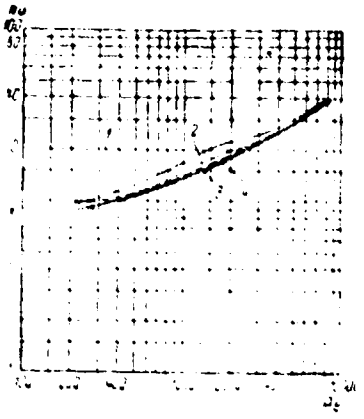

Fig. 88. Comparison of the average heat-transfer coefficient in tubes of various relative lengths with the heat-transfer coefficient beyond the thermally stabilized section (turbulent flow of a liquid metal).
(1) $\frac{l}{d} = 20$; (2) $\frac{l}{d} = 50$; (3) $\frac{l}{d} = 100$;
(4) $\frac{l}{d} = \infty$ (for a stabilized section).

Theoretical investigations of heat transfer during turbulent flow of a liquid metal in the entrance section of a tube were conducted by Deyssler, and also by Popendik and Palmer. Deyssler analyzed the case of constant heat flow along the heat-transfer surface by taking the steady-state velocity profile of the tube. Popendik and Palmer examined the case of constant tube-wall temperature and disregarded the turbulent thermal conductivity of the liquid, due to which their calculations are accurate only for the region of low Pe numbers.

The results of these studies for an entrance section with a relative length of $l/d = 4.6$ are shown in Fig. 89 as the dependence of the average value of the Nu number for the entrance section on the Pe number. The experimental data of

Johnson, Hartnett, and Clabaugh [119], obtained in tests using the same relative length with eutectic Pb—Bi, are shown in the same illustration. Tests with mercury were conducted by the indicated authors with similar results; Popendik and Harrison measured the heat-transfer coefficient for very short tubes (/d = 1 to 2), also using mercury.

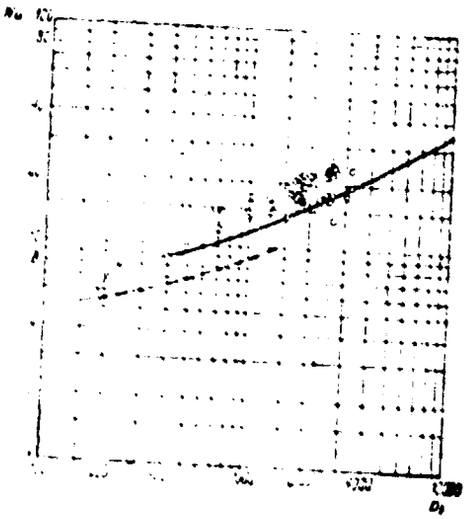

Fig. 89. Heat transfer in the entrance section of a circular tube during turbulent flow of a liquid metal. (1) Deissler solutions; (2) Popendik and Palmer solution; - experimental data of Johnson et al.

According to the data of Johnson et al, for a Pb—Bi alloy the length of the thermally stabilized section does not exceed thirty times the diameter of the tube (on the average, ~28d) and is independent of the Re and Pr numbers. This length is somewhat more than that obtained by Seban and Shimazaki [48] by theoretical means (l_T = 16d), assuming constant temperature at all points of the heat-transfer surface. A typical graph comparing experimental and theoretical values of the local coefficients of heat transfer in the entrance section of a tube is shown in Fig. 90. On the graph, the ratio of the tube length to its diameter is plotted along the abscissa and along the ordinate, the ratio of the local heat-transfer coefficient to the average value for the entire tube.

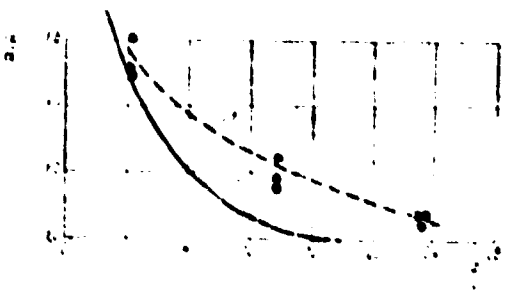

Fig. 90. Comparison of calculated and experimental values of the local heat-transfer coefficients for a liquid metal in the entrance section of a tube.
(1) Experimental data of Johnson et al;
(2) Seban and Shimazaki solution.

Laminar flow in tubes. For laminar-flow conditions, certain results of investigations of heat transfer in liquid nonmetals have been applied to liquid metals. For example, the coefficient of heat transfer to a liquid metal within the entrance section of a circular tube under conditions of constant heat flow along its length must equal $48/11 \cdot \lambda/d$, where d is the diameter of the tube.

Graetz gave a theoretical solution to the problem of heat transfer in the entrance section of a tube during laminar flow of an incompressible liquid; the wall temperature was assumed constant and the flow velocity profile to be piratolic. For result of the solution, see Fig. 91. The notations on the coordinate axes are interpreted in the following manner.

where q is the heat flux, kcal/m^2 hr;

F is the heat-transfer surface, m^2;

t_{ent} t_{ex} are the average temperatures of the liquid at the entrance and exit of the tube, respectively, °C;

L is the length of the tube, m;

G is the mass flow rate of the liquid, kg/hr.

There is still very little experimental data accumulated on heat transfer to liquid metals under laminar flow. The investigations on heat transfer to mercury and a Pb—Bi alloy conducted by Johnson, Hartnett, and Clabaugh [119] under laminar and transition conditions for a flow of metal indicated that in the area of low Pe numbers ($Pe < 100$) the intensity of heat transfer falls sharply (see Fig. 92).

Best Available Copy

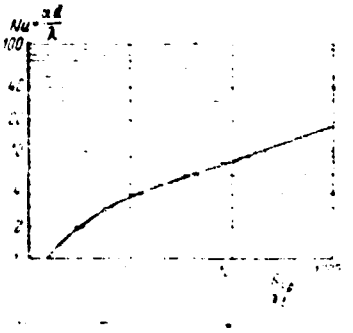

Fig. 91. Heat transfer during laminar flow of a liquid in the entrance section of a tube (t_w = const).

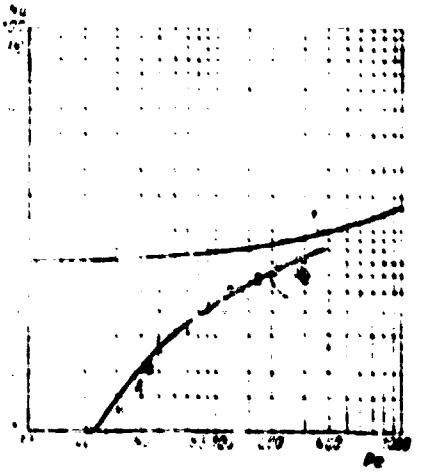

Fig. 92. Heat transfer to mercury and to eutectic Pb—Bi alloy during laminar flow of a liquid metal in a circular tube. (1) Martinelli-Lyon solution; (2) experimental data of Johnson et al; □ - mercury; ○ - eutectic Pb— Bi.

Heat transfer during flow of a liquid metal in the space between tubes (longitudinal flow past tube banks). Heat transfer in small heat exchangers using alkali metals has been studied by Tidball [162]. Investigations were conducted on a laboratory-type shell-and-tube heat exchanger which consisted of nineteen tubes with an outside diameter of about 3 mm inclosed in a cylindrical shell with an inside diameter of 22 mm; molten sodium flowed longitudinally past the tubes. A sodium-potassium eutectic alloy (78% K) was circulated inside the tubes. The flow around the tube cluster was not longitudinal, strictly speaking, because lateral baffles were installed inside the shell. By measuring the heat-transmission coefficient the average coefficient of heat transfer from the sodium between the tubes was computed by the author, while the coefficient of heat transfer from the alloy flowing inside the tubes was calculated with the Martinelli-Lyons [131] formula. The results of the experiments are shown in Fig. 93.

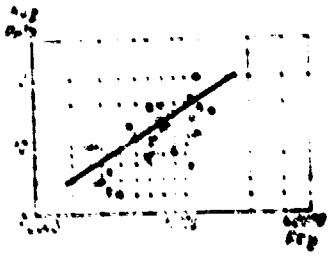

Fig. 93. Heat transfer in the space between tubes of small heat exchangers; sodium and Na—K alloy.

Brooks and Rosenblatt [47] studied heat transfer from sodium to a sodium-potassium alloy in a shell-and-tube heat exchanger. Inside the shell of the heat exchanger Na—K (56% K) alloy circulated, flowing logitudinally past a bank of 72 double tubes ("tube in a tube"). Sodium circulated in the inner tubes and the space between the outer and inner tubes was filled with a Na—K alloy. The tubes were made of nickel. Together with the heat exchangers, Brooks and Rosenblatt conducted measurements of the heat-transfer coefficient with a steam generator using a sodium-potassium alloy. In principle, the structure of the steam generator was analogous to that of the heat exchanger; the space between the outer and inner tubes was filled with mercury. Type 347 stainless steel was used for the tubes.

The heat-transfer coefficients in the space between tubes were computed by the authors from the heat-transfer coefficients in a heat exchanger and in the evaporator of a steam generator; only tests with a horizontal heat exchanger were considered, since in a vertical position the free convection of the liquid metal in the space between tubes began to effect the heat-transfer process.

The results of the experiments of Brooks and Rosenblatt (Fig. 94) are described by the following functions:

$$\text{Nu} = 0.34\,\text{Pe}^{0.6}\left(\frac{F_1}{F_2}\right)^{0.2},$$

where the Nu and Pe numbers were calculated using the outside diameter of the tube bank;

F_1 is the cross-sectional area for passage of the liquid, m^2;

F_2 is the heat-transfer surface, m^2.

Because the relative spacing of tubes in the evaporator bank was substantially larger than for the heat exchanger, the ratio F_1/F_2 fluctuated within broad limits in the tests of Brooks and Rosenblatt.

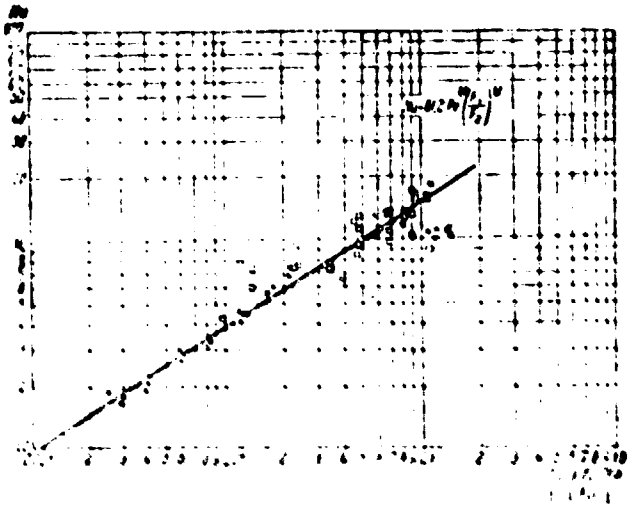

Fig. 94. Results of Brooks' and Rosenblatt's experiments on heat transfer in the space between tubes of a heat exchanger and a water evaporator using alkali metals. . = evaporator with forced circulation; ⁻ = evaporator with natural circulation; X = heat exchanger.

Heat transfer during transverse flow past tube banks. Moe, Dropkin, and Dwyer [101] conducted tests on heat transfer for a transverse flow of mercury past a staggered tube bank. They studied the effect on heat transfer of the following factors: velocity of the flow of metal, the relative positions of the tubes in the bank and the material of the tube surfaces.

The relative separation with respect to the width of the bank was $S_1/d = 1.38$ and with respect to its depth, i.e., in the direction of the flow of metal, was $S_2/d = 1.19$. Copper served as the material for the tubes; their outer surfaces were chrome plated. Several tests were conducted on tubes which had not been

chrome plated; this permitted the mercury to form an amalgam with the surface of the tube and wet it well. In tests with a chrome-plated surface it was found that for tubes located in the interior of the bank (beginning with the third row), the dependence of the heat-transfer coefficient on the flow velocity of the metal can be represented by the expression:

$$\alpha = [illegible]\, v_{max}^{[illegible]}.$$

where α is the average heat-transfer coefficient over the circumference of the tube kcal/m^2 hr $^\circ$C;

v_{MAX} is the velocity of the liquid-metal flow in space between the tubes computed for the narrowest section of the bank, m/sec;

d is the outside diameter of the tubes in the bank, m;

ν is the kinematic viscosity of the liquid metal, m^2/sec.

The authors obtained the following function for the heat-transfer coefficient on a copper heated surface:

$$\alpha = 10.8\, v_{max}^{0.[illegible]}.$$

A comparison of the experimental data for both surfaces is given in Fig. 95.

Heat transfer from the tubes in the first row of the bank is shown in Fig. 96. As is clear when Figs. 95 and 96 are compared, a noticeable reduction in heat transfer for the first row of the bank in comparison with the third and others was observed only for tubes with a chrome-plated surface.

MacGoff and Maustellor studied heat transfer to a Na—K (56% K) alloy as it flows transversely past staggered and in-line tube banks. A Na—K alloy also circulated inside the tubes, and the heat-transfer coefficient in the space between tubes was determined by calculating the heat-transmission coefficient. The diameter of the tubes was 12.5 mm; in the in-line bank they were arranged

with relative spacings of $S_1/d = 1.24$ (with respect to the width of the bank) and $S_2/d = 1.08$ (with respect to the depth of the bank); in the staggered bank, the spacing was $S/d = 1.21$, and was the same for both the width and depth of the bank. In the Reynolds-number range $300 < Re < 70{,}000$ the authors obtained a heat-transfer coefficient for rows of tubes located in the interior of the bank which can be represented by the equations:

for a staggered bank

(65)

for in-line bank

(66)

The same notations are used in Formulas (65) and (66) as in Formulas (63) and (64).

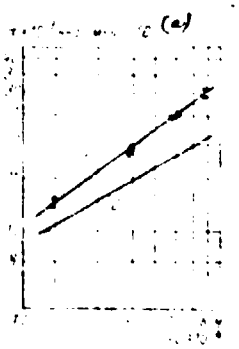

Fig. 95. Heat transfer from tubes of a staggered bank, immersed in a transverse flow of mercury (for rows of tubes located in the interior of the bank). (1) Copper tube surface, (2) chromeplated tube surface.
(α) $\times 10^{-3}$, kcal/m^2 hr °C.

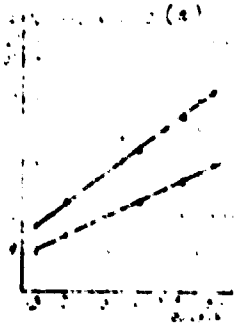

Fig. 96. Heat transfer from tubes of the first row of a staggered bank, immersed in a transverse flow of mercury. (1) Copper tube surface; (2) chromeplated tube surface.
(α) $\times 10^{-3}$, kcal/m^2 hr °C.

24. Heat Transfer during Boiling and Condensation

Heat transfer for boiling liquid metals. The amount of experimental data in the literature on heat transfer from boiling liquid metals is meager.

The experimental data of Farmer and Lyon on the boiling of sodium, a sodium-potassium alloy, cadmium, and mercury (pure and containing added wetting agents) are shown in Table 20. This data is also graphically shown in Figs. 97 through 99, and in Fig. 100 a comparison of the heat-transfer coefficients of various boiling liquids is given.

TABLE 20

Experimental Data on Heat Transfer from Boiling Liquid Metals

(A) Liquid	(B) Temperature t, °C	(C) Material of the heated surface	(D) Temperature drop t, °C	(E) Range of heat fluxes q, kcal/m² hr
(F) Mercury		(K) Cadmium		
(G) Mercury containing 0.1% sodium		(L) Copper		
(H) Mercury containing 0.02% magnesium and traces of titanium		(M) Chrome		
		(N) Type 316 stainless steel		
(I) Sodium-potassium alloy (56 to 59% K)				
(J) Sodium				

NYL-554

TABLE 20 continued

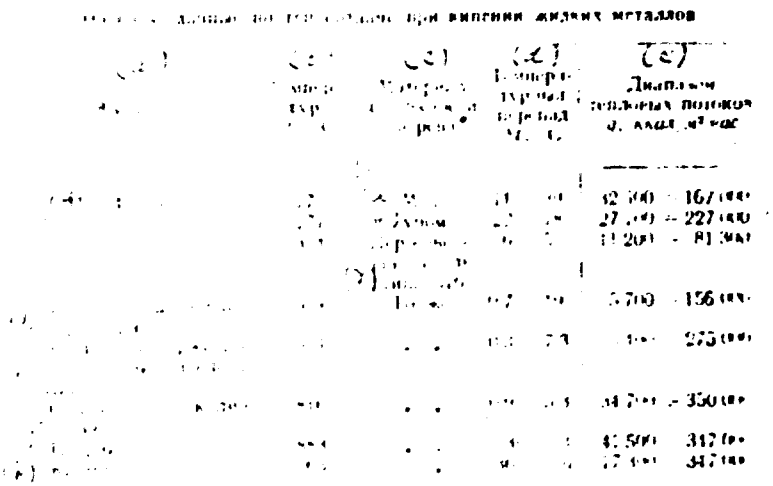

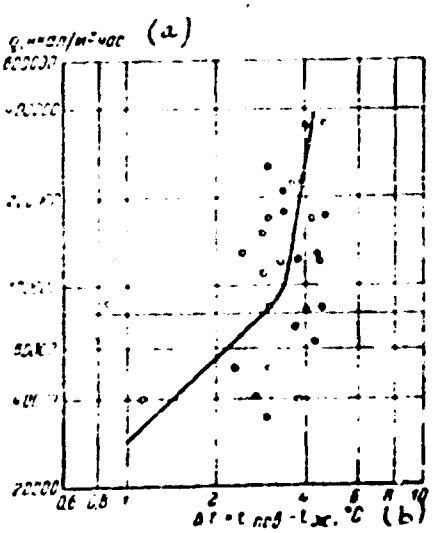

Fig. 97. Heat transfer from boiling sodium and boiling sodium-potassium alloy (56 to 59% K). ● - Sodium ○ - Na—K alloy. (a) q, kcal/m^2 hr; (b) temperature drop equals the temperature of the surface minus the temperature of the liquid °C.

MCL-554

Best Available Copy

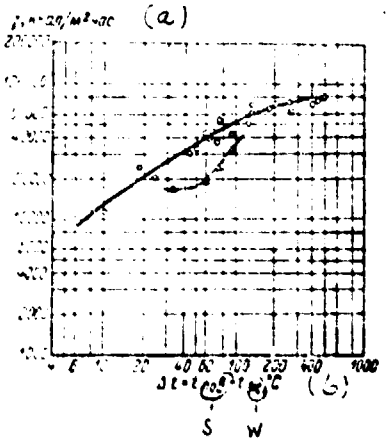

Fig. 98. Heat transfer from boiling mercury and cadmium.

○ = Mercury; △ = cadmium.

(a) q, kcal/m^2 hr; (b) temperature drop equals the temperature of the surface minus the temperature of the liquid, °C.

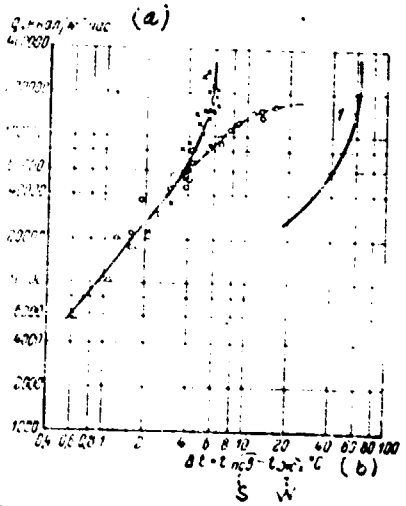

Fig. 93. Heat transfer from boiling mercury containing additives of Na, Mg, Ti. (1) Farmer solution; ○ = 0.1% Na; ✕ = 0.02% Mg and 0.0001% Ti. (a) q, kcal/m^2 hr; (b) temperature drop equals the temperature of the surface minus the temperature of the liquid °C.

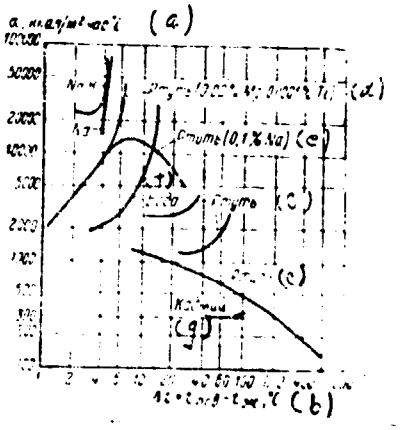

Fig. 100. Heat transfer from various boiling liquids. (a) α, Kcal/m^2 hr °C; (b) temperature drop equals the temperature of the surface minus the temperature of the liquid, °C; (c) mercury (d) mercury (0.02% Mg and 0.001% Ti); (e) mercury (0.1% Na); (f) water; (g) cadmium.

An examination of the table and graphs clearly shows that sodium, sodium-potassium, and mercury containing dissolved additives yield the maximum intensity of boiling heat transfer; here the temperature drops between the liquid and wall do not exceed 11° C. On the curve corresponding to heat transfer to mercury which contains 0.1% sodium, a maximum is observed indicating the beginning of film boiling, as vapor bubbles, forming on the heating surface, unite into one continuous film and the intensity of heat transfer falls sharply.

An important factor affecting the process of heat transfer from boiling liquid metals is the wetting of the heating surface by the boiling liquid. If the liquid metal does not wet the heating surface, then film boiling can become the

only type of boiling possible; this was observed, for example, with boiling mercury and cadmium on a stainless-steel heating surface. When 0.1% sodium, or 0.2% magnesium and 0.0001% titanium is added to mercury; the heat-transfer coefficient during boiling increases by approximately ten times, whereas the effect of adding sodium and magnesium (with traces of titanium) on heat-transfer varies.

With boiling mercury and a copper heating surface (as is known, copper and mercury form an amalgam) a heat-transfer coefficient twice as large as that for boiling at a chrome-plated surface is obtained.

With film boiling of liquid metals the heat-transfer coefficient can be even lower than the heat-transfer coefficient for free convection without boiling. As Farmer found,* in cooling the identical surface with boiling and nonboiling mercury, ~ 240 kcal/m^2. hr $^\circ$C was obtained for the first case, and ~ 2400 kcal/m^2. hr $^\circ$C for the second. The heat-transfer coefficient for film boiling of a liquid metal is usually so low that the use of liquid metal heat-transfer media under there conditions has no comparative advantage, for example, over water (see Fig. 100). Therefore it is necessary to secure good wetting of the heating surface by a liquid metal.

The data given above was obtained after prolonged tests; it is impossible to confirm that in the process of prolonged operation of heat exchangers the intensity of heat transfer during boiling will remain unchanged.

Heat transfer for condensing liquid-metal vapors. Nusselt's well-known theoretical solution pertaining to the case of laminar flow of a condensate film forming on a vertical plate yields the following expression for the average heat-transfer coefficient over the surface:

---

* Confirming the experimental results of the Central Scientific Research Institute for Boilers and Turbines obtained in 1937 through 1939 — editor's note.

$$\bar{\alpha} = 1.47 \left(\frac{\lambda^3 \rho^2 g}{\mu^2}\right)^{\frac{1}{3}} \left(\frac{4G}{\mu}\right)^{-\frac{1}{3}} = 0.943 \left(\frac{\lambda^3 \rho^2 g r}{\mu L \Delta t}\right)^{\frac{1}{4}}. \qquad (67)$$

Where G is the condensate mass flow rate per unit width of film, kg/m·hr;

r is the latent heat of vaporization (condensation), kcal/kg;

L is the length of the plate, m;

Δt is the difference in temperatures of the wall and the condensing vapor, °C.

This function is also shown in Fig. 101, using as coordinates the values

$$\left(\frac{\mu^3}{\lambda^3 \rho^2 g}\right)^{\frac{1}{3}} \quad \text{and} \quad \left(\frac{4G}{\mu}\right).$$

The theoretical formula for condensation of vapor for a single horizontal tube (or for several horizontal tubes in a vertical bank) takes the following form:

$$\alpha = 0.725 \left(\frac{\lambda^3 \rho^2 g r}{\mu \sum D \Delta t}\right)^{\frac{1}{4}}, \qquad (68)$$

where $\sum D$ is the sum of the diameters of all the tubes forming the condensation surface.

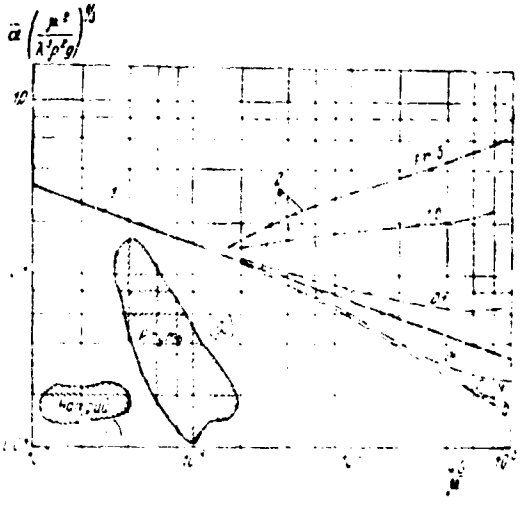

Fig. 101. Heat transfer for condensation of the vapors of some liquid metals. (1) Nusselt solution; (2) Seban solution. (a) mercury; (b) sodium.

It is to be expected that Formulas (67) and (68) are useful for calculating heat transfer during the condensation of liquid metals, since the value of the Prandlt number does not affect the results of the theoretical solution for laminar flow of a condensate film.

An analytic investigation was conducted by Seban for heat transfer during condensation with a Prandtl number varying from 0 to 5 for turbulent film flow (Fig. 101). It was found that in this case the Nusselt number for liquid metals ($Pr = 10^{-2} - 10^{-3}$) can be smaller than the Nusselt number given by the theory

of the laminar flow. Experimental data on condensation of mercury vapors are also shown on Fig. 101. As is clear from the figure, the observed heat transfer coefficient is significantly less than the calculated one. This difference can be explained by the presence of additional thermal resistance on the separation surface between condensate and wall.

Experimental data on heat transfer during condensation of sodium vapors are given in Table 21 and in Fig. 101. These data refer to condensation on the outer surface of a tube consisting of a number of sections and made of stainless steel and nickel (by sections). The tube was placed at a 45° angle to the horizontal; its length was 130 mm and diameter 30 mm. Although it was to be expected that the heat-transfer coefficient for the inclined surface would be less than the theoretical value found for a vertical surface, the difference between theory and experiment was extremely great.

TABLE 21

Heat Transfer for Condensing Sodium Vapors

(A) Temperature °C	(B) Heat flux kcal/m² hr	(C) Temperature difference	(D) Heat-transfer coefficient, kcal/m² hr °C	(E) $Re = \frac{4G}{\mu}$	(F) Heat-transfer coefficient according to Nusselt, kcal/m² hr °C

Таблица 21

Теплоотдача при конденсации паров натрия

(А) Температура пара, °С	(Б) Тепловой поток, ккал/м²час	(В) Температурный напор, °С	(Г) Коэффициент теплоотдачи, ккал/м²час°С	(Д) Re $\frac{4G}{\mu}$	(Е) Коэффициент теплоотдачи по Нуссельту, ккал/м²час°С
640	150 (144)	2.7	556 (88)	140	826 (132)
725	192 (184)	3.3	58 (88)	200	713 (114)
870	260 (249)	4.1	63 (101)	325	616 (98)

For rough calculations it is possible to assume that the values of heat-transfer coefficients for condensing liquid-metal vapors will equal 8 to 10% of the theoretical values.

CORROSION PROPERTIES OF STRUCTURAL MATERIALS IN LIQUID METALS

(KORROZIONNYYE SVOYSTVA

KONSTRUKTSIONNYKH MATERIALOV V ZHIDKOMETALLICHESKIKH SREDAKH)

Chapter IV

By studying the reaction of a liquid metal and the solid surface of some structural material (also a metal as a rule), it can be established that the intersolubility of the metals and the formation of intermetallic compounds play a major role in this process. A definite role is played by the formation of chemical compounds of the oxide type in a system and the penetration of liquid between the grains of the solid metal. By analyzing the equilibrium conditions for the chemical reactions accompanying the reaction of a metal with a surface washed by it, it is possible to ascertain the direction of the process but not its rate, which must be determined by experimental means.

When the intersolubility of the liquid metal and the wall material within the working temperature range is very low, then, as shown experimentally, it has little effect on the corrosion resistance of the material.

The formation of intermetallic compounds is undesirable; in certain cases,

however, a film of the compound protects the surface of the material from the aggressive action of the medium.

A temperature differential in the system affects the solubility characteristics. It often happens that solubility is very low under isothermal conditions, since solubility is accelerated by the transfer of solutes from a hot region of the system to a cold region, where these solutes separate out of the solution. They settle on the surfaces of tubes and can sometimes clog them. The effect of anisothermal conditions on the corrosion rate differs for different materials. For example, the rate at which iron dissolves in mercury depends strongly on the difference in the temperatures of the hot and cold regions, while the rate at which iron dissolves in sodium depends only slightly on the temperature difference. Certain impurities in a liquid metal, oxygen for example, accelerate the rate of dissolving.

Any component of the material may be transferred from one part of a system to another, even when no temperature gradient exists. In the first place, such transfer can result from the use of dissimilar metals in different parts of the system. Actually, let us assume that part of the system is made of metal A and part of metal B, and that the metals A and B are able to form a chemical compound or a solid solution. If metal A dissolves in the liquid (even if only in very small amounts), it will be transferred by the liquid to the surface of metal B and react with the latter. In theory, such a transfer can continue indefinitely; in practice, however, it will gradually decelerate, since the layers of the solid solution (compound) prevent metal A from reaching the surface of metal B. In the second place, certain elements are transferred when there is a difference in electric potential between the liquid metal and the wall. Some authors recommend using this effect, called electrolytic diffusion, to reduce corrosion in a liquid-metal medium.

The formation of chemical compounds on the surface of structural materials is chiefly due to the presence of impurities in the liquid metal. For example, admixed oxygen causes a film of a material's own oxide to form on the surface, provided that this oxide is chemically more stable than the oxide of the liquid metal. By comparing the free energy of reaction for oxidation of metals, it can be established which particular oxide will most probably form.[1] The oxide film on the surface of a material can have a positive or negative effect on increasing corrosion resistance, depending on whether it is dense and stable or porous and unstable.

Sometimes the corrosive effect of a liquid metal is diminished by an admixture of special substances - inhibitors. Introducing, for example, titanium or zirconium into mercury can eliminate corrosion of the steel in a mercury installation. The mechanism by which inhibitors function is unclear. Nevertheless, it is known that where the presence of oxygen in the system increases corrosion, the effect of the inhibitors is based on binding the oxygen into oxides which are insoluble in the liquid metal[2].

The role of penetration of liquid between grains of the solid material in the overall process of corrosion depends on the composition of the material and the condition of its surface (i.e., its treatment), on the distribution of internal

---

[1] The greater the free energy of formation of the chemical compound, the greater the probability of a formation reaction.

[2] A hypothesis of the mechanism of the action of inhibitors in mercury has been set forth by academician N. T. Chalkov (N. T. Chalkov and M. N. Zavas: Effect of a Mercury Heat-transfer Medium on Steel in Power Plants, Izd. AN SSSR, 1956). Editor's note.

stresses in the surface layer, etc. A typical example of intergranular penetration is the interaction of mercury and a brass surface.

At high liquid-metal flow rates, especially with the heavy metals where the flow has considerable kinetic energy, erosion of structural materials becomes noticeable. As yet very little experimental data has been accumulated on this question. According to American data the maximum permissible liquid-metal velocities are taken to be ~3 m/sec (for bismuth, lead, and mercury) and ~8 m/sec (for sodium and Na-K alloy).

Laboratory tests of the stability of materials in liquid-metal media are usually conducted under conditions similar to actual conditions. The liquid container is made either of the specimen material or a material which does not interact with the liquid. The surface of the liquid metal is protected from oxidation by a cushion of inert gas. Translation of the specimen relative to the molten metal is achieved by free convection of the liquid, rotation of the specimen or specimen holder, or forced motion of the liquid. Tests of surface erosion of the material under cavitation are conducted at lowered pressures. In all cases the degree of wettability of the surface of the specimen by the liquid metal is checked.

Table 13 contains a summary of the information on the corrosion resistance of structural materials in liquid metals at three temperatures: 300, 600, and 800°C.

In compiling the table of corrosion resistance, the following values of the rate of corrosion were used, to correspond to "good," "limited," and "poor" stability of a material in a medium.

Such relatively strict requirements for corrosion resistance are set because the walls of liquid-metal heat exchangers are made, as a rule, rather thin so as to obtain the largest possible heat-transfer coefficients.

Stability	Rate of corrosion, mm/year
Good	Less than 1
Limited	From 1 to 10
Poor	Above 10

More detailed information on the corrosion resistance of various materials in liquid-metal media is given below.

25. Sodium, Potassium, and their Alloys

(Table 23)

Metallic materials. Information on the stability of certain materials in alkali metals has been accumulated over the many years in which the alkali metals have been produced and used. However, this information pertained to the low-temperature range, as a rule only slightly exceeding the melting point of the metal. Under these conditions, it was found for example that normal mild steel does not suffer under the aggressive effect of molten sodium, even under very prolonged action (10-15 years). In the course of continuous service of sodium-cooled aviation internal-combustion motor valves, relatively little corrosion of heat-resistant alloys (13 to 15% Cr, 13 to 15% Ni, 1.75 to 3% W) was noted for an alkali metal medium at t 500-550°C. Until liquid metals became widely used as heat-transfer media, high working temperatures were encountered only during the production of Na-K alloys by distilling a sodium and potassium chloride compound. In this case, the alkali metals were in contact with types 304 or 316 stainless steel at 900°C and gradual carburization of the steel surface was observed.

Recent extensive investigations showed that there are many structural

materials suitable for use in an alkali metal medium (see Table 23).

The corrosive effect of sodium, potassium, and their alloys on materials is minimal as compared to other liquid-metal heat-transfer media (Li, Ga, Hg, Sn, Pb, Bi). However, it increases sharply with an oxygen content greater than 0.01-0.02% in the liquid metal, and when there are considerable temperature differences in the system.

Laboratory investigations into the stability of various materials in liquid sodium* have been conducted by many scientists with broad variations in the following variables: temperature (up to 900°C); duration of experiments (up to 5,000 hours); number of admixtures in the metal; the size and shape of the test specimens; the temperature difference between individual portions of the system; metal flow velocity; and composition of the test material. In certain instances, substances intended to prevent liquid-metal oxidation by chemically binding oxygen (beryllium and calcium) were specially added to the flow. Unfortunately, the investigations were conducted, as a rule, without sufficiently accurate determination of the oxygen content of the sodium, which is attributable to the difficulty of sampling the liquid metal and the methods of analysis themselves (see Chapter VII).

The surface of carbon steel, as a rule, is decarburized by the action of the alkali metals. This occurrence was noted by all the investigators who performed metallographic analysis of the surface layer of specimens after the tests. The intensity of decarburization of low-alloy steels depends on the amount of oxygen in the sodium, the temperature, and the chromium content of the steel.

---

* All information given below for sodium pertains to potassium and Na-K alloys as well, excepting instances where specific reference is made.

MCL-554

TABLE 22

Corrosive Resistance of Structural Materials in Liquid-metal Media

| Liquid metal | > | | |

TABLE 22 (cont')

Corrosive Resistance of Structural Mater_ s in Liquid-metal Media

Nonferrous metals

(o) Nickel and nickel alloys (with Fe, Cr, & Mo)

(p) Nickel alloys (with copper)

(q) Platinum, gold, silver

(r) Titanium

(s) Zirconium

Nonmetals

(t) Aluminum oxide (dense)

(u) Graphite (dense)

(v) Beryllium oxide (dense)

(w) Magnesium oxide (crucible)

(x) Porcelain & other silicates

(y) Pyrex glass

(z) Titanium oxide & zirconium oxide

(aa) Fused quartz glass

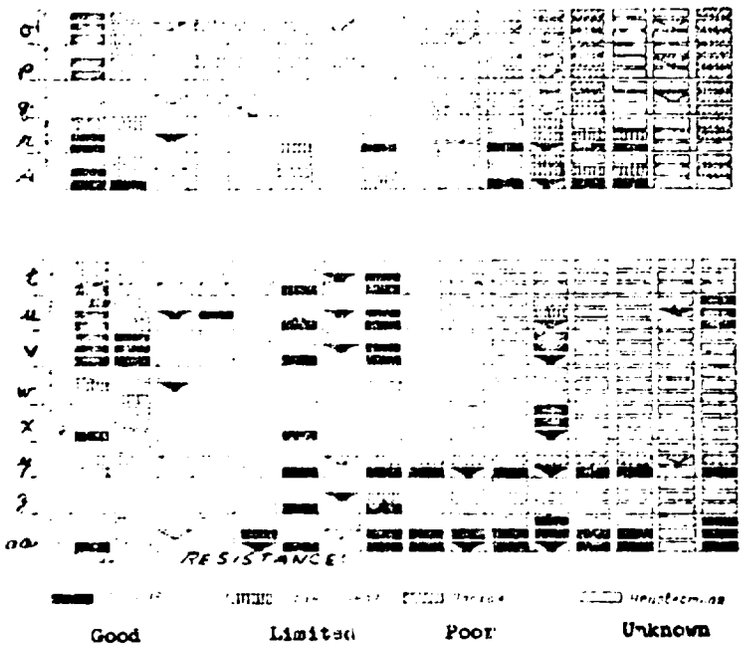

(1) Heat-transfer medium solidifies at a temperature above 300, 600, or 800°C, respectively.

(2) Poor resistance of graphite to action of K and good resistance to action of Na.

(3) Good resistance of W and poor resistance of Mo, Nb, and Ta to action of Ga.

(4) Limited resistance of Inconel to action of Pb.

TABLE 23

Stability of Structural Materials in a Medium of

Sodium, Potassium, or Their Alloys

Ferrous metals

1. Armco iron
2. Carbon steel
3. Gray cast iron
4. SAE 52100 (1.45% Cr, 1.0% C)
5. Sichromo 3S (3% Cr, 0.5% Mo, 1.5% Si)
6. Steel 2-9% Cr, 0.5-1% Mo
7. Stainless steels 18-8
8. Stainless steel 310 (25% Cr, 20% Ni)
9. Ferritic stainless steels (27% Cr)
10. Norbhite (26% Cr, Si, Mo, Cu)
11. High-speed steel (18% W, 4% Cr, 1% V)
12. Invar (36% Ni)
13. Fernico (28% Ni, 18% Co)
14. Alnico 5 (Ni, Co, Al, Cu)
15. Hadfield's manganese steel
16. Nitralloy G (nitrided)
17. Brazing alloy (80% Fe - 20% P)

Nickel and nickel alloys

19. Nickel
20. Inconel (13% Cr, 6.5% Fe)
21. Nichrome (15% Cr, 25% Fe)
22. Monel (30% Cu)
23. Hastelloy A, B, C
24. Brazing alloys Ni-Mn, Ni-Mo, Ni-P

Temperature, °C

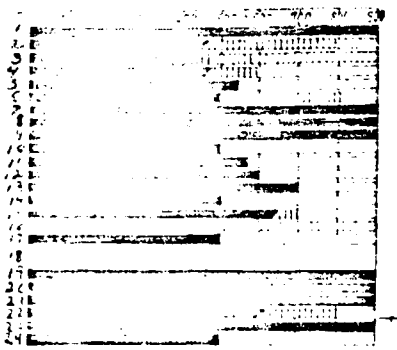

MCL-554.

TABLE 23 (cont')

Stability of Structural Materials in a Medium of

Sodium, Potassium, or Their Alloys

25. Copper and Copper Alloys

26. Copper (oxygen-free & deoxidized P)

27. Copper (electrolytic)

28. Copper with Be (2% Be)

29. Aluminum bronze (5-8% Al)

30. Cupronickel & supernickel (20 or 30% Ni)

31. Brass (40% Zn)

32. Nickel silver (17% Zn, 18% Ni)

33. Refractory metals

34. Niobium

35. Molybdenum

36. Tantalum

37. Titanium

38. Tungsten

39. Vanadium

40. Zirconium

41. Chromium

42. Other metals

43. Cobalt and high-cobalt alloys

44. Aluminum 2S and 3S

45. Aluminum 24S and 52S

46. Al-Si (Eutectic 12% Si)

47. Beryllium

48. Sb, Bi, Cd, Ca, Au, Pb, Se, Ag, S, Sn

Temperature, °C

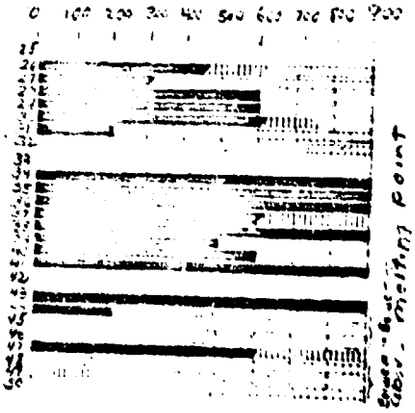

MCL-554

TABLE 23 (cont')

Stability of Structural Materials in a Medium of

Sodium, Potassium, or Their Alloys

Other Metals

49. Magnesium

50. Pt and Si

51. Nonmetals (refractoriness depends on purity, density, and external conditions)

52. Al_2O_3 (sapphire or alundum)

53. BeO (very dense)

54. MgO

55. Quartz

56. Darkoid

57. Asbestos

58. Silicone Rubbers

59. Teflon

60. High-density grapuite

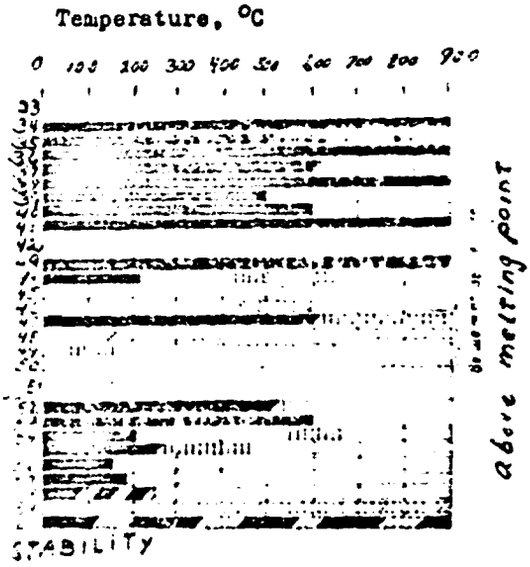

a) Good (suitable for long-term use)

b) Limited (for short-term use only)

c) Poor (unsuitable for use as structural material)

d) Unknown (insufficient data)

When alloyed austenitic steels are present in the same sodium circuit, the decarburization rate increases, resulting, apparently, from the intensive absorption of the transported carbon by certain alloying additives (chromium, niobium, tantalum), capable of forming carbides. The intensity of decarburization is minimal in steels of the ferrite class, alloyed with chromium. A 1-2% chromium content in steel, evidently, is sufficient to reduce decarburization to a minimum. If the chromium content is less than 1%, carburization is noticeable even with a low content of oxygen in the sodium (less than 0.005%). It was observed that decarburization of carbon steel proceeds more intensely at 700°C than at 800°C. This is due to the lower diffusion rate of carbon in the austenite into which the steel ferrite is transformed when heated to 800°C.

Cast iron is unfit for use in a sodium medium at high temperatures since its surface layer becomes saturated with liquid metal. Cast-iron specimens became both deformed and enlarged after being in a sodium-potassium medium.

The stainless nickel-based austenitic steels and alloys (Inconel, etc.) are quite stable in sodium at temperatures below 650°C, where the temperatures of the hot and cold regions of the circuit differ by less than 150°C. Nickel begins to wash out of steel and transfer to a relatively cold region at temperatures above 650°C. As shown by chemical analysis, the crystals deposited in the cold region contain 90% Ni and 9% Cr (the remainder is Fe and Mn).

If the oxygen content of the sodium exceeds the saturation limit, destruction of the stainless-steel surface due to intergranular penetration of the liquid metal becomes evident at as low as 350°C. A brittle layer which breaks up at the slightest deformation of the surface appears on the surface. The influence of the relative oxygen content of sodium on the corrosion resistance of type 347 stainless steel is illustrated in Fig. 102. Analogous data on the stability of Armco iron in a sodium circuit made of nickel is shown in Fig. 103.

The corrosion resistance of austenitic stainless steels is more sensitive to the oxygen content of the sodium than that of ferritic steels.

Many investigators noted that austenitic stainless steels are carburized in an alkaline-metal medium. The carburization becomes noticeable at temperatures above 550°C. Figure 104 shows a carburized layer on the surface of a type 304 stainless steel specimen [102]. At a temperature of 800°C the depth of carburization reached 0.25 mm in 100 hours. The source of carbon in the system was the graphite crucible used for the liquid metal. The carburization can be attributed to transport of carbon from a carbon-steel surface to the stainless-steel surface, if both surfaces are washed by the same liquid metal. Another source of carbon in the system is the carbon dioxide included as an impurity in the composition of the protective gas cushion.

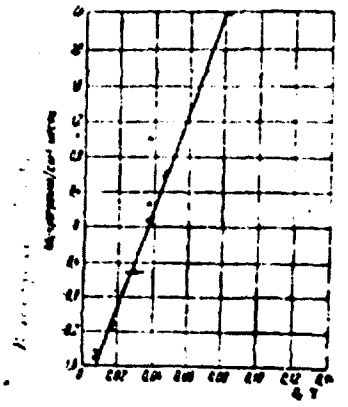

Fig. 102. Corrosion rate of type 347 stainless steel as a function of oxygen content of sodium at t = 540°C.

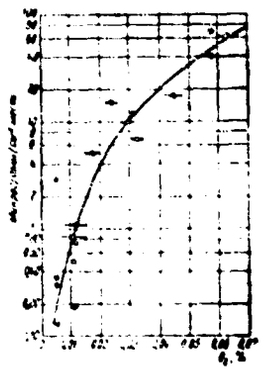

Fig. 103. Corrosion rate of Armco iron as a function of oxygen content of sodium at $t = 540^{\circ}C$.

Sometimes carburization of the surface can prove to be beneficial, since it increases the hardness of the metal and its resistance to wear, but when steel which can undergo plastic deformation is required, it is harmful.

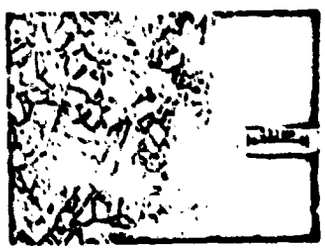

Fig. 104. Carburization of the surface layer of type 3C4 stainless steel specimen.

Heat-resistant alloys are about as corrosion resistant in a sodium medium as the stainless austenitic steels. Cobalt-base alloys (S-590 and S-816), as well as nickel-base (Inconel, Inconel-X), and pure nickel show no traces of the effect of sodium up to 550°C. The results of experiments on the stability of certain steels and heat-resistant alloys in molten sodium are given in Table 24.

TABLE 24

Stability of Some Structural Materials in Liquid Sodium

Material	Temperature, °C	Oxygen content of Sodium, %	Rate of corrosion, microgram/cm² month	Test conditions (Static or Dynamic)
Iron	510	0.01	200	Dynamic
Carbon steel	500	0.01	100	Static
Steel, 1.25% Cr-0.5% Mo	500	0.01	100	S
Steel, 2.25% Cr-1% Mo	510	0.01	100	D
Steel, 5% Cr-0.5% Mo	510	0.01	100	D
Steel, 5% Cr-0.5% Mo	500	0.01	100	S
Steel, 5% Cr-0.5% Mo	500	0.1	1800	S
Steel, 5% Cr-0.5% Mo	500	0.5	5500	S
Steel, 7% Cr-0.5% Mo	500	0.01	100	S
Steel, 7% Cr-0.5% Mo	500	0.1	2000	S
Steel, 7% Cr-0.5% Mo	500	0.5	6000	S
Steel, 9% Cr-1% Mo	510	0.01	100	D

TABLE 24 (cont')

Stability of Some Structural Materials in Liquid Sodium

Material	Temperature, °C	Oxygen content of Sodium, %	Rate of corrosion, $\frac{\text{microgram}}{cm^2\ month}$	Test conditions (Static or Dynamic)
Steel, 9% Cr-1% Mo	500	0.01	100	Static
Steel, 9% Cr-1% Mo	500	0.1	2000	S
Steel, 9% Cr-1% Mo	500	0.5	5400	S
Steel, 9% Cr-1% Mo	715	0.01	400	S
Steel, 9% Cr-1% Mo	715	0.5	37000	S
Steel, 12% Cr	510	0.01	100	Dynamic
Steel, 12% Cr	500	0.01	100	S
Steel, 12% Cr	500	0.1	700	S
Steel, 12% Cr	500	0.5	5100	S
Steel, 12% Cr	715	0.01	400	S
Steel, 12% Cr	715	0.5	26000	S
304 (Stainless Steel)	510	0.01	100	D
304 " "	500	0.01	100	S
304 " "	500	0.1	"	S
304 " "	500	0.5	200	S
304 " "	6[illegible]	0.01	100	D
304 " "	715	0.01	100	S
304 " "	715	0.5	"	S
347 " "	510	0.01	100	D

TABLE 24 (cont')

Stability of Some Structural Materials in Liquid Sodium

Material	Temperature, °C	Oxygen content of Sodium, %	Rate of corrosion, $\frac{\text{microgram}}{cm^2\ month}$	Test conditions (Static or Dynamic)
347 (Stainless Steel)	500	0.01	100	Static
347 " "	500	0.1	500	S
347 " "	500	0.5	500	S
347 " "	648	0.01	100	Dynamic
347 " "	715	0.01	100	S
347 " "	715	0.5	"	S
310 " "	715	0.01	100	S
310 " "	715	0.5	"	S
Inconel-X	510	0.01	100	D
Inconel-X	648	0.01	100	D
Inconel-X	715	0.01	100	S
Inconel-X	715	0.5	"	S
A-286	648	0.01	100	D
A-286	715	0.01	100	S
A-286	715	0.5	"	S
17-14 Cu-Mo	648	0.01	100	D
17-14 Cu-Mo	715	0.01	100	S
17-14 Cu-Mo	715	0.5	"	S
18 Cr-35 Ni	715	0.01	100	S

MCL-554.

TABLE 24 (cont')

Stability of Some Structural Materials in Liquid Sodium

Material	Temperature, °C	Oxygen content of Sodium, %	Rate of corrosion, $\frac{\text{microgram}}{\text{cm}^2 \text{ month}}$	Test conditions (Static or Dynamic)
18 Cr-35 Ni	715	0.5	•	S
Molybdenum	715	0.01	100	S
Molybdenum	715	0.5	8000	S
Hastelloy	715	0.01	100	S
Hastelloy	715	0.5	•	S

• Considerable specimen weight increase was observed.

A considerable transfer of certain elements from one portion of the system to another, especially if these portions are made of dissimilar materials, is frequently observed in sodium circuits. Such transfer can be intensive even where there are no temperature differences in the system. For instance, it was noted [102] that a layer of Ni-Mo alloy (Fig. 105) gradually forms on the surface of a molybdenum specimen, when it is acted upon by liquid sodium in a nickel container. Dissolving in sodium and diffusion to a solid surface take place for both nickel and molybdenum, since Ni-Mo also forms on the surface of the container. As a result of the process described, the surface layer of the

specimen becomes hard and brittle.

Another similar example is the transport of aluminum by sodium to an iron surface accompanied by formation of the intermetallic compound Fe-Al.

Experiments have shown that the following substances are unfit for use, due to their great solubility in sodium and potassium: Sb, Bi, Cd, Au, Pb, Se, Ag, and Sn. Magnesium has limited stability in alkaline metals and can be used in contact with Na-K only at low temperatures. Platinum is quickly corroded by vapors of alkali metals but is not noticeably soluble in liquid sodium or potassium. Na-K alloy does not affect platinum at room temperature; at 600°C, however, the rate of corrosion is fairly high.

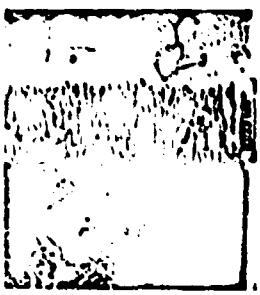

Fig. 105. Formation of Ni-Mo on the surface of a molybdenum specimen in a sodium medium.

1) Ni-Mo; 2) molybdenum specimen; 3) Vickers hardness: 1,250; 4) Vickers hardness: 140.

The reaction of sodium with copper is accompanied by the formation of Na-Cu on the surface of the copper. This process becomes noticeable at t 300°C. If a copper capsule is filled with sodium and held for 100 hours at t = 980°C, then when the capsule is opened it will be empty and its walls will contain the alloy

Na-Cu which is characterized by great hardness and brittleness.

Zirconium does not dissolve noticeably in sodium up to 600°C. The rate of corrosion of zirconium depends to a very great degree on the oxygen content of the liquid metal, since in the $Zr-O_2-Na$ system there takes place selective oxidation of Zr, which has greater affinity for oxygen than Na has. A dark layer of dioxide (ZrO_2) gradually forms on the surface of the zirconium. As a result of the transfer which occurs intensively at temperatures of about 500°C and up, the surface layer of the material becomes hard and brittle. Figure 106 shows the increase in hardness of the surface layer of a zirconium specimen in a sodium medium at a temperature of 500°C, with ~ 0.01-0.1% oxygen contained in the liquid metal [45]. The distance from the surface into the specimen is plotted along the abscissa and the hardness in Rockwell numbers on the ordinate. With an oxygen content greater than 0.005% in the Na, the rate of oxidation of Zr is approximately constant and corresponds to a weight gain equal to ~ 500 microgram/cm² month. Zirconium can be protected from corrosion by adding to it an oxygen-absorbing substance. For example, alloys of zirconium and titanium have good stability in sodium.

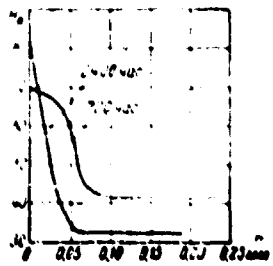

Fig. 106. Increase in surface-layer hardness of a zirconium specimen in a sodium medium (H_R in Rockwell hardness).

The behavior of hafnium in sodium is analogous to that of zirconium.

The corrosion rate of beryllium in alkali-metal media becomes noticeable when the oxygen content of the alkali metals exceeds 0.01%. The oxide film forming on the surface of beryllium protects the metal from further destruction only in a motionless sodium medium. Introducing calcium into sodium in quantities of about 2% noticeably reduces the rate of corrosion.

Nonmetallic Materials. Ordinary glass at $t<300^{\circ}C$ is not adversely affected by sodium; at higher temperatures "Pyrex" glass breaks up quickly, whereas "Vicor" glass is useful up to 400°C. The presence of oxygen in the liquid metal is very harmful to the corrosion resistance of glass.

Darkoid (rubber, impregnated with a fireproof substance) is used successfully in contact with sodium at relatively low temperatures (100-120°C).

Asbestos can be utilized for gland packings operating in a sodium medium at temperatures up to 150-170°C and pressures up to 3-4 gage atmos. At a temperature of 200°C and higher, however, asbestos starts to react with the alkali metals.

Certain silicone rubbers lose their elasticity as a result of the action of sodium and potassium.

Teflon (tetrafluoroethylene) disintegrates completely under the action of Na, and becomes a black powder.

Carbides of tungsten, titanium, chromium, and tantalum bound with nickel or cobalt are not affected by the aggressive action of molten sodium.

The oxides of aluminum, magnesium, titanium, and zirconium, and other substances chemically stable with respect to sodium have a relatively porous structure. Hence, they can absorb molten sodium and crack when sharp variations of temperature occur. When the density of the oxides is artificially raised by alloying, they become suitable for use.

The Behavior of Graphite in Molten Sodium. A stability test of graphite in motionless sodium showed that the loss in the weight of graphite specimens rises, if there is a high concentration of potassium in the sodium (0.01% and higher) and sodium simultaneously washes the surface of the graphite and stainless steel. In this case, intensive carburization of the surface layer of the steel occurs. The oxygen concentration and temperature of the liquid metal also affect the rate at which the graphite dissolves.

Certain experimental data pertaining to static tests of the stability of graphite specimens in sodium poured into steel and nickel capsules are given in Table 25. During investigations into the stability of AGOT graphite the appearance of small cracks on the surface of the specimen was discovered, which was not true of the more fine-grained AWG and AUF graphites. A cylindrical stainless-steel capsule, into which a hollow graphite rod with a longitudinal groove on the side was tightly fitted, was used to study the behavior of graphite in a flowing metal. The groove was connected with the interior of the hollow rod through holes at the top and bottom of the rod. Sodium was poured into the capsule-and-rod-assembly, which was then heated to 800°C at the bottom while the temperature at the top was maintained at 400°C, resulting in natural circulation of the metal: upward, through the center of the rod, and downward, along the groove. After 432 hours of operation, the side groove turned out to be completely clogged up in the cold region by a substance containing 8.5% Na and 91.5% C with a melting point at least above 600°C. The surface of the graphite in the lowest part of the capsule (in the hot region) was destroyed. Consequently, in this case carbon was transported from the hot region to the cold region. No carburization of the steel surface of the capsule was observed at temperatures below 550°C.

TABLE 25

Data of Static Tests of the Stability of Graphite Specimens in Sodium

Grade of Graphite	Capsule material	Temperature, °C	Duration of test, hours	Change in specimen weight, %	Remarks
AGOT	347 Steel	750	163	9.1	Intensive carburization of steel
AUF	347 Steel	750	202	50	Idem
AGOT	Ni	750	216	0	No change noted in state of specimen
AGOT	347 Steel	675	423	9.0	Intensive carburization
AGOT	347 Steel	675	648	7.5	Idem
AGOT	347 Steel	675	1454	17.5	Idem
AGOT	347 Steel	600	163	0.13	Moderate carburization
AGOT	Ni	600	220	0	---
AUF	347 Steel	600	650	1.63	Moderate carburization
AGOT	347 Steel	600	1968	0.92	Idem
AGOT	347 Steel	525	341	0.07	No carburization observed
AUF	347 Steel	450	166	9.3	---
AUF	347 Steel	450	640	0	No change noted in state of specimen
AUF	347 Steel	450	2284	0.19	No effect of sodium on specimen observed

It was established that at $t \sim 400$-$500^{\circ}C$ and above, the internal cavities (pores) of graphite immersed in sodium are completely filled by the sodium. A graphite rod with one end dipped in sodium ($t = 550^{\circ}C$) so that $\sim$ 150 mm of its length was above the liquid,* became completely "saturated" with sodium within [illegible]. The volume of the internal cavities amounted to approximately 22% of the [illegible]. At $t = 550^{\circ}C$ during this period (50 hours) only 60% of the volume of the cavities were filled with sodium.

Data describing endurance tests of graphite under conditions of sharply changing temperatures of a liquid metal are available in the literature. Table 26 gives the results of "thermal shock" tests conducted with different liquid metals, using cylindrical graphite specimens 20 mm in diameter and 25 mm in length. The tests consisted of preheating the specimens to the temperature specified in the table and then plunging into a relatively cool liquid metal.

---

* The space above the level of the liquid was filled with an inert gas (helium).

TABLE 26

Test Data for Thermal Shock of Graphite Specimens

Temperature of preheated specimen t, °C	Liquid Metal	Temperature of metal t, °C	Test Results
900	Na	150	Specimen destroyed, surface wetted by sodium
700	Na	150	Idem
600	Na	150	Specimen retained its initial appearance, surface wetted by sodium
2500	Sn	300	Specimen retained its initial appearance, no wetting
1500	Bi	300	Idem
20	Al	1100	"

Stability of Heat-Resistant Materials in Sodium at High Temperatures.

The information given above pertains to the stability of structural materials at temperatures not exceeding 600-700°C, as a rule. Tests of certain heat-resistant materials in a sodium medium in a considerably higher temperature range (800-1,500°C) were conducted by Reed [143]. The results of his experiments are given in Table 27. According to the stability-test data for a molybdenum wire in sodium vapor at $t = 1,500$°C, sodium causes intergranular corrosion, which can be considered relatively weak when the extremely severe test conditions are taken into account. As can be seen from Table 27, the degree of corrosion

of the oxides of magnesium, aluminum, and zirconium is determined by the degree of purity and the porosity of the specimens.

TABLE 27

Corrosion of Some Heat-Resistant Materials in Sodium

(Under Static Conditions)

Material	Temperature of sodium t, °C	Duration of test τ, hrs	Change in weight of specimen, %	Test Results
Molybdenum (99.9% pure)	900	168	0.001	No corrosion observed
	1300	100	—	Intergranular corrosion at a depth of 0.025 mm
Tungsten (99.9% pure)	900	168	from 0.07 to 0.01	Not affected by corrosion
Tantalum (99.9% pure)	900	168	from 0.09 to 0.01	Not affected by corrosion, specimen surface sometimes becomes darker
Kennametal-(K138A)-80% TiC, 15% Co, 5% (WC + TaC)	900	168	from 0.07 to 0.20	Very little corrosion

TABLE 27 (cont')

Corrosion of Some Heat-Resistant Materials in Sodium

(Under Static Conditions)

Material	Temperature of sodium t, °C	Duration of test τ, hrs	Change in weight of specimen, %	Test Results
AGO graphite	900	168	6.0	Corrodes
	900	841	60.0	Corrodes highly
Monocrystal of silicon carbide	900	168	1.0	Insignificant corrosion
Synthetic spinel	925	168	100.0	Dissolves completely in sodium
"Korgonite" aluminum oxide, 6% porosity	940	168	—	High corrosion, disintegrates into small block grains
Aluminum oxide (synthetic sapphire)	900	168	1.0	Insignificant corrosion, material remains transparent
Magnesium oxide, 12% porosity	940	168	1.2	Material becomes blacker and swells

TABLE 27 (cont')

Corrosion of Some Heat-Resistant Materials in Sodium

(Under Static Conditions)

Material	Temperature of sodium t, °C	Duration of test τ, hrs	Change in weight of specimen, %	Test Results
Magnesium oxide (single crystal)	925	168	0.02	Does not corrode
Zirconium oxide, 23% porosity	890	168	3.7	Corrodes, specimens disintegrated
Molybdenum disilicide (cast)	900	168	—	Very little corrosion
Thorium oxide	925	168	0.06	Not affected by corrosion

26. Lithium

(Table 28).

Lithium belongs to the alkali metals; however, in its chemical properties it is closer to the alkali-earth elements. This explains why Li behaves more aggressively with respect to structural materials than do sodium or potassium. Admixtures in the liquid metal have a definite effect on the stability of materials with respect to lithium. So far, there is not enough experimental data to permit quantitative evaluation of this effect.

Lithium nitride (Li_3N), which forms when nitrogen reacts with either the solid or molten metal, is extremely aggressive with respect to structural materials. No material has been found (of the metals or ceramics) which is capable of successfully resisting corrosion in a medium of molten lithium nitride.

Oxygen is more likely to be found in lithium as the hydroxide (LiOH) than as the oxide itself (Li_2O), since it is known that atmospheric moisture prevents oxidation of lithium. Like Li_3N, molten lithium hydroxide is aggressive with respect to structural materials. When heated to 455°C LiOH decomposed, forming lithium oxide. LiH and Li_2O react with the majority of metal oxides.

TABLE 28

Stability of Structural Materials in a Lithium Medium

Temperature, °C

a) Ferrous metals

b) Pure iron

c) Low-carbon steel

d) Low-chromium steel (4130)

e) Ferritic chromium stainless steel

f) Austenitic chrome-nickel stainless steel

g) Nonferrous metals

h) Al, Bi, Cd, Pb, Mg, Pt, Au, Ag, Si, Sn, Zn

i) Beryllium, chromium, vanadium

j) Zirconium, titanium

k) Niobium, tantalum, molybdenum

l) Nickel and nickel-base alloys

m) Cobalt-base alloys

n) Nonmetals

o) Quartz

p) Glass and silicates

q) Graphite

r) Rubber and plastics

s) M_gO

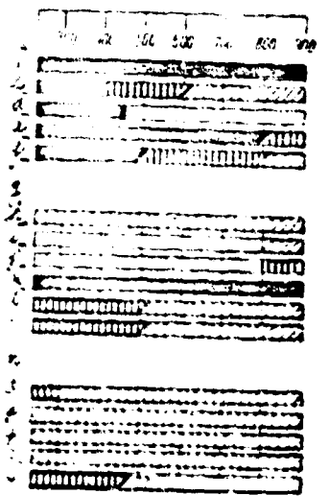

Stability

Good — Limited

Poor — Unknown

Admixtures of chlorine are present in lithium both in the free form and lithium chloride (LiCl), which heavily corrodes iron and copper surfaces.

Lithium hydride is formed when water vapor or hydrogen reacts with the liquid metal; at high temperatures it reacts with metals and ceramic materials.

Liquid lithium also reacts strongly with metal carbides.

Some impurities (the oxide, hydroxide, nitride, and hydride) can be removed from the molten metal by filtration. It was noted that a stainless steel screen used to filter the impurities gradually disintegrated; destruction was caused chiefly by nickel washing from the steel.

The stainless chrome-nickel steels can be used at $t > 550^{\circ}C$ only where there are little oxygen and nitrogen in the liquid metal and the temperature differences in the system are small. Corrosion of stainless steel in a lithium medium is accompanied by strong intergranular penetration by the liquid metal. Fig. 107 shows penetration of lithium all the way through the wall of a type 316 stainless-steel tube 102 . The wall is 0.9 mm thick; a small quantity of nitride (0.1%) had been added to the lithium beforehand. Under the same conditions but with no nitride in the liquid metal, the depth of intergranular penetration amounted to only 0.05 mm.

Fig. 107. Intergranular penetration of lithium into the wall of a stainless-steel tube held at $t = 870^{\circ}C$ for about 100 hours.

Fig. 108. Lithium washing nickel from type 304 stainless steel.
1- Vessel of type 304 stainless steel; 2- iron vessel.

A picture of lithium selectively washing nickel from type 304 austenitic stainless steel is shown in Fig. 108 [102]. The temperature of the lithium was 1,000°C, the test lasted for 400 hours. The figure shows the transformation of austenitic steel into ferrite (in the surface layer) caused by the washing out of nickel.

The rate of corrosion of stainless steel is especially high when the vessel holding the liquid metal contains a considerable quantity of iron. In this case the nickel washed out of the steel diffuses through the lithium to the surface of the iron.

Low-carbon type 316 stainless steel or type 347 steel is recommended for use as structural material for equipment which must operate in a lithium medium at temperatures to 700°C. Type 310 stainless steel can be used in the 700 to 1,000°C temperature range. Molybdenum, tungsten, niobium, tantalum, and Armco-iron have satisfactory corrosion resistance in lithium at temperatures up to 800°C.

The corrosion resistance of Monel metal (68% Ni; 1.25% Mn; 1.0% Fe; 0.05% Si; the remainder Cu) in a medium of liquid lithium is very low; at 300°C Li

dissolves up to 18% of the Monel metal.

At a temperature of about 1,000°C, beryllium quickly disintegrates in a lithium medium. The corrosion rate of Be at $t \sim 500°C$ is $\sim 1{,}600$ microgram/cm^2 · month.

It has been noted that at $t \sim 1{,}000°C$ tungsten disintegrates in molten lithium in an armco-iron vessel.

When lithium reacts with zirconium, a dull film of zirconium nitride (ZrN) forms on the zirconium surface; this is due, evidently, to the presence of nitrogen (in the form of Li_3N) in the lithium.

The following metals cannot be recommended for use in view of their poor corrosion resistance in lithium: Al, Ba, Bi, Ca, Cd, Au, Pb, Mg, Pt, Si, Ag, Sr, Tl, Sn, Zn, Cu, Ni, and the Ni-base alloys.

Quartz has satisfactory stability only in a lithium medium free of the oxide and nitride, and then only at temperatures to $\sim 280°C$. Lithium silicide (Li_6Si_2) forms at higher temperatures. If standard technically-pure metal is melted in a quartz vessel, its walls almost immediately disintegrate. Standard glass is also unfit for use in a lithium medium.

Most ceramic materials are corroded by lithium; we recommend melting lithium in steel or iron crucibles.

Molten Li penetrates to the inner pores of magnesium oxide but does not cause corrosive disintegration.

27. Gallium

(Table 29)

Gallium is the most dangerous of all the liquid metals examined, from the standpoint of its corrosive effect on materials. Only few materials (fireproof

oxides, quartz, graphite, tungsten, and tantalum) have satisfactory stability in Ga at high temperatures.

The mechanism of the interaction of Ga with structural materials is determined by a number of conditions, the temperature level being the most important. For example, at temperatures up to 600°C the corrosion rate of tantalum is determined chiefly by the dissolving intensity of the solid material, whereas at 600°C the diffusion of gallium into the surface layer of Ta begins to predominate, accompanied by the formation of a chemical compound. Elements with similar chemical properties often behave differently in a gallium medium. For example, molybdenum reacts with Ga to form several products, including one in solid solution. At the same time, tungsten, whose chemical compounds are isomorphic with molybdenum compounds, does not react with gallium up to 800°C. Gallium can wet magnesium oxide but does not wet the oxides of beryllium or aluminum. The oxides of Mg, Be, Al, and the majority of ceramic substances are satisfactorily stable in a medium of liquid Ga. Aluminum disintegrates quickly in a gallium medium even if its surface is anodized.

The data shown in Table 29 refer mostly to tests on materials in motionless or nearly motionless gallium. Let us consider some of these data in more detail.

At $t \geq 600°C$ and higher, chromium disintegrates in the presence of liquid gallium; it is also known that these metals are not intersoluble and that chemical compounds do not form between them. Hence, Cr can be expected to be stable enough in gallium at temperatures below 600°C. Gallium reacting with titanium forms the chemical compound Ga_3Ti. Such elements as Cu, Pt, Zr, Ni, V, Mn, Ag, Au, Ce, Pr, Cd, Fe, Ge, Sn, and In are evidently not suitable for practical use; they form solid solutions with gallium. However, there are data in the literature to the effect that Cu, Pt, and Zr are not affected by corrosion in a gallium medium at temperatures of about 100°C.

TABLE 29

Corrosion Resistance of Structural Materials in a Medium of Gallium

a) Ferrous metals

b) 18-8 Stainless steel

c) Stainless steel, 16% Cr

d) Tool steel (W, Cr, Mo, V)

e) Iron

f) Nonferrous metals

g) Tungsten

h) Tantalum

i) Alloy, 93% Ta, 7% W

j) Niobium

k) Molybdenum

l) Titanium

m) Lead

n) Chromium

o) Manganese

p) Alloy, 50% Cr, 50% Mn

q) Nickel

r) Alloy, 80% Ni, 20% W

s) Zirconium

t) Magnesium

u) Copper

v) Platinum

w) Aluminum

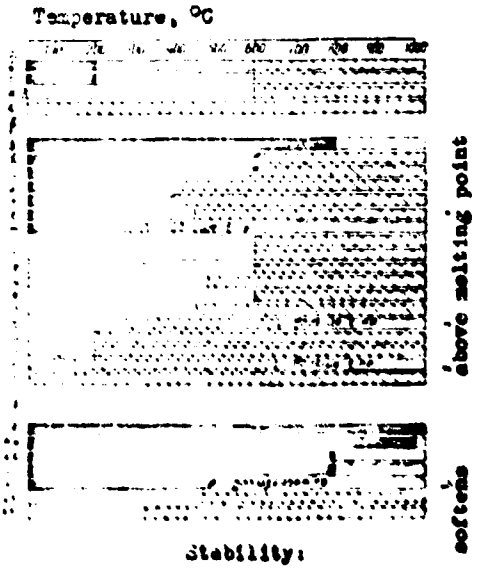

x) Ag, Ca, Cd, Co, Sn, Zn

y) Nonmetals

z) Quartz

aa) Sintered BeO

bb) Graphite

cc) ZrO_2

dd) Pyrex glass

ee) Sintered MgO

ff) Rubber

NCL-554

The solubility of tantalum in gallium amounts to 0.14% at 500°C and 4.2% at 600°C. A tantalum-tungsten alloy (93% Ta, 7% W) has somewhat higher corrosion resistance than pure tantalum.

Crucibles made of beryllium oxide are not affected by the aggressive action of gallium up to temperatures on the order of 1,600°C (for brief service) and 800°C (for extended service). Special investigations have verified the good stability of BeO up to 1,000°C.

Molten silicon oxide has good stability in gallium at temperatures to ~ 1,200°C; the resistance drops in the presence of oxygen.

Alundum crucibles are not at all affected by gallium at t = 1,000°C.

Zirconium oxide is wetted by gallium at high temperatures, and the liquid metal penetrates deep into the solid material.

Plastics and rubber show satisfactory stability in a gallium medium up to their temperatures of thermal dissociation.

28. Mercury

(Table 30)

Carbon steels and alloy steels. Extensive investigations of the corrosive effect of mercury on structural materials were conducted with respect to the use of indirect (mercury-water) installations in power engineering.

Carbon steels and alloy steels are not affected by corrosion when briefly subjected to the action of mercury. However, prolonged tests of large plants showed that a residue of crystallized iron and its oxide gradually builds up on the inside walls of carbon steel tubes in the relatively cold sectors of the system.

Laboratory tests on the stability of materials were conducted, as a rule, with natural convection of the liquid at temperatures up to 800°C and relatively

low metal flow rates (0.01-0.05 m/sec). The corrosion rate was determined as a function of: the chemical composition of the material, additives to the mercury, duration of the experiment, and temperature. It turned out that low-alloy steels, such as the steel with 5% Cr, 0.5% Mo, and 1% Si, are more stable in mercury than carbon steels. Moreover, adding certain elements, in particular titanium and magnesium, to the mercury sharply reduced the rate of corrosion. Furthermore, it seems that when the mercury moves, even at small velocities, and differences exist in the system, although small, the corrosion of steel increases noticeably.

The major factor in the mechanism of interaction of mercury with a steel surface is apparently the dissolution of iron, which takes place at a rate determined by the value of the diffusion coefficient for iron in mercury. Inasmuch as the concentration of iron in the mercury layer adjacent to the surface reaches saturation very quickly, the rate of the process as a whole is determined by the rate at which the dissolved iron particles are diverted into the volume of the liquid metal. This saturation point very much depends on temperature, amounting to $1.5 \cdot 10^{-6}$% at 25°C and $7.6 \cdot 10^{-5}$% at 700°C. As shown by experiment, for 100°C temperature increases above 500°C, the corrosion rate of carbon steel in mercury increases roughly five-fold. For example, at 500°C the corrosion rate was found to equal 5 mm/year, while at 800°C it is 560 mm/year.

The influence of the composition of steels on their corrosion resistance in mercury is illustrated in Table 31. As the table shows, carbon steels have good stability in flowing mercury at temperatures below 400°C, limited stability up to 550°C, and poor stability at higher temperatures. The anticorrosion properties of carbon steel improve when the following elements are added: Cr, Si, Ti, Mo; introducing aluminum into the steel does not produce a positive effect. Good steel stability can be achieved up to temperatures of the order of 600°C by

successfully combining alloying elements, especially chromium, silicon, and molybdenum.

TABLE 30

Stability of Structural Materials in a Mercury Medium

a) Ferrous metals and iron-base alloys

b) Ferrous metals (Ti and Mg in Hg)

c) Low-carbon steel

d) Low-carbon steel with 0.1-4% Al

e) Low-carbon steel with 4% Cr

f) Steel with 5% Cr

g) Low-carbon steel with 0.5% Mo

h) Low-carbon steel with 0.5% Mo

i) Low-carbon steel with 1-3% Si

j) Low-carbon steel with 1-2% Ti

k) Low-carbon steel with 2% Al and 2% Cr

l) Nitralloy (1.23% Al, 1.49% Cr)

m) Low-carbon steel with 5.7% Cr and 1.2% Cu

n) Low-carbon steel with 4.5% Cr and 4.5% Mo

o) Low-carbon steel with 5.7% Cr, 1.2% W

p) Low-carbon steel with 15-20% Mn and 3% Si

Temperature, °C

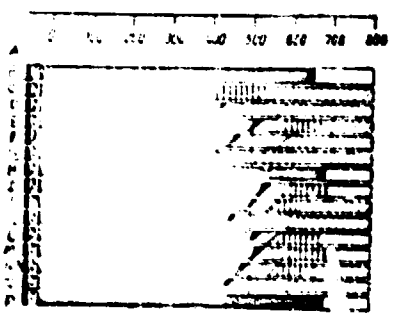

TABLE 30 (cont')

Stability of Structural Materials in a Mercury Medium

q) Low-carbon steel with 6% Cr,
0.5% Al, and 3% Mo

r) Sicromo 53 (5% Cr, 0.5% Mo, 1.5% Si)

s) Low-carbon steel with 5.5% Cr,
0.5% Mo, and 1.4% Si

t) 304 and 310 Stainless steels (Cr)Ni)

u) High-nickel steels Ni-Fe and Ni-Cr-Fe

v) Ferritic stainless steels (Cr)

w) Nonferrous metals

x) Tungsten

y) Molybdenum

z) Chromium

aa) Beryllium

bb) Ta, Nb, Si, Ti, V

cc) Ni, Cu, and their alloys

dd) Cobalt and stellite

ee) Pt, Mn, Zr

ff) Al, Bi, Cd, Ce, Au, Pb, Mg, Ag, Sn, Zn

gg) Nonmetals

hh) Glass

ii) Ceramics

jj) Graphite

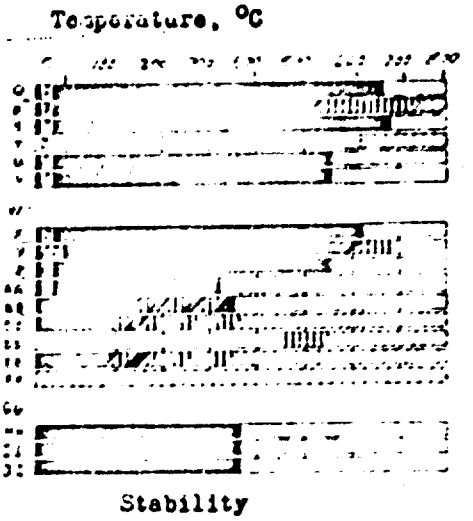

MCL-554

A 0.2-0.4% chromium content reduces the corrosion rate of the steel by about six times. Adding 4% Cr is much less effective, due to the formation of a chromium-oxide film on the surface of the material; this film is very thick and as a result does not adhere sufficiently well. The corrosion rate of steel containing 5% Cr is only half the corrosion rate of carbon steel.

Small quantities of molybdenum ($\sim$ 0.5%) do not improve the anticorrosion properties of steel, while adding 20% Mo decreases the rate of corrosion at 650°C to a negligibly small value.

Silicon added to steel in quantities of 1-3% reduces the corrosion rate by approximately 90% at 640°C.

Steel containing 1-2% titanium is 4-5 times more stable than carbon steel.

Nitralloy (1.23% Al; 1.45% Cr) has the best anticorrosion properties of the steels with chromium and aluminum. Its corrosion rate in flowing mercury at t = 650°C is 4 mm/year, which is about 10% of the corrosion rate of carbon steel under the same conditions. The solubility of nitralloy in mercury is about the same as the solubility of pure iron.

Steel containing 1-2% Cr, 0.5-0.6% Mo, and 1-2% Si, which is used in the operation of mercury-vapor trilers proved to be about 20 times more stable than carbon steel. The high-chrome ferritic steels showed good stability in motionless mercury at 650°C; no tests in a moving medium were made. As shown by experiment, at high temperatures (t >650°C) the anticorrosion properties of chrome-nickel austenitic steels are unsatisfactory in moving mercury. Nickel-base alloys displayed good stability in motionless mercury at 550°C.

TABLE 31

Stability of Steels of Various Compositions in Flowing Mercury

Material	Duration of test, hrs	Maximum Temperature in system, °C	Rate of corrosion: microgram / cm^2·month	Rate of corrosion: mm/year
Carbon steel (mild)	10000	482	7000	4
	10000	538	15000	9
0.2% C	10000	593	37000	22
	10000	649	88000	53
Steel, aluminum alloyed				
0.1% Al	162	625	28,000	17
0.2% Al	48	650	18,000	11
0.5% Al	257	615	64,000	40
1% Al	95	620	52,000	32
2% Al	113	630	69,000	43
4% Al	19	650	7,000	4
Chromium steel				
0.2% Cr	46	650	13,000	8
0.5% Cr	138	615	7,000	4
4% Cr	138	625	23,000	14
5% Cr	10,000	482	3,000	2
Molybdenum steel				
0.5% Mo	161	670	86,000	53
20% Mo	64	650	500	0.3

ORNL-554.

TABLE 31 (cont')

Stability of Steels of Various Compositions in Flowing Mercury

Material	Duration of test, hrs	Maximum temperature in system, °C	Rate of Corrosion	
			microgram / cm^2·month	mm/year
Silicon steel				
1% Si	67	640	7,000	4
2% Si	107	640	11,000	7
3% Si	67	640	7,000	4
Steel, titanium alloyed				
1% Ti	329	620	9,000	6
1% Ti	329	675	39,000	24
2% Ti	329	625	7,000	4
2% Ti	329	640	15,000	9
Steel, alloyed with aluminum and chromium				
0.1% Al; 0.1% Cr	136	625	46,000	29
0.5% Al; 0.5% Cr	137	630	37,000	23
2% Al; 2% Cr	48	620	44,000	27
2% Al; 2% Cr	142	650	13,000	8
Nitralloy (not nitrided)				
1.23% Al; 1.49% Cr	165	650	7,000	4
	2	615	6,000	4

TABLE 31 (cont')

Stability of Steels of Various Compositions in Flowing Mercury

Material	Duration of test, hrs	Maximum temperature in system, °C	Rate of Corrosion	
			microgram / cm^2·month	mm/year
Steel, alloyed with chromium and copper				
5.7% Cr; 1.2% Cu	161	670	8,000	5
Steel, alloyed with chromium and molybdenum				
0.5% Cr; 0.5% Mo	140	650	6,000	4
4.5% Cr; 4.5% Mo	140	640	6,000	4
4.9% Cr; 0.5% Mo	161	670	86,000	53
Steel, alloyed with chromium and tungsten				
5.7% Cr; 1.2% W	100	600	26,000	16
Steel, alloyed with molybdenum and silicon				
15% Mo; 3% Si	89	655	1,000	0.6
20% Mo; 3% Si	68	655	500	0.3

TABLE 31 (cont')

Stability of Steels of Various Compositions in Flowing Mercury

Material	Duration of test, hrs	Maximum temperature in system, °C	Rate of corrosion: microgram/cm²·month	Rate of corrosion: mm/year
Steel, alloyed with chromium, molybdenum, and silicon 4.5% Cr; 0.5% Mo; 1.23% Si	140	640	6,000	4
Silcrome SS 4 to 6% Cr; 0.45 to 0.65% Mo; 1-2% Si	10,000	482	300	0.2
	10,000	538	800	0.5
	10,000	593	1,800	1.1
	10,000	649	4,000	2.5
Steel 5.5% Cr; 6.4% Mo; 1.4% Si	280	588	700	0.4
	982	620	800	0.5
	111	650	800	0.5
Steel, alloyed with aluminum, chromium, molybdenum, silicon 0.8% Al; 5% Cr; 0.5% Mo 0.9% Si	450	650	64,000	38
Type 304 Stainless steel 18% Cr; 8% Ni	450	652	32,000	20

MCL-554

TABLE 31 (cont')

Stability of Steels of Various Compositions in Flowing Mercury

Material	Duration of test, hrs	Maximum temperature in system, °C	Rate of corrosion	
			microgram / cm^2·month	mm/year
Type 310 Stainless steel				
25% Cr; 20% Ni	400-500	650	77,000	47

Remarks: A minus sign denotes loss in weight of specimen.

The influence of additives to Hg on the corrosion rate of carbon steel is illustrated in Table 32. The best additive from the standpoint of reducing corrosion is titanium. The presence of 0.001% Ti in mercury reduces the rate of corrosion (at 650°C) to a negligibly small value; at a temperature of 455°C a similar effect is produced by adding 0.0001% Ti; Zr, Cr, Ni, and Al can also serve as inhibitors (decelerators) of corrosion, but more of these elements should be introduced into the liquid metal in the case of titanium. Adding Cu, Pb, and Sn increases the aggressive effect of mercury on carbon steel.

Certain other substances are frequently introduced into mercury in addition to corrosion inhibitors. This has two purposes: 1) reduction of oxidation of the steel surface, which also tends to improve wettability and thus improves the heat-transfer conditions; 2) removal of the free oxygen, nitrogen, and water

vapor from the mercury, increasing the effectiveness of the main inhibitor. Consequently, these additives should have greater chemical affinity for oxygen and nitrogen than the inhibiting substance (most often titanium) and the material of the surface (mostly iron). The most suitable elements for these purposes are magnesium and calcium; Mg is preferred because of its better availability and its better solubility in Hg. The addition of 0.002% Mg leads to complete absorption of the free oxygen in mercury.

TABLE 32

Influence of Additives to Mercury on the Corrosion Rate of Carbon Steel

Element added (a)	Duration of test, hrs (b)	Temperature, °C (c)	Corrosion rate	
			micrograms/cm²·month (d)	mm/year (e)
(a)	(b)	(c)	(d)	(e)
Nothing added, the same	From 40 to 175	[illegible]	[illegible]	4 53 560 2580 222 173 173 49 0.37
0.25% Cr 1% Ni		[illegible]	<500 <500	<0.3 <0.3
[illegible] Ti [illegible] Ti 0.04% Zr [illegible] Zr	From 100 to 2,000	[illegible]	<500 <500 <500 [illegible]	<0.3 <0.3 <0.3 0.06

MCL-554

Alkali metals can be used to some extent to improve the ability of mercury to wet steel. For example, in mercury-vapor plant service, sodium and iron form the compound $Na_2O \cdot Fe_2O_3$ which is insoluble in mercury and settles in the tubes of the system, possibly clogging them.

Other metals and alloys. Very little information has been accumulated on the stability of nonferrous metals and alloys in a flowing mercury medium. The only materials whose anticorrosion properties have been thoroughly examined are molybdenum, tungsten, and stellite.

It has been established that the following metals are fully acceptable in the manufacture of equipment for mercury-vapor installations: W, Mo, Cr, and Be. It can be assumed that Ta, Si, and Ti also have satisfactory anticorrosion properties. The following metals and alloys have limited stability with respect to mercury: Ni, Inconel, Monel metal, Cu, Cu-base alloys, Co, stellite, Pt, Mn, and Zr. Certain metals dissolve well in mercury: Al, Bi, Cd, Ca, Au, Pb, Mg, Ag, Sn, and Zn. Alloys containing appreciable quantities of these elements should not be used in contact with mercury.

Nonmetallic materials. Evidently, ceramic materials are suitable for use in a mercury medium. Carbon does not dissolve in Hg, at least up to 350°C; hence, graphite can be expected to be fairly stable in a mercury medium.

29. Lead, Bismuth, Tin, and Their Alloys

Pb, Bi, and Sn are alike in the magnitude of their corrosive effect on structural materials (Table 33).

Lead. Certain impurities of liquid lead, primarily oxygen, antimony, arsenic, tin, and zinc, exert a harmful effect on the stability of iron and steels in a lead medium. There is still little data accumulated which would permit a quantitative evaluation of this effect; this is due first of all to the

to the difficulty of conducting an accurate analysis of the oxygen content of lead.

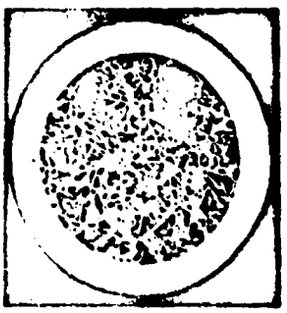

Fig. 109. Precipitation of iron crystals in a flow of lead in a cold portion of the circuit.

The stainless steels in the 400 series, standard carbon steel, molybdenum, and nickel have satisfactory corrosion resistance in a motionless lead medium at temperatures to 500°C. The stainless steels in the 300 series have considerably lower anticorrosion properties.

A quartz-tube circulation circuit was used at the Oak Ridge National Laboratory of the USA [102] to study the transport of structural materials by flowing lead. Replaceable specimen tubes, each 450 mm long, were installed in the hot and in cold portions of the circuit. During testing of iron-chrome-alloy specimens, iron crystals were found to precipitate in the cold area. Some of the crystals settled on the surface of a specimen tube and some circulated in the lead flow. Figure 109 shows a cross section of the tube, together with the solidified lead and crystals of iron in its mass.

TABLE 33

Stability of Structural Materials in Lead, Bismuth, and Alloys of Lead, Bismuth, and Tin

a) Ferrous metals

b) Carbon steel

c) Iron

d) Low-chrome steel (2-9% Cr)

e) High-chrome steel

f) 347 Stainless steel (18% Cr, 8% Ni, Nb)

g) Gray cast iron

h) 18-8 Stainless steel

i) Nonferrous metals

j) Tantalum and niobium

k) Zirconium

l) Beryllium

m) Chromium

n) Titanium

o) Aluminum

p) Inconel (13% Cr, 6.5% Fe)

q) Hastelloy C

r) Manganese

s) Copper

t) Nickel

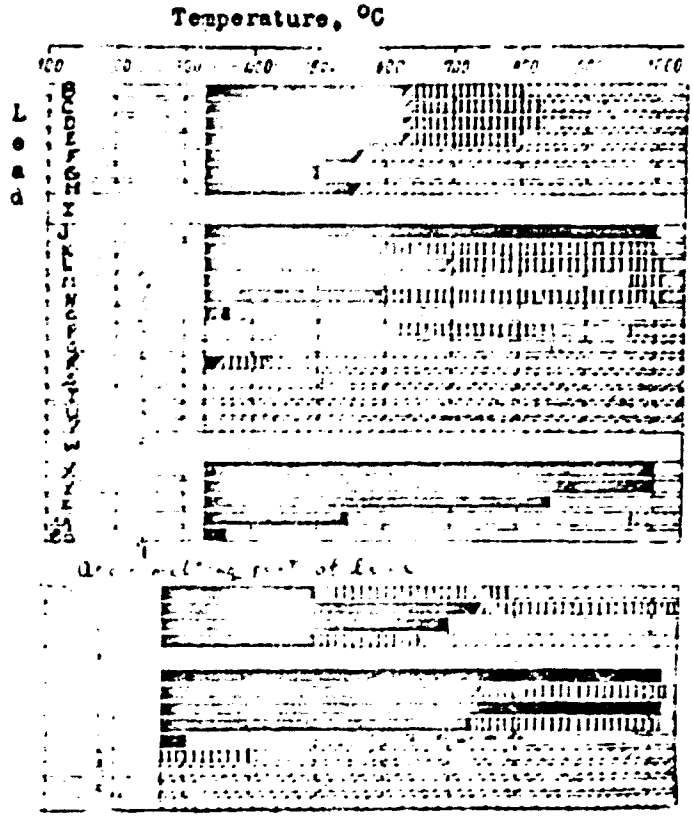

u) Monel metal

v) Platinum

w) Nonmetals

x) Beryllium oxide (sintered)

y) Quartz

z) Porcelain

aa) Graphite

bb) Pyrex glass

MCL-554

TABLE 33 (cont')

Stability of Structural Materials in Lead,

Bismuth, and Alloys of Lead, Bismuth, and Tin

cc) Ferrous metals

dd) High-chrome stainless steel (27% Cr)

ee) Iron

ff) Carbon steel

gg) Stainless steel (Cr-Ni)

hh) Nonferrous metals

ii) Molybdenum

jj) Chromium

kk) Beryllium

ll, Niobium

mm) Aluminum

nn) Copper

oo) Nickel

pp) Manganese

qq) Platinum

rr) Nonmetals

ss) Graphite

tt) Vicor

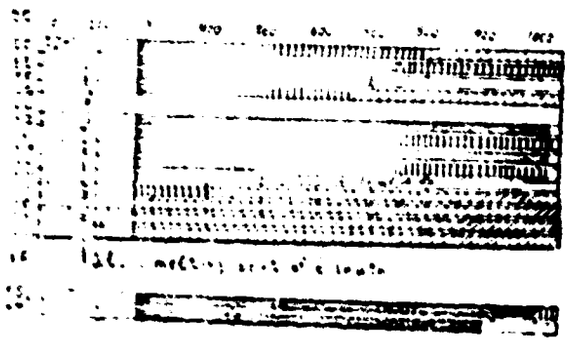

ORNL-554

TABLE 33 (cont')

Stability of Structural Materials in Lead,

Bismuth, and Alloys of Lead, Bismuth, and Tin

uu) Nonferrous metals

vv) Iron

ww) High-chrome steel

xx) 310 Stainless steel

(25% Cr, 20% Ni)

yy) Chrome-molybdenum steel

zz) Carbon steel

ba) 18-8 Stainless steel

bb) Steel (16% Cr, 3% Ni)

bc) Nonferrous metals

bd) Beryllium

be) Aluminum

bf) Hastelloy A, B, C

bg) Aluminum Bronze (10% Al)

bh) Inconel (13% Cr, 6.5% Fe)

bi) Copper, brass, Monel metal

bj) Nickel and manganese

bk) Nonmetals

bl) Pyrex glass

Eutectic alloy of lead with bismuth

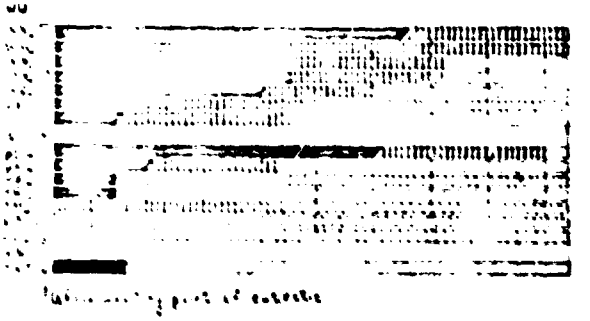

TABLE 33 (cont')

Stability of Structural Materials in Lead,

Bismuth, and Alloys of Lead, Bismuth, and Tin

bm) Ferrous metals

bn) Iron and carbon steel

bo) Cray cast iron

bp) 18-8 Stainless steel

bq) Nonferrous metals

br) Tungsten

bs) Beryllium

bt) Zirconium

bu) Titanium

bv) Aluminum

bw) Nonmetals

bx) Pyrex glass

Eutectic alloy of lead with bismuth and tin

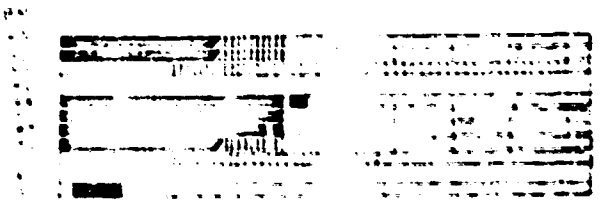

1- Good (suitable for extended service)

2- Limited (used only for brief applications)

3- Poor (unsuitable as structural material)

4- Unknown (insufficient data)

Crystallization gradually led to complete clogging of the tube and cessation of circulation. As shown by experiment, intensive transport of iron occurs at as small a difference in the hot and cold regions of the system as 0.0001%.

When similar experiments were conducted with nickel and molybdenum specimens no dissolution or transport of specimen material by the lead was observed. In these experiments, temperature of the lead was 600°C in the hot region and 550°C in the cold region.

The impurities contained in zirconium greatly influence its stability. For example, lead penetrated to a depth of about 0.025 mm into a specimen of zirconium with admixtures of magnesium and carbon held in a lead medium for five days at 1,000°C. In this case the crystals (grains) of zirconium in the penetrated zone did not change, as was shown by metallographic analysis. At the same time, lead did not penetrate as far into a specimen with a smaller admixture content after tests under the same conditions.

As Table 33 shows, certain metals (Cu, Ag, Sn, Zn, and Mn) cannot be recommended for use in a Pb medium even at low temperatures.

The majority of fireproof oxides and silicates have good resistance to the aggressive effect of Pb.

Carbides* have poor stability in lead.

During solidification, lead sometimes adheres to the surface of quartz and causes it to crack.

Bismuth. Bismuth reacts strongly with iron at temperatures above the point of austenitic transformation.

Beryllium is satisfactorily stable in a bismuth medium at temperatures up to 700°C, but at 1,000°C the corrosion rate becomes intolerably high.

---

* The experiments were conducted with intergranular-type carbides.

Bismuth has a more corrosive effect on stainless steel than lead does. Austenitic stainless steels containing nickel turn out to be less stable than chromic stainless steels such as type 446 steel.

Chrome-molybdenum and chrome-silicon steels (composition: 2.25% Cr; 1% Mo and 0.5% Cr; 1.5% Si) showed good stability in a bismuth medium under static conditions at a temperature of 500°C. The depth of intergranular penetration of bismuth in the surface layers of these steels amounts to no more than 0.1 mm/year. Magnesium, zirconium, and titanium in quantities of 0.005-0.05% give the best results as corrosion inhibitors. Steels with a high chromium content have lower corrosion resistance than medium and low-alloy chrome steels.

Crystallization of a Fe-Cr alloy in the cooler portion of the circuit is observed where there are considerable temperature differences in a stainless-steel system with flowing bismuth, as in the experiments with lead (see above). The time interval required for the entire pipe system to become clogged with crystals of the alloy can be relatively short (300-400 hours).

If the surface of the steel has oxidized noticeably, insoluble accumulations of the oxide Bi_2O_3 can be observed to form in the cold portions of the system.

The intensity of transfer of steel components by bismuth greatly decreases when zirconium and magnesium are added to the liquid metal. Thus, for instance, chrome-steel tubes 10-15 mm in diameter become completely clogged with the substances which have precipitated in the cold portion after 300-400 hours of operation, if the bismuth contains no additives. At the same time, when 0.01-0.1% Zr and 0.01-0.1% Mg are added to the liquid metal, no clogging of tubes more than 10 mm in diameter is observed even after 10,000-20,000 hours of continuous operation.

The decrease in the transport of steel components upon addition of zirconium to bismuth is usually attributed to the absorption of zirconium on the

Best Available Copy

steel surface and the formation of a layer on it protecting the material of the wall (mostly iron) from dissolution.

Unlike lead, bismuth reacts strongly with zirconium.

Nickel and nickel-base alloys disintegrate quickly in a liquid-bismuth medium. Cu, Mn, Mg, Zn, Pt, and Cr cannot be used in contact with bismuth. These metals form eutectic alloys with bismuth which have the following melting points, respectively: 270.3; 268; 260; 254.5; 266; and 139°C; and the following content of the elements listed, in per cent: 0.2; 0.6; 0.54; 2.7; 1.0; and 42.

Quartz was used successfully to manufacture vessels for liquid bismuth at working temperatures of 500 to 1,000°C. It should be borne in mind that bismuth wets quartz surface, "sticks" to it, and, expanding during solidification, can cause the material to crack.

Carbon is soluble in bismuth to 0.012% at 1,385°C and 0.017% at 1,408°C; at 1,000°C to substantially less than 0.01%. Graphite crucibles were used as liquid bismuth containers (~ 1,000°C) and showed fairly satisfactory corrosion resistance. Nonetheless, cases where crucibles were broken as the metal solidified in them were frequent.

The stability of heat-resistant metals in bismuth at high temperatures. Tests of certain heat-resistant materials in bismuth medium in the high-temperature range (800-1,500°C) were carried out by Reed [143]. The results of his experiments are given in Table 34.

TABLE 34

Corrosion of Some Heat-resistant Materials in Bismuth

(under static conditions)

Material	Temperature of bismuth, °C	Duration of experiment, hours	Content in bismuth after experiment, %	Experimental results
Molybdenum (99.9% pure)	1000	167	0.06	No corrosion observed, surface wetted by bismuth
	1430	2	—	No corrosion observed
Tungsten (99.9% pure)	1000	167	0.001	
Tantalum (99.9% pure)	1000	227	011	Strongly pronounced intercrystallitic disintegration, surface wetted by bismuth
Rhenium	1000	250	0.006	No corrosion observed
Kennametal				

TABLE 34 (cont')

Corrosion of Some Heat-resistant Materials in Bismuth

(under static conditions)

Material	Temperature of bismuth, °C	Duration of experiment, hours	Content in bismuth after experiment, %	Experimental results
Kennametal (K136A) (TiC = 80%, Co = 15% WC - TaC = 5%)	1000	188	0.01 Ti 0.02 Co	No corrosion observed
MPG graphite	1400	168	—	
MPT graphite	1400	168	—	
Silicon carbide (SiC)	1000	227	0.17 SiC	Specimen crumbled
Aluminum oxide	1000	150	0.0002 Al	No corrosion observed
Aluminum oxide, "Alundum" type	1345	2.5	0.99 Al	Corrodes slightly
Magnesium oxide	1000	227	0.01 Mg	Very slight corrosion

TABLE 34 (cont')

Corrosion of Some Heat-resistant Materials in Bismuth

(under static conditions)

Material	Temperature of bismuth, °C	Duration of experiment, hours	Content in bismuth after experiment, %	Experimental results
Zirconium oxide	1000	167	0.003 Zr	No corrosion observed
Molybdenum disilicide	1400	168	—	
	1000	337	0.002 Mo	
Thorium oxide	1000	167	0.06 Th	Corrodes slightly
Titanium carbide	1000	167	0.001 TaC	No corrosion observed
"Vicor" glass (tubes for specimens)	1000	167	0.002 Si	

The eutectic alloy of bismuth and lead (56.5% Bi; 43.5% Pb). Low-carbon steel is quite stable in Bi-Pb alloy to 500°C, provided the alloy is not permitted to oxidize. By transporting the steel carbides into the spheroidal state the

temperature limit indicated can be raised to 700°C, i.e., approximately to the austenitic transformation point. Certain investigators assumed that lead and the bismuth-lead alloy affect only the cementite component of steel without changing its ferrite component: for practical use they recommend one of the industrial brands of steel with a maximum carbon content of 0.12%.

Like lead and bismuth, the Pb-Bi alloy is more aggressive toward austenitic stainless steels containing nickel than toward chrome stainless steels.

The rate of corrosion of type 410 stainless steel in a eutectic bismuth-lead alloy (as in the case of bismuth) decreases in the presence of titanium. It has been established that adding titanium reduces in particular the rate of solubility of chromium in the liquid metal, simultaneously reducing the rate of solubility of iron.

Cast iron is liable to crack under prolonged service in Pb-Bi and therefore cannot be recommended for practical applications.

Surfaces of tungsten electrodes used to measure liquid-metal flows with magnetic flowmeters (see Chapter VI), gradually become dull in a eutectic Pb-Bi medium. This phenomenon is attributed to oxidation of the tungsten caused by oxygen contained in the alloy.

Tin. The corrosive effect of tin on structural materials is fundamentally determined by the intensity of intergranular penetration of liquid metal into the surface layer of the material. Intergranular penetration strongly affects the properties of metals, in particular, their ductility. If the material is affected by internal stresses, its stability with respect to liquid tin decreases greatly.

Tin reacts strongly with iron at temperatures above the point of austenitic transformation.

Cast iron and carbon steels have limited corrosion resistance in tin at temperatures up to 500°C; the austenitic and ferritic stainless steels are not

recommended for use at temperatures above 400°C.

Beryllium and titanium are not affected adversely by tin up to 500°C; the stability of zirconium in this temperature range is limited.

The elements W, Mo, Ta, Nb, Cr, and V can be used as structural materials for service in a tin medium.

The following elements cannot be recommended in view of their high solubility in liquid tin: Al, Ag, Au, Cd, Co, Cu, In, Mg, Ni, Pb, Pt, Se, Sb, and Zn.

Bismuth, lead, and tin alloys. The solubility of standard aluminum in the Bi-Pb-Sn eutectic alloy with a 45-v difference in the electric potentials of the wall and the liquid amounts to ~ 3%, while anodized aluminum under the same conditions dissolves in quantities of only 0.15%. When there is no potential difference, at the same temperature the solubility of anodized aluminum amounts to 0.9%.

The alloy containing 92% Pb and 8% Sn proves to be more aggressive with respect to Armco-iron and carbon and chrome steels than does pure lead.

Stability of heat-resistant materials in tin at high temperatures. Tests of certain heat-resistant materials in a tin medium in the high-temperature range (800-1,500°C) were conducted by Reed [143]. The results of his experiments are given in Table 35.

30. Transport of Activity in Liquid-metal Systems

The liquid metal circulating in the system becomes radioactive due to irradiation in a nuclear reactor. Under powerful irradiation, the activity of sodium is comparable to the activity of radium, which makes it difficult for the service personnel to approach the system when repairs are needed. In order to

reduce overall activity of the system to a safe level by removing the sodium from it, it is necessary to drain or flush 99.9999% of the metal.

TABLE 35

Corrosion of Certain Heat-resistant Materials in Tin

(under static conditions)

Material	Temperature of tin, °C	Duration of experiment, hours	Content in tin after experiment	Experimental results
Molybdenum (99.9% pure)	1000	338	1.69	Heavy corrosion
	1500	2	0.07	Heavy corrosion, molybdenum crystals in tin
Tungsten (99.9% pure)	1000	40	0.001	Negligible corrosion
Tantalum (99.9% pure)	1700	1	0.37	Heavy corrosion
Rhenium	1500	840	0.006	No corrosion detected

TABLE 35 (cont')

Corrosion of Certain Heat-resistant Materials in Tin

(under static conditions)

Material	Temperature of tin, °C	Duration of experiment, hours	Content in tin after experiment	Experimental results
Kennametal (K1384) TiC = 80%, Co = 15% WC - TaC = 5%	1000	168	0.003 Ti 3.42 Co	Washing out of cobalt from the alloy observed
AUF graphite	from 800 to 2,000	1	—	No corrosion detected
	1500	840	—	
Molybdenum disilicide	1000	168	0.0004 Mo 0.01 Si	Moderate corrosion
	1500	168	—	Heavy corrosion
Tantalum carbide	1000	168	0.98 Ta	Moderate corrosion
"Vicor" glass (tubes for specimens	1000	168	0.08 Si	Corrodes slightly

TABLE 35 (cont')

Corrosion of Certain Heat-resistant Materials in Tin

(under static conditions)

Material	Temperature of tin, °C	Duration of experiment, hours	Content in tin after experiment	Experimental results
Chromium carbide	1500	168	—	No corrosion detected
Tubes made of "Morganite" aluminum oxide	1740	1	—	

The activity of the metal remaining in the drained system risers, due to the presence in it of even negligible quantities (less than 0.001%) of radioactive admixtures having a long half-life. Amounts of admixtures which are negligible from the standpoint of their influence on the corrosion resistance of the materials and on the heat-transfer properties of the metal can prove to be intolerable due to the danger caused by radiation. The corrosion products of the structural materials form part of these admixtures. Corrosion proceeding even at a very negligible rate frequently causes considerable activity to spread throughout the entire circuit. Fission products of the nuclear fuel which get into the circuit of the heat-transfer medium are a source of activity, together with the metal itself and its admixtures.

Radioactive elements contained in the liquid-metal systems emit, as a rule, gamma- and beta-rays; in this case the gamma-radiation plays the major role, since beta-rays are completely stopped by the walls of the pipelines and boilers of the circuit.

The results of certain experimental studies of the transport of radioactive elements in sodium circuits made of type 347 stainless steel are discussed below. The method of determining the intensity of transport was common to all the experiments. An active source of known strength is made of stainless steel. It is placed in a sodium circuit made of the same kind of steel, but not active. The rate at which steel is removed from the source, in micrograms per square centimeter of surface per month, is determined by measuring the cumulative activity on the walls of the circuit. The value obtained in this manner differs from the rate of corrosion of the material in that it does not include the steel components dissolved in the liquid. Furthermore, in this case the transfer can be determined for the steel as a whole and for each of its radioactive components individually.

The transport is determined either in sealed containers (capsules) of small volume or in experimental loops (circuits). The capsule takes the form of a hollow cylinder, 25 mm in diameter and ~ 50 mm in height, in which specimens of the material studied and an active source are placed. The capsule is filled with sodium and placed in a muffle furnace where it is held for a given period of time. While in the furnace, the capsule is continuously rotated in such a way that the liquid metal washes the surface of the specimens at a given rate. After this the capsule is opened and the surface of the specimens studied to determine the depth of diffusion of the radioactive elements. If diffusion at the surface is not the object of study, the capsule itself can be used to determine the amounts of activity transported, and it is not necessary to place

specimens in it.

The installation of Fig. 110 is constructed on a similar principle, making it possible to study the influence of the oxygen content of Na on the intensity of activity transfer. It consists of two parallel vertical tubes joined at the bottom by a horizontal tube. An active source made of type 347 steel is placed in the bottom of one elbow and a test specimen of this steel in the bottom of the other elbow. The whole device is attached to a vibrating frame. The average rate at which the radiation source and the specimen are washed by the liquid is ~ 0.15 m/sec.

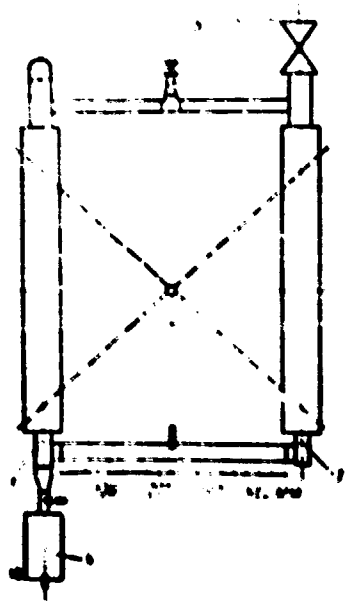

Fig. 110. Set-up for studying the influence of the oxygen content of sodium on the rate of activity transport. 1- active source; 2- valve for sodium; 3- specimen; 4- cold trap; 5- inert gas feed line.

A capsule in which liquid metal circulates by free convection or by means of a magnet is convenient in determining the intensity of transport of the material as a whole. A device of this type is shown in Fig. 111. Sodium is poured into a stainless-steel capsule into which are also placed a holder with the source of radioactivity, up to 10 steel test specimens, and a sampling ladle. The upper part of the capsule is connected to a glass-tube system fitted with stopcocks. As shown in the figure, the design of the device makes it possible to replace specimens and to remove the sodium selected for analysis from the capsule protected by the inert gas, without disturbing the source of activity.

Figure 112 shows a diagram of a set-up for studying the transport of radioactive elements in sodium contained in a circular tube. The tube is placed on a round plate. A special kinematic device communicates a reverse-rotating motion to it; the average liquid flow velocity reaches 4.5 m/sec.

Natural circulation circuits, with temperatures in their ascending and descending portions of 500-600°C and 100-150°C, respectively, are also used to study activity transport.

Very valuable results are produced by experiments conducted in forced circulation loops as well as in loops installed inside nuclear reactors. In the latter case it is possible to study the influence of radiation on the transfer process. Only one experimental installation of this type is known to exist at present. It was designed so as to fit completely into one of the ducts of an experimental reactor. The installation includes a section heated by the reactor,* an electromagnetic pump, and a heat exchanger in which irradiated sodium transmits its heat to a sodium-potassium alloy circulating in the secondary (nonradioactive) circuit. The entire assembly is cylindrical, ~4 m long and 140-170 mm in diameter. The total amount of sodium in the system is ~1,800 g;

* This section is also equipped with an electric heater.

it flows at ∽ 10 liters/min at maximum and minimum temperatures of 480°C (at the heated sector) and 310°C (at the outlet of the heat exchanger). The system is equipped with several shields which retain the neutron flux to prevent activation of the secondary circuit.

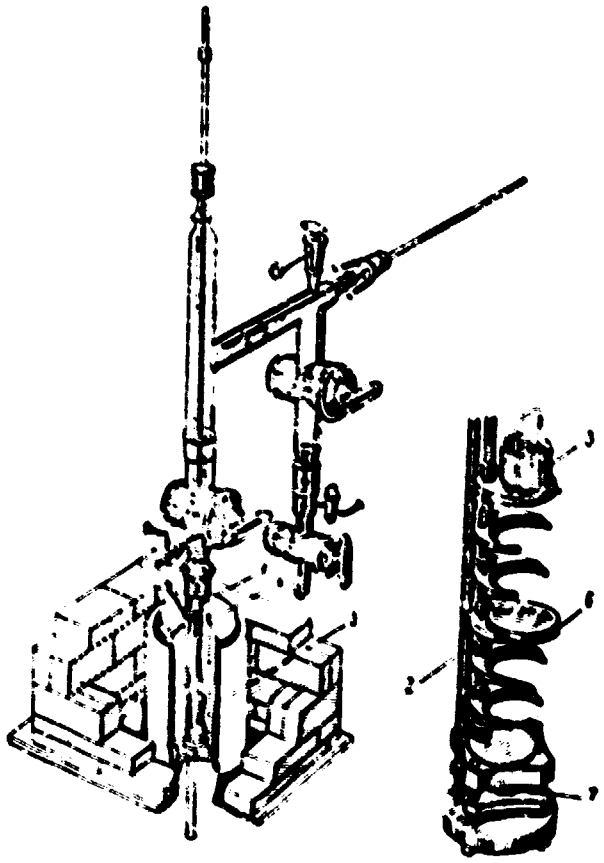

Fig. 111. Capsule for studying transport of activity by sodium under isothermal conditions. 1- Stainless-steel capsule; 2- holder; 3- sampling ladle; 4- furnace; 5- magnetic coil for stirring sodium; 6- specimen; 7- active source

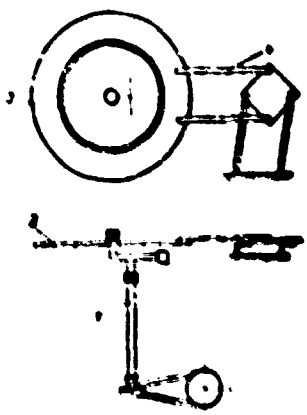

Fig. 112. Installation for studying transport of radioactive elements in sodium: 1- shaft; 2- plate; 3- tube with sodium; 4- linkage.

Experimental results. Table 36 gives some experimental figures on activity transport, obtained with the installations just described. If we take into account the considerable difference in the conditions under which these experiments were conducted, they may be considered to agree satisfactorily. As the table shows, the relationships between the rates of transport of individual elements were about the same in all the experiments.

TABLE 36

Rate of Transport of Certain Radioactive Elements by Sodium

(in $\frac{\text{microgram}}{\text{cm}^2 \text{ month}}$)

Specimen: type 347 stainless steel, $t \sim 500^\circ C$

O_2 content in Na, %	Capsules			Forced-circulation circuit	U-shaped capsule (Fig. 110)	Natural circulation circuit	Forced-circulation unit *	Ring-shaped tube (Fig. 11... *
	Isothermal conditions					Nonisothermal conditions		
	—	0.003	0.001	0.006	0.003	—	0.0035	0.003
Duration of experiment (in days)	30	79	10	20	7	101	80	28
Fe^{59}	3	0.7	0.4	2	2	—	—	—
Co^{60}	0.4	0.2	0.2	0.2	0.02	0.05	6	3
Ta^{182}	—	5	5	35	1	—	—	—
Mn^{54}	—	—	—	—	5	6	—	—

* Specimen made of type 316 stainless steel.

The values of activity transfer rates obtained in tests conducted by Haag [93], using an experimental loop placed inside a nuclear reactor, are given in Table 37. By apparent transport rate (see Table 37) for a given element is meant the decrease in the weight of steel corresponding to the value of the transported activity determined for a given isotope. The apparent rates are not the same for different isotopes since the intensity of the transport of an element is not proportional to its concentration in the steel. The individual transport rates given in Table 37 were determined by the apparent rates, allowing for the content of the given isotope in steel.

As shown by experiments, the following radioactive isotopes (all gamma emitters) basically determined the activity transport: Ta^{182}, Mn^{54}, Co^{60}, and Fe^{59}.

From the standpoint of effect on transport intensity, the composition of the active source, in particular the impurities in it, is of great importance. For example, tantalum and cobalt, present in stainless steel as foreign impurities are intensive gamma-emitters. The isotope Mn^{54} is formed from Fe^{54} in accordance with the (n,p) reaction occurring during irradiation of steel. Data from radiochemical analysis of a steel specimen which had sustained a neutron flux of $0.54 \cdot 10^{14}$ neutron/cm^2·sec for 35 days are given in Table 38. The table gives only the main gamma-emitters with half-lives of more than 30 days.

TABLE 37

Rate of Transport of Certain Radicactive Isotopes Contained in Stainless Steel (according to data for an experimental loop with 0.0034 oxygen content in sodium)

Isotope	Half-life	Apparent transport rate, $\frac{\text{milligram}}{\text{cm}^2 \text{ month}}$	Individual transport rates, $\frac{\text{milligram}}{\text{cm}^2 \text{ month}}$	Transport rate with respect to cobalt-60
Co^{60}	5.3 years	0.0032	$2.7 \cdot 10^{-6}$	1
Mn^{54}	315 days	0.13	—	—
Ta^{182}	115 days	0.20	$2.0 \cdot 10^{-4}$	75
Fe^{59}	46 days	0.012	$8.3 \cdot 10^{-3}$	3100
Cr^{51}	26.5 days	0.0006	$1.0 \cdot 10^{-4}$	40

It appears that heat treatment of steel influences the intensity of activity transport. For example, annealed specimens of 347 steel give a higher transport rate than specimens which have not been annealed. The surface cleanness of the source of activity and of the nonactive metal washed by the sodium played a dominant role. The most effective methods of cleaning stainless-steel surfaces are: washing with pure sodium, acid etching, electropolishing, and

high-temperature annealing in a hydrogen atmosphere.

Experiments conducted with ferritic steels and zirconium show that their activity transport rates are less than or equal to the transport rates for austenitic stainless steels.

The influence of the material of the tubes of the experimental circuit on the intensity of activity transport was specially studied. It appeared that in using the same source material (type 347 stainless steel) the intensity of transport to the surface of 316 and 347 steels was the same.

The value of the activity transferred to unit surface of the circuit is in inverse proportion to the ratio of this surface to the surface of the source. The parts of the system located closer to the source prove to be more highly activated.

The oxygen content of the sodium has a decided effect on the transport rate. According to Shaw [93] the transport rate of the isotopes Co^{60}, Fe^{59}, Ta^{182}, and Mn^{54} increases by 54, 17, 5, and 4 times, respectively, as the oxygen content of the sodium changes from 0.0027 to 0.0099%.

The addition of certain substances (inhibitors) to sodium reduces the intensity of transport. The action of transport inhibitors, apparently, is based on the decrease in the concentration of oxide in the liquid metal and on the formation of a protective layer on the surface of the steel which hampers the diffusive exchange between active and nonactive atoms.

The inhibitor should be soluble in the liquid metal and should have a low neutron absorption cross section to avoid parasitic capture of neutrons in the reactor; its irradiation products should not have high activity or long half-life.

TABLE 38

Data from Radiochemical Analysis

of an Irradiated Specimen of Type 347 Stainless Steel

(neutron flux: $0.54 \cdot 10^{14}$ $\frac{\text{neutrons}}{\text{cm}^2 \cdot \text{sec}}$, irradiation time: 25 days)

Radioactive isotope	Half-life	Number of decays per minute per gram of steel	Content of given element in the specimen, wt%
Fe^{59}	46 days	$1.7 \cdot 10^{10}$	66.4
Co^{60}	5.2 years	$7.3 \cdot 10^{9}$	0.071
Ta^{182}	117 days	$2.7 \cdot 10^{10}$	0.088
Mn^{54}	310 days	$8.7 \cdot 10^{7}$	—
Sb^{124}	60 days	$1.7 \cdot 10^{8}$	0.004
Ag^{110}	270 days	$1.4 \cdot 10^{7}$	0.0013
Zn^{65}	250 days	$1.3 \cdot 10^{7}$	0.0027

TABLE 39

Comparison of Effectiveness of Various Inhibitors of Activity Transport

(quantity of inhibitor, 1% by weight; specimen: type 347 steel)

Inhibitor	Oxygen content in sodium in ten-thousandths of a per cent		Free energy of oxide formation, kcal/gram-atom of oxygen	Effectiveness of inhibitor *
	Initial (before addition of inhibitor)	Final (after addition of inhibitor)		
Barium	42	27	115	17
Strontium	30	74	122	12
Calcium	45	27	133	10
Titanium	39	34	92	6.4
Antimony	30	43	40	5.7
Magnesium	38	19	127	5.6
Cerium	17	66	96	2.8
Tin	21	44	49	2.7
Nickel	28	78	43	1.8
Beryllium	23	75	121	0.7
Cesium	38	58	82	0.7
Chromium	19	26	71	0.5
Sodium	—	—	90	—

* The effectiveness of the inhibitor is defined as the ratio of the activity transport rate in pure sodium (no inhibitor) to the transport rate in the presence of an inhibitor.

MCL-554

A comparison of the effectiveness of various transport inhibitors is given in Table 39. As can be seen from the table, substances characterized by greater free energy of oxide formation, i.e., having greater chemical affinity for oxygen (see Chapter II) are generally better inhibitors. Substances whose energy of oxide formation is less than that of sodium (cesium, chromium, etc.) only increase the transport rate. In this case, the oxide protective film on a steel surface is destroyed rather than the inhibitor being oxidized. This is also shown by the increase in the oxygen content of the sodium (see Table 39). No distinct relationship is observed between the decrease in concentration of oxide in the sodium when an inhibitor is added to it and the effectiveness of the latter. The best transport inhibitor is barium. When 1% barium is added to sodium, the transport rate of Ta^{182} greatly decreases (10^4 times) as does the transport rate of Mn^{54}, Fe^{59}, Cr^{51}, and Co^{60} to a lesser degree (Co^{60} by 7 times). In order to make it possible to recommend using barium as an inhibitor under industrial conditions, it is necessary to find reliable methods of removing its oxide from the system.

It has been established that the amount of substance transported increases exponentially with temperature in accordance with equation:

$$\log A \quad \text{const} - \frac{8.39 \cdot 10^3}{T}, \qquad (69)$$

where A is the activity measured by the number of separate decays per minute per gram of material (stainless steel); T is the absolute temperature.

Experiments conducted using free convection of the liquid metal showed that the presence of a temperature drop in the system does not noticeably influence the intensity of activity transport. The experiments were conducted with relatively small concentrations of oxygen, and type 347 stainless steel served as the material for both the activity source and the capsule for the metal.

Time does not have as decided an effect on the rate of transfer as do the temperature and oxygen content. Tests carried out using various experimental set-ups gave different results for the function relating the amount of activity received by a steel surface and the time. It has been established that the depth of the activated layer can reach 2.5 mm after an installation has been operating for five months at a temperature of 400-450°C. It may be assumed when designing liquid-metal-reactor cooling circuits that the amount of activity received by the surface of the circuit is proportional to the length of operation.

The liquid flow velocity has little effect on the intensity of activity transport. The same can be said for the influence of a strong neutron flux (up to 10^{13} neutron/cm^2·sec) on a specimen.

The results of the experiments make it possible to revise the upper limit of the rate of activity transport in industrial installations.

The concentration of atoms of any radioactive element in structural material[1] located in the core of a reactor obeys the following law:

$$\frac{dN^*}{d\tau} = e - \lambda N^*, \qquad (70)$$

where N^* is the concentration of activated atoms in steel irradiated inside a reactor, atom/g;

e is the rate of formation of a given radioactive element as a result of the absorption of neutrons, in atoms per second per gram of material;

λ is the radioactive decay constant of the given substance; 1/sec;

τ is the time of operation of the installation at a given neutron flux density, sec.

---

[1] In this case, stainless steel.

Integrating Eq. (70) for an initial concentration N^* equal to zero produces the following expression:

$$N^* = \frac{a}{\lambda}(1 - e^{-\lambda t}). \tag{71}$$

Since the activity A of a given element is expressed by the number of nuclear decays per second per gram of material, equal to λN^*, we have

$$A = a(1 - e^{-\lambda t}). \tag{72}$$

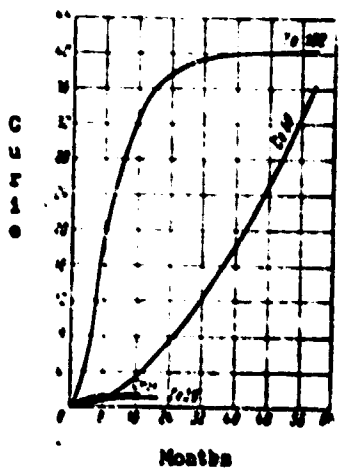

Fig. 113. Activity transport in a hypothetical system.

Let us calculate the activity of material removed from a reactor by sodium. The quantity of activated atoms N_b^* removed from the reactor obeys the equation:

$$\frac{dN_b^*}{dt} = RN^* - \lambda N_b^*, \tag{73}$$

where R is the intensity of activity transport (in grams per second), i.e.,

the specific transport rate (in grams per second per unit surface), multiplied by the area of the source of activity.

The value λN^{*}_{D} entering into Eq. (73) represents the rate of decay of the transported atoms. Combining Eqs. (71) and (73) we get:

$$\frac{dN_D}{dt} + \lambda N_D^{*} = \frac{R}{\lambda} \sigma (1 - e^{-\lambda t}) \quad . \tag{74}$$

Integrating Eq. (74) for a transported activity of zero at the initial instant of time gives:

$$N_D^{*} = \frac{R\sigma}{\lambda^2} (1 - e^{-\lambda t} - \lambda t e^{-\lambda t}) \tag{75}$$

Then the total activity transported, expressed in terms of the number of nuclear decays per second, is

$$A_D = \lambda N_D^{*} = \frac{R}{\lambda} \sigma (1 - e^{-\lambda t} - \lambda t e^{-\lambda t}) \tag{76}$$

Table 50 and Fig. 113 give data for an approximate calculation using the method described for a hypothetical thermal-neutron reactor. The transfer of radioactive Fe, Cr, Ta, and Co was computed, i.e., the elements which settle on the surface of steel, since the radioactive isotopes Ag, Sb, Sn, and Zn evidently remain dissolved in the liquid sodium. The values of the rate of transport obtained in experiments with a liquid-metal loop placed inside a reactor were used in the calculations. The neutron flux was assumed to equal 10^{14} neutrons/cm^2 sec; the area of the surface of the reactor absorbing this was assumed to be 10^6 cm^2. Only gamma-radiation was computed since the beta-rays were stopped by the tube walls.

TABLE 40

Activity Transport in a Hypothetical System

Radioactive isotope	Content in stainless steel, %	Specific rate of transfer $\frac{\text{microgram}}{\text{cm}^2 \text{ month}}$	$\frac{K}{\lambda}$	$\frac{\text{Curie}}{\text{g}}$	Number of γ-quants per decay	Time, months	$1-e^{-\lambda t}$	Transported activity A_b, curie
Cr^{51}	17	10	13	3.72	0.03	1	0.181	0.263
						2	0.455	0.662
						4	0.812	1.18
						6	0.945	1.37
						9	0.992	1.44
						max	1.0	1.45
Fe^{59}	70	10	21.7	0.0556	1	1	0.079	0.095
						2	0.241	0.290
						4	0.552	0.665
						6	0.765	0.922
						12	0.974	1.17
						max	1.0	1.20
Ta^{182}	0.01	200	1068	0.0189	2	1	0.015	0.606
						4	0.132	5.33
						6	0.309	12.5
						12	0.658	26.6
						24	0.939	37.9
						36	0.991	40.0
						60	1.0	40.4

TABLE 40 (cont')

Activity Transport in a Hypothetical System

Radioactive isotope	Content in stainless steel, %	Specific rate of transfer $\frac{\text{microgram}}{\text{cm}^2 \text{ month}}$	$\frac{R}{\lambda}$, g	σ, [illegible], %	Number of γ-quants per decay	Time, months	$1-e^{-\lambda t}$	Transported activity A_b, curie
Co^{60}	0.05	3	274	0.47	2	1	0.00006	0.0155
						6	0.00206	0.532
						12	0.0079	2.03
						24	0.029	7.48
						36	0.059	15.2
						60	0.142	36.6

The radiation level caused by settling of active substances in the circuit can be calculated for the system with a given arrangement of equipment, provided that the distribution of activity along the inner surface of the circuit is uniform. Calculations showed that after six months of continuous operation of a hypothetical reactor, the part of the circuit located outside of the zone affected by the neutron flux becomes so contaminated by radioactivity that access of personnel to it must be limited to 40 hours a week. After 36 months of operation, the time of access is reduced to several hours. These data were obtained on the assumption that the rate of accumulation of activity in the system is constant with time. Since, in fact, the transport rate gradually decreases with time, the

true danger of radiation sickness among personnel will be less.

(End of Chap er IV)

PART TWO

DESIGN AND OPERATION OF LIQUID-METAL SYSTEMS

CHAPTER V

SYSTEM DESIGN

(PROYEKTIROVANIYE SISTEM)

31. General Principles of Equipment Layout

The individual units of a liquid-metal circuit should not be located too close together, since there must be free access to any point of the system.

The layout of equipment in a liquid-metal installation should provide for possible natural circulation of the metal in the system, for example during an emergency shutdown of the circulation pump. For this purpose, the source of heat for the system should be installed in the lower part of the circuit, and the heat-removal unit at the top.

Arrangement of Tubing. All the tubing in the circuit should be placed at an angle to the horizon in order to make it easier to load and flush the system as well as to drain the liquid metal from the installation. With the tubes arranged horizontally, as the system is loaded by pushing the metal from the tank under the pressure of an inert gas, gas pockets form. If this happens, it is necessary to drain the gas from each pocket separately. Loading the circuit under vacuum makes it possible to avoid the appearance of gas pockets, but requires a large amount of time and is inconvenient when charging operations are repeated frequently. In horizontal tubing some of the liquid may remain after drainage, forming plugs of solidified metal or its oxides. Such plugs make flushing and further operation of

the circuit more difficult.

Electromagnetic liquid-metal pumps should also be at an angle to the horizon, with the pressure end higher than the suction end. Gas bubbles getting into the flow can become trapped in the pump duct, since gaseous substances are not affected by a magnetic field and therefore cannot be moved by the pump. Gas entering the pump causes unstable operation and reduced efficiency. This undesirable effect (especially dangerous at low metal flow velocities, when the gas bubbles cannot be carried away by the flow of liquid), is excludedaltogether when the pump is arranged as described above (the bubbles rush upward under the pressure of the liquid and under the effect of their own buoyancy).

Normally a pipe angle of about 3° is adequate to assure complete drainage of the metal from the circuit. Units of the installation being designed which are difficult to drain must be fitted with special heated drainage lines.

Position of the breather (expansion) tank in a circuit. An expansion breather tank is an inherent part of any liquid-metal circuit, since the volume of metal increases quite a bit upon heating. For example, when the temperature was raised from 40 to 650°C, the volume of a sodium-potassium alloy (44%K) increased by 20%.

It is most advisable to locate the expansion tank in the upper part of the circuit, where the pipeline supplying inert gas to the installation can also be connected. The gas bubbles entrained in the liquid will be caught in the tank, and at the same time, a leak in the gas ducts will not cause leakage of the molten metal.

It is recommended that the expansion tank be situated on the suction side of the liquid-metal pump, i.e., where the pressure inside the circuit is minimal. In this event, the inert gas can be maintained at low pressure in the tank, as a result of which its walls can be made relatively thin. Furthermore, such location of the expansion tank makes it possible to combat cavitation at the pump intake by raising the pressure of the inert gas in the tank.

Position of dump (loading) tank. The drainage of liquid metal from a system has its own peculiarities, depending on the arrangement of equipment used. If the circuit includes a loading (dump) tank and an expansion tank (Fig. 114) the metal can be drained into the dump tank under the effect of gravity; to speed draining of the system the feed of inert gas in the expansion tank can be increased and, simultaneously, some of the gas in the dump tank can be released. A drain valve must be installed on the pipe connecting the circuit with the loading tank.

In the event the dump tank is simultaneously used as an expansion tank (Fig. 115), there is no drain valve in the system and drainage is carried out just by dropping the pressure in the dump tank and feeding some inert gas into the upper part of the circuit.

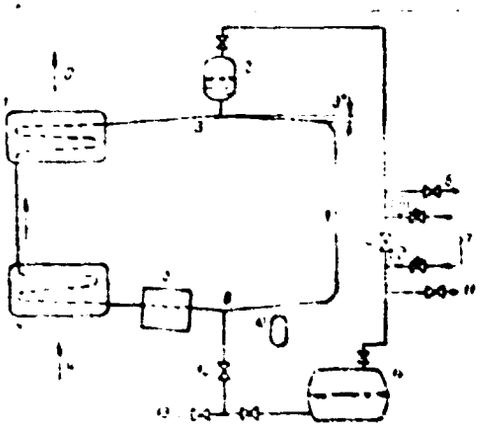

Fig. 114. Diagram of equipment layout in a liquid-metal circuit (variant I).

(1) Heat exchanger for removing heat;

(2) expansion tank; (3) upper point of circuit;

(4) valve for equalizing pressure in the inert gas system;

(5) pump; (6) and (11) valve for blowing inert gas through the system and evacuating;

(7) inert-gas feed line; (8) low point of circuit;

(9) heat exchanger for supplying heat;

(10) cold trap; (12) drain valve; (13) valve for flushing the system; (14) dump (loading) tank.

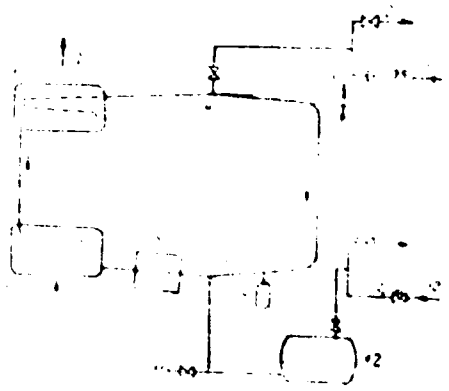

Fig. 115. Diagram of equipment layout in a liquid-metal circuit (variant II).

(1) Heat exchanger for removing heat; (2) and (8) valve for blowing inert gas through the system and evacuating; (3) and (10) inert-gas feed line; (4) upper point of circuit; (5) pump; (6) heat exchanger for supplying heat; (7) low point of circuit; (9) cold trap; (11) valve for flushing the system; 12) dump (loading) tank.

The second tank location (Fig. 115) is less desirable since, first of all, the absence of a drain valve requires constant checking of the gas pressure in the expansion tank in view of the fact that the level of the liquid metal in the circuit must be constant, and, secondly, the line feeding inert gas to the upper point of the circuit, usually of a small diameter (5 to 10 mm), in operation can become plugged with solidified metal or its oxides, which will cause difficulties in drainage.

The volume of the dump tank should be 1.5— 2 times the volume required for loading the metal system (in solid form). This tank-capacity margin is necessary in view of the following considerations: (1) the volume of metal can increase due to heating in the tank or if hot metal enters the tank during drainage; (2) a need to refill the liquid metal can arise during operation; and (3) a part of the volume of the tank should be occupied by inert gas.

Separate lines draining individual portions of the circuit should be connected to the dump tank. In order to ensure the reliability of the drainage (loading) line, it is recommended that two valves be installed on it in series. It is convenient to connect a feed line for the liquid used for flushing the circuit between the valves, as shown in Fig. 115. It is not advisable to use drainage line sectors with frozen-in metals instead of drain valves, because of the need for special means of cooling and heating the line and undesirable delays arising during loading and drainage of the system.

The diameter of line required for sufficiently fast drainage depends on the particular peculiarities of the system: its capacity, equipment layout, etc. It has been established by experience that using of drain lines 50 mm in diameter with circuit lines 200 mm in diameter and drain pipes 25 mm in diameter with pipelines 75 mm in diameter does not cause any difficulties in drainage. Use of drain pipes 10 to 12 mm and less in diameter is not recommended even for low-capacity liquid-metal circuits.

Position of outlets for monitoring and measuring instruments. Liquid metals or their vapors getting into circuit instrumentation outlets can cool there, plugging the outlets with solidified metal and oxides. Hence, it is advisable to design the outlets so that they are heated by the fluid circulating in the main conduit. The intensity of natural convection of a liquid metal in an outlet will, evidently, vary depending on the location of the outlet with respect to the main duct. It is very desirable to situate the outlet above the main duct where heat transfer through natural convection is the most intense. Locating an outlet below the main conduit is inadvisable because it is not well heated, and the metal will remain in the outlet after the circuit is drained.

The diameter of the outlet should be at least 5 to 6 mm in order to avoid clogging.

Arrangement of cold traps in sodium and sodium-potassium circuits. Cold traps for sodium and potassium oxides are installed in the coldest sectors of the circuit, making it possible to achieve sufficiently low temperature of the liquid metal in a trap with minimum heat loss. Cold traps constructed as cooled settling tanks (see Chapter VII) are, as a rule, connected to a horizontal portion of the main duct and installed below it (Figs. 114-115). Such a trap should be equipped with a drain line and valve for removal of accumulated oxides.

Cold traps constructed as cooled filters (see Chapter VII) are installed parallel to the main duct of the circuit.

32. Behavior of Structural Materials in Liquid Metal Circuits

The physical and chemical properties of liquid metals differ greatly from the properties of fluids used in power engineering (water, steam), as a result of which the proper selection of materials in the design stage is impossible without thorough study of these properties. For example, the high thermal conductivity of liquid metals leads to the possibility that sharp local temperature variations may appear (thermal shocks), promoting additional thermal stresses in the metal wall.

Therefore, critical parts of equipment should be designed not only for tensile strength and creep strength but for resistance to thermal shock as well. The specific problem of corrosion of various structural materials in liquid metal (see Chapter IV) can also serve as an example.

During the transfer of heat through the walls of pipes, collectors, etc. in liquid-metal heat exchangers, a considerable part of the total temperature drop is formed by the temperature drop in the wall, since, as a result of a high heat-transmission coefficient, the temperature drop on the liquid-wall boundary is negligible. At the same time, the thermal stresses arising in the metal of the wall are proportional to the temperature difference across it. Therefore, in designing liquid-metal heat exchangers, special attention should be paid to the possibility of the appearance of thermal stresses.

Thermal stresses should be calculated for both steady-state operation of the installation as well as for non-steady-state conditions, where the stresses can be maximum. The results of calculations for determining the stresses in the housing of a molten-sodium-cooled reactor are known. For a sharp rise in sodium temperature from 370 to 425°C, as can happen under sharp increases in the power of the installation, the thermal stresses in a chrome-nickel-stainless-steel housing can reach 2,700 kg/cm^2.

Most of metal-fatigue tests, relating degree of deformation of a specimen and the number of loading cycles to rupture have been carried out in the air. The following is known about the fatigue strength of steels in liquid metals.

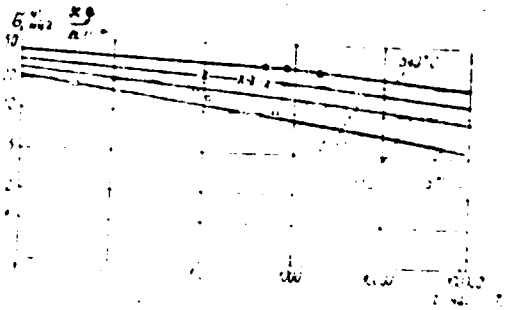

Fig. 116. Comparison of the creep resistance of type 347 stainless steel in molten sodium and in air. Tests in sodium: ● – 540°C; X – 595°C; ○ – 650°C; □ –705°C. ——— are data on tests in air at same temperatures.

Bending tests conducted on specimens of type 347 stainless austenitic steel placed in molten sodium at a temperature of 725°C, showed that the fatigue strength of the material does not drop when air is replaced by liquid metal. Tests of the same steel to rupture under prolonged loading in air and sodium led to similar results (Fig. 116).

The effect of sharp temperature variations on the serviceability of steel was studied using an experimental circuit consisting of a pipeline to the inside of which type 347 stainless-steel specimens were welded (Fig. 117). A tubular specimen 200 mm in diameter and 900 mm long was preheated to the desired temperature. Thermal shock was applied to the specimen by pumping a relatively cold sodium-potassium alloy through it.

The maximum temperature of the specimen amounted to 480°C and the maximum

rate of cooling to 130°C/sec, with an over-all temperature drop of 270°C. Metallographic analysis showed that the thermal stresses arising under these conditions caused intercrystalline cracks to appear in the metal, resembling fatigue cracks. The cracks appear at points of stress concentration and propagate along inclusions in the metal. The results of thermal fatigue tests of steel show that failure of the specimens was caused by the following factors:

(1) Defects in butt welds;

(2) poor-quality machining of the metal surface;

(3) internal defects in the pipe walls.

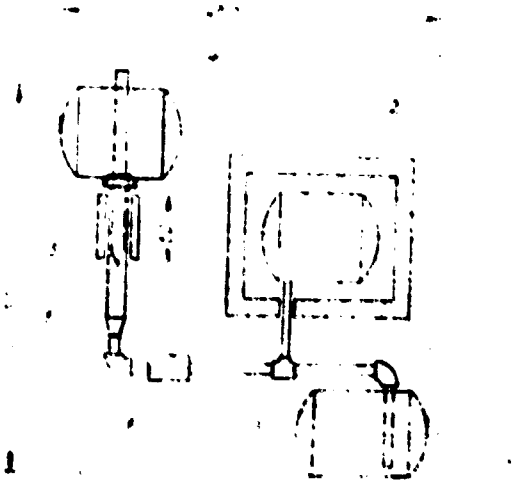

Fig. 117. Diagram of experimental liquid-metal circuit designed to test pipe specimens under thermal shock. (1) Specimen; (2) alloy preheating tank; (3) dump tank; (4) upper tank; (5) heater; (6) pump.

In the first case two lengths of pipe were butt-welded with a ring lining; the ring was not fitted tight enough to the pipe surface, so that during welding some of the metal flowed into the wedge-like gap formed. When the weld seam shrank a fissure formed in this spot, which is why a fatigue crack formed.

In the second case, the pipe wall was prepared for welding with a dull tool, causing failure. The cold hardening of the surface material occuring when the surface was treated contributed to the decrease in fatigue strength.

The third case pertains to the cracking of a pipe where it extended into the opening of the pipe sheet; the crack was caused by a defect in the material of the pipe.

In calculating structures for creep strength, it must be borne in mind that the harmful influence of the internal stress concentrations on the creep resistance of a metal increases with rising temperature. The internal stress concentration also reduces the corrosion resistance of the metal, which in turn tends to decrease its strength. For example, a case is known where numerous cracks appeared in the spot where steel pipes were welded into the pipe sheets of a sodium-to-water heat exchanger; the cracks first appeared on the water side as a result of corrosion. The water preheater made of type 304 heat-resistance steel failed after two sharp rises in the temperature of the sodium to 425°C, having functioned for only 48 hours. It turned out that the water entering the preheater had high content of chlorides, which react with austenitic steels.

As shown by the results of an endurance test of a model of a sodium-heated bent-tube water-vaporizer (Fig. 172), metal failure (appearance of cracks) is detected in the spot where the tubes were welded into the massive pipe sheet, i.e., in the region of the greatest bending moment. A similar model with lighter pipe sheets did not fail under identical test conditions.

Behavior of welded, soldered, and detachable joints in sodium.

Experience in the operation of sodium circuits shows that welds possess the same corrosion resistance as the base metal (usually stainless steel of austenitic or ferritic type). Slag cannot be permitted to form in the weld, since the slag will be washed away by the liquid metal.

When using soldered joints, it should be borne in mind that certain solders (silver, for example) do not have adequate corrosion resistance in liquid sodium. An alloy containing 60% manganese and 40% nickel, as well as the chrome-nickel-silicon alloys, can be recommended for use as solders.

On the basis of laboratory investigations (see Chapter IV), one could conclude that liquid-metal circuits should not be made of dissimilar materials, since transfer of certain chemical elements from one material to another was observed. However, no transfer can be observed under operating conditions. For example, sections of a sodium circuit which had functioned in the Knolls Atomic Power Laboratory (USA) for several years were made of several different materials (austenitic stainless steel, nickel, Inconel, and ferritic steel), and no interaction between them was detected.

When there is close contact between any two metallic surfaces in liquid sodium (for example, the male and a female threaded surfaces, or a valve and its seat), two undesirable phenomena are observed. The first is surface abrasion, and the second, self-welding. Abrasion can be avoided by the proper selection of the structure of parts joined, for example, by the use of tapered threads instead of conventional thread when necessary. Furthermore, special treatment of the surface (nitriding or chrome plating) can be used. Nitriding at a depth of from 0.025 to 0.075 mm effectively prevents abrasion. The use of lubricants such as mineral oils or disulfides of molybdenum and graphite to reduce abrasion is not recommended since these substances cannot adhere to the friction surfaces, and furthermore they react with the molten sodium.

The self-welding of parts occurring as a result of prolonged contact under pressure and at high temperatures is best avoided by using dissimilar materials for the contacting surfaces. Special surface treatment (nitriding, for example) also counteracts self-welding

Quality control of structural materials. A high standard of quality is required of materials used to manufacture equipment for liquid-metal circuits. The material of pipe walls, collectors, tanks, etc., must be free of blow holes, cavities, and nonmetallic (slag) inclusions, since the slightest seepage of air into the system or leakage of the liquid metal (radioactive, in many cases) is permissible.

Ultrasonic defectoscopy, which is not always absolutely reliable, is frequently used to detect blow holes and cavities inside the metal. Small cavities in the material can be detected by color defectoscopy. This method is also useful in detecting nonmetallic slag inclusions.

Such inclusions are extremely dangerous, since they remain undetected during seepage tests of the assembled liquid-metal circuits even when a helium leak detector with an extremely sensitive mass-spectrometer is used, permitting the detection of the slightest seepage of helium from the circuit. In service, the slag inclusions start to interact with the molten metal, gradually being washed out by it; this can cause a dangerous leak.

Especially strict standards should be applied to material for the tubes of heat exchangers.

33. Design of Piping

Calculation of thermal stresses. The operating conditions for piping in liquid-metal circuits differ from those for conventional piping in that the operating temperatures are higher and the possibility of thermal fatigue of the material of the walls is greater.

The stress caused by thermal expansion in the wall of piping operating at a high temperature should not exceed the following values:

$$\sigma_t \leq A(1.25\sigma_c + 0.25\sigma_t). \qquad (77)$$

in which σ_c is the permissible tensile stress for a given material at room temperature;

σ_t the same at the operating temperature;

K safety factor allowing for a decrease in the strength of the material under the effect of cyclic variations in temperature.

As Eq. (77) shows, the value σ_t is determined chiefly by the permissible stress for a cold metal, deviating from it by at most 16.7%. This is explained by the fact that with rising temperature the modulus of elasticity of the material and thus the elasticity of the pipe wall, rises despite a decrease in strength.

Formula (77) gives the minimal value of the effective stress, which must be increased if other additional loads act on the wall of the pipe (internal pressure, gravity). In this case the value of the additional stress should be added to the second term in the parenthesis of Eq. (77). As a rule this will not exceed $0.25\sigma_t$. Actually, the stresses due to internal pressure are usually negligibly small due to the low pressure in liquid-metal circuits and relatively great thickness of the pipe walls. At the same time, the piping supports are designed in such a way that the stresses in the metal caused by the structure's own weight amount to $0.25\sigma_t$. Hence, the total value of the second term in the parenthesis of Eq. (77) is equal to about $0.5\sigma_t$. This value makes up a significant proportion of the total stress σ_t in the low- and medium-temperature ranges, but at temperatures above 600°C it is inconsequential since at $t > 600°C$ the stress σ_t drops sharply.

The value of the coefficient K in Eq. (77) is selected in accordance with the number of thermal cycles in the operation of the installation, depending on the operating conditions. If the installation is subjected to the effect of less than 7,000 cycles, then in a majority of cases it turns out that the coefficient K can be assumed to equal unity; if the number of cycles exceeds 7,000, K decreases, reaching 0.5 when the number of cycles equals 250,000 and more.

It should be noted that piping is more durable with respect to thermal shock than are other elements of liquid-metal installations. First of all, they have greater elasticity and can withstand considerable plastic deformation without breaking. Secondly, the pipelines are thoroughly heat-insulated on the outside, as a result of which their temperature is close to that of the liquid metal and the temperature drops across the pipe walls are low. Since the internal heat stresses in the wall are proportional to the given temperature drop they may also be low. These ideas are confirmed by experiment. During numerous thermal shock tests (the number of cycles reached several thousands) of a pipeline with molten sodium flowing through it, no traces of wall failure were discovered, despite the fact that the rate of the temperature variation reached 500 deg/sec.

In designing pipelines it is not necessary to make calculations for creep, since a slight deformation due to creep is not dangerous. Furthermore, such deformation relieves the internal stresses in the metal arising at high temperatures. Creep is dangerous only when the region of deformation is not uniformly distributed along the length of the pipe, but occurs in only a limited section of pipe. Local deformation can increase gradually and lead to failure.

A means of combating the appearance of thermal stresses in a pipeline is prestretching, where the rough piping is made somewhat shorter than required and then artificially stretched in the cold state during assembly. The internal stresses in the metal caused in this fashion decrease with rising temperature; therefore, it is as serviceable at high temperatures as at low.

The question of compensating for thermal expansion should be given careful attention when designing pipelines, since the operating temperatures and the coefficients of thermal expansion of the piping material are great in this case. Actually, types 304, 316, 321, 347, and 310 austenitic stainless steels have a coefficient of linear expansion about 40% greater than that of the carbon steels (Fig. 118), possessing, at the same time, fairly low thermal conductivity (Fig. 119).

Satisfactory compensation for thermal expansion can be achieved in the circuit by including bent-tube sections, possessing the required elasticity. In using corrugated pipes or bellows, they should be arranged strictly vertically, in order to assure reliable drainage of the liquid metal. However, the installation of compensating devices should be avoided if possible, since they reduce the strength and the reliability of the structure.

In assembling installations, it should be borne in mind that the relative displacement of liquid-metal piping when the system is heated can be greater than the displacement of standard piping due to the greater working temperature of the liquid.

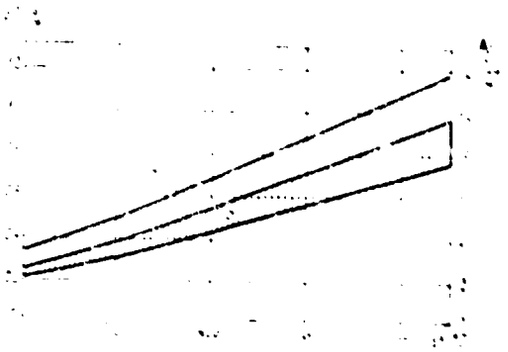

Fig. 118. Linear expansion of certain steels.

(A) Austenitic steels; (B) ferritic steels.

Δt Difference between working and room temperatures.

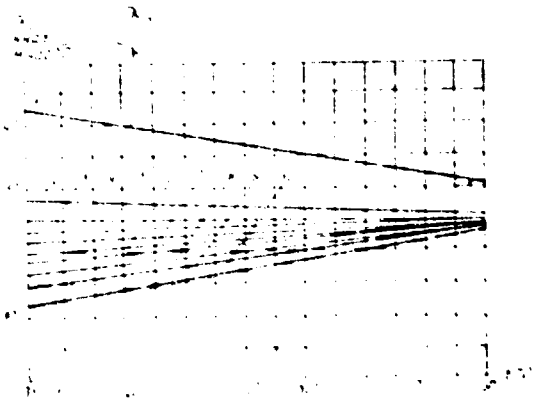

Fig. 119. Thermal conductivity of certain steels.
(1) Carbon, 0.2% C; (2) 1% Cr; 0.5% Mo;
(3) 2% Cr; 0.5% Mo; (4) 5% Cr; 0.5% Mo;
(5) 2.5% Cr; 0.5% Mo; (6) 3% Cr; 0.5% Mo; 1.25% Si;
(7) 5% Cr; 0.5% Mo; 1.5% Si; (8) 27% Cr;
(9) 18% Cr; 8% Ni; (10) 25% Cr; 20% Ni.

Pipeline junctions. Only seamless pipes should be used for piping in liquid-metal circuits.

Whereever possible, the pipelines should be joined by butt welding. Butt welding has the following advantages: (1) The quality of weld seams can be easily inspected by x-ray defectoscopy; (2) the flexibility of the pipeline does not decrease noticeably. It is recommended that pipelines be butt-welded, employing gaskets. Where possible the gasket rings are removed mechanically after welding, in order to make it easier to drain the liquid metal from the piping. A high-quality weld is produced when special gasket rings are used which melt during welding (Fig. 120). Good results in pipelines are obtained by welding with tungsten electrodes in an argon-protective atmosphere.

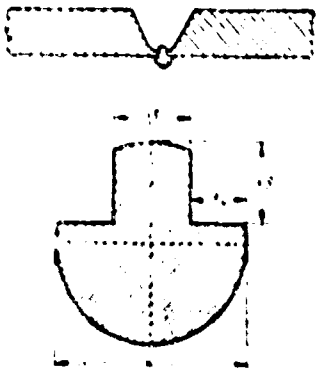

Fig. 120. Use of special gasket rings in butt welding of pipelines.

If the diameter of the joined pipes is 25 mm or less, it is recommended that unions be used. The use of gaskets in this case is inadvisable, since the cross section for the passage of liquid is sharply reduced.

In design, it is necessary to avoid welded joints with sharp transitions from one thickness to another; for example, in butt-welding two pipes, the thickness of the wall of one of the pipes should be changed smoothly along its length, so that at the weld the walls of both pipes have identical thicknesses; i.e., it is necessary to take measures to prevent internal stress concentrations in the metal (see Figs. 121 and 122).

Welds serving to hold elements of the circuit to beams, stands, etc., should be welded along the entire length so as to secure good thermal contact between the fixtures and the welded part and in this manner to prevent the appearance of thermal stresses.

The following welding standards are compulsory in the Knolls Atomic Power Laboratory (USA):

1. If the seam functions under load, it should be filled with weld metal along the entire thickness of the wall.

2. Corner-weld joints of parts are undesirable and are allowable only when the thicknesses of the parts in the weld region are identical.

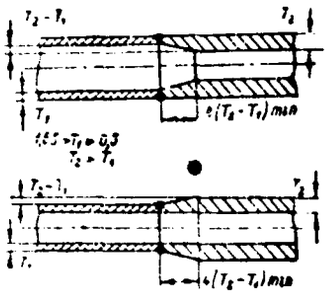

Fig. 121. Recommended structures of butt-welded pipeline joints.

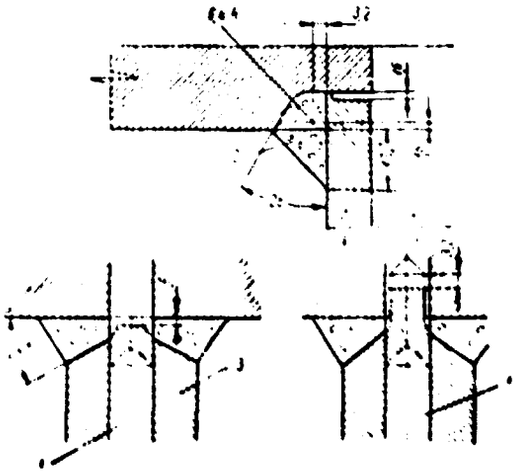

Fig. 122. Recommended structure of welds for high-temperature service.

(1) Drilled after welding; (2) corner seam;

(3) nipple.

The possibility of cracks appearing in the welds decreases when electrodes made of a material with high ferrite content are used. However, when the seam is subjected to a high temperature (above 550°C), a considerable ferrite content in the weld metal is unacceptable, since it promotes increased brittleness of the material as a result of the presence of the sigma-phase in it.

Flange couplings in sharply changing temperature conditions are not noted for high reliability and their use in liquid-metal circuits should be restricted to instances where other types of joints cannot be used, for example, when joining parts made of dissimilar materials or when there is a need for frequent replacement of parts of the circuit.

In designing flange couplings, a material for the bolts should be used with a smaller coefficient of thermal expansion than the material of the flange itself.

The selection of material for gaskets is determined by the operating conditions of the flange coupling. Copper and aluminum gaskets can be used in sodium at temperatures below 200°C, and stainless steel or nickel gaskets at temperatures above 200°C. The "ball in cone" gasketless type of flange coupling is one of the most reliable, although the integrity of its seal can be affected when it is frequently assembled and disassembled. Threaded coupling of pipelines for liquid-metal installations can be recommended only for brief service at low temperatures (below 250°C). Threaded pipe couplings for sodium and sodium-potassium* are assembled with special lubrication; the most satisfactory results are shown by a lubricant consisting of a mixture of lead oxide (PbO) and glycerin. It should be borne in mind that the lubricant can be a source of impurities for the circulating metal.

---

* Such couplings are not recommended for pipes with diameters larger than 25 mm.

Coupling unions with thoroughly tight surfaces are suitable for coupling carbon-steel and stainless-steel piping. They are about as reliable as flange couplings. Unions for pipelines with diameters below 25 mm, through which a sodium-potassium alloy was pumped at temperatures up to 550°C, were subjected to operational tests and showed satisfactory serviceability.

Copper piping with bronze fittings can be used in working with a sodium-potassium alloy at temperatures below 120°C. However, sharp temperature variations in the liquid metal (thermal shocks) should be considered. The fact of the matter is that bronze becomes highly strain-hardened during assembly of pipeline couplings. For this reason, stresses due to strain hardening are added to the internal stresses in the wall of the union due to thermal fluctuations, and the union can crack.

Stainless-steel fittings remain serviceable at elevated temperatures (up to 750°C).

34 Thermal Insulation

The following are the specific quality requirements for thermal insulation of liquid-metal circuits: the insulating material should not react chemically with the liquid metal; as far as possible, the insulation should be impregnable to the liquid metal; the mechanical and thermal properties of the insulation should not change when irradiated.

Let us list the more widely-used thermal materials:

1. Fire-resistant high-density mineral fiber.

2. Compressed mineral wool or glass fiber.

3. Loose mineral wool or glass fiber (density not greater than 100 kg/m^3).

4. Asbestos, with low content of water of crystallization in the form of thread or packed (amosite).

5. Special molten aerogel.

6. Magnesia (85%).

7. Molten diatomite.

8. Molten calcium silicates.

9. Stainless steel chips.

10. Slag wool.

11. Metallic foil with a filler of any of the above materials.

Information on certain properties of the thermal-insulation materials are given in Table 41.

TABLE 41

Properties of Thermal-insulation materials

Thermal-insulation materials	Density, kg/m^3	Maximum operating temperature t, °C	Linear shrinkage after 24 hours of operation at maximum operating temperature, %	Force required to compress material by 5%: Shear stress τ_{sp}, kgf/cm^2	Initial material, kgf/cm^2	After 24 hours of operation at maximum operating temperature, kgf/cm^2	Amount of moisture absorbed, % by volume
Molten aerogel	290	760	0.5	2.8	8.4	9.8	1.4
Diatomite	385	1050	3.0	4.9	6.8	7.8	1.8
Calcium silicates	175	650	1.5	4.2	9.1	9.1	1.8
Magnesium oxide (85%)	190	330	0.5	2.8	3.15	2.5	0.7
Molten anosite	270	400	0.5	3.9	0.56	0.28	0.9
Foamed mineral wool	305	650	0.5	2.8	0.77	0.78	

Rocksil, a long-fiber white mineral wool [136] , is used to insulate the Na-K piping and heat exchangers used in the fast-neutron reactor (under construction at Dounreay)(Britain). This material is extremely porous and contains up to 95% air by volume, and at the same time has good heat-resistant properties and is suitably chemically inert up to 750° C.

Interaction of thermal insulation materials with alkaline metals. Sodium and Na-K alloy react quite strongly with minerals containing chemically-bound water. This, however, does not preclude the use of such materials for insulating small experimental installations.

Packed mineral wool, special aerogel, molten diatomite, and molten amosite proved to have satisfactory chemical stability with respect to sodium under industrial service conditions. These materials were not completely impregnable to the liquid metal, even though their density was much higher than the density of mineral wool, glass wool, or stainless steel chips.

Temperature conditions of insulation service. In selecting the type of thermal insulation, consideration must be given to, specifically, the temperature conditions under which it will function. Table 41 shows the maximum operating temperatures for various types of insulation. Preheating the circuit by electric heaters is caused by local overheating of the thermal insulation as compared to operating conditions. Since thermal insulation which has greater temperature stability usually has greater thermal conductivity, it is advisable in some cases to insulate piping in two layers. The first layer, immediately next to the pipe, is made of a more temperature-stable and more conductive material, and the second layer of a material with better thermal insulating properties but lower temperature stability.

Thermal conductivity of insulating materials. Curves of the thermal conductivity of various thermal-insulation materials as a function of temperature are

given in Fig. 123. As the figure shows, molten aerogel has the lowest thermal conductivity.

The thermal conductivity of a thermal-insulation material is greatly influenced by the nature of the surrounding medium. In contrast to standard power installations where air at atmospheric pressure is the medium, in nuclear-fuelled installations, thermal insulation can operate in rarefied air or any kind of gas. Gasses with low molecular weight, helium for example, can raise the thermal conductivity of an insulator by 2-3 times. On the contrary, the thermal-insulation properties of a material can improve in gas having a high molecular weight, or in rarefied air. The influence of rarefaction is felt at pressures below 10 mm Hg. The thermal conductivity of insulators having small internal pores (molten aerogel) is less sensitive to changes in the nature of the surrounding medium than are other insulators.

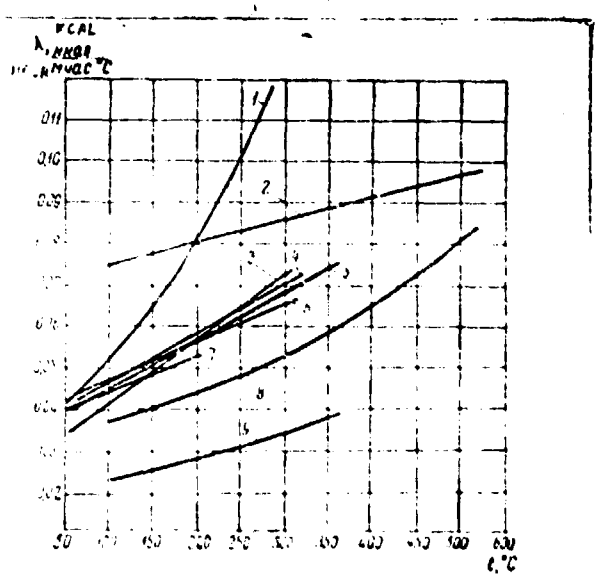

Fig. 123. Thermal conductivity of some thermal-insulation materials.

(1) Stainless steel chips; (2) diatomite; (3) mineral wool fiber (γ = 140 kg/m^3); (4) amosite; (5) pressed mineral wool in blocks; (6) calcium silicates; (7) magnesia (85%); (8) fireproof fiber (γ = 220 kg/m^3); (9) aerogel (LK-61).

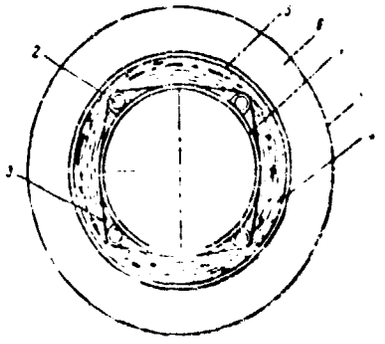

Fig. 124. Assembly of thermal insulation on a pipeline.
(1) Pipeline; (2) tubular heater; (3) heater tracing; (4) very dense fireproof fiber; (5) leak indicator; (6) molten aerogel; (7) outer jacket.

Tables 42 and 43 present data permitting a comparison of thermal insulation made of molten aerogel with standard insulation.

TABLE 42

Comparison of Heat Loss Through Layers of Various Thermal Insulation Materials of Identical Thickness (temperature of surface of pipe: 455°C, temperature of surrounding medium: 27°C)

Type of insulation	Thickness mm	Temperature of outer surface of insulation, °C	Heat loss per linear meter, kcal/hour	Ratio of heat losses
		Pipe 200 mm in diameter		
Molten aerogel	75	43	160	0.48
Standard insulation*	75	56	332	1.00
Fireproof mineral fiber	20	45	181	0.54
Molten aerogel**	55	—	—	—
		Pipe 50 mm in diameter		
Molten aerogel	50	46	87	0.48
Standard insulation	50	61	180	1.00
Fireproof mineral fiber	20	49	107	0.59
Molten aerogel	30	—	—	—

* In this case "standard" means a thermal insulation having a thermal conductivity of 0.07 kcal/m hour°C at a temperature of 260°C.

** Compound insulation consisting of an inner layer of fireproof mineral fiber and an outer layer of molten aerogel.

TABLE 43

Economy on Material Resulting from Switching from Standard Thermal Insulation to Molten Aerogel Insulation (temperature of surface of pipe: 455°C, temperature of surrounding medium: 27°C)

Insulation material	Thickness of insulation, mm	Temperature of surface of insulation, °C	Heat loss per linear meter, kcal/hour	Material used per linear meter: Volume, m^3	Material used per linear meter: Weight, kg	Relative consumption of material: Thickness of insulation	Relative consumption of material: Volume	Relative consumption of material: Weight
	Pipe 200 mm in diameter							
Standard insulation*	75	56	332	0.07	19	1.0	1.0	1.0
Molten aerogel	32	63	328	0.025	7	0.42	0.35	0.37
	Pipe 50 mm in diameter							
Standard insulation	50	61	180	0.018	5	1.0	1.0	1.0
Molten aerogel	17	73	180	0.004	1.2	0.33	0.23	0.25

* "Standard" insulation in this case means a thermal insulation having a thermal conductivity of 0.07 kcal/m hour °C at a temperature of 260°C.

Most of the materials used do not lose their thermal insulation properties after prolonged immersion in water and subsequent drying, except for molten aerogel which should be protected from the effect of moisture by covers or jackets.

Radiation was not observed to affect the properties of any of the insulation materials studied.

Assembly of thermal insulation on pipelines. Figure 124 shows schematically a cross section of pipeline with thermal insulation, electric heaters, and a liquid-metal leak indicator mounted on it. The leak indicator consists of a metal ring insulated electrically from the pipeline. Liquid metal flowing through a leak creates electrical contact between the ring and the wall of the pipeline, which can be recorded by special devices informing the personnel operating the installation of an accident. The leak indicator can be located not only between layers of insulation (Fig. 124), but also directly on the surface of the pipe, which permits speedier discovery of the leak.

The two-layer insulation shown in the figure was used successfully in several semi-industrial liquid-metal installations. The inner layer of insulation was fitted to the pipe by means of a fireproof cord (glass fiber, etc.), and the outer layer by means of a metal tape, followed by asbestos sheathing. Finally, the surface of the insulation is covered by a layer of cement protecting it from moisture. Sometimes the insulation is protected from mechanical damage by a metal jacket.

Chapter VI

EQUIPMENT FOR LIQUID-METAL SYSTEMS

(OBORUDOVANIYE ZHIDKOMETALLICHESKIKH SISTEM)

35. Mechanical Pumps

Mechanical pumps, which surpass electromagnetic pumps in efficiency and cost less, are frequently used in liquid-metal reactor systems.

Centrifugal pumps, whose hydraulic characteristics and design fully meet the requirements for extended operation at constant feed and head, are the most commonly used circulation pumps for primary circuits. Reciprocating pumps are used only as auxiliary units, since they have a low discharge rate and create a pulsating pressure. A reciprocating pump with a separating diaphragm is, furthermore, unreliable in extended service because of the danger of diaphragm failure.

Since liquid metals follow the general principles of hydraulic resistance, the section between the inlet and outlet valve is designed in accordance with the standard formulas for liquids.

The major problem with mechanical pumps is the design of seals and bearings reliable in extended service where there is to be no access for inspection or repairs.

Seals should completely exclude the possibility of leakage of the liquid metal or seepage of air into the pump in order to avoid chemical reaction with the coolant.

In designing bearings for liquid-metal pumps it sometimes is necessary to use the pumped medium as a lubricant, i.e., to use a liquid with poor lubricating properties.

Considerable difficulties arise in selecting a material for components of bearings and seals since the use of diverse materials in a system leads to the possibility of transport of individual constituents of the material by the molten metal.

Mechanical pumps use diaphragm and gas seals as well as seals of frozen metal — the coolant.

Table 44 gives certain data for mechanical pumps which have performed successfully for 1,000 hours and more. All the pumps, with the exception of one reciprocating pump, are single-stage centrifugal pumps for pumping liquid sodium in closed circuits. The reciprocating pump was designed for special technological processes requiring low delivery and relatively high pressures. Table 44 gives the maximum value of hydraulic efficiency for the pumps, including the drive.

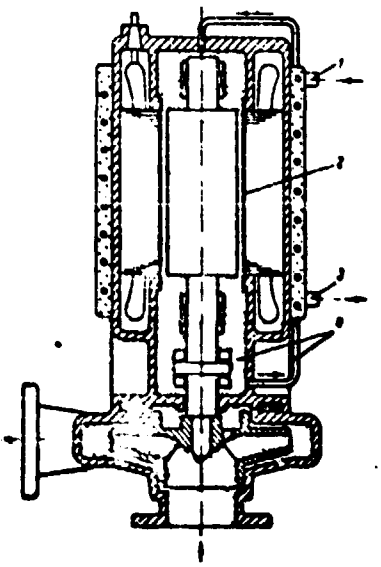

Рис. 125. Насос с герметизированным ротором

Fig. 125. Canned-rotor pump.

(1) Coolant inlet; (2) diaphragm;

(3) coolant discharge (4) liquid metal.

Impellers for centrifugal pumps are designed according to specifications for conventional liquids. The clearance at the sealing bush, however, should be increased by 1.5 to 2 times; this is especially important when using austenitic steels, which have a high coefficient of heat expansion.

Complete airtightness of the working volume, especially necessary in moving radioactive liquids, is achieved by diaphragm-seal pumps. The operation of diaphragm seals is based on separation of liquid metal from air by an airtight nonmagnetic shell. The rotor inside the shell is submerged in the liquid being

pumped and obtains its torque from a rotating external magnetic field.

Diaphragm seal pumps are made in two main varieties: canned-rotor and magnetic-drive.

Canned-rotor pumps. Figure 125 shows a canned-rotor pump. The impeller of the pump is fitted directly on the rotor of a polyphase motor submerged in the pumped liquid. A thin cylindrical membrane makes the bearings and the rotating parts completely airtight. The shielded insulated windings of the stator are located outside the membrane. The rotor is rotated as in a standard polyphase motor. The stator winding and the liquid metal in the region of bearings and rotor are cooled. Thus, the temperature in the drive section can be considerably below the temperature in the section between the inlet and the outlet valve and, consequently, the problem of insulation of the stator winding is not the restricting factor in setting the temperature limit of the pumped liquid.

In designing such pumps, the problem of bearings operating with liquid metal as a lubricant is compounded by the problem of creating a strong cylindrical membrane which will cause the least power loss in the motor. Losses due to eddy currents in the membrane result in a reduction in the overall efficiency of the motor and in a need to remove the heat resulting. Installation of a membrane in the motor clearance is the reason that the designed ratios normal for an induction motor cease to be optimal.

The counter torque developed as a result of the presence of the membrane can be derived from the general expressions for the case of a hollow cylinder placed in the air gap of an induction motor [Ref.].

$$\mu_0 = \frac{\delta}{\delta + \beta_2}, \qquad (78)$$

here $K_T = \frac{T}{a^2 B^2 L}$ and $\Omega = \frac{4\pi^2 nat}{\rho_s}$,

where T is the torque, dyne·cm;

a is the radius of the cylinder, cm;

t is the thickness of the cylinder wall, cm;

L is the axial length of the field, cm;

n is the field frequency, rev/sec;

ρ_s is the resistivity of the cylinder, emu.

B is the maximum magnetic flux density, gauss.

The dimensionless coefficients α and β determine the resistance and the inductive reactance of the cylinder, respectively.

In case of a long cylinder where magnetic materials are used in the electromagnetic system of a motor, the theoretical values of the coefficients are equal to:

$$\alpha = 2 + 2\left(\frac{a}{\delta}\right)^2,$$

where δ is the size of the air gap.

Since the term $2\left(\frac{a}{\delta}\right)^2$ is negligibly small as compared to motors, the term for motors fed by currents of normal frequency and fitted with a thin membrane made of a material of high electrical resistance, Eq. (76) can be presented as

$$K_T = \frac{\alpha}{\beta}. \qquad (78) \qquad (79)$$

from which

$$T = \frac{2\pi a^2 B^2 L t}{\rho_s} \text{ dyne·cm.}$$

TABLE 44

Mechanical Pumps for Liquid Metals

Type of pump	Purpose	Efficiency %	Advantages	Disadvantages
Centrifugal, with canned rotor	Low Capacity	65	Reliable seal	Operating temperature is limited to 300°C when conventional bearings are used. Maintenance complicated.
Centrifugal, with magnetic drive	Low capacity. operating temperature not above 250°C	60	Reliable seal	Low operating temperature complicated maintenance.
Centrifugal, with freeze seal	Wide capacity range. High temperature (to 700°C)	75	Maintenance convenient. No rubbing parts in liquid metal	Danger of leakage when circulation of cooling system ceases
Centrifugal, with gas seal	Wide capacity range. Moderate temperature.	75	Reliable seal. No rubbing parts in liquid metal	Monitoring of level of metal in pump tank required as well as addition of purified inert gas to motor.
Centrifugal with, gas seal on shaft	For nonradioactive metal. Wide capacity range. High temperature (to 750°C)	75	Maintenance simpler than in previous pumps	Monitoring of level of metal in the pump and addition of purified inert gas required.
Reciprocating, with gas seal	Low capacity and temperature	10—20	High pressure	Rubbing parts are in liquid metal.

Since the power loss

$$H = 2\pi nT \text{ approx.} \qquad (80) \qquad (80)$$

we get, substituting the expression for T into (80)

$$H = \frac{4.10 \cdot 2\pi^2 n^2 \gamma L a^2 B^2}{\rho_0} \text{ em. W.}$$

Substituting for certain values, we obtain the following formulas for calculating the power loss in the membrane:

$$H = \frac{3.85 \cdot 10^{-4} n^2 L D^2 B_m^2}{\rho_0} \text{ em. W.} \qquad (81) \qquad (81)$$

where ρ_0 is the resistivity of the membrane, ohm-cm

$B_m = \frac{2}{\pi} B$, the average magnetic flux density;

D, the diameter of the cylinder, cm.

In designing the pump motor keeping in mind the goal of maximum overall efficiency, it is necessary, first of all, to try to reduce the flux density as compared to conventional standards.

If the expressions for the losses in an induction motor are combined with the formula for the losses in the membrane, the required equation for designing the pump motor can be derived.

The back emf induced in the phase of any induction motor is obtained from the equation

$$E = 4.44 \cdot 10^{-8} K_w f T \Phi_m \text{ v} \qquad (82) \qquad (82)$$

where f is the frequency, cps;

T, the number of turns in a phase;

Φ_m, the total magnetic flux per pole pair, maxwells

K_w the coefficient for the winding arrangement ($K_w = 0.955$ for tight winding).

Equation (82) differs from the conventional transformer formula in coefficient K_w which allows for the arrangement of the winding.

Using Eq. (82) for three-phase current and disregarding the resistance of the stator, we get the following expression for the power fed to the motor:

$$Q = 10.9 \cdot 10^{-13} \pi K_w B_m (ac) D^2 L n \cos\varphi, \quad \text{watts} \qquad (83) \qquad (83)$$

where B_m is the average flux density in the air gap, gauss;

(ac), the specific electric load in ampereturns per centimeter of the length of the gap circumference;

n, the synchronous speed, rev/sec;

D, rotor diameter, cm;

L, rotor length, cm.

From Eqs. (81) and (83) we derive an expression for the relative losses in the membrane in terms of the basic parameters of an induction motor:

$$Z_0 = \frac{N}{Q \cos\varphi} = \frac{0.0\,\text{Xa}\,l\,N R_0}{K_w B_m (ac) \cos\varphi}, \qquad (84) \qquad (84)$$

in which $\cos\varphi$ is the power factor.

Equation (84) shows that the relative losses in the membrane are directly proportional to the diameter of the rotor and do not depend on its length. Consequently, it is advisable to use the greatest possible L/D ratio.

For preliminary calculations for a pump motor, in addition to (83) and (84), a knowledge of the relative losses in the copper of the rotor and the stator is required.

The current in the rotor rods can be determined from the equation

$$I_0 = \frac{K_w N_{ph}}{N_{R_0}} I_1 \cos\varphi \qquad (85) \qquad (85)$$

where N_{Sc} is the total number of stator conductors;

N_{Rc} is the total number of rotor conductors;

I_p, the phase current of the stator.

The current in the rotor rings is

$$I_b = \frac{N_{Rc}}{\pi p} \cdot \qquad (86)$$

where p is the number of pole pairs.

The total losses in the copper of the rotor are

$$H_{Rc} = \frac{10^{-8}(\pi K_w)^2 \rho_t L_B D^2 (\omega)^2 \cos^2\theta}{A_B N_{Rc}} \text{ om} \qquad (87)$$

Here ρ_c is the resistivity of the rotor conductors, uohm·cm;

A_b is the cross section of one rotor rod, cm^2;

L_b is the effective length of the rod, equal to the length of the rod plus the quantity

$$\frac{2N_c d_m A_B}{\pi p^2 A_c} \text{ cm};$$

d_m is the average diameter of the ring, cm;

A_c is the cross section of the ring, cm^2.

Using the expression derived and Eq. (83), we obtain the following equation for the relative losses in the copper of the rotor

$$z_{Rc} = \frac{20.5 K_w \rho_t (\omega) L_B \cos\theta}{A_B N_{Rc} B_{av} L} \cdot \qquad (88)$$

Similarly, for the losses in the copper of the stator, we get the following:

$$z_{st} = \frac{20.5 \rho_t (\omega) L_B}{K_w A_b N_{Sc} B_{av} L \cos\theta} \cdot \qquad (89)$$

where A_b is the total cross section of copper per stator slot, cm^2;

N_{ss} is the number of stator slots;

L_T is the average length of conductor, equal to half the average turn length, cm.

Equations (83), (84), (88), and (89) make it possible to calculate the total losses in the motor and to determine the optimum ratios of the basic values.

The presence of liquid metal in the gap between stator and rotor increases the overall losses. These additional losses are made up of "ventilation" mechanical losses and losses due to eddy currents passing through the liquid. Actually, both types of losses are very small and need not be taken into account.

Losses can also be caused by the peculiarities in rotor design. It is not advisable to submerge a laminated rotor core in liquid metal. In such conditions, the insulation between the laminae would become quickly disrupted and would serve as a source of contamination for the liquid metal, which is undesirable. In view of this, rotors are made either solid with copper rods in the slots or are sealed from the outside with a sheath of thinwalled tube of magnetic material in order to prevent an increase in the "air" gap. However, due to the relatively large "air" gap necessary and the shielding effect of the fixed membrane, neither design of the rotor core brings about a noticeable drop in motor efficiency.

In view of the need to use the pumped liquid metal as a lubricant for bearings in canned-rotor pumps, a type of hydrostatic bearing has been used, i.e., a bearing in which pressure in the lubricating layer is maintained by an external source. The main advantage of a hydrostatic bearing over an ordinary hydrodynamic bearing consists in the opportunity of considerably increasing the specific load.

Figure 126 [84] shows a cross section of a bearing and a view of an inside bearing surface. The neck of the shaft has a collar having several pockets, each of which is individually fed with liquid metal from one common receiver. The

liquid flows out of the bearing along its edges as well as through longitudinal grooves between the pockets. The longitudinal grooves serve to exclude the possibility of pressure equalization in the central part of the bearing by overflow along the circumference. Calculations show that introducing longitudinal grooves in a bearing having a ratio L/D≥ 2 doubles its load capacity.

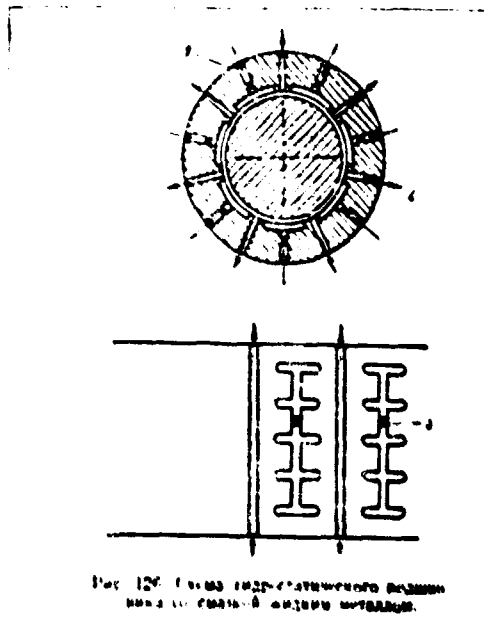

Fig. 126. Diagram of hydrostatic bearing lubricated by liquid metal.
(1) Liquid inlet; (2) liquid outlet; (3) throttle washer.

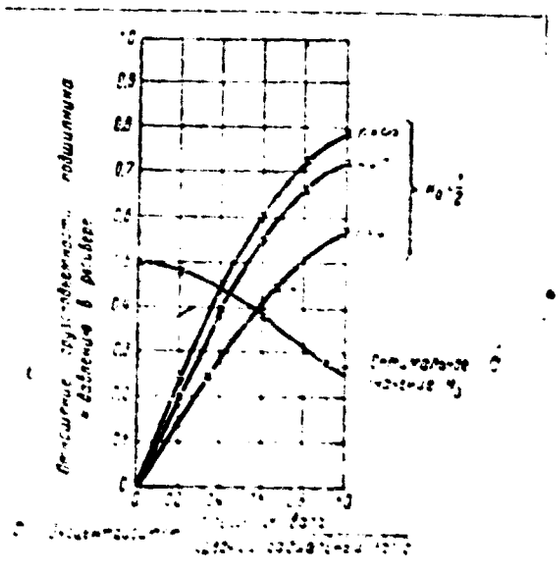

Fig. 127. Characteristics of a hydrostatic bearing.

(a) Number of pockets; (K_p) ratio of pressure in pocket to pressure in the receiver.

(b) Relationship of bearing capacity to receiver pressure; (b) optimum value of K_p;

(c) eccentricity = $\frac{\text{shaft displacement}}{\text{average radial clearance}}$

The bearing acts as follows. At no load, the shaft occupies a central position with respect to the bearing bushing. Individual throttle washers are adjusted in such a way as to secure identical pressure in all the pockets. During

operation, any displacement in the shaft toward any pocket will cause the pressure in it to rise and the pressure in the diametrically opposite pocket to drop correspondingly, and, consequently, will give rise to restoring force. The cross grooves of the pockets are intended for establishing an "oil" wedge during emergency interruptions in liquid input; the bearing functions as a hydrodynamic bearing.

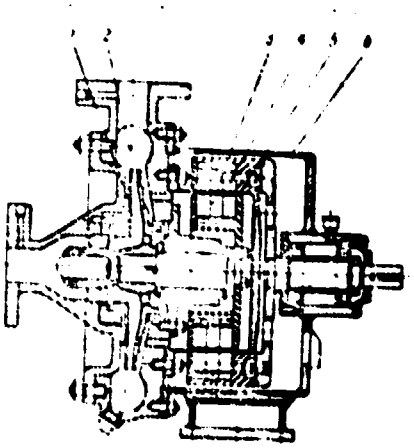

Fig. 128. Centrifugal pump with magnetic drive.
(1) Impeller; (2) frame; (3) driven magnets;
(4) driving magnets; (5) membrane;
(6) housing.

Figure 127 shows analytical curves characterizing a hydrostatic bearing of the design discussed. To avoid variations in the load capacity of the bearing it is considered advisable to have an odd number of grooves, numbering at least five.

Pumps with magnetic drive. Figure 128 shows an airtight pump with a magnetic drive; it is a combination of a centrifugal pump with a permanent-magnet clutch. In this case the use of permanent magnets drive ensures high reliability as compared with electromagnets, as well as compactness. The magnetic coupling consists of driving and driven disks fitted with horseshoe magnets. When the drive rotates, the magnets of the driving disk attract the magnets of the driven disk and cause the impeller shaft to rotate.

The working volume of the pump is covered by an airtight hood which is attached to the housing. The thinwalled nonmagnetic membrane forming the cylindrical surface of the hood is located in the gap between the poles of the magnets. Pumps of such design of up to 20 hp at 1,500 rpm [45] are manufactured in Britain. The transmission of considerable power by means of magnetic clutches is difficult from the design point of view owing to the difficulty of arranging the required number of magnets. The pressure in the operating chamber of the pump depends on the strength of the membrane whose thickness is limited by the size of the gap between the poles of the magnets. The selection of the permissible liquid-metal temperature is to a considerable extent determined by the operating conditions of the pump-shaft bearings since the pumped medium serves as the lubricant.

Pumps with gas seals. Pumps with gas seals do not require seals for the liquid metal itself; they are equipped, therefore, with relatively simple packings. Centrifugal pumps with gas seals have long shafts, whose upper bearings are located outside the zone of the liquid metal and its vapors. A device

for regulating the level of liquid metal in the working volume of the pump should be provided.

Pumps of this type are equipped with seals of inert gas which fills the space over the free surface of the liquid metal. Rotating and labyrinth seals are used.

When some gas leakage into the atmosphere is tolerable, ordinary gland packing or face-to-face type contact packing can be used. The latter packings perform reliably with lubrication; however, there is danger that the lubricant will penetrate into the working space of the pump with contamination of the liquid metal.

Gas may not leak into the atmosphere when radioactive liquid metals are involved. One of the designs for this case is shown in Fig. 129.

The gas-sealed centrifugal pump shown in Fig. 129 was designed and manufactured by the Knolls Atomic Power Laboratory for eutectic Na-K. The capacity of the pump is 115 m^3/hour at 1,750 rpm, a 23-m head, and a Na-K temperature of 355°C. The electric motor and the bearings are located over the free surface of the liquid metal in an atmosphere of inert gas, they are protected from flooding by a pipeline coupling the working volume of the pump to a large-capacity external overflow reservoir. In the top part of the pump tank there is labyrinth seal on the shaft to restrict gas leakage when the housing of the motor is removed, and to protect the bearings and the electric motor from the vapors of the pumped metal. During operation, gas pressure in the upper and lower chambers is identical and no gas leaks into the atmosphere. The external surface of the upper housing is cooled by air from the fan which cools the motor. All parts of the pump which come into contact with the Na-K eutectic or its vapors are made of type 18-8 stainless steel.

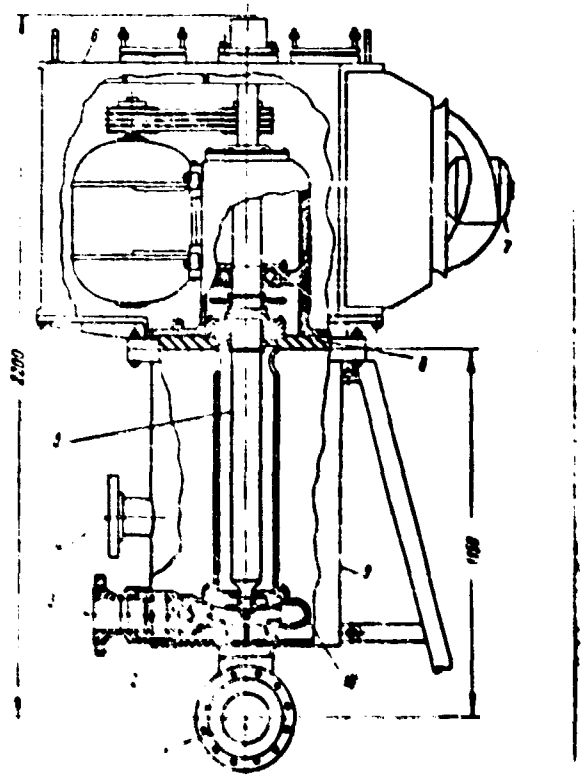

Fig. 129. Centrifugal pump for Na-K alloy with labyrinth gas seal.

(1) Suction; (2) impeller; (3) discharge; (4) overflow connection; (5) shaft; (6) motor housing; (7) cooling fan; (8) labyrinth seal; (9) pump tank; (10) casing.

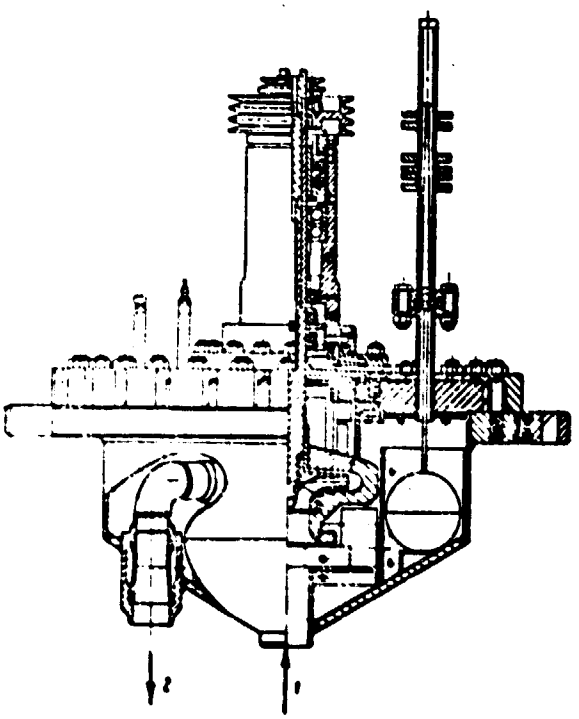

Рис. 130. Центробежный насос с торцовым газовым уплотнением

Fig. 130. Centrifugal pump with face-to-face gas packing.
(1) Liquid inlet; (2) outlet.

NSL-55A

Figure 130 shows a centrifugal pump of the Oak Ridge Laboratory 145 designed for a liquid-metal temperature of up to 750°C. The face-to-face contact-type seal is located in neutral gas over the free level of the hot liquid. Local cooling of the casing and the neck of the shaft is provided to ensure normal operating conditions for the packing. White-graphite ceramic and hardened-steel rings were used for the rubbing elements of the seal. The fixed breakable flange joints of the pump are fitted with metallic oval-shaped gaskets.

A liquid-metal reciprocating pump with a gas seal has been employed in the chemical industry at temperatures up to 250°C with heads up to 7.6 m. In this case, no special problems arose with respect to the seal or rubbing elements. Leakage through the piston was returned to the settling tank of the pump and the rod was sealed with ordinary soft packing in order to retain the inert gas in the settler in the space behind the piston. The valves were of special shape, designed to prevent jamming or clogging by metal oxides.

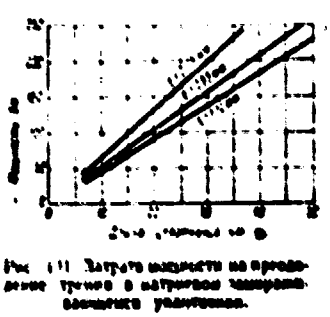

Fig. 131. Power consumed in overcoming friction in a frozen-sodium seal.
(a) Thickness of the layer of liquid metal.
(a) Power, watts; (b) seal length, cm.

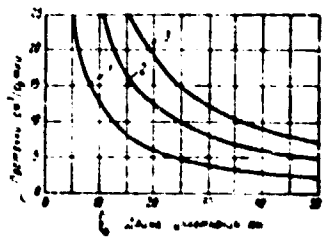

Рис. 132. Зависимость величины протечек через натрием замораживающий участок уплотнения от его длины при различных перепадах давления на уплотнении (Δp).

Fig. 132. Leakage through a frozen-sodium seal as a function of its length at various pressure drops at the seal (Δp).

(1) Δ_p = 1.4 atmos; (2) Δ_p = 2.8 atmos;

(3) Δ_p = 4.2 atmos; n = 1,800 rpm;

d_{shaft} = 69.5 mm. (a) Leakage, cm^3/24 hours;

(b) seal length, mm.

Pumps with frozen seals. In principle, frozen seals consist of a friction bearing with a small clearance filled with liquid metal. The neck of the shaft rubs against the surface of the frozen metal forming a thin but sufficiently viscous film of metal. The film is maintained in the liquid state due to the heat of friction, but in view of its high thermal conductivity it quickly dissipates the heat. As a result, it does not become thick enough to cause a considerable leakage of metal. The heat of the hot metal and the heat of friction is continuously removed by means of special cooling by liquid or gas.

The power spent to overcome friction is directly proportional to the length of the seal and inversely proportional to the thickness of the layer of liquid metal (Fig. 131) [45].

The magnitude of leakage through the seal is determined by the velocity of liquid flow through a narrow annular slot at varying pressure. Figure 192 gives data on leakage when the shaft seal is 69.5 mm in diameter and rotates at n = 1,800 rpm.

Of great importance for normal performance of the seal is the cooling temperature and the purity of the liquid metal, since the seal acts like a cold trap with respect to impurities (see Chapter VII). The contamination of sodium by oxides in the freezing seal can lead to jamming and breakdown of the pump; in this connection the oxygen content of the metal should not exceed 0.005%.

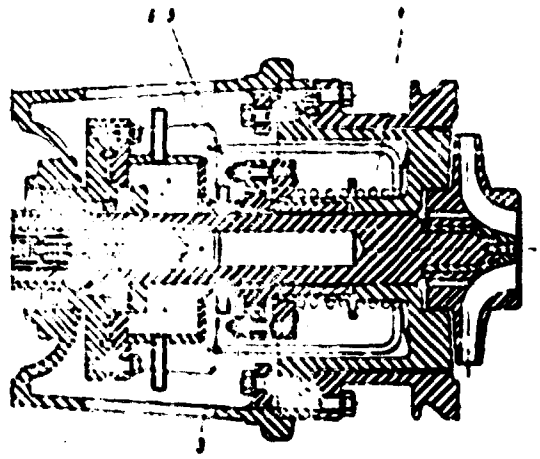

Рис. 133. Центробежный насос для натрия с замораживающимся уплотнением.

Fig. 133. Sodium centrifugal pump with a frozen seal.

(1) Inert gas space; (2) leakage trap;

(3) frozen sodium; (4) heater;

(5) molten sodium with a temperature of

not more than 100-110°C;

(6) cooling-medium inlet.

It is advisable to thermally insulate the seal from the whole system and to place a liquid metal inlet space immediately next to it. The frozen zone should be as short as possible in order to reduce the power expended for friction.

The length of the seal was from 6 to 19 mm in the pump shown in Fig. 133. The free surface of the liquid metal was protected from oxidation by inert gas.

The frozen seal is not capable of withstanding pressure drops greater than several tenths of an atmosphere.

When a horizontal shaft arrangement is used it is necessary to take measures to ensure that the shaft deflection at the seal will not exceed 0.1 mm. Play of the shaft should not exceed 0.025 mm to avoid plastic deformation of the frozen metal as well as excessive heat release. With a horizontal shaft, in the event the pressure of the liquid metal in the slot is less than the pressure of the inert gas, the liquid-metal film may rupture and the gas penetrates into the working volume of the pump. Vertical-shaft pumps are not liable to these shortcomings. Figure 134 shows an American sodium centrifugal pump with a frozen seal, designed for a capacity of 5.3 m^3/min and pressure head of 30.5 m at a temperature of 650°C. The pump has a vertical shaft fitted with a frozen seal and an airtight housing filled with inert gas. The shaft seal, 76 mm in diameter is located under the lower bearing at a distance of 380 mm from it. For cooling the upper surface of the housing a ring 508 mm in diameter and 152 mm long is provided. The parts of the pump are made of type 410 stainless steel; there is no need to work harden the surface of shaft necks under the seals after polishing for this type of steel.

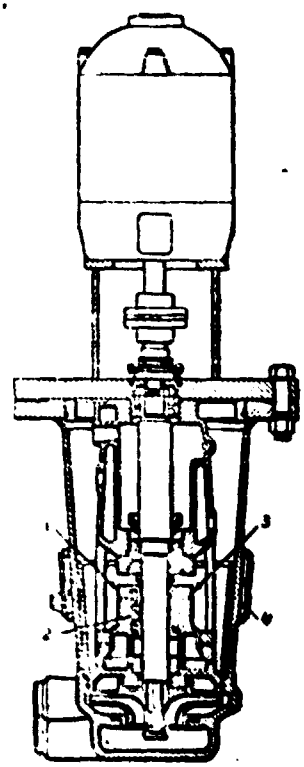

Fig. 134. Sodium centrifugal pump with a frozen seal and vertical shaft.
(1) Inlet for coolant (toluene); (2) frozen-sodium ring; (3) coolant outlet; (4) cooling jacket.

Figure 135 shows an experimental curve for the power lost due to the seal of this pump. The maximum starting moment for a shaft 76 mm in diameter is 4.15 kgfm. As the temperature of the solidified metal nears the melting point, the cohesive forces diminish, and consequently, the starting moment diminishes. Sealing with a metal which has high thermal conductivity makes it possible to have a temperature in the circular slot close to the freezing point. The curves in Fig. 136 represent the characteristics of the sodium seals shown in Figs. 137 and 138 [84].

As shown by experience a seal ring with conical exterior and cylindrical interior, forming a cone-shaped metal film 0,5 mm thick from the gas side and 1,5 mm from the liquid-metal side, performs more smoothly than a ring of cylindrical shape. Evidently, with diminishing radial gap the solid inclusions in the the liquid metal can gradually become ground down before they cause damage to the neck of the shaft.

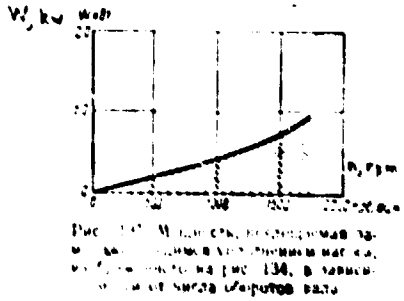

Fig. 135. Power taken up by the frozen seal of the pump shown in Fig. 134 as a function of the number of revolutions of the shaft.

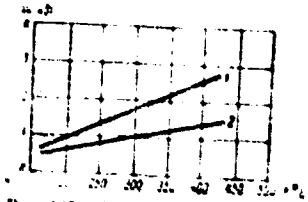

Fig. 136. Cooling capacity for a frozen seal as a function or sodium temperature.
(1) Seal, Fig. 137; (2) seal, Fig. 138.
(number of shaft revolutions: 1,200 rpm; seal temperature: 50°C; pressure drop 0.035 kg/cm^2).

The seal sleeve of the pump shown in Fig. 137 has milled double-thread helical channels for the coolant, which flows downward in one helical channel and upward in the other.

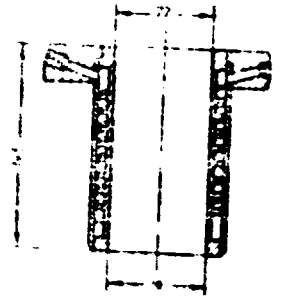

Fig. 137. Frozen-sodium seal with one cooling channel.

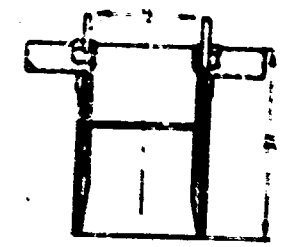

Fig. 138. Frozen-sodium seal with two cooling channels.

A design with two independent cooling channels is shown in Fig. 138. The lower cooling circuit is formed by a double helical channel. The cooling circuit precools the liquid metal in the region of the large radial gap, where foreign inclusions are precipitated before they can settle in the upper section of the of the slot. The upper cooling circuit consists of an annular chamber which ensures freezing of the liquid metal in the region of the narrow annular slot. The shortlength and the small radial gap in the region of the frozen metal decreases the rotating and the starting moments.

Centrifugal pumps with frozen seals are convenient to operate and repair. They have high efficiency due to the absence of rubbing elements immersed in liquid metal. If the circulation of the coolent (water, toluene, etc.) which freezes the seal is interrupted, the seal does not fail at once, as a result of which there are always several minutes for emergency measures.

Rotating frozen seals are not suitable for use with liquids containing abrasive particles which cause rapid wear of the shaft and the seal.

36. Electromagnetic Pumps

In addition to mechanical pumps, electromagnetic pumps are used for pumping liquid metals, which have low electrical resistance as compared to other liquids.

Electromagnetic pumps are lower in efficiency and larger in size and weight than mechanical pumps, but they find acceptance due to the following advantages:

1) Possibility of complete airtightness of the assembly owing to the absence of seals of any type;

2) simple operation and repair owing to the absence of moving or rotating parts (bearings) requiring replacement or lubrication;

3) convenience of location in a system due to the absence of special tanks with a free surface for the suction end;

4) possibility of adjusting the discharge over a wide range by changing the input voltage.

Electromagnetic pumps are economically practical only for pumping alkali metals having a relatively high specific weight and low electrical resistance. The energy consumed in pumping them is relatively low, and in this respect the efficiency does not exert a decisive influence on the selection of the type of pump.

To date, considerable experience has been accumulated in operating various types of electromagnetic pumps in large experimental plants. The American General Electric Company has built and tested a 115 m^3/hour electromagnetic pump for the marine power plant on the submarine "Sea Wolf".

In all electromagnetic pumps, the motor law is used, i.e., force is created by a conductor carrying electricity in a magnetic field. The current flows along the liquid metal— which plays the part of the conductor— in a direction perpendicular to the lines of force; the liquid travels perpendicular to the directions of the current and the lines of the field; the direction of displacement is determined by the left-hand rule.

Types of electromagnetic pumps. According to the principle of operation, electromagnetic pumps are classified as induction and conduction pumps. In both classes of pumps, the magnetic field is generated by cores installed in the immediate vicinity of the duct. In induction pumps, the electrical current is excited in the liquid metal by coils external to the duct, while in conduction pumps the current is fed in and removed via busbars connected directly to the duct. Conduction pumps can operate on both direct and alternating current.

The most important types of electromagnetic pumps are listed below:

Conduction pumps

1. Direct-current pump.

2. Alternating-current pump.

Induction pumps

1. Helical induction pump.

2. Flat-type linear induction pump.

3. Annular linear induction pump.

4. Induction pump with rotating field.

In helical pumps the liquid metal acquires a rotating motion, in linear pumps translational motion only. In all types of linear induction pumps a sliding field of polyphase current is used.

Very advanced designs of conduction pumps, both d-c and a-c, as well as flat-type linear induction pumps are available at present. Helical and annular induction pumps are being studied in Britain and the USA. Pumps with rotating magnets are manufactured only in small quantities by industry in the USA.

A common shortcoming of conduction pumps is the large amount of currents which require current-conducting busbars of large cross section that must be connected to the thinwalled liquid-metal ducts.

The advantages of electromagnetic d-c pumps include simplicity of design, convenience in operation, and dependability of the electric insulation. There is experience with continuous service of such pumps with liquid-metal temperatures of up to 600°C with natural air cooling of the winding.

The overall efficiency of d-c pumps, including losses at the power supply, is about 15-20% for small pumps and 40-50% for large assemblies, fed from homopolar generators. Furthermore, since the demands on the electric insulation are not severe, these pumps may be operated under intensive radiation without creating great difficulties.

An advantage common to a-c electromagnetic pumps is the possibility of using ordinary sources of supply for them. At high capacities they are comparable in size and efficiency to d-c pumps.

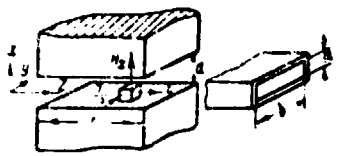

Рис 139 К выводу уравнений, характеризующих движение жидкого металла в магнитном поле насоса

Fig. 139. Quantities involved in equations characterizing the flow of liquid metal in the magnetic field of a pump.

A disadvantage of a-c pumps is the need of special cooling by forced circulation of air or some fluid. Furthermore, they are more complex to produce and more expensive than d-c pumps. The majority of electric-insulation materials used for windings in a-c pumps are sensitive to radioactivity.

The main advantage of induction pumps is that they do not require high currents in or out of a thinwalled duct by means of heavy busbars from special power supplies.

Pumps with rotating magnets, which do not require current-conducting busbars and have a simple power supply, are of definite interest.

The fields of application of the various types of electromagnetic pumps depend on their particular features. The a-c conduction pumps are used for small assemblies; a-c pumps are best for bismuth in assemblies of various capacities. Induction pumps are used to move liquid metals having low resistivity, low

viscosity, and low density (sodium-potassium alloy, sodium, and lithium). Helical induction pumps are effective at low capacities and high pressure heads, and linear induction pumps for high capacity at various pressures. Table 45 indicates the types of electromagnetic pumps recommended for use under different operating conditions [42].

Table 46 gives the basic characteristics of some electromagnetic pumps which have been constructed [43].

Design of electromagnetic pumps. Let us present the basic equations common to all types of pumps, characterizing the flow of liquid metal in the magnetic field of the pump [43].

TABLE 45

Types of Electromagnetic Pumps Recommended for Various Operating Conditions

Discharge and pressure head	Sodium Na-K alloy	Bismuth
$<5 m^3$/hour, <2 kg/cm^2	A-c conduction pump operating on line frequency through a transformer	A-c conduction pump operating on line frequency through a transformer
5-20 m^3/hour, <2kg/cm^2	Linear induction pump. Conduction pump operating on line frequency with a separate transformer or connected to it	Conduction pump operating on line frequency with or without a transformer
$<10 m^3$ hour, ~ 7 kg/cm^2	Helical induction pump	Helical d-c pump. Helical a-c conduction pump with a separate transformer
$<20 m^3$/hour, ~ 4 kg/cm^2	Linear induction pumps. D-c and a-c conduction pumps operating on line frequency with separate transformers	D-c and a-c conduction pumps with separate transformers
$<200 m^3$/hour <7 kg/cm^2	Linear induction pumps. D-c and a-c conduction pumps at a lowered frequency with separate transformers	D-c and a-c conduction pumps at lowered frequency with separate transformers
$>200 m^3$/hour, >7 kg/cm^2	Linear induction pumps. D-c conduction pump	D-c pump. A-c conduction pump at lowered frequency with a separate transformer

TABLE 46

Main Features of Electromagnetic Pumps

Type of pump	Metal	Capacity, m^3/hour	Pressure, kg/cm^2	Power, kW	Efficiency, %	Power factor	Voltage, V	Current, amp	Frequency, cps	Characteristics of cooling device
Conduction										
A-c	Flat type	1.6	1.0	0.05	4.0	0.26	—	—	-	—
A-c	Sodium potassium at 400°C	5.5	0.7	0.10	—	—	—	—	-	—
D-c helical	Bismuth at 500°C	0.2	4.2	0.02	1.0	—	1.2	1 400	-	—
D-c helical	Bismuth at 200°C	2.7	4.2	0.31	12	—	0.6	4 400	-	—
D-c helical	Sodium potassium at 250°C	81.6	2.8	6.2	44	—	0.75	19 000	-	—
D-c helical	Bismuth at 550°C	546	5.3	77	30	—	2.6	100 000	-	—
D-c helical	Sodium at 410°C	2260	5.3	320	50	—	2.5	200 000	-	—
Induction										
Helical	Sodium at 400°C	6.8	4.2	0.77	22	0.56	—	—	50	3—4 kw
Helical	Sodium at 400°C	85	2.8	6.4	18.5	0.8	—	—	25	28.3 m^3/min air

TABLE 46 continued

Main Features of Electromagnetic Pumps

Type of pump	Metal	Capacity, m^3/hour	Pressure, kg/cm^2	Power, kw	Efficiency, %	Power factor	Voltage, v	Current amp	Frequency, cps	Characteristics of cooling device
Annular	Sodium potassium at 175°C	115	1.0	3.0	36	0.22	—	—	50	3.5 kw
Annular	Sodium at 500°C	109	3.5	10.3	36	0.3	—	—	50	10 kw
Annular	Sodium at 400°C	327	5.3	320	45	0.48	—	—	50	—
Flat type	Sodium at 370°C	2260	2.8	25	36	0.45	—	—	60	5606 m^3/min air

If an element of liquid with dimensions dx, dy, and dz (Fig. 139) is placed in a magnetic field with strength H_x (oersted) and a current flows along the element with density I_y (ampere/cm^2), then in the z direction it will experience a force

$$\frac{dF_z}{dz} = \frac{I_y H_x}{10} \quad (90) \qquad (90)$$

The total pressure developed by the pump when its effective length is l, is

$$P_z = \int_0^l \frac{I_y H_x}{10} dz \quad (91) \qquad (91)$$

Then the power at the pump discharge is

$$P_0 = \frac{P_z q}{10^7} \text{ em} \quad (92) \qquad (92)$$

in which q is <u>sh</u> Y cm^3/sec;

a and b are the dimensions of the cross section of the channel, cm (see Fig. 139);

v is the velocity of metal flow in the duct, cm/sec.

The basic power losses consist of resistance losses in the liquid metal (P_p), in the windings (P_w), in the duct walls (P_s), as well as the hydraulic losses to friction of the liquid against the duct walls (P_h).

The resistance losses in the liquid metal can be determined by the following equations:

$$P_p = abl\rho \int_0^l I_y^2 dz \text{ em.} \quad (93) \qquad (93)$$

where ρ is the electrical resistivity of the metal, ohm·cm.

The ordinary methods of calculating hydraulic friction losses cannot be used in designing electromagnetic pumps in view of the high conductivity of the liquid metal and the effect of the magnetic field on it. When the liquid moves,

currents are induced in it; the interaction of these currents with the magnetic field leads to the formation of forces which cause additional resistance to displacement and, consequently, to an increase in hydraulic losses.

The head expended in overcoming friction in a rectangular duct with a high ratio of length to sides, is determined from the expression

$$h = \frac{c_f l v^2}{ag}, \qquad (94)$$

where c_f is the friction coefficient;

l is the length of the duct;

v is liquid flow rate;

a is the length of the longest side of the cross section of the duct; and

g is the gravitational acceleration.

For turbulent flow in a duct with smooth walls and where the magnetic field has a noticeable effect, the coefficient of friction can be determined from the conventional equation

$$\frac{1}{\sqrt{c_f}} = 4 \lg (\mathrm{Re}\sqrt{c_f}) - 1{,}6 \qquad (95)$$

where $\mathrm{Re} = \frac{lva}{\nu}$

ν is the kinematic viscosity of the liquid, cm^2/sec.

Investigation of the influence of a magnetic field on the flow of mercury showed that the effective viscosity of liquid increases with rising field strength. In this case, the coefficient of friction can be determined from the equation

$$\frac{1}{\sqrt{c_f}} = \frac{\mathrm{Re}}{\mathrm{Re}_M} \left| \qquad (96)$$

where μ_m is the magnetic permeability of the liquid;

H_a . magnetic induction, gauss

μ . dynamic viscosity, gauss/cm·sec;

ρ . electric resistivity of the liquid, ohm·cm.

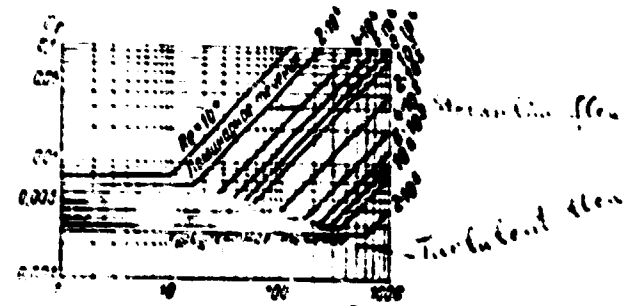

Fig. 140. Graph for calculating the coefficient of friction during flow of liquid metal through a rectangular duct in a magnetic field.

If it is assumed that Eq. (95) is correct for small values of m and Eq. (96) for large values of m, then the function $\zeta = f(m)$ can be represented graphically for various Re (Fig. 140).

To design induction pumps, basic equations can be derived giving the relationship among the pump parameters and the electrical quantities (current density, voltage in the winding, magnetizing ampere-windings) as well as for calculating the efficiency of the pump. Corresponding calculated dependences are given in the paper mentioned above [3]. This paper also gives the basic equations for designing d-c conduction pumps allowing for the influence of an effect analogous to the reaction of the armatures of electric motors or allowing for compensation for this effect by means of a compensating winding. These same equations can be used to design a-c conduction pumps but allowances should be made for the influence of losses owing to eddy currents in the metal as well as induced currents in the compensating winding and in the duct walls.

D-c conduction pumps. Figure 141 shows schematically a d-c conduction pump. A rectangular duct, which is a section of the liquid-metal piping, is situated between the poles of the electromagnet. The current, fed by copper busbars brazed to the duct, passes through the liquid and part through the duct walls. In order to reduce power losses to the minimum, the duct walls are made as thin as possible and of a material with high electrical resistance. Some of the current in the liquid metal passes through the strong magnetic field zone, giving rise to axial forces moving the metal, and some, traveling around the strong field zone (see Fig. 142 a), to a considerable extent is lost to effective operation of the pump. These losses can be reduced by installing special insulating shields in the magnetic field, lengthening the path for parasitical currents in the way shown in Fig. 142 b.

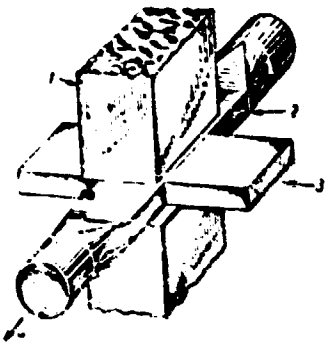

Рис. 141. Схема кондукционного насоса постоянного тока.

1 — полюс магнита; 2 — канал; 3 — шина; 4 — поток жидкости.

Fig. 141. Schematic diagram of a d-c conduction pump.

(1) Magnet pole; (2) duct; (3) copper busbar; (4) liquid flow.

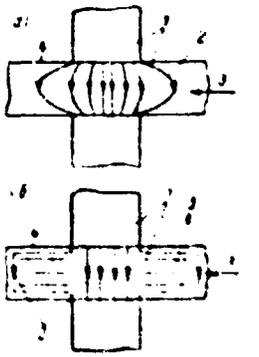

Fig. 142. Distribution of lines of current in liquid metal:

(a) Without insulating shield;

(b) with insulating shield.

(1) Copper busbars; (2) current lines;

(3) liquid-metal flow; (4) duct wall;

(5) insulation shields.

An analysis of the equation of metal flow in the magnetic field of the pump shows that for constant current the capacity and pressure head are related linearly; this is confirmed by the experimental characteristics of similar pumps (see Fig. 143).

The magnetic field created by the current passing through the liquid distorts the basic magnetic flux, increasing it at the inflow side, and decreasing it at the discharge side of the metal; this leads to reduced pump capacity. For

small pumps, with a strong magnetic field and relatively weak currents, such a drop in efficiency is of no substantial consequence. However, for pumps of considerable capacities operating with larger currents and long poles, it is necessary to compensate for the nonuniformity of the magnetic field.

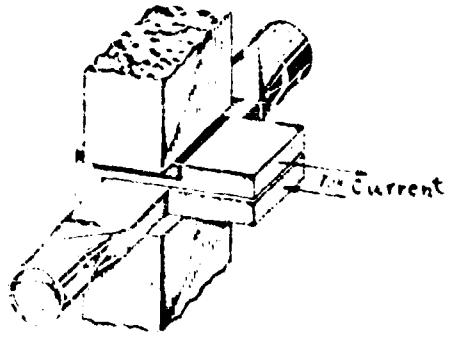

Рис. 143. Компенсация неоднородности магнитного поля с помощью изменения направления тока

Fig. 143. Compensating for a nonuniform magnetic field by means of changing the direction of the current.

Compensation is achieved by two means.

The first of these consists in passing a current flowing opposite to the direction of the current in the liquid metal through a conductor located under or over the duct (Fig. 143). A certain variation of this method is the use of two-stage pumps with horseshoe-shaped ducts. In this case the field generated

by one arm of the duct is compensated by the field of the other arm.

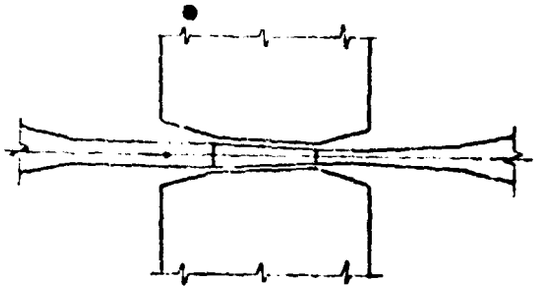

Рис. 144. К компенсации неоднородности магнитного поля с помощью клиновой формы зазора между полюсами магнита.

Fig. 144. Compensation of a nonuniform magnetic field by changing the shape of the gap between the magnetic pole pieces.

The second method consists in providing a wedge-shaped gap between the poles so that the magnetic gap is wider at the input to the duct (Fig. 144). In addition, the cross section of the duct is tapered as a result of which the velocity of the metal rises to such a degree that the counter emf, and, consequently, the current density in the magnetic field zone remains constant. The disadvantage of the latter method consists in the fact that complete compensation occurs only at specific values of the current and field strength.

A problem common to all electromagnetic pumps is maintaining sufficiently low temperature at the electric winding. In this type of pump its temperature can be reduced to the desired level by removing the field winding

sufficiantly far from the duct with the molten metal as well as by inserting thermal insulation between the duct and the pole pieces.

The type of field winding used in the pump electromagnet is dictated chiefly by service requirements. Independent field windings are usually multi-turn types and have a high working voltage. Here the main problem consists in cooling the electric insulation of the winding. On the other hand, a series winding may consist only of several copper turns (or of only one turn for large pumps) with a large cross section. Inasmuch as the voltage drop across such a winding usually does not exceed one volt, the problem of electric insulation is solved quite simply. For example, because of natural circulation of the air, air-cooled pumps operated without excessive heating of the winding for liquid-metal temperature of up to 430°C, which made it possible to use lacquer-coated insulation.

The duct of the pumps described either is welded (from metal sheet) or made by shingling a thin-walled round pipe to the required shape. The thickness of the duct wall is 0.5-1.5 mm.

The absolute dimensions of the cross section of the duct are governed, mainly, by the hydraulic losses, which become great if the cross section of the duct is too small.

The material of the duct walls depends on the type of liquid pumped; it is most common to use stainless steel for sodium and chrome steel for bismuth. Austenitic type 18-8 steel has suitable values of electric resistivity in the range of operating temperatures ($72 \cdot 10^{-6}$ ohm-cm at 20°C and $108 \cdot 10^{-6}$ ohm-cm at 500°C). Steels with high chromium content have about the same values of electric resistance etc. . The use of low-chrome steels is undesirable inasmuch as they oxidize heavily in air at high temperatures, which is impermissible in the duct walls, that are, as a rule, very thin.

It is desirable that the duct walls which are parallel to the surface of

the pump poles have good magnetic properties, and the walls which are connected to the electrodes be nonmagnetic. The stainless steels in the austenitic class are nonmagnetic, whereas the chrome steels are good ferromagnetics.

If magnetic steel is used for the tube, the walls connected to the electroles close off some of the main flow and weaken the field near the electrodes, which must be taken into account during calculations. Due to the fact that large magnetic fluxes are usually used in pumps, this weakening of the field is slight.

The copper busbars brazed to the walls of the duct sometimes should be split up into several different parts, making it possible to reduce the thermal stresses arising as a consequence of the difference in the thermal expansions of the busbar and the material of the duct. It should be considered that the material of the busbars (copper), when operating at high temperatures, oxidizes heavily in the air. At 500°C the rate of oxidation is ~ 2,5 mm per year. Oxidation can be reduced by having the busbars operate in a jacket filled with inert gas.

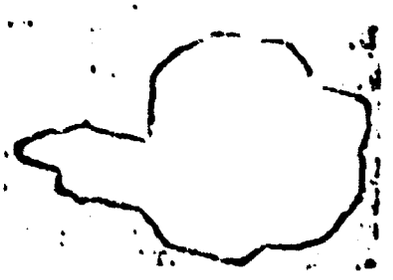

Fig. 143. [illegible]

Fig. 143. Small d-c conduction pump.

Permanent magnets can be used in d-c pumps, but then the size and the cost of the assembly increases, as a result of which they can economically be used only for small pumps.

Large amounts of current must be supplied to d-c pumps (from one to several thousand amperes) at low voltage (about 1 to 2 v). Rectifiers and homopolar generators are used as power sources for currents with such parameters. Two types of homopolar generators are now in use: a submerged-commutator, a disk-commutator. In the first of these, the armature is fully submerged in the liquid metal; in the second, the armature is wetted by the metal only where the commutators are located. Homopolar generators are manufactured which generate current up to 100,000 amp with an efficiency of 80%.

Figure 145 shows a small d-c conduction pump 171 ; results of tests on it are given in Fig. 146.

A large d-c pump with a capacity of 115 m^3/hour and pressure of 1.65 atmos abs, intended for pumping Na-K alloy in a nuclear-reactor system, has been designed and tested. The duct of the pump consists of a conical nichrome tube with an average cross-section dimension of 38 x 83 mm and a wall thickness of 0.64 mm. The magnet poles are 100 mm wide and 380 mm long; the width of the magnetic gap varies from 4.7 mm at the input to 3.8 mm at the output.

The field winding consists of two copper turns 152 x 152 mm in cross section connected in series with the busbars supplying current to the liquid metal.

The duct and magnet are situated inside a welded stainless-steel jacket which is intended to retain the liquid metal in case the duct walls are damaged. Mica insulation of the ducts and the electromagnet core, with no external cooling, is used in the pump design. The pump is fed by a water-cooled rectifier supplying 20,000 amp at 1 v.

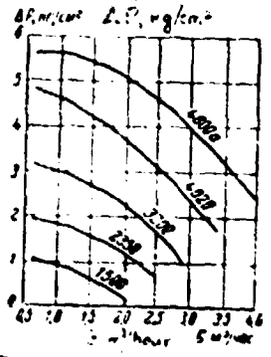

Рис. 146. Результаты испытаний кондукционного насоса постоянного тока, изображенного на рис. 145

Fig. 146. Test results for the d-c conduction pump shown in Fig. 145.

Figures 147 and 148 show characteristics of the pump for a liquid-metal temperature of 250°C.

A larger pump with a homopolar generator, designed to operate in the primary sodium system of a reactor, is shown in Fig. 149 171 . The pump is rated for a liquid-metal flow amounting to 2,250 m^3/hour at a pressure head of 5.3 kg/cm^2. It consumes 250,000 amperes at 2.5 v. The cross section of the duct for transfer of the liquid between the poles of the magnets was 150 x [illegible] mm with the length of the duct being 1,070 mm and its walls 1.6 mm thick. The flow rate of sodium in the duct was 10 m/sec. The homopolar generator is driven by a 1,250 hp electric motor.

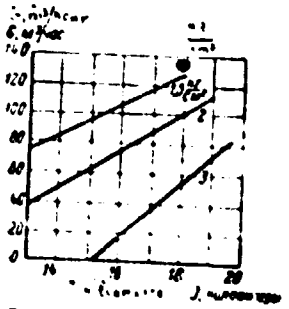

Рис. 147. Зависимость производительности индукционного насоса постоянного тока от величины потребляемого тока

Fig. 147. Dependence of the capacity of a d-c conduction pump on the amount of current used.

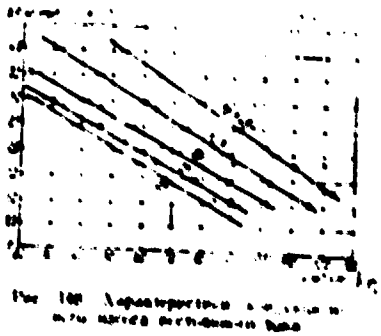

Рис. 148. Характеристики индукционного насоса постоянного тока

Fig. 148. Characteristics of a d-c conduction pump.

D-c pumps were successfully used to pump a liquid metal at a temperature of 800°C; it was cooled solely by natural convection of the surrounding air and radiation.

A-c conduction pump. An a-c conduction pump is similar in principles of performance and design to d-c pump described above. A prerequisite for operation of the pump is that the current generating the magnetic flux be in phase with the current flowing through the liquid metal. This condition is satisfied by connecting the field winding in series with the pump duct.

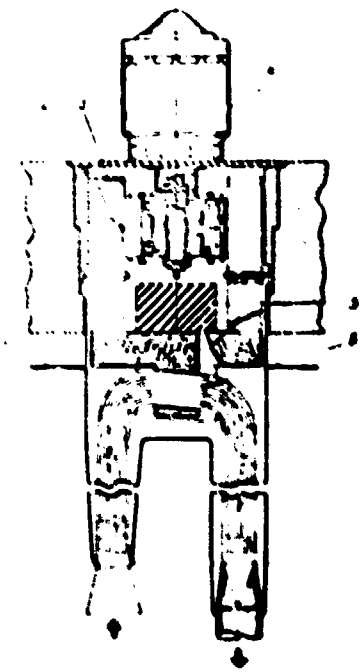

Fig. 149. Large conduction d-c pump with a homopolar generator:
(1) Sodium level; (2) copper busbars;
(3) weld, filled with sodium;
(4) electric motor; (5) magnet core;
(6) [illegible].

This pump does not need cumbersome power supplies. A power transformer, whose magnetic core is connected into the magnetic circuit of the pump, is used for this purpose.

The magnetic circuits of the transformer and the pump can be connected by different methods. Four possible ways are shown in Fig. 150. The most widely used pumps are those shown in Figs. 150 a and 150 b. The design shown in Fig. 150 b is simple to produce and is used for small pumps. The characteristics of such a pump, pumping mercury at $t = 100^{\circ}C$ are given in Fig. 151 and in Table 47. The pump weighs 39.5 kg and has dimensions of 220 x 229 x 178 mm.

A general view and the characteristics of an a-c conduction pump for moving alkaline metals is given in Figs. 152 and 153.

It is advisable to use a single-turn field winding in a-c conduction pumps, inasmuch as the dimensions of the pump are increased when there are many turns and the power factor drops. In order to reduce the leakage flux of the winding it should be made as small as possible and placed as close as possible to the magnetic gap.

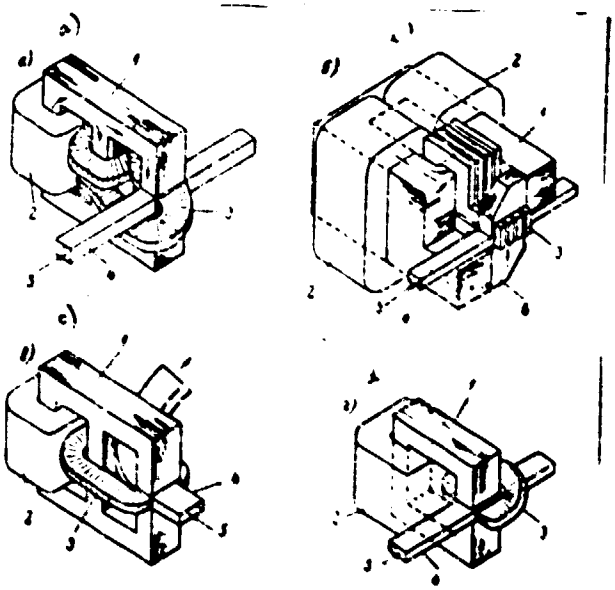

Fig. 150. A-c conduction pumps connected to a transformer (types a, b, c, and d).

(1) Core; (2) primary winding; (3) secondary winding; (4) tube; (5) liquid metal; (6) pole piece.

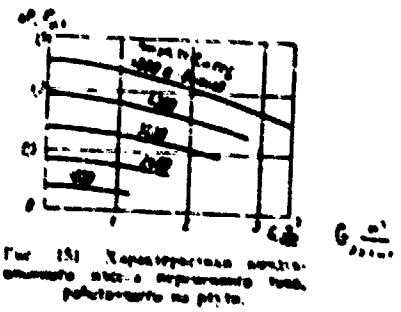

Fig. 151. Characteristics of an a-c conduction pump moving mercury.

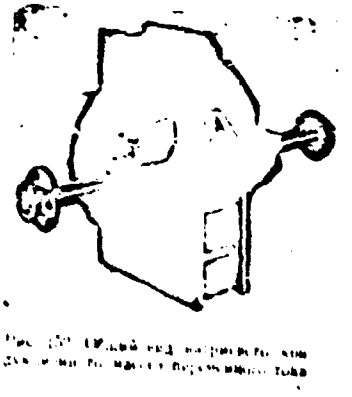

Fig. 152. General view of a sodium ece conduction pump.

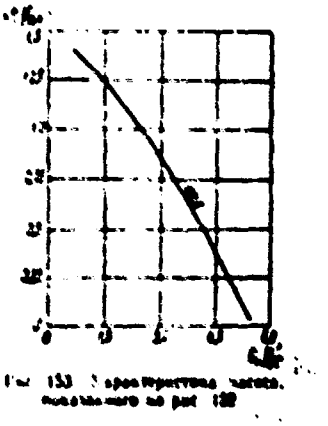

Fig. 153. Characteristic of the pump shown in Fig. 152.

TABLE 47

Design and Performance Characteristics of an A-c Mercury Pump Connected with a Transformer

Characteristic	Value
Nominal diameter of tube, mm	19
Cross section of duct, mm^2	8.6X 24
Thickness of duct walls, mm	0.56
Cross section of primary winding, cm^2	25.8
Cross section of core of the primary winding, cm^2	46.5
Cross section of secondary winding, cm^2	9.76
Nominal primary amperetums	48,00
Power consumed, kw	1.45
Power factor	0.32
Maximum pressure head, kg/cm^2	1.2
Maximum capacity, m^3/hour	3.2
Maximum efficiency, %	6.5

The efficiency of a-c conduction pumps does not exceed 10-15% as a result of considerable power losses, i.e., it is lower than in d-c pumps (to 40%). One of the main sources of losses is due to the fact that in the liquid metal flow, which is equivalent to the short-circuited turn of a transformer, the alternating magnetic field induces a parasitic emf.

As shown by Blake [42], when an a-c conduction pump has large dimensions, its efficiency and power factor can be brought closer to those of an a-c pump by reducing the frequency of the supply current to 5 to 10 cps.

Helical induction pumps An induction pump with a helical flow of liquid is similar in principle of operation and characteristics to an asynchronous motor. The pumped metal fills the annular gap between two thin-walled tubes separated by helical partitions into several channels. A three-phase multi-polar winding, similar to that in a motor stator, surrounds the outer pipe. A fixed core, made of sheet steel, and used in rotor blocks of induction motors, is situated in the inside tube; a diagram of the pump is shown in Fig. 154.

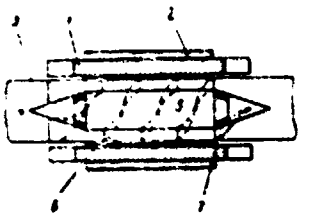

Рис. 154. Схема спирального индукционного насоса.

Fig. 154. Diagram of a helical induction pump.

(1) Multi-phase winding; (2) yoke;

(3) tube; (4) liquid metal; (5) rod;

(6) guides; (7) copper ring.

A three-phase winding serves to create a rotating magnetic field, which induces an emf in the liquid and gives rise to currents in the liquid similar to the currents generated by the rotor of an induction motor. The interaction between the field and the currents in the liquid forces the latter to rotate around the inside tube and, thanks to the helical partitions, to flow axially. Copper rings, closing the current circuit, are welded to the inside wall of the duct at the inlet and outlet. Helical liquid collectors adjoin both ends of the annular passage. These collectors are connected with the suction and pressure outlets of the pump, respectively.

Since eddy-current losses arise in the walls of the tubes forming the annular pump duct, the thickness of these walls should be minimal. The winding of the

stator located directly at the outer wall of the duct is protected from overheating by a layer of thermal insulation as well as by forced air cooling. The operating conditions for winding insulation can also be complicated by the effect of radioactivity. It is possible that the problem of protecting insulation from the effect of heat as well as radiation may be solved by using ceramic insulating materials.

It is advisable to use helical pumps at relatively high liquid heads (see Table 45), as well as when the structure must be as compact as possible. The high pressure drop in the pump is achieved by selecting a small pitch angle for the helical baffles so that the pumped liquid will be affected by each of the poles many times.

Sodium pumps of this type have been constructed for a rated head of up to 7.5 kg/cm^2.

Figure 155 and 156 show the characteristics of one of these helical induction pumps having a sodium-pumping capacity of 90 m^3/hour at a head of 1.5 kg/cm^2. The pump weighs about 700 kg and requires about 30 m^3 of air per minute for cooling.

Flat and annular linear induction pumps. In principle, the action of a flat linear induction pump is similar to that of the helical pump; however, it differs substantially from the helical pump in design and characteristics.

During the operation of the pump, the liquid metal flows in a thin-walled duct of rectangular cross section. In high-capacity pumps, the duct is formed by a number of parallel flat tubes connected at the inlet and the outlet of the pump by common fittings. Polyphase, multi-polar current windings are situated on both sides of the duct, creating a sliding magnetic field. This field induces currents in the liquid and causes the liquid to be displaced along the duct.

It has been established that a length-to-width ratio for the sections

forming the ducts 25 : 1 is the most satisfactory from the standpoint of obtaining acceptable efficiency and a cos φ with 60-cycle current.

The pump winding is situated on a metallic core, with a layer of insulating material between the duct and the core. Also, provisions must be made to compensate for the difference in thermal expansions of the duct and the external housing of the pump. The housing is air or water cooled to maintain the winding at the required temperature.

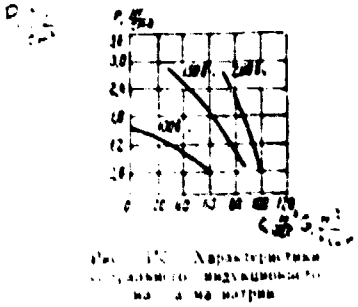

Fig. 155 Characteristics of a helical induction pump operating on sodium.

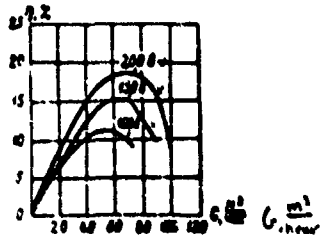

Fig. 156. Emf of a helical induction pump operating on sodium as a function of efficiency.

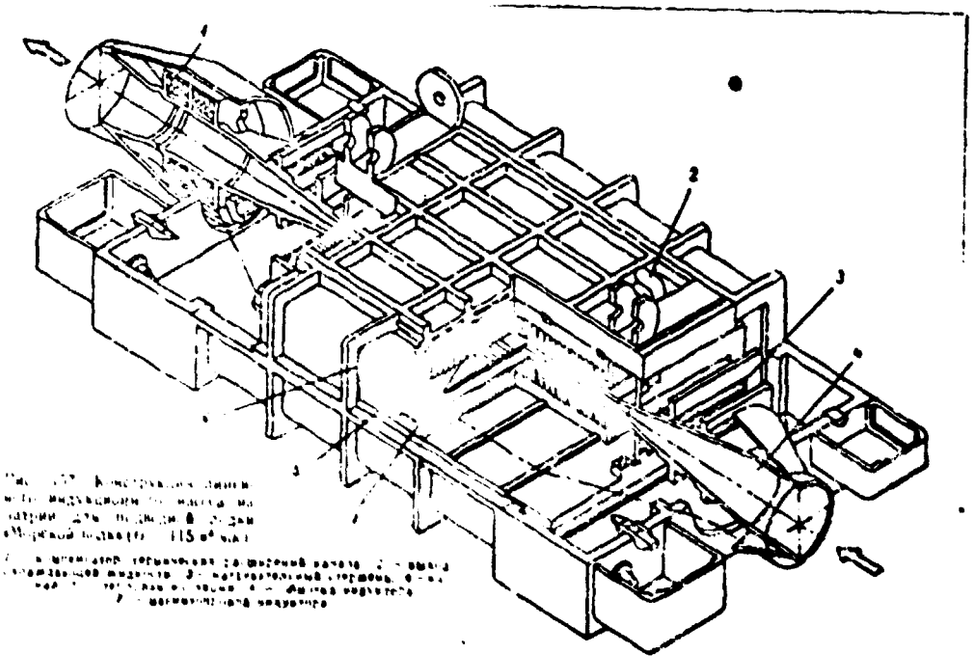

Fig. 157. Design of a linear induction sodium pump for the submarine "Seawolf" (Q = 115 m³/hour).
(1) Duct heat expansion compensator; (2) discharge of cooling liquid; (3) heating rod; (4) duct; (5) thermal insulation (6) inductor windings; (7) inductor magnetic circuit.

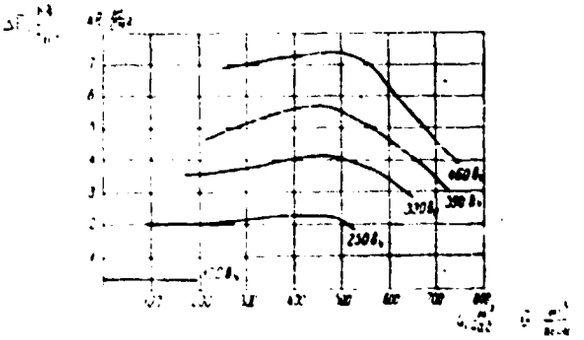

Fig. 158. Characteristics of a linear induction sodium pump.

Fig. 157 shows the design of one such pump (for the submarine "Seawolf"), and Figs. 158 and 159 show the characteristics of a linear pump.

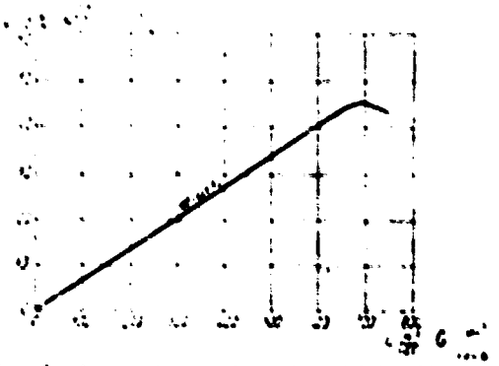

Fig. 159. Dependence of efficiency on discharge for a linear induction sodium pump.

ACL-554

It is advisable to use this type of induction pump in the event a reduction in the power consumed in pumping and the dimensions of the pump are the chief considerations. The efficiency of larger pumps reached 45% at $\cos\varphi = 0.42$. Several types and sizes of flat linear pumps have been tested in detail and some of them performed over long periods of time at liquid-metal temperatures of 400-450°C

Fig. 160. General view of a linear induction pump with an annular gap (the housing has been removed).

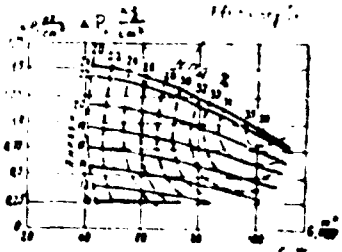

Fig. 161. Characteristics of the linear pump with an annular gap shown in Fig. 160.

TABLE 48

Technical Data on Linear Induction Pumps Produced by the Firm "English Electric"

Characteristic	Pump number					
	IA	6	10	10	15	20
Liquid being pumped	NA		Na—K (30%K)		Na	
Capacity, m^3/hour	7.2	40.7	108	108	270	685
Pressure, kg/cm^2	1.5	1.2	1.1	1.0	1.1	2.1
Total length (including the diffuser), mm	510	1020	1960	—	2 000	2 280
Total height, mm	150	305	510	—	610	610
Over-all width, mm	150	405	760	—	1 070	1 220

TABLE 48 continued

Technical Data on Linear Induction Pumps Produced by the Firm 'English Electric'

Characteristic	Pump number					
	IA	6	10	10	15	20
Diameter of the outlet aperture of diffuser, mm	25	51	102	—	152	213
Weight, kg	365	2500	6800	—	12 500	16 000

Lately, much attention is being given to annular-gap linear induction pumps for moving liquid metal. Giving the walls of the duct a cylindrical shape somewhat increases pump efficiency as compared with flat-type pumps by cutting edge losses in the gap and makes it possible to use duct walls which are quite thin, although possessing adequate strength.

A general view of an annular-gap linear pump and its characteristics (for a sodium-potassium alloy) are given in Figs. 160 and 161 [171] .

37. Heat Exchangers and Steam Generators Operating on Sodium and a Sodium-Potassium Alloy

Liquid metals possessing favorable heat-transfer and nuclear properties, a high boiling point, and stability at high temperatures are promising heat-transfer media for nuclear-reactor cooling systems. Liquid metals are the only possible coolants for fast reactors.

Using liquid metals as heat-exchange media permits operation at a high temperature without considerable pressures, which makes it possible to obtain a relatively high efficiency for the plant with relatively simple and inexpensive heat-exchange equipment.

Heat exchangers functioning on lithium, lead, or lead-bismuth alloys have not as yet received extensive application and have been used mostly in small experimental plants. Considerable experience has been gained in designing, manufacturing, and operating experimental and semi-industrial heat exchangers operating on sodium and sodium-potassium alloys. These metals have high thermal conductivity, a low melting point, a high boiling point, and good thermal stability. Na and Na-K alloy also have low corrosion activity when impurities have been removed: low-carbon, chrome, and chrome-nickel stainless steels, nickel, inconel, and zirconium are corrosion resistant in these media and in the working temperature range. Very little power is needed to pump these metals due to their low specific gravity and low viscosity (about as much, for instance, as needed for pumping water). Due to low electric resistance, sodium and Na-K alloys can be successfully circulated in systems by electromagnetic pumps, which operate with these metals at relatively high efficiencies.

The disadvantage of Na and Na-K alloys is their relatively low heat capacity, as a result of which it takes a greater flow of metal than of water to remove heat for identical temperature drops.

Several specific requirements should also be considered when designing heat exchangers and steam generators operating on sodium and Na-K alloys:

1. Maintaining complete air-tightness of the device. The possibility of leakage of the liquid metal, which is sometimes radioactive, as well as its combination with water or the air should be precluded. The reaction of alkali metals with water is accompanied by liberation of gaseous hydrogen and a large amount of heat and can lead to breakdown of the plant. On combining with the air, the molten metal is readily combustible; this presents a danger to service personnel. Furthermore, scientists have established that there is a sharp rise in the corrosive activity of alkali metals when they are contaminated with oxygen and poorly soluble oxides form.

These oxides are also dangerous with respect to clogging of piping, especially with respect to the cold sections.

In view of the high operating reliability requirements, designs with two working fluid circuits, separated by a third liquid-- an interlayer --not reacting with the working fluids, have received acceptance. The introduction of an interlayer sharply increases the over-all thermal resistance to heat transfer in the apparatus. In the intermediary heat exchangers installed between the nuclear reactor and the steam generator, sodium is used as the third liquid; in vapor generators, the layer between the liquid metal and the steam-water circuit is usually mercury. The appearance of a leak in one of the circuits is established by variations in the pressure of the interlayer, in view of which constant monitoring of the pressure in the working chamber of the interlayer is set up.

In order to make the structure extremely leakproof, all joints should be welded, including the connections of tubes to tube-sheets. In addition to the

standard methods for checking welded seams, x-ray and gamma-ray analyses, leak tests with a helium leak detector and supersonic defectoscopy are used to check welds.

2. Maintaining a high degree of cleanliness in the system. All the internal surfaces of the heat exchanger should be thoroughly cleansed of dirt and grease, for which purpose the assembled device is degreased (by dichlorethane or some other grease solvent), flushed, dried, and filled with an inert gas (argon, nitrogen, or helium). The metal should be drained completely and it should be impossible for gas pockets to form when the heat exchanger is being filled. Maintaining cleanliness of the heat exchanger during operation is achieved by methods which are common for the entire system.

3. Providing preheating of the sodium circuit of the heat exchanger. In order to avoid the dangers connected with clogging of the ducts, the heat exchanger should be uniformly heated to a temperature exceeding 98°C prior to the start of circulation. For this purpose the heat exchangers are provided with different types of electric or steam-heating systems.

In designing heat exchangers special attention should be paid to compensation for thermal expansion.

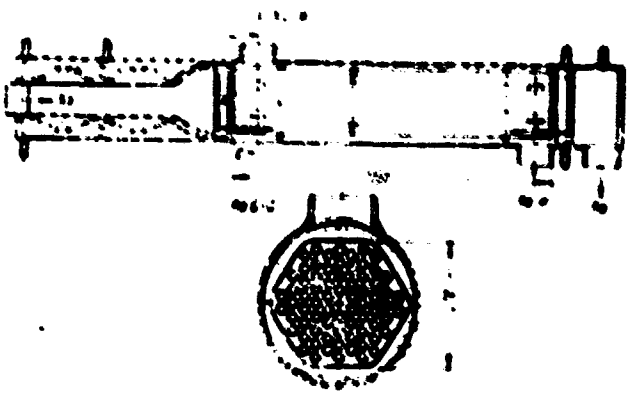

Fig. 162. A sodium-- Mo-K --alloy double-tube heat exchanger.

Some important conclusions relating to serviceability of structures under conditions of thermal stress were accumulated in operating heat exchangers.

In the event the steam and sodium circuits of a steam generator are not separated from each other by walls filled with a third liquid, it is desirable to have the liquid metal circuit capable of withstanding the maximum pressure of the steam circuit. In order to avoid a sharp rise in pressure, the sodium circuit should be provided with a safety valve of large cross section. A pressure rise in the system when water penetrates into it can be accompanied by sharp local temperature rises. Hence it is important to equip the installation with automatic devices which could cut off the heat exchanger from the rest of the system in an emergency and quickly interrupt the supply of water to the system.

A description of certain designs of heat exchangers and steam generators, in which sodium and Na-K alloy act as heat transfer media, is given below.

Heat Exchangers. Fig. 162 shows a counter-current, single-pass, tube-and-shell heat exchanger in which the heat is transmitted from the sodium cooling the reactor to a Na-K alloy. The double concentric-tube and the double-tube sheet system is used in the heat exchanger. Sodium flows through the inner tubes, the annular gap between the tubes is filled with motionless sodium (the interlayer), while an Na-K alloy circulates in the space between the tubes. There are no baffles in the space between the tubes. The inner tubes are diffusion-bonded to the outer tube sheets, one of which is directly welded to the shell of the heat exchanger and the other is welded to the shell through a bellows compensator. The outer tubes are diffusion-bonded in the inner tube sheets, at one of which a bellows thermal-expansion compensator is also situated.

The Na-K alloy flows into the heat exchanger through six connecting pipes situated at its 'cold' end and flows out through six connecting pipes on the opposite side. The heat exchanger consists of two sections which can be connected to the system in parallel or in series. One of the sections can be completely

disconnected to investigate the effect of decreasing the total heat-removal area. In order to study the effect of the position of the device on its operation, one of the sections was arranged vertically and the other horizontally.

Altogether, 72 double tubes 12.5/0.85 mm and 16/1.0 mm in diameter were installed in the heat exchanger. The heat-transfer area, calculated from the external diameter of the outer tubes, came to 3.73 m^2 for each section or 7.46 m^2 for the heat exchanger as a whole.

Grade L nickel (99.4% Ni, 0.1% Cu, 0.15% Fe, 0.2% Mn, 0.05% Si, and a maximum of 0.02% C) which has a high thermal conductivity was selected as the tube material. All the remaining components of the heat exchanger were made of type 347 stainless steel.

The sodium flow through the heat exchanger amounted to 46.2 tons/hour and of the Na-K alloy to 47.0 tons/hour, the sodium temperature at the inlet was 510°C and of the Na-K alloy at the outlet 472°C. Given these flow rates, the over-all coefficient of heat transfer amounts to 4,880 kcal/m^2 · hour °C and the heat removal to 930,000 kcal/hour.

The advantage of the design discussed consists in the relatively low hydraulic resistance of the heat exchanger shell.

The disadvantage of the design is the inaccessibility for inspection and maintenance of the inner tube sheets as well as the considerable thermal resistance of the double-tube system.

Figs. 163 and 164 show a counter-current, single-pass, sodium-- Na-K --alloy heat exchanger with flat L-shaped tubes. The heat exchanger is intended to serve the same purpose as the preceding one and is designed to operate with the same heat-exchange sodium parameters.

The sodium and Na-K alloy flow along different staggered tube banks, entering at the front of the heat exchanger and flowing out of the side. The space between the tubes is filled with a sodium interlayer. The utilization of heat tubes makes /262

it possible to do without special thermal expansion compensators.

Continuous tubes, cylindrical in shape at the point where they are connected to the tube sheets, are used in the structure. Flat tubes were obtained by shingling tubes 19/0.9 mm in diameter to dimensions of 26 x 6 mm. Such dimensions for the tube cross section were established as being the most favorable from the standpoint of obtaining the greatest heat-transfer area while preserving an acceptable hydraulic resistance.

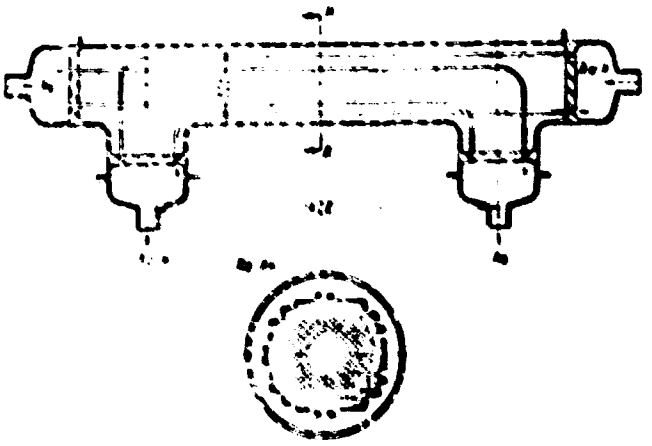

Fig. 16j. Sodium-- Na-K --alloy heat exchanger with flat L-shaped tubes.

A total of 170 tubes were installed in the heat exchanger; Na-K alloy flows in 86 of them and sodium in 84. The effective heat-exchange area, calculated from the external area of the tubes, amounts to 5.55 m^2. The heat-transfer coefficient for rated operating conditions is 9,750 kcal/m^2 · hour °C, and the heat removal is equal to $1.01 \cdot 10^6$ kcal/hour.

The heat exchanger is all-welded; the grade L nickel tubes were diffusion-bonded into the tube sheets in a protective atmosphere of helium.

The advantage of this design consists in relatively low hydraulic resistance for both heat exchangers, high over-all heat-transfer coefficient, and accessibility of the tube sheets for maintenance.

A disadvantage of the design is the large size of the heat exchanger and the high manufacturing costs. Manufacturing costs can be reduced considerably by employing round tubes, but then the dimensions increase considerably and the heat-transfer coefficient drops.

Fig. 165 shows a counter-current single-pass Na-K alloy sodium heat exchanger of the tube-and-shell type with no intermediate medium (interlayer). The heating medium is an Na-K alloy, which flows downward inside 35 tubes 9.5/0.6 mm in diameter. Sodium flows inside the shell in the space between the tubes. The tubes are so arranged in the bank that the centers of the circumferences formed by their cross sections are situated at the vertices of equilateral triangles whose sides are each 15 mm long.

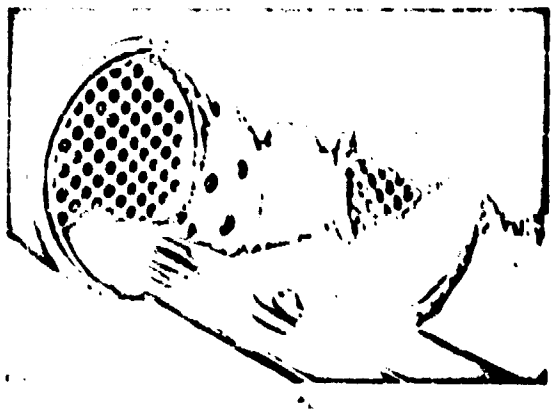

Fig. 164. Separation of a bank of flat tubes of the heat exchanger shown in Fig. 163.

The lower tube sheet is connected to the shell through a bellows compensator. The Na-K alloy discharge pipe is connected with the shell by a protective covering which prevents escape of sodium into the atmosphere if the bellows compensator is damaged. In order to secure the required rigidity of the structure, the heat exchanger is equipped with four baffles which support the tube bundle. The baffles are segments joined by two tie rods. There is a clearance of 0.4 mm between the tubes and the openings in the baffles, which is enough to permit the space between the tubes to be considered as having no baffles when calculations are made. The tubes are rolled in the tube sheets and welded in an inert gas atmosphere. Suitable drain and vent pipes are provided in the heat exchanger to secure complete evacuation of gas in charging and complete drainage of metal after operation. The heat exchanger is made of type 316 stainless steel. It is rated for the following data:

Total heat removal, kcal/hour	925,000
Effective heating area, m^2	1.45
Average temperature difference between heat exchangers, °C	50
Na-K alloy volume, m^3	0.0142
Sodium volume, m^3	0.0099

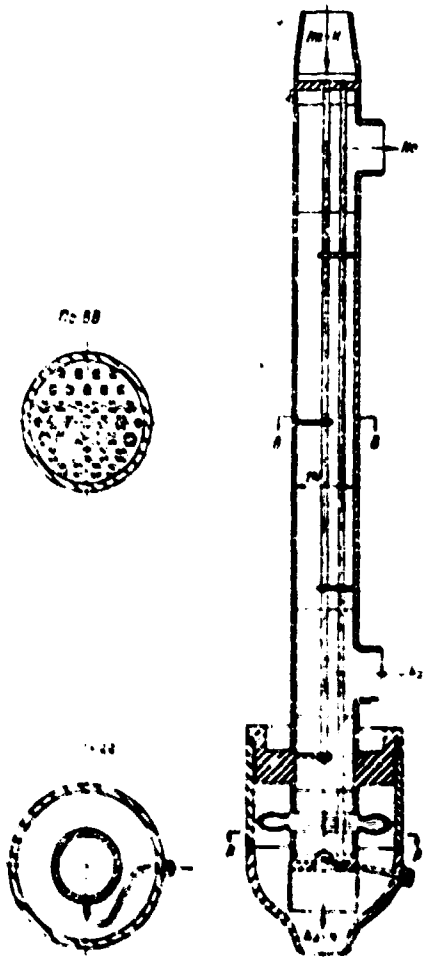

Fig. 165. A sodium-- Na-K --alloy heat exchanger with partitions in the shell.

Fig. 166 shows a small tube-and-shell counter-current-type heat exchanger. Its design is simple; the shell has neither internal baffles nor thermal-expansion compensators. Cylindrical liquid-metal flow distributors were installed at the connection joints.

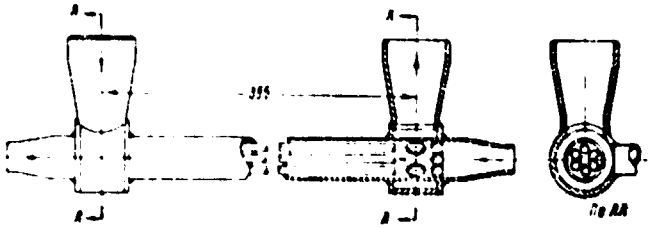

Fig. 166. Small alkali -metal tube-and-shell heat exchanger.

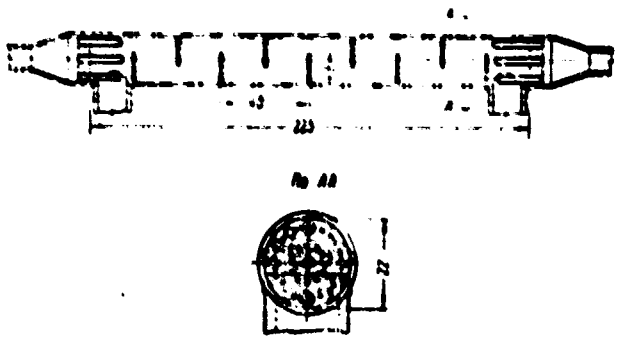

Fig. 167. Small alkali metal tube-and-shell heat exchanger with baffles inside the shell.

A 304-stainless-steel tube with an external diameter of 284 mm serves as the shell; the material of the seven tubes of the heat exchanger, 6/0.9 diameter, is also 304 steel.

The heat exchanger has a heat-transfer coefficient on the order of 10,000 kcal/m^2 · hour °C for an over-all heat flow of 25,000 kcal/hour. It has a relatively low hydraulic resistance in the space between the tubes.

Fig. 167 also shows a small tube-and-shell heat exchanger of the countercurrent type. Its design is similar to that discussed above, with the exception of the baffles inside the shell. The heat exchanger is made of stainless steel.

The heat-transfer coefficient is ~ 12,000 kcal/m^2 · hour °C for a total heat removal of ~ 25,000 kcal/hour.

The heat exchanger is characterized by a high heat-transfer coefficient in the space between the tubes.

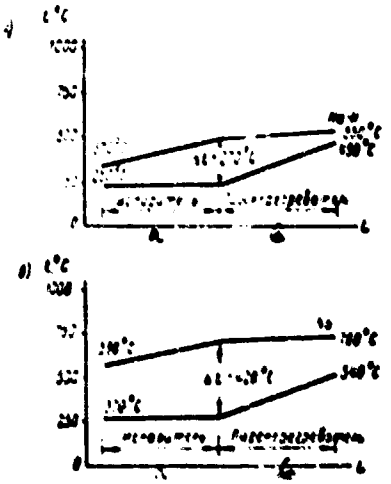

Fig. 168. Temperature distribution along the heating area in sodium and sodium-potassium alloy steam generators with a thermal capacity of 1,000 kw. (a) Vaporizer; (b) Steam superheater.

Steam Generators. The design peculiarities of steam generators using alkali metals as a heating medium are governed, mostly, by the high operating temperature of the heat-transfer media and the need to prevent contact between the molten metal and water or steam.

The low thermal capacity of sodium and Na-K alloys causes high temperature drops in the heat exchangers. The differences in the temperatures of the water (steam) and the liquid metal are usually also very high, as can be seen, for example, from Fig. 168a and b which show the distribution of temperatures of heat-transfer media along the heat-exchange surface in Na and Na-K steam generators with a thermal capacity of 1,000 kw.

As a result, the selection of structural materials and the problem of thermal stress in steam-generator elements acquires primary importance. A serious problem is, for example, the compensation of the expansion caused by the different elongations of the tubes and the shell of the steam generator.

Fig. 165 shows a steam generator with a capacity of 3 tons/hour at a pressure of 33.7 gage atmos and a saturated-steam temperature of 260°C with natural circulation in the steam-water circuit. The steam generator consists of two evaporators, a steam superheater, and a drum. Na-K alloy is used as a heating medium; it enters the steam superheater at a temperature of 482°C and pressure of 3.4 gage atmos, then passes along parallel pipelines to the evaporators; the Na-K leaves them at a temperature of 326°C. Water enters the drum and then flows to the common collector through two down-pipes and then to the evaporator and back to the drum. To prevent water from flowing into the steam superheater a cyclone water separator was installed at the steam outlet of the drum.

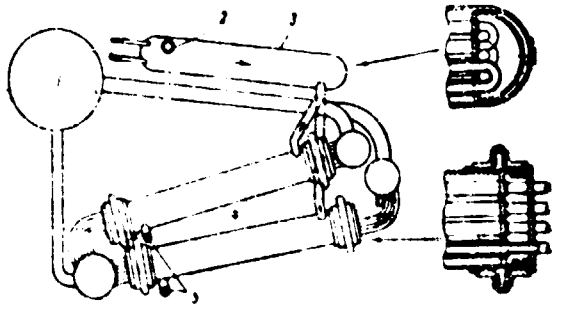

Fig. 169. Na-K alloy steam generator with natural circulation in a steam-water circuit.
(1) drum; (2) Na-K inlet; (3) steam superheater; (4) evaporators; (5) Na-K outlet.

The concentric-tube design has been used to prevent the possibility of contact between the Na-K alloy and water and steam. The annular space between the tubes is filled with mercury. Pressure in the space between the tubes is maintained at 13.6 to 17 gage atmos by means of a cushion of inert gas (helium). The Na-K alloy flows in the space between the tubes of the steam superheater and the evaporator washing the surfaces of the outer tubes longitudinally. The steam superheater consists of a multipass (from the steam side) tube-and-shell heat exchanger and the evaporator consists of tube-and-shell counter-current heat exchangers.

The thermal expansion of the steam superheater tubes is compensated by means of a "floating head" device; bellows compensators connecting the inner tube sheet with the shell are used for this purpose in the evaporator.

Outer tubes 45/2.5 mm in diameter made of EI211(EI1) steel and inner tubes

38/3 mm in diameter made of SA260 steel are used in the steam generator.

Fig. 170 shows a steam generator with forced circulation in a steam-water circuit. It is intended for the same plant and operates on the same parameters as the preceding steam generator.

It has two drums, two evaporators, and a steam superheater. The liquid-metal circuit is fitted with valves making it possible to pass the Na-K through the evaporators either in series or in parallel. The evaporators and the steam superheater are made as multipass (for water or steam) and single-pass (for Na-K alloy) heat exchangers. The alloy flows in the space between the tubes, washing the surfaces of the outer tubes. The annular gap is filled with mercury to avoid the possibility of contact between the Na-K alloy and water.

The thermal expansion of the tubes is compensated by free shifting of the tube sheet of the inner tubes in the shell. The evaporators and the steam superheater are identical in design. The outer tubes 45/2.5 in diameter are made of SA213T11 steel and the inner tubes, 38/3 in diameter, of SA213T19 steel.

Fig. 171 shows an evaporator in which thermal expansion is compensated by utilizing U-tubes. The considerable difference in the temperatures of the hot and the cold branches of the tubes, however, can cause thermal stresses to appear in the tube sheet of this evaporator.

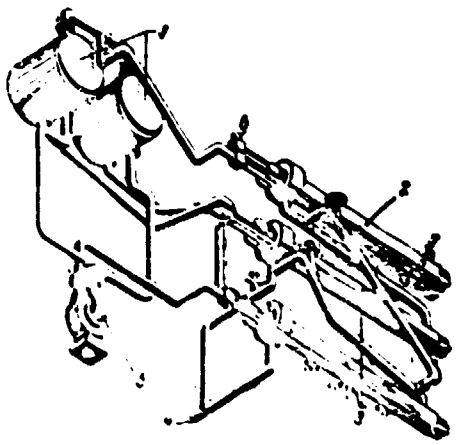

Fig. 170. Na-K alloy steam generator with forced circulation in the steam-water circuit.
(1) drums; (2) steam superheater; (3) evaporator; (4) Na-K outlet; (5) pump; (6) steam discharge; (7) Na-K inlet.

Compensation in the steam generator shown in Fig. 172 is achieved by the use of bent tubes. Considerable stresses rise at the tube-sheet connections; nevertheless a steam generator of this design served without damage for 1,000 hours.

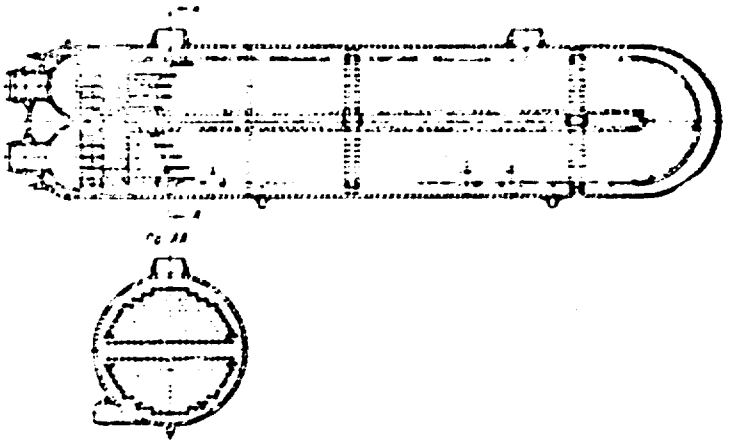

Fig. 171. U-tube evaporator.

Fig. 173 shows a helical-tube steam generator. About the same problems arise in this design as in the preceding version.

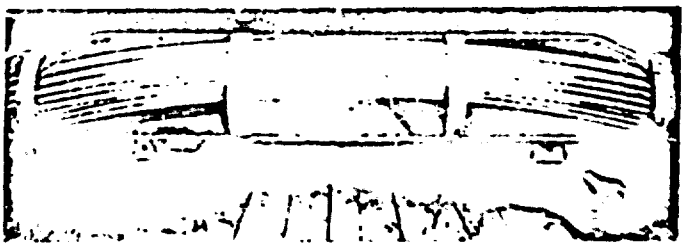

Fig. 172. Bent-tube steam generator.

The problem of thermal-expansion compensation can also be solved by employing the "tube-in-tube" design (Fig. 174). Here one of the tube sheets must absorb considerable strain. The design is also complicated by the fact that the outer tube must have a diameter large enough to maintain an acceptable rate of flow of liquid metal in the annular space.

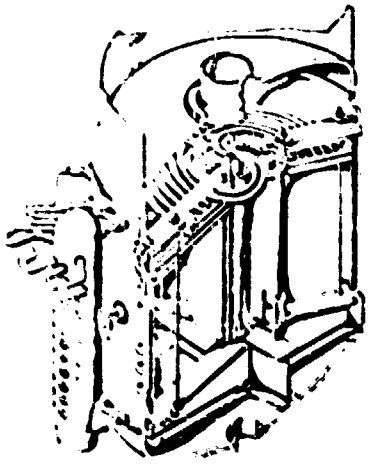

Fig. 173. Helical-tube steam generator.

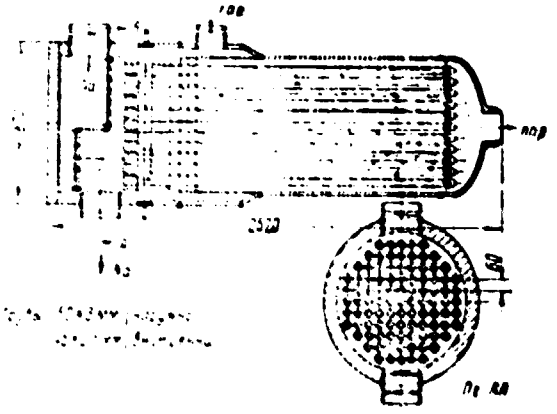

Fig. 174. Utilization of the 'tube-in-tube' design for a sodium steam superheater.
(a) Tubes 50 x 3 mm (outer); (b) tubes 45 x 2.5 mm (inner).

The need for reliable separation of the alkali -metal circuit from the steam circuit led to the double-wall tube having longitudinal grooves on the contacting surface of the tubes (Fig. 175). The grooves are filled with some chemically neutral liquid or gas at a specified pressure.

Experimental data on heat transfer in heat exchangers and steam generators. The results of the measurements of the heat-transfer coefficient in a sodium-- Na-K alloy heat exchanger with flat nickel tubes (see Figs. 163 and 164) [47] are given in Fig. 176. The equivalent hydraulic diameter of the channel formed by the cross section of the flat tube was taken as the defining dimension in calculating the quantity Re. The same figures illustrate the relative arrangement of the tubes of the heat exchanger and their basic dimensions. In calculating the heat-transfer

coefficient the effective heat-exchange surface was determined by projecting the inner surface of the tubes with the heating medium (sodium) on the tubes with the heated medium (alloy). At low alloy flow rates a sharp drop in the intensity of heat transfer is observed (see Fig. 176), which is explained by the authors of ref. [47] by the nonuniform distribution of the flow in the tubes of the heat exchanger, which are of different lengths.

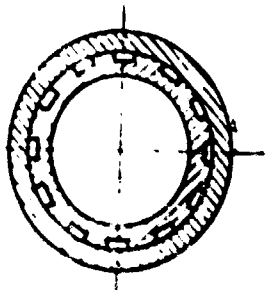

Fig. 175. Grooves on the surfaces of double tubes for alkali-metal steam generators.

The dependence of the heat-transfer coefficient on the Pe number for a tube-and-shell sodium-- Na-K alloy, double-tube heat exchanger (see Fig. 162) are given in Fig. 177. The Pe number was determined by the external diameter of the outer tube. The same figure shows the calculated dependence for the heat-transfer coefficient found assuming the absence of free convection in the mercury interlayer between the tubes. In the calculations, the coefficients of heat transfer from the walls of the tubes to the liquid metal were determined by the Martinelli-Lyon formula [see formula (55), Chapter III] . The experimental data (see Fig. 177) indicate a substantial difference in the heat work of horizontal and vertical heat

exchangers. For low metal-flow rates in a vertical heat exchanger, some rise in the intensity of heat exchange is observed. It is caused, evidently, by the influence of additional buoyancy arising as a result of temperature variations in the liquid along the height of the heat exchanger and the increasing rate of its motion in the space between the tubes and inside the tubes.

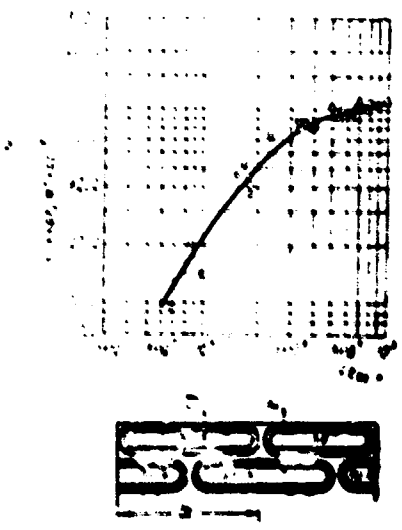

Fig. 176. Heat-transfer coefficient in a sodium-- Na-K alloy, flat-tube heat exchanger.
(a) K, kcal/m^2 hour °C.

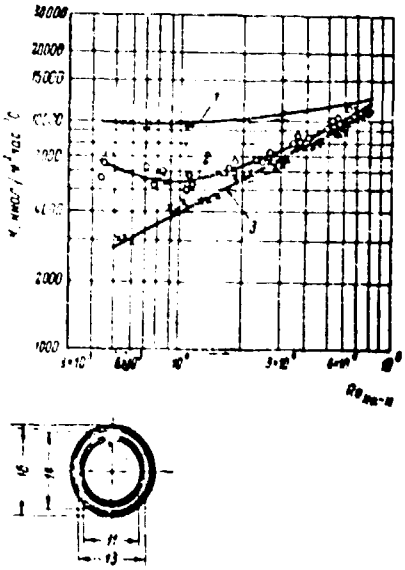

Fig. 177. Heat-transfer coefficient in a sodium-- Na-K alloy, double-tube heat exchanger.

(1) calculated curve; (2) vertical heat exchanger; (3) horizontal heat exhanger.

(a) K, kcal/m^2 hour °C.

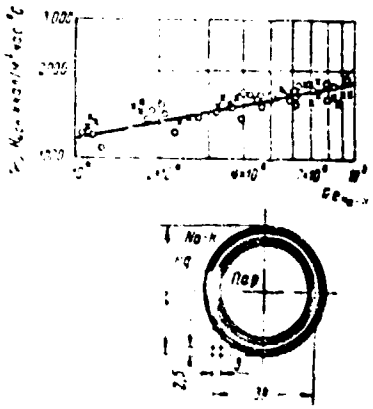

Fig. 178. Heat-transfer coefficient in the evaporating section of a Na-K alloy double-tube steam generator.

0 - forced circulation of the steam-water mixture;

X - natural circulation of the steam-water mixture.

(a) K_{exp}, kcal/m^2 hour °C.

The values of the heat-transfer coefficient in the evaporating section of a Na-K alloy double-tube steam generator (see Fig. 169) are given in Fig. 178.

38. Accessories

Accessories (various types of valves) are important components of liquid-metal systems. Their design and materials should meet certain requirements:

1) high corrosion resistance in liquid metals;

2) adequate strength at elevated temperatures;

3) high strength of the structures with respect to thermal shock;

4) zero seepage of liquid metal along the stem of a valve operating in the primary circuit;

5) no welding of a valve to the seat.

The valve housing can be made of type 347 stainless steel, which showed good results under tests for intergranular corrosion in sodium. Forged rather than cast valve housings are used to secure the necessary leaktightness.

Thermal shock tests of 347 steel valve castings and forgings showed that, as a result of plastic deformation, stress relaxation occurs even when local stresses exceed the yield point. However, in design, sharp variations in the thicknesses of housing walls should be avoided.

Heat-resistant type 316 steel is used for high liquid-metal temperatures.

It is desirable to install the valves in parts of the system where the temperature does not exceed 650°C in order to prevent welding of the valves to the seats. Seats of conventional design made of stellite perform satisfactorily in sodium at a temperature to 950°C, but do not always guarantee complete leaktightness of the duct. When the duct must be spanned with absolute reliability, frozen metal can be used in the duct. The freezing can be done in small sections of the pipeline and at places where rapid opening or spanning of the duct is not required; in this respect the use of this type of seal on the drainline is not practicable.

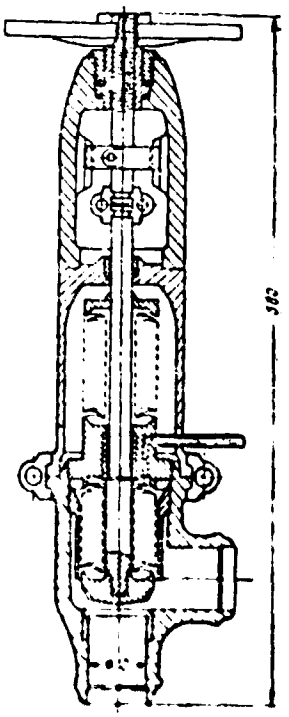

Fig. 179. Double-bellows gating valve d_y = 50 mm.

Experiments with various packings for valve stem gaskets (graphite powder, asbestos, lead cerria, metallic nickel powder, and other materials) did not produce positive results.

Of late, types of seals with no packing have proved satisfactory in liquid-metal systems. Bellows-type seals have gained wide acceptance, and in certain critical instances, double bellows with an interlayer of gas.

The use of valves with frozen seals on the stem is proving to be effective. The outer end of the stem is enclosed in a hollow head intensely cooled by water. The thin annulus between the stem and the head is filled with liquid metal which forms a sealing plug upon freezing. Inasmuch as the shear strength of the metals

used for this purpose is not high, the frozen ring can be easily cut off at the surface of contact with the stem when the latter rotates.

The greatest danger to this type of seal is an interruption in the cooling-water circulation. The frozen plug, however, remains for a period of one minute or more; i.e., there is sufficient time to start an auxiliary cooling system. The service life of the frozen seal is unlimited provided the sealing metal is free of foreign solid particles, which exert an abrasive action on the surface of the steel.

Fig. 179 shows a double-bellows gate valve, $d_y = 50$ mm. Inasmuch as the bellows membranes (sylphons) have a relatively low natural frequency vibration, when they are used there is the danger that high-amplitude resonant oscillations will appear. In designing, it is recommended that the difference between the frequency of the pulses and the natural frequency of membrane vibrations be not less than 15%.

Vibration of the bellows can occur in regions of sharp change in flow direction and at high discharges. This can happen in gate valves, in view of which the bellows are protected from hydraulic shock by suitable shields.

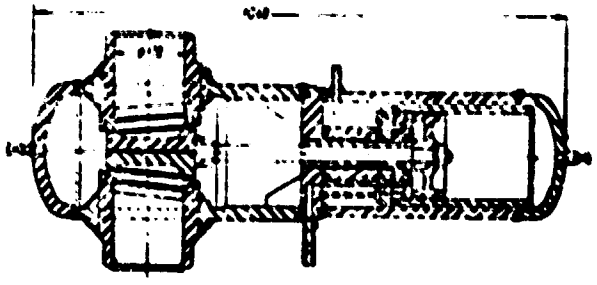

Fig. 180. Gate for a sodium pipeline $d_y = 174$ mm.

Fig. 180 shows a piston-controlled gate for a sodium pipeline, d_y = 178 mm. Inasmuch as the medium moved is the working fluid in this case, seepage through the piston ring is of no great significance.

Fig. 181 shows schematically a valve with integral electric drive. The winding of the stator is separated from the rotor by a steel or inconel shell 1.6 mm thick. The valve is controlled by a switch which causes rotation of the poles of a three-phase electric motor with an induction winding. The rotor follows the rotation of the switch in the same direction and at the same rate, simultaneously shifting in an axial direction, opening or closing the valve.

Fig. 182 shows a cut-off valve installed in a sodium pipeline, d_y = 76 mm. All parts of the valve are made of type 316 stainless steel. Stellite has been welded on to the supporting surfaces. The guide bushing of the casing is made of stellite 21 and the piston ring of stellite 25. The valve is operated hydraulically, and the pumped sodium is used as the hydraulic fluid.

Fig. 183 shows a rocking feed valve for a sodium pipeline, d = 203 mm. The valve is closed on all sides; hence there is no problem of sealing off any of its elements. The sliding bearings are protected from contamination by the sodium flow by special baffles.

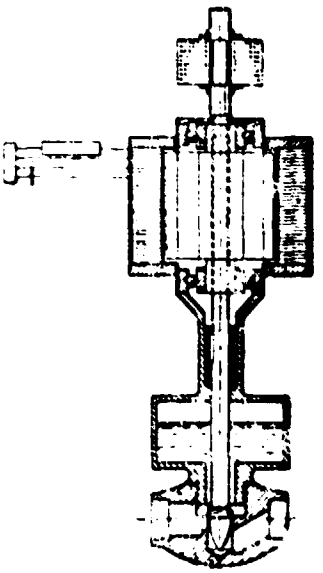

Fig. 181. Valve with integral electric drive.

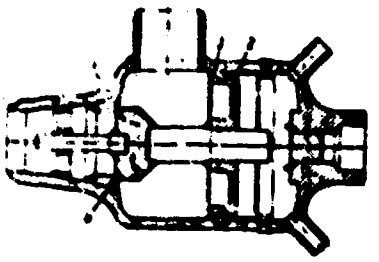

Fig. 182. Check valve for a sodium pipeline, d_y = 76 mm.
(1) valve; (2) piston; (3) guide bushing; (4) stellite beading.

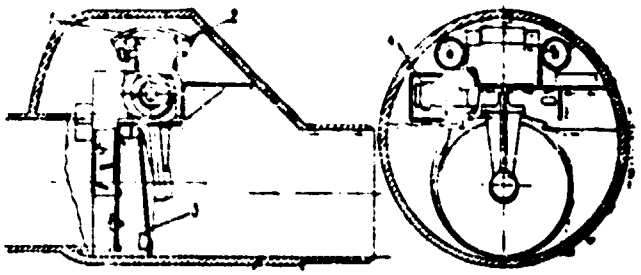

Fig. 183. Rocking feed valve for a sodium pipeline, d_y = 203 mm. (1) counterweight; (2) counterweight spring; (3) valve gate; (4) spring of pivot gate.

Fig. 184 shows a ball feed valve installed on a pipe, d_y = 3 mm. The valve permits the liquid to flow in one direction only and acts under the effect of the pressure drop on it. The ball is made of type 440 stainless steel, the other parts of 316 stainless steel. The valve was tested successfully with sodium at temperatures up to 760°C.

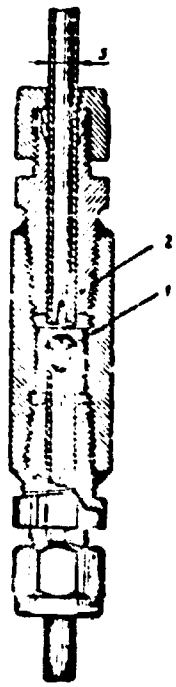

Fig. 124. Ball feed valve for a sodium pipeline, d_y = 3 mm.
(1) Ball, d = 6 mm; (2) aperture for passage of sodium when ball is raised.

39. Instrumentation

General. Peculiarities in the design of measuring devices in liquid-metal systems are governed mainly by the type of heat-transfer media and the magnitude of the operating temperature of the instrument. In modern installations this varies between 100 and 600°C. The operating pressure does not substantially affect instrument design since it is normally relatively low.

Owing to the specific properties of liquid metals, especially their high electrical conductivity, their use as heat-transfer media led to the construction of devices formerly not commonly used, for example, electric level indicators and magnetic flowmeters.

The peculiarity in the operation of measuring devices in liquid-metal systems lies in the fact that the degree of purity of the metal influences their efficiency inasmuch as the presence of oxides and other impurities alters such properties as electrical conductivity, for example, and promotes clogging of the inlet and outlet leads of the devices.

The fact that at room temperature the majority of the metals used are in the solid state can be utilized to diminish the danger brought about by leakage of metal inside the device. An example of this is a pressure gage in sodium systems consisting of a pressure transmitter and the measuring (secondary) device itself, which records the gas pressure in the pressure transmitter cavity. If the length of the inlet main of the secondary device is sufficiently large, then the metal will freeze in this main in case of a leak inside the transmitter. Special experiments were conducted to determine the length of tube which ensures solidification of sodium in it for the above temperature (and other) conditions. The test results are given in Table 49 and in Fig. 185, which show the distance traveled by the sodium in an uninsulated steel tube, d = 6.5 mm, to the place where it solidifies as a function of the temperature of the surrounding medium (air). As shown by the experiments, neither the temperature of the metal nor its pressure exerts any substantial effect on the magnitude of this distance.

Best Available Copy

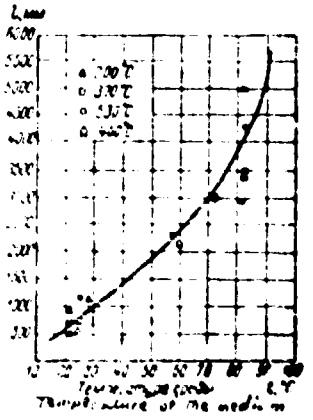

Fig. 185. Solidification of sodium in a steel tube cooled by the natural convection of the surrounding air.

The presence of relatively cold zones inside the measuring devices is undesirable inasmuch as the metal vapors condense in these zones, causing eventual plugging of the internal orifices of the device. Hence, intensive and fairly uniform heating of all its joints should be maintained.

TABLE 49

Length of Tube Required for Solidification of Sodium Flowing Through it

(under conditions of cooling by natural convection of the

surrounding air)

Tube material	Internal diameter of the pipe, d, mm	Sodium temperature, t, °C	Sodium pressure, p, gage atmos	Temperature of the surrounding medium, t, °C	Length required, ℓ, m
Copper	6.3	315	7.0	80	2.05
•	6.3	315	7.0	80	2.30
Stainless steel	6.8	315	7.0	80	>6.10
Same	15.8	295	7.0	80	>18.3
•	15.8	315	7.0	50	7.5
•	15.8	300	7.0	70	8.95
•	15.8	327	7.0	80	11.50
•	4.6	370	8.8	80	3.65
•	15.8	310	7.0	70	7.30
•	15.8	150	7.0	60	5.50
•	15.8	540	7.0	60	7.70
•	15.8	540	7.0	60	7.00
•	4.6	370	8.8	60	2.20

Temperature measurement. Fig. 186 shows a highly sensitive and mechanically stable platinum resistance thermometer used for measuring the temperature of molten sodium. The accuracy of the instrument amounts to $\pm$ 0.5°C for temperature ranging to 120°C and $\pm$ 1.5°C for temperatures to 550°C; its response was better than 3-4 sec. The minimum depth of thermometer immersion in the liquid metal is ~50 mm. The calibration of the thermometer is completely reliable at temperatures to 550°C and does not vary under the influence of the radioactivity of the liquid metal. In order to measure temperatures above 550°C, apparently, a resistance thermometer with a tungsten sensitive element is required.

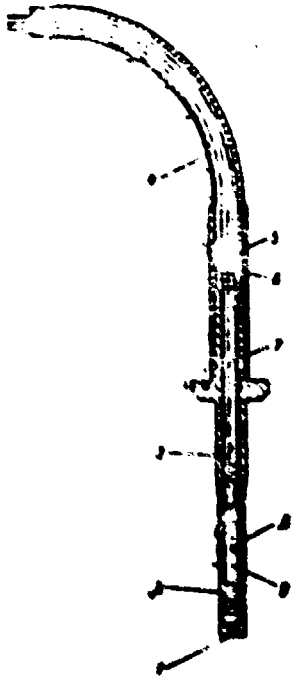

Fig. 186. Platinum resistance thermometer used to measure the temperature of molten sodium.
(1) diffusion-bonded plug; (2) platinum wire; (3) inconel wire; (4) cable; (5) alundum cement; (6) glass plug; (7) insulator; (8) stainless-steel tube; (9) cold core.

Thermocouples are used when the dimensions of the temperature sensor must be as small as possible. Thermal electrodes of chromel-alumel thermocouples are usually placed in stainless steel shells 1.5 mm and 3 mm in diameter and insulated by powdery magnesium oxide. Thermocouples are inserted into the interior of the system in a relatively cold spot in order to secure sealing of the inlet by solidified metal. A thermocouple jacket inlet outside the cold zone is sealed by brazing. The end of the jacket is welded on permanently, in such a way that after mounting the hot junction of the thermoelectrode wires can be easily removed from the jacket, permitting replacement of thermocouple wires. Since the magnesium oxide absorbs moisture and as a result loses its electric insulating properties, the insulation should be protected from contact with water and water vapors.

It is desirable to calibrate every thermocouple of such design individually, inasmuch as their results can differ from the standard curve. The response of the thermocouples is about 1.0-1.5 sec; the maximum measuring error is $\pm$ 2°C at a temperature on the order of 500 - 600°C. The longest thermocouples made have been seven meters. The temperature limit for application of thermocouples of this design depends on the decreased insulation resistance at elevated temperatures and is probably $\sim$ 1,000°C. A thermocouple with a jacket diameter of 1.5 mm was used under radioactive conditions to measure the temperature of sodium washing the heat-generating unit of an experimental nuclear reactor. The high flexibility and strength of the thermocouple makes it possible to lead them through long channels with many bends.

The temperatures of tube surfaces of a liquid-metal circuit can be measured by conventional thermocouples insulated by a glass thread and attached to the surface by standard methods (caliking, by means of clamp sheets, etc.). Welding thermocouples to a steel surface by discharging a bank of capacitors has become common. A corresponding device can be used for welding thermoelectrode wires and welding the hot junction of a thermocouple to the wall of a protected jacket. The

thermocouple to be welded on is clamped either by a conventional pair of electric-insulated pliers or in a special clamp and applied to the welding site. The welding is done by an electric arc generated between the junction of the thermocouple and the specified sector of the surface during the discharge of capacitors.

Pressure measurement. Standard manometers with a Bourdon-tube sensitive element have been used to measure pressure in systems containing a sodium-potassium alloy. Plugging of the tubes was observed in certain instances, caused, apparently, by insufficient purity of the liquid metal. Precise pressure measurements in sodium systems is difficult with Bourdon tubes inasmuch as the manometer has to be constantly heated which contributes an error in its readings. When the tubes are plugged up by solidified sodium, they are usually disabled, since attempts to melt the metal out lead to failure of the tube or to intolerable changes in its elastic properties. Manometers are sometimes installed on special containers filled partially with liquid metal and partially with inert gas (Fig. 187). The main difficulty in the operation of separate-container manometers is the condensation of metal vapors in the upper, colder part of the container and the resulting plugging of the inlet piping of the manometer. It is recommended that the containers be fitted with metal-vapor condensers in the form of cooled tubes of the greatest possible cross section (see Fig. 187). The container should be fitted with a liquid-metal level indicator. Sometimes two level indicators are installed, electrically connected with solenoid valves controlling the inflow of inert gas into the container and its outflow from the container, which makes it possible to maintain a constant metal level in the container and protects the gas pipelines and the manometer from spattering by molten metal.

Remote-reading diaphragm pressure sensors are also used to measure pressure. Figs. 188 and 189 show pressure transmitters with single and double diaphragms rated for operation at pressures to 7 gage atmos and temperatures to 500-600°C. They are installed directly on the piping of the system. Under any temperatures

and pressures the diaphragm of the transmitter can be installed in a position close to the null* by forcing air into its cavity; the error of the device, due to variations in the elastic properties of the diaphragm under temperature fluctuations, is insignificant.

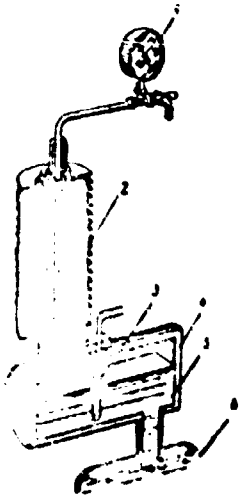

Fig. 187. Manometer with a separater container.
(1) manometer; (2) metal-vapor condenser; (3) level indicator; (4) separater container; (5) liquid metal; (6) pipe.

The diameter of the tubing, by means of which the sensor is connected to the liquid metal intake, is 50 mm.

Double-diaphragm transmitters are more advantageous in measuring high pressures and less dangerous in service, since they prevent metal from falling into the pneumatic system in the event one of the diaphragms fails. Pressure variations in the space between the diaphragms influence the magnitude of pressure transmitted to the air gap if the areas of the diaphragms are dissimilar. This makes it necessary

* Zero position corresponds to equal pressure on both sides of the diaphragm.

to maintain constant artificial pressure in this space. Inconel X is the material of the diaphragm and inconel is used for the casing and sensor. The limit of measurement is regulated by changing the pressure in the air gap or by means of altering the position of the nozzle (see Fig. 189).

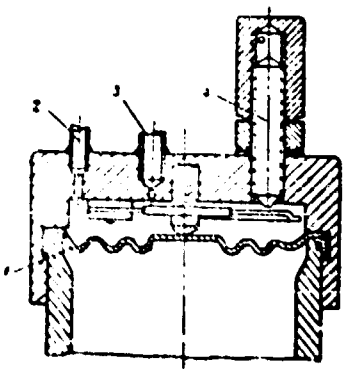

Fig. 188. Single-diaphragm pressure transmitter.
(1) diaphragm; (2) outlet to manometer; (3) gas lead-in; (4) nozzle.

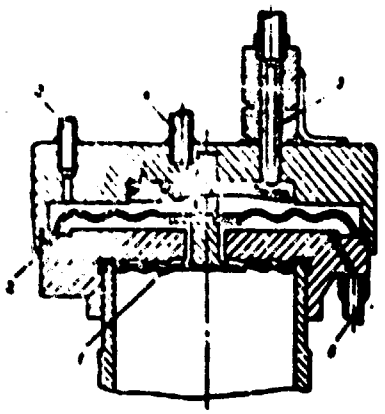

Fig. 189. Double-diaphragm pressure transmitter.
(1) and (2) diaphragms; (3) outlet to manometer; (4) gas lead-in; (5) nozzle; (6) gas led into cavity between diaphragms.

The accuracy of diaphragm pressure transmitters is about $\pm$ 3%; their response, 10-15 sec. This type of pressure transmitter performed satisfactorily in liquid-metal (sodium) installations continuously for two years.

The relatively slow response of pneumatic transmitters makes it necessary to switch to the use of an electrical pressure transmitting system. Fig. 190 shows the circuit of a fast-response pressure-signal transmitter which works on the principle of variation of the inductance of a pick-up coil when the pressure in the system changes. When the pressure rises above the permissible level, a relay is actuated which starts the signal device. In operation this type of pressure-signal transmitter proved to be very dependable; the deviation of the pressure at which the relay was actuated from the selected pressure did not exceed 0.3-0.4 kg/cm^2. The response of the signal transmitter was better than 0.2 sec.

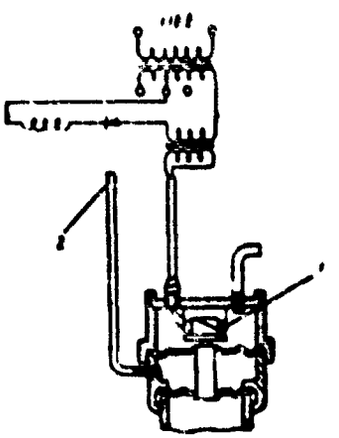

Fig. 190. Diagram of inductance pressure signal transmitter.
(1) inductance coil; (2) air lead-in.

An inductance pick-up with elastic-bellows pressure transmission is shown in Fig. 191. The lower bellows maintains the pressure-tightness of the system; it is in direct contact with the liquid metal. The lower bellows is connected to the upper bellows (which has a spring inside) by means of a stainless steel rod. The stiffness of the spring should be great enough in comparison to the stiffness of the lower bellows to prevent chance deformations of the latter or deformations of the connecting rod caused by temperature variations from reflecting / on the position of the core affixed to the upper bellows. The core is made of soft iron and acts as the fixed core of a transformer. Each of the windings of the transformer has two coils which are wound so as to prevent an effect of temperature on their total resistance. Inasmuch as the core shifts upward or downward under pressure variations, the voltage at the transformer output turns out to be proportional to the measured pressure. The upper part of the device is protected from the effects of high temperature by cooling of the finned supports by the natural convection of the surrounding air. In the event of failure of the lower bellows the metal freezes in the narrow annulus about the central rod. If, however, some metal leaks through the annulus, it will freeze in the cavity of the upper bellows.

Devices of the types described have been employed for measuring low (to 2 kg/cm^2) as well as considerable pressures (to 25 kg/cm^2) in sodium circuits. Their response was better than one second. Tests of the devices showed that they stand up well under repeated (to 5,000 cycles) pressure increases from zero to 20 kg/cm^2 at temperatures of about 500°C. No clogging of the bellows by sodium oxide occurred. The fact that the operating temperature in the lower part of the device is sufficiently high apparently plays a favorable role here.

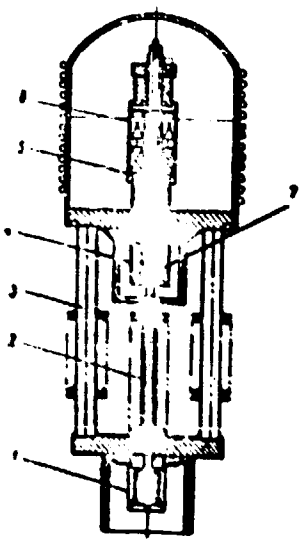

Fig. 191. Inductive pick-up elastic-bellows-actuated pressure transmitter.

(1) lower bellows; (2) rod; (3) finned support; (4) upper bellows; (5) core; (6) transformer; (7) spring.

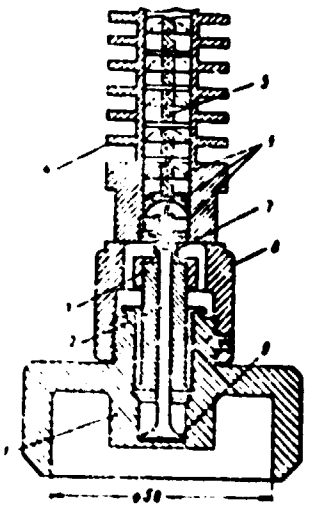

Fig. 192. Capacitive pressure transmitter.
(1) diaphragm; (2) rod; (3) metalloceramic [sintered metal-powder] cylinder; (4) fins; (5) conductor; (6) insulator; (7) contact spring; (8) housing; (9) mica lining.

A capacitive-type sensor can be used to measure pressure. A schematic diagram of a capacitive pressure pick-up is given in Fig. 192. The housing of the transmitter is turned from Inconel-X. The thickness of the diaphragm serving as one of the plates of a variable capacitor is 0.5 mm. The second plate of the capacitor is held in place by means of a hollow cylinder made of pressed powdered metal material and serving simultaneously as a seal for the liquid metal (in the event the pressure-tightness of the diaphragm fails) and as the electrical insulation of the plate. The upper part of the transmitter is finned to improve cooling.

This transmitter can measure pressures equal to 15 kg/cm^2. It can operate at a temperature of the surrounding medium up to 100-150°C and at temperatures of the liquid metal up to 450°C. The accuracy in determining pressure is ± 0.015 kg/cm^2.

A disadvantage of capacitive pickups is the instability of calibration caused, mainly, by temperature variations of the liquid metal. As a result of this they find wide acceptance only as pressure-signal transmitters.

Electric-resistance pressure transmitters, consisting of diaphragm sensors with strain gages attached to the diaphragms, turned out to be less suitable for use than types of transmitters just discussed.

Flow measurement. Permanent-magnet flowmeters have received the widest acceptance for measuring liquid-metal flow. This type of flowmeter consists of a nonmagnetic section of the liquid-metal pipeline placed between the poles of a magnet. Normally, stainless steel is used for this section. Two electrodes are welded or brazed to the pipeline at two diametrically opposite points located in a plane perpendicular to the direction of the lines of force of the magnet and to the direction of liquid flow. The indicator is a standard millivoltmeter connected to the electrodes. The emf generated by the flowmeter is proportional to the liquid flow rate.

Permanent-magnet flowmeters have certain advantages over electromagnetic flowmeters. In using electromagnets it is necessary to separate the signal caused by the inductance of the magnet coil from the signal generated by the liquid flow. Furthermore, electromagnets require voltage regulation for the winding supply. It is advisable to use electromagnetic flowmeters in measuring flows of liquids with high electrical resistance. As a rule, permanent-magnet flowmeters are used in liquid-metal systems.

As shown by experience in the operation of sodium circuits, these devices do not introduce additional hydraulic resistance to the system, they can operate over wide ranges of temperature and discharge, and they have high sensitivity and fairly reliable calibration.

If measurement of the flow does not have to be especially accurate, the magnetic flowmeter can be installed without precalibration. Computations for a

Best Available Copy

flowmeter are made in the following manner. The emf developed by it is

$$E = BVd\,10^{-4}, \tag{97}$$

where E is the emf in microvolts;

B, the magnetic induction in the gap between the magnet poles, gauss;

V, the liquid flow rate, cm/sec;

d, the internal diameter of the pipeline, cm.

Several correction factors must be introduced into Formula (97). The first of them (K_1) accounts for the electrical resistance of the pipe wall and is defined by the formula:

$$K_1 = \frac{2\frac{d}{D}}{\left[1+\left(\frac{d}{D}\right)^2\right]+\frac{\rho_f}{\rho_w}\left[1-\left(\frac{d}{D}\right)^2\right]}, \tag{98}$$

where $\frac{d}{D}$ is the ratio of the internal and external diameters of the pipe;

$\frac{\rho_f}{\rho_w}$ is the ratio of the electrical resistivities of the liquid (ρ_f) and the material of the pipe (ρ_w).

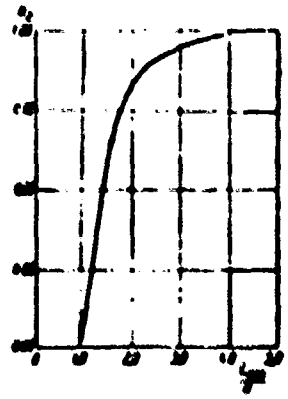

Fig. 193. Correction factor K_2 in Formula (100) for magnetic-flowmeter calculations.

The factor K_1 is introduced into Formula (97) only when computing for flowmeters whose pipes have conducting walls.

The corrective factor K_2 accounts for the nonuniformity of the magnetic field along the length of the pipe. The values of K_2 are given graphically in Fig. 193 as a function of the ratio of the length of the pole-piece of the magnet* to the internal diameter of the pipe.

Finally, the correction factor K_3 accounts for the effect of temperature on the properties of the magnet and on the size of the gap between the poles. If the temperature of the magnet changes from t_1 to t_2, the factor K_3 can be found by means of the equation:

$$K_3 = \frac{1 - \frac{(B_{t_2} - B_{t_1})(t_m - 25)}{B_{t_1}(t_m - 25)}}{1 - \frac{b}{a} 12.5 \cdot 10^{-6}(t_m - t_b)}, \qquad (99)$$

where a is the length of the gap between the magnet poles, cm;

b is the length of the base to which the magnet is attached, cm;

t_m is the temperature of the magnet in the vicinity of its poles, °C;

t_b is the temperature of the magnet in the vicinity of its base, °C;

B_{t_1} is the magnetic induction in the gap between the poles for a magnet temperature t_1, gauss;

B_{t_2} is the same for a temperature t_2.

Allowing for the correction factors K_1, K_2, and K_3, Formula (97) appears as:

$$E = 3.6 \cdot 10^{-4} \frac{BG}{d} K_1 K_2 K_3 v_a. \qquad (100)$$

---

* The length of the pole-piece is understood to mean its dimension along the direction of liquid flow. If the pole-piece has a circular cross section, this dimension is equal to the diameter of the circle.

where E is the emf in microvolts;

B is the magnetic induction in the gap between the poles, measured at a temperature of 25°C, gauss;

G is the volumetric flow of liquid metal, m^3/hour;

d is the internal diameter of the pipeline, mm.

The electrical resistance of the contact between the wall of the pipe and the liquid was not taken into account in deriving Eq. (100). Experiment shows that the presence of the resistance greatly affects the readings of the flowmeter. It can be assumed that when the walls of the pipe are wetted by the liquid metal (as in the case of sodium circuits) the value of the contact resistance is negligibly small. Figs. 194 through 197 are nomograms and graphs for correction factors which make it possible to make approximate calculations for magnetic flowmeters when they operate with sodium and Na-K. The rules for applying these nomograms are identical with those for the nomograms presented in Figs. 61 through 64 (Chapter III).

When the flowmeter is in service it is periodically necessary to check the value of the magnetic induction B; at high temperatures it gradually falls.

The materials of the pipe and the electrodes welded to it should be, if possible, identical to avoid the appearance of parasitical thermal emf's. However, if dissimilar materials must be used, temperature differences between the welded points of the electrodes should be avoided.

Liquid metal flow is measured not only by magnetic flowmeters, although they have received the widest acceptance. Standard nozzle-type flowmeters, with specially heated pressure lines, can be used for flow measurements. In order to measure the pressure head in the nozzle, heated differential manometers, filled with the same liquid metal as the entire system, are employed. It is feasible to use special containers which are periodically fed by inert gas and which separate the cavity of the manometer from the system.

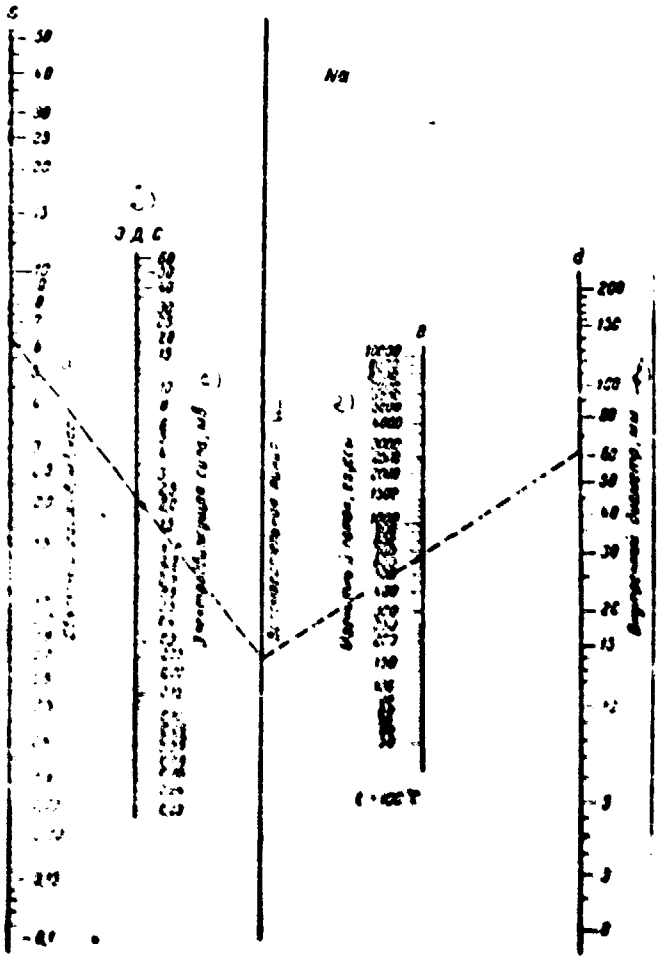

Fig. 194. Calculation of the emf of a magnetic sodium flowmeter.

(a) Volumetric flow, m^3/hour; (b) emf; (c) electromotive force, microvolts; (d) auxiliary line; (e) magnetic flux, gauss; (f) internal diameter, cm.

Liquid-metal level measurement. The simplest indicator of metal level in any reservoir is a conducting rod lowered into the reservoir to a certain depth and insulated electrically from it. The rod is connected to a low-voltage circuit which is closed when its end comes into contact with the liquid metal. The losing of the circuit actuates a visual, audio, or some other type of signal. Spark plugs of internal combustion engines with elongated central electrodes can be used for level indicators. The contact-type indicators are used mostly to signal changes in level. A disadvantage of these indicators in continuous operation is that the metal vapors condense on the insulator at the point where the rod enters the reservoir (if the temperature in this spot is relatively low) and cause a short circuit. If the indicator operates at high temperature, the insulators prove to be insufficiently stable in metal vapors, as shown by experience in operating sodium circuits.

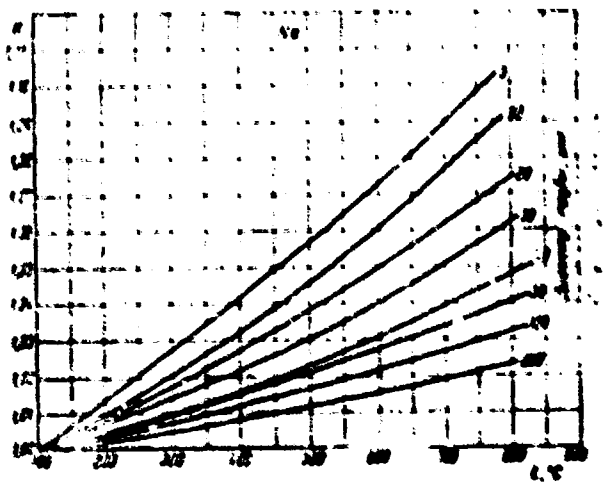

Fig. 195. Correction factor for temperatures $t = 100°C$ for the computed value of emf of a magnetic sodium flowmeter.

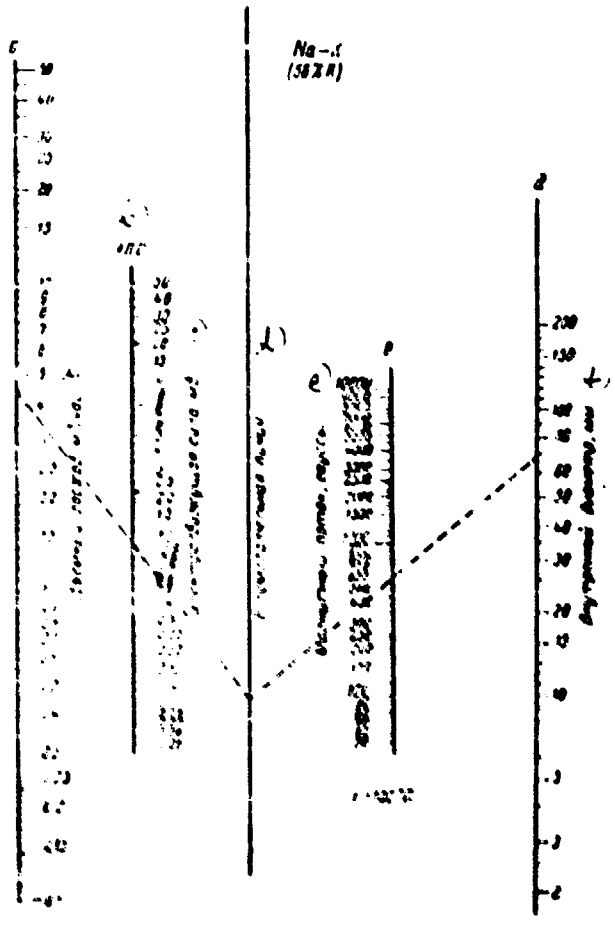

Fig. 196. Computation of the emf of a magnetic Na-K (565 K) flowmeter.

(a) Volumetric flow, m^3/hour; (b) emf; (c) electromotive force, microvolts; (d) auxiliary line; (e) magnetic flux, gauss; (f) internal diameter, mm.

Electrical indicators of a more complex design, used to measure the level of radioactive sodium, which have shown high dependability under continuous operation, are described below. Two types of level meters were developed: with two rods fixed to the upper cover of a liquid-metal reservoir; and with a tube-like rod fixed to the bottom of a reservoir. The general appearance and the electrical circuit of the first type of level meter are shown in Figs. 198 and 199, and a general view and the circuit of the second type, in Figs. 200 and 201. The difference between the maximum levels measured by these devices is about 1,000 mm. They function on the same principle. The liquid metal in a reservoir shorts out certain sectors of the rods (2) (Fig. 198) between themselves or taps some of the resistance of the cylindrical rod (1) (Fig. 200), shorting it with the reservoir housing. As can be seen from the circuit (Fig. 199), the total measured resistance of the level meter of the first type is determined by the length of the section of rods above the level of the liquid metal as well as by the resistance of a corresponding section of tubes (3) (see Fig. 198). Hence, the total resistance of the level of the first type is not a linear function of variations in metal level in contrast to the second type of level meter, the resistance of the tubular rod (1) (Fig. 200) of which is directly proportional to level variation. A standard resistance is built into both devices and serves to calibrate and check the functioning of the electrical measuring circuit. A special resistance is switched into the circuit to compensate for resistance variations in the rods with temperature variations. The maximum error in level measurement amounts to 6%.

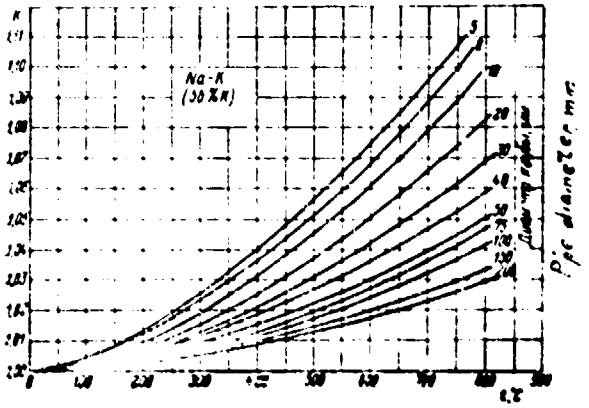

Fig. 197. Corrective factor for temperature $t = 100^{\circ}C$ for the computed value of emf of a magnetic Na-K (56% K) flowmeter.

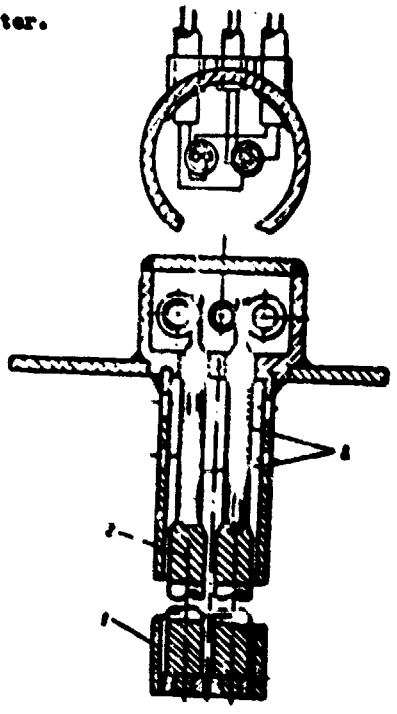

Fig. 198. Double-rod electric level indicator.

(1) protective housing; (2) rods; (3) tubes.

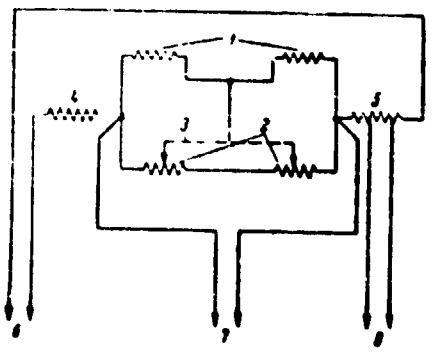

Fig. 199. Circuit of a double-rod electric level indicator. (1) tube resistance; (2) rod resistance; (3) liquid metal; (4) compensating resistance; (5) standard resistance; (6) power supply; (7) and (8) to indicating device.

The basic factors adversely affecting the operation of electric level meters are the resistance of the measuring rod-liquid contact and the accumulation of a layer of liquid-metal oxides on the rod surface. In working with sodium, contact resistance is noticeable only during the first period of operation, i.e., until the rod is completely wetted by the liquid.

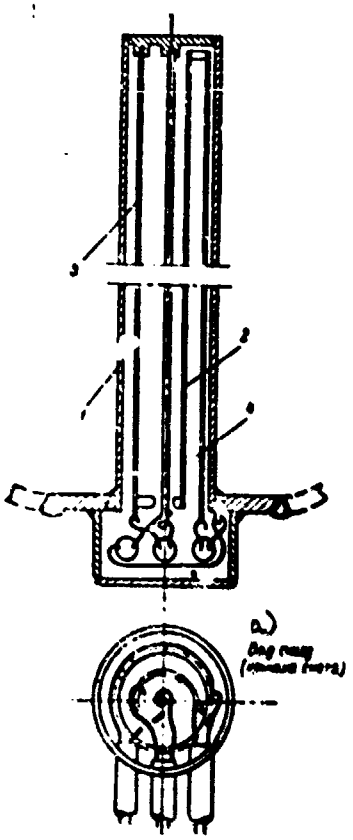

Fig. 200. Electric tubular-rod level indicator.

(1) tubular rod; (2) compensating resistance;

(3) standard resistance; (4) mineral wool.

(a) View from the bottom (cover removed).

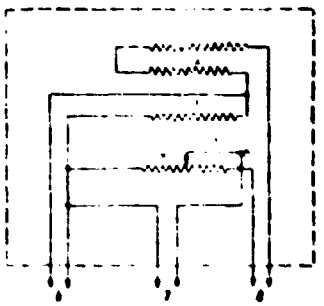

Fig. 201. Circuit of an electric tubular-rod level indicator. (1) and (2) compensating resistances; (3) standard resistance; (4) rod resistance; (5) liquid metal; (6) and (7) to indicating device; (8) power supply.

Float-type level indicators are also used to measure liquid level. In these devices of more complicated design, the displacement of the float is normally transmitted to an indicating device through a diaphragm, bellows, or some other elastic element. The indicating device consists of a voltmeter, and the signal transmitter is a moving transformer core. Float-type level indicators were made to measure liquid levels from 300 to 1,800 mm at operating temperatures up to 400°C. These devices have the following disadvantages:

1) Readings of the device depend on the density of the liquid, and, consequently, vary together with changes in its temperature.

2) It is impossible to make level measurements in a small-capacity tank, inasmuch as there is a minimal permissible float volume whose value depends on the characteristics of the elastic element.

The error of float-type level meters amounts to about ± 1% of the limiting value of the measured level.

CHAPTER VII

OPERATION OF LIQUID-METAL SYSTEMS
(EKSPLUATATSIYA ZHIDKOMETALLICHESKIKH SISTEM)

The use of liquid metals as coolants introduces special features into the operation of laboratory and industrial plants. This fact applied to all the metals under consideration, although the alkali metals possess specific properties that permit their separate consideration.

Experience in the operation of systems with nonalkali metals basically was acquired during the study of mercury-water power plants. Nonalkali metals are distinguished by their relatively great chemical stability under atmospheric conditions. This fact considerably facilitates their use during the filling, emptying, repairing etc., of systems. Conversely the strong chemical activity of alkali metals causes additional operating difficulties. Such difficulties are connected both with the presence of additional complex equipment necessary for the protection of metals from oxidation, for their purification, for the withdrawal of samples, etc., as well as with the greater danger to the attendant personnel inherent in the use of Na, Na-K, and Li, due primarily to their high inflammability. Problems in purifying, sampling, etc., are also encountered in practice in the case of nonalkali metals, but, as a rule, they can be solved very easily. Methods of purifying some of these metals used under laboratory conditions are described in Chapter II, "Chemical Properties." Methods of purification of nonalkali metals used in industry have received little study. For example, it is known that mercury may be purified by using substances (titanium, magnesium), which bind certain

impurities (oxygen in particular), into insoluble compounds which float on the liquid metal and can be removed from its surface, if need be.

The method of operation of liquid-metal power plants is governed by the following:

1. The presence of an inert gas in the system.

2. The necessity of sampling the metal to determine the concentration of oxides and other impurities.

3. The utilization of devices for purifying the metal that are characteristic particularly of sodium circuits.

4. The necessity of special heating for the system.

5. The appearance of considerable internal stresses in the structural material during fluctuations in the temperature of the liquid metal.

40. Preparing the System for Operation

Leakage Tests. Leakage tests of the circuit are made in the following ways:

1. By checking the leakage of kerosene filling the space being tested.

2. By hydro-sampling.

3. By X-rays and gamma rays.

4. By detecting leaks with a helium leak detector.

The latter method is the most reliable. When a vacuum exists within the container being tested and there is a helium medium outside of it, a leak detector with a sensitive mass spectrometer makes it possible to detect a crack through which the leakage of helium amounts to no more than $2 \cdot 10^{-11}$ m^3/hr. If the use of a helium leak detector is neither possible nor feasible, leak detectors utilizing halogen-containing organic materials may be used to locate the leak.

When testing the leaktightness of a container, good results are sometimes obtained by creating air pressure in the container or by creating pressure from some other gas and by coating the surface of welds, flange unions, etc. with a

soap emulsion before testing them. However, there have been cases of leakage of a liquid metal in places where gas bubbles were not observed during soap emulsion tests.

Preliminary Washing. Before the circuit is loaded with metal, all of its components must be completely cleansed of foreign matter (dirt, oil, etc.) which might react with the liquid metal afterwards or else clog up the main ducts.

To remove traces of oil or grease from the internal surfaces of the pipes, various degreasing agents are used. These surfaces may be treated with pickling solutions. It is essential to ensure that after washing there remain no traces of wetting material in the system, in particular, traces of degreasing agents containing hydrocarbons. As is known, the presence of hydrocarbons in a system can cause carburization of the surface of stainless-steel pipes, while the presence of halogen-substituted hydrocarbons in sodium and sodium-potassium circuits is even more dangerous, since these substances react violently with alkali metals.

The most convenient way of removing wetting materials from the circuit is to use water entering under strong pressure. After this washing, the circuit must be carefully dried in a vacuum or in a stream of inert gas.

Special Features in the Preparation of Sodium for Charging into the Power Plant. Before filling a system with sodium it is necessary to carefully free the surface of the metal from oxide[1] and from the layer of lubricant which preserves the metal from oxidation while it is being kept in iron barrels or other containers. After preliminary mechanical purification of the surface layer, the sodium is loaded in individual blocks or briquets into the melting tank, where it should be kept at a temperature of approximately 250°C for several days, thus partially

---

[1] To remove the oxide film from the surface of the metallic sodium, a 10-20% solution of isopropyl alcohol in kerosene is recommended.

cleansing the metal of organic substances. Then, in order to remove the oxides, the sodium is cooled down to 120°C and is passed through porous metal filters, the diameters of the openings of which are no more than 15 μ. These filters may be inserted into the charging line of the circuit. To facilitate the drainage of sodium, a drainage line equipped with a valve was set up parallel to the filters. The filters must be constructed in such a way that they can be removed from the circuit for cleaning and washing.

For preliminary purification of sodium, filters in the form of cold traps may also be used.

Pre-heating the Circuit. Before being filled with liquid metal, the entire power plant must be heated to a temperature exceeding the melting point of the metal.[1] Electric and steam heating are used, the former being more common than the latter.

When the section being heated is small, or when its configuration is complicated, a wire or ribbon wound around the section and protected by a heat-resistant electrical insulator may serve as the heater. To heat large sections, heaters made individually in the form of ceramic cores or tubes with wire or ribbon, etc. wound around them are used. These heaters are attached directly to the surface being heated.

Electrical induction heating is effective for components made of carbon steels. However, when applied to austenitic steels, this method requires a current of very high frequency and is therefore not advantageous.

Steam heating takes place in the following way. One pipe or several pipes of small diameter through which steam circulates are placed in direct contact with the liquid metal duct.

The circuit must be heated in such a way that the temperature in different

---

[1] Sodium-potassium circuits usually do not require pre-heating.

sections is approximately the same all of the time. It is desirable that the rate of heat increase should not exceed 5-10 degrees per hour. These measures make it possible to avoid excessive stresses in the structural material.

Filling the System with Liquid Metal. Before being loaded, the system is evacuated or filled with an inert gas, after the latter has been blown through the system repeatedly for the purpose of removing all the oxygen from it. Vacuum filling may be used in those cases where gas pockets may form in the circuit. During filling, the liquid may enter the system either under the pressure of an inert gas above the level of the metal in the load tank or else through the action of gravity. Sometimes the metal is pumped into the circuit. The first of the above-mentioned methods is the simplest and most convenient. The second method is rarely used, since the load tank is frequently a drainage tank at the same time and is therefore located in the lower part of the circuit.

Before charging, the temperature of the metal in the load tank must be approximately equal to the temperature of the heated circuit.

Solid sodium may be charged into the load tank with the aid of the double lock shown in Fig. 206. The sodium briquet being loaded is placed in the intermediate chamber of the lock, after inert gas has been blown through it.

Level indicators for the metal in the load tank and in other parts of the system serve to regulate the process of charging the circuit. The charging process may also be regulated according to the readings of thermocouples located at various sections of the circuit.

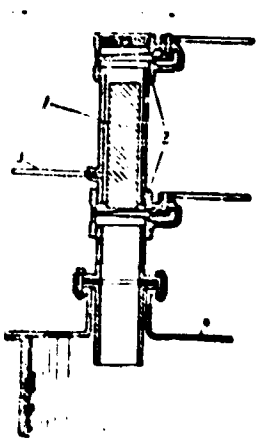

Fig. 202. Double Lock for Loading Sodium into the Load Tank.

(1) A sodium briquet; (2) Gates; (3) Inert gas feed; (4) Tank.

41. Detection of Leaking Metal

Leakage of liquid metal from the circuit into the surrounding medium or into the circuit of another coolant may have dangerous consequences. The degree of danger from a leak is determined by a number of factors; e.g., the size and location of the leak, the temperature of the liquid metal, etc. When checking the leaktightness of the system during its operation, special attention must be given to the welds, especially those welds in which excessive concentrations of internal stress are possible (the places where the tubes are welded to the tube sheets etc.). A leakage of metal may occur as a result of breakdown of bellows, membranes, or other thin-walled components, and also as a result of poor quality manufacture and welding of tubes (slag inclusions, confusion). To a lesser degree the leakage of metal through a crack may be caused by corrosion of the walls of the tubes or the heat-exchangers.

If the metal escaping is radioactive, devices serving to measure the activity of the air must be used in order to detect it. Reduction of the level of the

liquid in the expansion tank is another indication of metal leakage. However, this method is not very reliable, since temperature fluctuations in the system have an effect on the level of the liquid.

A leakage of Na or Na-K alloy in a circuit is noticeable because of the liberation of white fumes of sodium oxide. The fumes may be detected either visually or with the aid of television equipment, photoelectric cells, or chemical air-analyzers.

The most convenient and reliable method of detecting a leak is based on the closing of an electric circuit by the escaping metal. The main difficulty in the manufacture of such devices results from the necessity of making a reliable electrical insulator for the contact wire in order to ensure unimpeded contact between the escaping metal and this wire. If one contact wire is used, a short circuit occurs between the wire and the surface of the container or pipe containing the liquid metal. If two wires are used, the circuit is closed between them. The use of two wires is preferable, since the closing of the circuit takes place in a small gap, and the reliability of detection of the leak is greater. The best insulators for the contact wire are ceramic beads, the shape of which enables the liquid to touch different parts of the wire freely.

The possibilities of using thermistors for detecting leaks (according to a local increase in temperature) in those parts of the system where contact signalers cannot fit are being studied.

Timely detection of a leak of metal in heat-exchange apparatus, especially a steam generator, is of great importance. Sodium steam generators frequently have a system of tubes with double walls between which a heat-transfer interlayer is located. An increase of pressure in the space where the interlayer is located indicates the presence of a leak.

42. Repair and Washing of Sodium Circuits

Repair of a Sodium Circuit. The performance of work on an operating sodium circuit requires that certain measures be taken to avoid oxidation of the metal.

If the circuit is repaired after having performed a large amount of work, the circuit must be entirely drained of sodium and washed thoroughly, before the repairs are started. When the amount of work performed by the circuit is small, two methods of decreasing oxidation of the metal during repairs are recommended:

1. The sodium is drained out of the circuit or out of that part of the circuit which is to be repaired. After the pressure of the inert gas in the system has been lowered to approximately 0.05 gage atmos, an opening 20-50 mm in diameter (depending on the diameter of the tube) is drilled through the wall of the section of the tube being removed. An empty rubber balloon (Fig. 203) is inserted into the opening and is filled with gas, so that the pressure in it exceeds the pressure in the circuit by 0.1-0.2 atmos abs. Thus oxidation of the metal by atmospheric air is avoided. When drilling the hole for the balloon, it is necessary to prevent steel shavings from falling into the tube. After the section of the tube being removed has been cut, a layer of sodium oxide forms around the balloon on the wall of the tube and must be removed with cotton wool or with a rag moistened with alcohol. After the dismantled (or newly manufactured) tube section has been returned to its proper place, the gas is let out of the balloon and the balloon is removed from the opening, into which a plug is then welded.

The above method is used for pipes with a diameter of 100 mm or more. In the case of tubes with smaller diameters, rubber plugs may be used instead of balloons.

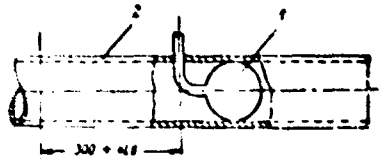

Fig. 203. Use of a Rubber Balloon to Protect Sodium from Oxidation During Repairs to the Circuit.
(1) Balloon; (2) tube.

2. To protect sodium from oxidation, the metal itself may be used artificially frozen in one of the sections of the tube. This method is less convenient than the first, since artificial freezing of the metal in a tube of large diameter takes a long time. Furthermore, the most effective method of cooling a pipe with water or ice is inadmissible from the viewpoint of safety. In practice, this method is applicable to tubes no more than 50 mm in diameter.

When cutting tubes containing frozen sodium, and particularly when cutting tubes containing frozen sodium-potassium, the cutting instrument must not be lubricated with any oils, since the latter vigorously react with alkali metals. After the tube is cut, the surface of the metal must be protected from further oxidation by a thick layer of insulating ribbon. Before the section of tube is welded into place, the sodium is removed from no less than 100 mm of the main tube with a knife or chisel, thus eliminating the possibility of its escaping in molten form from the tube during subsequent welding.

In case the repairs require a change of any section of the circuit, the welding must be done on the spot, after the metal has been completely drained out and the system filled with an inert gas under a pressure slightly exceeding that of the atmosphere. It is desirable that the circuit be washed before being repaired, but this is not mandatory.

Washing a Sodium Circuit after Draining the Metal. All the substances used in removing sodium residue from the system (with the exception of liquid ammonia) react chemically with it. Steam, water, methyl alcohol, and ethyl alcohol are most frequently used for washing. When these substances react with sodium, a chemical reaction of the following type takes place:

$$ROH + Na \rightarrow NaOR + \frac{1}{2} H_2$$

where the letter R represents the appropriate radicals (H, CH_3, and C_2H_5).

From the practical point of view the following particularities of the reaction are important:

1. Generation of a large quantity of heat, which can cause a great increase in temperature in various sections of the circuit.

2. Liberation of hydrogen, which increases the pressure in the system and in certain cases creates a danger of explosion of a mixture of hydrogen and oxygen inside the container or outside of it.

3. Formation of compounds of the NaOR type, which are insoluble in water, alcohol, etc and can therefore clog up the pipe.

In this connection, the possibility of carrying out a careful washing of the circuit is of great importance. The main task is to ensure that the liquid metal is fully drained out of all the units in the system. The power plant must be equipped with ducts of large diameter that are capable of relieving pressure when hydrogen is liberated during washing. The sections of the circuit, connected in parallel, are equipped, when possible, with shut-off valves, which enable each of the sections to be washed individually. Special care must be taken in washing parallel lines (e.g., the tubes of the heat exchangers), which must not overlap. Those components of the circuit which can be removed from the power plant are washed individually.

Alcohol Washing. The advantage of this method of washing is that during

vaporization the alcohol absorbs the heat, and thus its reaction with sodium is not very violent, in comparison with that of sodium and water. In order to increase the chemical activity of the washing reagent during washing, the alcohol may be gradually diluted with water.

This method has the following disadvantages:

The great inflammability of the alcohol and its vapors;

The possibility of a sudden increase in pressure as a result of liberation of hydrogen during the reaction between the alcohol and sodium in the circuit, a large part of the volume of which is occupied by the alcohol;

The possibility of decomposition and coking of the alcohol, when there are large quantities of sodium residue in the system;

The high cost of the alcohol.

The following procedure is recommended for washing:

1. Completely drain out the sodium and let the circuit cool down to a temperature lower than the boiling point of the alcohol (60-70°C);

2. Blow inert gas through the system;

3. Pour into the circuit a small quantity of ethyl or methyl[1] alcohol.

Add alcohol to the system, whenever the alcohol which has already been poured in stops boiling;

4. Wash the system after filling it with alcohol by turning on the circulation pump or by stirring the alcohol in some other fashion;

5. Drain off the alcohol and add 20% water to it;

6. Pour into the circuit a mixture of alcohol and water and wash the mixture;

7. Wash the circuit with pure water.

---

[1] Methyl alcohol reacts more vigorously with sodium than ethyl alcohol does.

This method of alcohol washing is recommended for small-scale power plants.

Water Vapor Washing. This method of washing has the following advantages:

The temperature at which washing takes place is higher than the melting point of sodium, thus furthering completion of the reaction;

The presence of a gaseous medium within the system reduces the possibility of a sudden increase in pressure in the system as a result of liberation of hydrogen;

Low cost.

The disadvantages of the method are as follows:

The low heat capacity of water vapor causes individual sections of the circuit to become overheated;

Because the water content in the system is low during the first stages of washing, the alkali forming during the reaction may be precipitated in solid form and clog up the tubing.

The following procedure is recommended for washing:

1. Completely drain the sodium from the circuit;

2. Fill the circuit with inert gas;

3. Blow dry saturated or slightly superheated water vapor under a pressure of approximately 1 atmos abs through the system, preheated to a temperature of 120-150°C;

4. Reduce the intensity with which the circuit is heated and blow moist water vapor through it. Then stop heating the circuit and gradually increase the moisture of the vapor;

5. Wash the system with water.

This method of washing may be recommended for semi-industrial and industrial power plants.

Instead of steam a moist inert gas may be used for washing. This makes it possible to avoid overheating of individual units of the power plant, since the inert gas absorbs a part of the heat generated during the reaction between the

water vapor and the sodium. During the first stage of washing, a mixture consisting of 95% gas and 5% water vapor is blown through the circuit. Then the feeding of inert gas into the system is gradually stopped, and washing with steam and water begins.

After the circuit has been washed, all the water in it must be completely removed. Drying is done best in a vacuum of several tenths of a millimeter of Hg and at a temperature of 100-150°C.

Liquid Ammonia Washing. The use of liquid ammonia to remove sodium residue gives good results. However, the necessity of creating great pressure in order to liquefy the ammonia (8 atmos abs at 20°C) limits the applicability of this method to laboratory power plants of small size.

The reaction between sodium and ammonia takes place fairly slowly and leads to the formation of sodium amide ($NaNH_2$). Since liquid ammonia does not react with the sodium oxide (Na_2O), which forms during the operation of the power plant, 2 to 5% ammonium chloride is added to the ammonia. Ammonium chloride reacts with sodium oxide forming sodium chloride, which has a low solubility in liquid ammonia (this solubility amounts to only 3% by weight).

Ammonium chloride should be added to the system only during the last stage of washing, when the quantity of metal in the circuit is comparatively small, since ammonium chloride reacts vigorously with sodium, and this reaction is accompanied by violent liberation of hydrogen.

As was shown by special studies, liquid ammonia does not cause any noticeable corrosion of stainless steel.

Destruction of Sodium and Sodium-Potassium. If it becomes necessary to destroy alkali metals, a number of methods of performing this operation can be recommended.

Burning. Sodium may be destroyed by burning it in air. The disadvantage of this method is that large quantities of toxic white fumes (sodium oxide) are formed. Alkali metals are burned in large open metal tanks. Smoke formation is reduced,

when the sodium to be burned is sprayed with an ordinary atomizer (this method is used in the chemical industry for the production of sodium peroxide). The molten metal is fed into the nozzle of an atomizer by a current of air, is sprayed out and burned in a special chamber. Most of the sodium oxide that forms settles on the walls of the chamber, and the residue is collected with the aid of cyclones, electrostatic dust collectors, etc.

Destruction of Sodium and Sodium-Potassium in Alcohol. Ethyl, methyl, and propyl alcohol may be used to destroy alkali metals. The metal being destroyed is added in small pieces or drop by drop to the vessel containing the alcohol. Part of this vessel is filled with inert gas. The reaction products are placed in water in order to render them completely harmless.

In view of the high cost of the alcohol and the danger of fire, this method is only used to destroy small quantities of metal.

Destruction of Sodium and Sodium-Potassium in Water. In this case the metal is destroyed either by spraying it with water or by feeding steam into the container. Special care must be taken to ensure that the hydrogen which forms in the container can escape from it freely and to ensure that the personnel performing this operation are protected from the fumes which are given off.

Spraying a liquid metal inside a large volume of water is safer when done at a considerable distance from the surface of the water. Special tests showed that during spraying of sodium at a depth of 3 m no noticeable fuming occurred on the surface of the water. The flow of sodium through the spraying nozzle amounted to 2,500 kg/hr in this case.

43. The Reaction Between Molten Alkali Metals and Water

Contact between alkali metals and water or water vapor may occur: (1) during the operation of an alkali-metal steam generator; (2) when an insufficiently dried circuit is filled with metal; (3) when the system is washed after having been used;

(4) when it is necessary to destroy the metal.

The Chemical Reaction $Na + H_2O$. The reaction between sodium and water takes place in accordance with one of the following equations:

$$2Na\ (solid) + H_2O\ (liquid) \rightarrow Na_2O\ (solid) + H_2\ (gas) + 31.08^{*}\ kcal/mole$$

$$Na\ (solid) + H_2O\ (liquid \rightarrow NaOH\ (solid) + \tfrac{1}{2}H_2\ (gas) + 33.67\ kcal/mole$$

Comparative calculations of the free energy available for these reactions show that at temperatures lower than the boiling point of sodium hydroxide (NaOH) (~~318°C) the reaction between sodium and water always leads to the formation of NaOH and H_2, even in the presence of an excess of sodium. At temperatures higher than 318°C the excess sodium enters into the reaction with NaOH, forming sodium oxide and sodium hydride, NaH, while at temperatures higher than 450°C sodium oxide and gaseous hydrogen are formed. The reaction between water and an Na-K alloy proceeds in a similar fashion. The reaction between sodium and water is practically irreversible.

The results of theoretical calculations of the final values of the temperatures and pressures created in a solid container, after completion of the reaction under consideration, are shown in Fig. 204.

---

* The heat effects of the reactions are given for a temperature of 25°C.

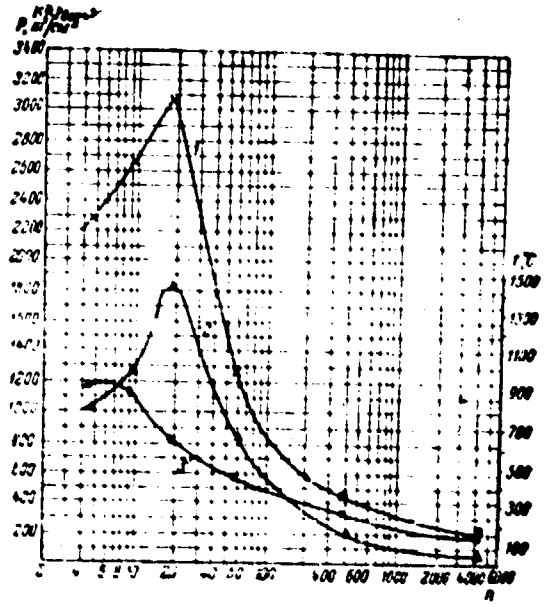

Fig. 204. Final values of the temperatures and pressures created in a solid container after completion of the reaction ($Na+H_2O$) compared to the ratio between the quantities of reacting substances.

1. P (adiabatic conditions); 2. t (adiabatic conditions); 3. P (isothermal conditions); g - the number of grams of water reacting with 23 grams of sodium.

The Mechanism of the Reaction. When liquid sodium comes in contact with water, the hydrogen liberated immediately separates the reacting substances, as a result of which the time necessary for completion of the reaction is determined mainly by the conditions under which the sodium and the water are mixed.

Special tests were made for the purpose of studying the nature of the action of the shock wave which forms during the reaction between alkali metals and water in a water medium at a depth of 3 meters. Mathematical treatment of the results of the tests showed that the energy of the shock wave forming during the reaction is comparatively slight and does not exceed 5 cal/g Na-K or 0.4% of the total quantity of energy liberated. The energy of the hydrogen bubbles constitutes the greater

part of the total energy (16%). Obviously, all the remaining energy is converted into heat.

Let us consider the question of the temperature characteristics of this process. If the reaction occurs with an excess of water, the heat generated is expended in evaporating the water. Therefore, the temperature in the reaction zone does not exceed the boiling point of water at the given pressure. If there is an excess of sodium, the heating in the reaction zone is stronger, since in this case only vaporization of the liquid metal can absorb the heat being given off, lowering the temperature to ~900°C (at atmospheric pressure).

44. An Inert-gas System

Liquid metals used as coolants react vigorously with the oxygen in air. Therefore, it is necessary in operation to protect the metal from oxidation by shielding it with a cushion of inert gas. Usually nitrogen, argon, and helium are used to create this protective cushion. Some of their physical properties are given in Table 50. Of the gases enumerated the most widely used is nitrogen, because of its maximum accessibility. Argon, being the heaviest inert gas, is most advantageously used in connection with constantly open or periodically opened containers of liquid metal. Helium has the best nuclear properties and is therefore used in systems containing a nuclear reactor.

Impurities in an Inert Gas. The following are the most important impurities: oxygen, hydrogen, water vapor, certain hydrocarbons, and to a lesser extent, carbon monoxide and carbon dioxide.

Oxygen is the most harmful impurity in an inert gas. The amount of O_2 admissible in the gas cushion is determined by assuming that all the oxygen enters into the reaction with the metal. It is obvious, therefore, that the greater the quantity of inert gas, the more carefully it must be cleansed of oxygen.

Table 50

Physical Properties of Certain Inert Gases

QUANTITY	DIMENSION	GAS		
		Helium	Nitrogen	Argon
Molecular Weight	-	4.003	28.016	39.944
Density at 0°C and 1 atmos abs (ρ)	g/liter	0.17846	1.25049	1.78394
Melting Point at 1 atmos abs	°C	-272.1	-210.02	-189.26
Boiling Point at 1 atmos abs	°C	-268.92	-195.808	-185.86
Critical Temperature t_{kr}	°C	-267.95	-147.16	-122.46
Critical Pressure P_{kr}	atmos abs	2.26	33.490	47.996
Specific Heat Capacity C_p	kcal/kg °C	1.251 (18°C)	0.2481 (20°C)	0.1252 (17.8°C)
Specific Heat Capacity C_v	kcal/kg °C	0.752	0.1774 (20°C)	0.075 (15°C)
Heat Conductivity Coefficient λ	cal/cm/sec°C	$34.3 \cdot 10^{-5}$	$58.0 \cdot 10^{-6}$	$38.2 \cdot 10^{-6}$

Hydrogen contained in an inert gas reacts with sodium, forming a hydride that is only slightly soluble in liquid metal (see Chapter I); thus it clogs the tubes of the system and also causes undesirable fluctuations in the reactivity of a fast reactor, if the hydride forms in the reactor circuit. The amount of hydrogen in an inert gas is usually small, and therefore it causes less difficulty during operation than oxygen does.

Water vapor is also an undesirable impurity in an inert gas, for when it reacts with sodium, it forms sodium hydroxide, which then decomposes into sodium oxide and sodium hydride.

The hydrocarbons present in an inert gas decompose at high temperatures in the presence of molten sodium, which first causes the total hydrogen content in the system to increase and then causes carburization of the surfaces of the steel components of the circuit. In order to reduce the concentration of hydrocarbons, the use of inert gas supplied by industry for gaseous-discharge illumination devices is recommended. The concentration of impurities in such a gas is approximately 0.005%; most of it is oxygen, while hydrocarbon impurities are almost totally lacking, since the compressors used to force the gas into the cylinders operate with a water lubricant instead of an oil lubricant.

If the liquid-metal circuit contains a nuclear reactor, it is necessary to take a number of additional factors into account when selecting the inert gas, the most important of these factors being the possibility of activation of the gas and the impurities contained in it. In spite of the low solubility of inert gases in liquid metal, such a possibility is not unlikely, since the gas, in the form of bubbles, may be carried by the current of the coolant into the active zone of the reactor. Of the above-mentioned gases (helium, argon, and nitrogen) only helium does not become activated in the reactor. Argon has a large neutron-capture cross section (0.6 barn for thermal neutrons) and, when activated, emits beta and gamma rays. Its half-life is 1.82 years. In this connection nitrogen is less dangerous,

since the half-life of the isotope N^{16} is comparatively small (7.3 sec). Table 51 gives a comparison of the nuclear properties of helium, nitrogen, and argon.

Table 51

Nuclear Properties of Certain Inert Gases

Isotope	Content	Cross Section			Neutron	Type of Reaction
	%	Absorption barns	Scattering barns	Total barns	Energy ev	
He	100	-	41 - 1.55	-	0.025	-
He^3	$1.3 \cdot 10^{-4}$	5000	-	-	Thermal	(n,γ) until transformed into He^4
He^4	100	-	-	-	-	(n,p) until transformed into He^3
N	100	1.45 - 1.86	-	12.7	0.025	-
N				9.96	10 - 200	-
N		0.1			Thermal	-
N^{14}	99.63	1.7	-	-	Thermal	(n,γ) until transformed into N^{15}
N^{14}	-	-	-	-	-	(n,p) until transformed into C^{14}
N^{14}	-	$1.9 \cdot 10^{-3}$	-	-	>10.7	$(n,2n)$ until transformed into N^{13}
N^{15}	0.37	$8 \cdot 10^{-5}$	-	-	Thermal	(n,γ) until transformed into N^{16}

Table 51 Cont'd

Nuclear Properties of Certain Inert Gases

Isotope	Content %	Cross Section Absorption barns	Cross Section Scattering barns	Cross Section Total barns	Neutron Energy	Type of Reaction
A	100	0.6	0.75	1.4	0.025	-
A^{36}	0.337	6	-	-	Thermal (n,γ)	until transformed into A^{37}
A^{38}	0.063	0.8	-	-	Thermal (n,γ)	until transformed into A^{39}
A^{40}	99.6	0.6	-	-	Thermal (n,γ)	until transformed into A^{41}
		$0.93 \cdot 10^{-3}$	-	-	1 Mev (n,γ)	until transformed into A^{41}

Determination of the Amount of Impurities in an Inert Gas. To detect oxygen concentrations of less than 0.01%, Winkler's method is used. This method is based on the absorption of oxygen by manganese hydroxide:

$$4Mn(OH)_2 + O_2 + 2H_2O \rightarrow 4Mn(OH)_3$$

$$Mn(OH)_3 + 3J^- + 3H^+ \rightarrow 2Mn^{++} + J_2 + 6H_2O$$

Thanks to certain improvements, the sensitivity of this method can be increased to 0.0005% O_2 with an average error of $\pm$ 0.00008%.

In a number of cases it is necessary to analyze the gas continuously for oxygen. Gas analyzers based on the reaction between oxygen and hydrogen in the presence of a catalyst (palladium or platinum) have been used successfully for this purpose.

The extent of the temperature increase of the catalyst during the reaction makes it possible to determine the concentration of O_2 in the gas entering the analyzer. The sensitivity of the device is approximately 0.01% O_2. It can be increased to 0.005%, if, instead of measuring the temperature of the catalyst, we determine the amount of water vapor formed with respect to the change in humidity (dew point) of the gas passing through the device.

The admixed hydrogen in the gas is determined by a similar method of catalytic combustion. Cupric oxide heated to 400°C may be used as a catalyst instead of palladium or platinum. The sensitivity of the method of catalytic combustion is approximately twice as great in the case of hydrogen as in the case of oxygen.

The amount of water vapor in the gas is determined by measuring the dew point. An especially great sensitivity in detecting water (several ten-thousandths of a percent) is obtained by burning the gas up to pressures of 10-20 atmos abs.

Serious methodological difficulties stand in the way of an accurate determination of the hydrocarbon content of an inert gas. The following methods of analysis are known: catalytic combustion (cupric oxide being the catalyst); measurement of the dew point in the gas after complete removal of moisture from it; ionization of the gas under low pressure (glow discharge), making it possible to detect traces of hydrocarbons and other impurities in noble gases.

Purification of Inert Gases. The maximum amounts of impurities permissible in inert gases are shown in Table 52. Additional purification of the gas, before filling the system with it, is necessary only when the gas is used in taking samples of the metal and in detecting oxygen in the sample, or when the gas is accidentally contaminated during transport, etc. The most reliable results in removing oxygen are obtained by bubbling the gas, first through a column containing hot Na-K alloy (150-200°C), and then through a column containing cold alloy (~20°C). It was found that the oxygen concentration in nitrogen decreases from 0.15 to 0.01%, after it has been passed under a pressure of 7 atmos abs through a column 100 mm in

diameter and 900 mm high, filled with a compact padding of steel shavings and half-filled with an Na-K alloy. It may be assumed that when the gas is bubbled through the alloy, hydrogen and water vapor are removed from it.

Table 52

The Admissible Content of Impurities in Inert Gases

Name of Impurity	Helium	Argon	Nitrogen
		%	
Purity of the gas	99.976	99.99	99.99
Oxygen	-	0.002	0.002
Hydrogen	0.00003	0.002	0.002
Nitrogen	0.001763	0.001	-
Carbon	-	0.003	-
Methane	0.000001	-	-
Carbon Dioxide	0.000581	-	-
Argon	0.000049	-	-
Moisture (dew point) °C	-	-60	-60

The removal of helium and argon from water vapor by blowing the gas over a layer of sodium flowing off the surface of a conical dome is a well-known experiment. Table 53 gives the results of purification with the aid of this device in relation to its operational time.

Table 53

Results of Removing Argon from Water Vapor

Duration of Experiment, hr	Partial Pressure of Water Vapor after Drying the Gas, mm Hg	Dew Point °C
2	0.5	-24.5
8	0.05	-45.7
120	$<$ 0.000015	-100

In the industrial synthesis of potassium, copper shavings heated to 600°C are successfully used to remove oxygen from nitrogen.

The moisture content of an inert gas may be considerably lowered by blowing it through activated aluminum oxide. During this operation the dew point of the gas is lowered at least to 6°C.

Small quantities of the gas are dried by freezing out the moisture in traps cooled by liquid nitrogen.

Traps for Liquid-metal Vapors. Alkali metal vapors may be removed from the gas by passing it through a stainless-steel screen immersed in Na-K alloy. During this operation the temperature must not exceed 40-50°C. If this device is used to remove sodium vapors from a gas, it is essential to use Na-K with an excess of potassium in order to counteract the increase in the melting point of the alloy that occurs during absorption of sodium.

45. Detection of Impurities in Sodium and in an Na-K Alloy

Sources of Impurities. Contamination of sodium[1] by impurities may occur either during its synthesis and transportation or during the operation of the power plant. Radioactive radiation of the metal in the nuclear reactor is conducive to the formation of impurities.

Technical grade sodium is a fairly pure product (Chapter II, Table 12). During transportation and charging into the power plant the metal is contaminated mainly by oxygen absorbed from the surrounding atmosphere and also by hydrogen and carbon contained in the protective lubricant. Metallic impurities fall into sodium mainly during welding, cutting, etc., as well as during assembling and repairing of the equipment. The impurity content is governed by the solubility of structural materials in the liquid metal and is usually low, especially at temperatures below 500-600°C. The gas cushion of the system contains several substances which can be sources of impurities (oxygen, water vapor, carbon dioxide).

The Effect of Impurities on the Operating Conditions of the Circuit. Impurities in alkali metals, as a rule, increase the rate of corrosion of structural materials and decrease the intensity of heat exchange; but when the metal is used to cool a nuclear reactor, the total activity level of the coolant increases. Furthermore, insoluble impurities can cause difficulties in the operation of the power plant, either fully or partially clogging up the tubes.

An admixture of oxygen is especially harmful. When the oxygen concentration in sodium is more than 0.005-0.01%, the aggressive action of sodium on structural

---

[1] All the information given from this point on concerning sodium also applies to a sodium-potassium alloy unless specific mention to the contrary is made.

materials increases noticeably.

An admixture of carbon causes carburization of the surfaces of the circuit components and an increase in the brittleness of the surface layer of the steel, which is dangerous in a number of cases (for the ports of the valves and the bushings of the pumps).

Calcium present in alkali metals is harmful, since it reacts with the nickel contained in stainless steel to form a compound of solid-solution type.

The main ducts of the process circuit become clogged up mainly as a result of the solid sodium oxide which accumulates in them. Due to the lower solubility of the oxide in the liquid metal at high temperatures (see Fig. 50) the most favorable conditions for full or partial clogging are created in the relatively cold sections of the system, especially at the entrance to the reactor. In the latter case, even partial clogging can have serious consequences, since it causes the liquid to be unevenly distributed to the different heat-generating components of the reactor, as a result of which certain components may become overheated. In order to avoid such occurrences, the oxygen concentration in the sodium must be kept at a low level. It may be assumed that with a relative concentration of O_2 equal to 0.001-0.002% oxide bottlenecks will not form, even in the coldest sections of the system.

Calcium also produces impurities of low solubility in sodium. Calcium reduces sodium oxide and forms solid calcium oxide.

Finally, organic compounds of the hydrocarbon type cause the pipes to become clogged up. These compounds produce insoluble precipitates, when they react with sodium.

Procedure for Sampling Metal. Sodium may be sampled for analysis by immersing a sampling tube into the system or by draining a portion of the metal into the sampler through a special tube.

The sampling temperature must not be lower than the temperature of the

circulating sodium, in order to avoid precipitation of impurities at the mouth of the sampler; their solubility in the metal decreases with decreasing temperature. Precisely for these reasons samples should not be taken from the load (drain) tank of the system.

Proper selection of the material for the sampler is important. If the metal being removed for analysis is drained through a tube, the tube must be made of the same material as the tubes of the circuit. However, the latter condition does not always have to be fulfilled. For example, a sampler in the form of a scoop used to determine the amount of iron impurity in Na, must be made of material not containing Fe (nickel, etc.). If the scoop is made of steel, treating the Na in the sampler with acid for the purpose of removing iron from it may distort the results of the analysis.

Sampling must take place in a shield of carefully purified inert gas. A sign of satisfactory purity of the gas is the retention of a mirror luster on the surface of the liquid sodium in the sampler over a long period of time. If the gas is insufficiently purified, the sample metal becomes covered with sulfur or a black film. This film must not be confused with the white oxide deposit which appears during cooling of metal containing more than 0.01% O_2, even in a medium of gas free of oxygen.

One of the devices used for sampling flowing or motionless metal at temperatures up to 650°C is shown in Fig. 205. A nickel scoop designed to hold approximately 1 g of Na is immersed in the liquid and is then removed from it and transferred into a chamber, where the sodium is amalgamated with mercury and the impurities are separated out of the basic metal. All these operations take place in an inert gas shield.

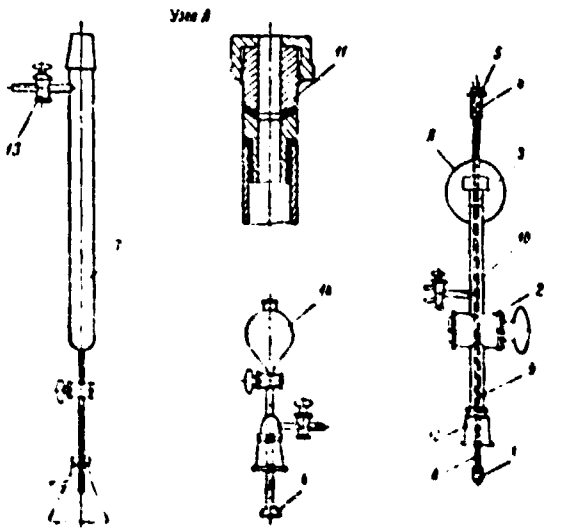

Fig. 205. Device for taking samples of sodium and preparing them for chemical analysis.

(1) scoop; (2) spigot; 3) and(11) gland; (4) sleeve; (5) clamp; (6) disk; (7) chamber; (8) hollow core; (9) wire; (10) chamber; (12) cone; (13) spigot; (14) flask for mercury.

As can be seen from Fig. 205, the scoop is fastened to the lower end of a hollow steel core by a long nickel wire bent in the form of a loop and passing through the core. The upper part of the core, together with the wire, is fastened in a Tygon sleeve by means of a screw clamp. The core is held in the glass chamber of the sampler by friction in a gland sealed with two rubber rings. The gland prevents gas from leaking out of the chamber, but at the same time permits the core and the scoop to move freely up or down. The sampler is attached at its lower end to the connecting tube of the valve, which cuts off the entire device (if need be) from the system. The moment of immersion of the scoop into the molten metal is determined by the closing of the electric circuit to which the core is connected.

After being filled, the scoop is raised and is cooled for a while in the upper part of the chamber. Then the spigot is closed and the sampler is detached from the valve and placed over the amalgamation chamber. After inert gas fed through a spigot has been blown through the chamber, the scoop moves downward, the clamp is loosened, and the nickel wire is removed from the core, as a result of which only the scoop containing the sodium remains in the amalgamation chamber. Then, with a constant current of inert gas flowing through the chamber, the sampler is quickly replaced by a flask containing mercury, after which the sample is amalgamated. The mercury enters the chamber through a hollow glass disk, which sprays it into fine drops, which condense the steam that formed during the reaction. The liquid in the chamber is stirred by agitating the scoop in it with a strong magnet. For complete amalgamation of the sodium sample 5 to 6 fifty-ml portions of mercury are sufficient. After the mercury in the chamber has been drained out, only alkali-metal oxides and other impurities insoluble in Hg remain. The sodium can be removed from the chamber by washing the chamber with a phenolphthalein solution. The remaining impurities are mixed with a small amount of distilled water and are immediately treated with a 0.01N solution of hydrochloric acid in a 5 ml microburet. While so doing, it is necessary to take into account the error in measurement resulting from absorption by the sample of carbon dioxide from the surrounding atmosphere. The remainder of the sample, i.e., the Na amalgam, is treated with a definite excess quantity of HCl in order to completely remove the alkalis, after which the amount of sodium in the sample may be determined.

If the sample is removed only for the purpose of determining the metallic impurities in the Na, special precautions against oxidation of the sample are unnecessary. In this case the sampler can be filled in an atmosphere of technical nitrogen. It is also possible to insert glass or metal tubes directly into the stream of sodium and suck liquid from it into the sampler. Samples were successfully

taken with Pyrex glass tubes, even when the temperature of the metal was 500-600°. However, when analyzing for oxygen, the use of such tubes is not recommended since oxides contained in the glass may dissolve in the sodium.

As was mentioned previously, instead of a sample being taken from the stream of liquid, sometimes part of the metal is drained into a container designed for further treatment and analysis of the metal. Figure 206 shows one of these devices. The essential component of the device is a steel beaker filled with pure inert gas and equipped with heated tubes 12 and 3 for feeding and draining the liquid metal. Fastened to the wall of the beaker is a manipulator enabling the metal beaker for the Na to be installed either at the outlet of the feed tubes or over the mouth of the amalgamation chamber. The liquid metal enters the beaker as a result of its own weight, after the valve is opened. After the sodium has circulated for a long time through tube 12, the beaker is filled, and tube 3 is placed directly under it. Tube 3 is usually connected to the drainage tank of the system.

When the beaker has been filled, it is placed over the chamber and is raised with the aid of a magnet, after which the manipulator is turned aside. Then the vent is opened, and the beaker with the hardened sodium is lowered into the chamber.

The rest of the amalgamation procedure is completely analogous to that described above for a sampler with a nickel scoop. 40-50 ml of distilled mercury is added drop by drop to the upper part of the chamber from the tank. In order to accelerate the amalgamation process, the chamber is heated slightly with the flame of a gas burner, and the beaker is shaken up and down in the chamber with the aid of a magnet. Then the amalgam is drained into the flask through a capillary tube. If the above-described operation is repeated 4-5 times, we can be sure that all the sodium has been removed from the sample.

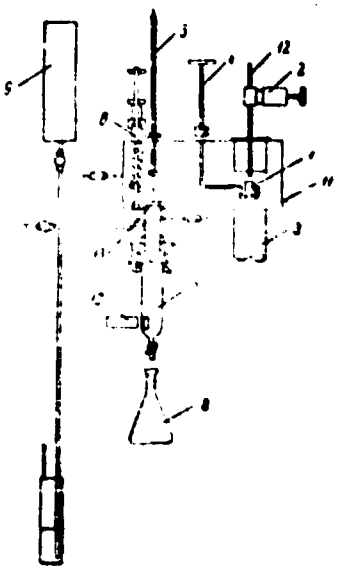

Fig. 206. Device for taking samples of sodium and preparing them for chemical analysis by draining part of the metal from the main duct.

(1) beaker; (2) valve; (3) drain; (4) manipulator; (5) magnetic core; (6) spring; (7) chamber; (8) flask; (9) container for mercury; (10) magnet; (11) common chamber; (12) tube; (13) vent.

The impurities remaining in the chamber are mixed with distilled water and are titrated with phenolphthalein for the purpose of determining the amount of sodium oxide in them. The amalgam previously drained from the device is also titrated, thus enabling the amount of sodium in the sample to be found. Then, using the result of the first determination, the concentration of oxygen in the sample can be calculated.

The beaker for the liquid metal is usually made of carbon steel or nickel and has the form of a cylinder 10 mm in diameter and 25 mm in height. Newly

manufactured beakers are annealed in a hydrogen medium at a temperature of ~1000°C, in order to remove the oxide film from their surfaces. Before beginning the sampling, several beakers (usually four) are placed in the chamber, and the entire apparatus is placed in a desiccator, where it is kept for a half-hour at a temperature of ~60°C. This makes it possible to get rid of the vapors adsorbed by their surfaces. Inert gas is blown through the chamber while it is in the desiccator. Then at the necessary moment the vent opens as a result of the excess pressure created in the chamber, and the beakers are transferred to the rotating support of the manipulator, after which the apparatus is ready for use.

During sampling the pressure of the inert gas in the container of the device is kept equal to 0.2-0.3 gage atmos. In order to avoid gas leaks, all the cores passing through the wall of the container are equipped with seals made of heat-resistant silicon rubber. The wall of the device contains an inspection window enabling the operator to control all the manipulations. The window is made of electrically-conducting glass. By passing a current through it, the temperature of the window may be maintained at a level of 200°C, thereby avoiding condensation of sodium vapors on its surface.

The above-described apparatus was used for a long time to determine the amount of oxide in sodium. In a range of oxygen concentrations equal to 0.001-0.02%, the maximum error in the determination amounted to 0.002%. The device was also used when working with Na-K alloy. In this case it was necessary to freeze the sample in the beaker with dry ice in order to prevent the alloy from reacting too quickly with the mercury.

Methods of Determining Impurities in Sodium and Na-K Alloy. Sodium. Traces of sodium may be detected by the highly sensitive method of neutron activity. The spectrophotometric method of analysis is sensitive to about one milligram of Na per liter of aqueous solution. In order to determine the amount of metal remaining in the system after it has been washed, the tagged atom method may be used. In

this case the radioactive isotope Na^{24} is added to the sodium.

Oxygen. The most widely used method of analysis is the amalgamation of a sample as just described, followed by titration of the impurities separated from the metal. This method, when carefully followed, enables the oxygen to be determined with an error of only 0.001% (by weight). If the amount of O_2 in the sample exceeds 0.01%, the error increases to ~0.002%. The use of amalgamation makes it possible to determine simultaneously the amount of sodium oxide (Na_2O), sodium hydride (NaH), and sodium hydroxide in the metal. Amalgamation of Na directly in a cold trap which collects the sodium oxide gives effective results. However, this method is often unacceptable since it involves the use of large quantities of mercury.

A fairly accurate analysis for oxygen may also be obtained by using a method involving the reaction between sodium and butyl bromide in xylene. In this case sodium bromide is formed, and the sodium oxide remains unaffected. The mixture of the excess butyl bromide and Na_2O remaining after the reaction is removed from the sodium bromide and is mixed with distilled water. The amount of sodium bromide in the mixture may be determined with the aid of silver nitrate. The error of this analysis is ±0.003-0.005% O_2. Cases have been reported, where the accuracy of the analysis was increased to 0.0006% O_2.

The last of the methods of analysis used is based on the reaction between graphite and the sample of sodium at high temperatures (t~ 2,300°C). The volume of carbon monoxide formed in this reaction depends on the amount of oxygen in the initial sample.

For an approximate determination of the amount of O_2 in the sodium under operating conditions, a simple device, called a bottleneck oxide indicator, is used. The bottleneck indicator (Fig. 207) is a small section of tubing inserted into the circuit parallel to the main duct and equipped with a nozzle (collar), a flow meter, a thermocouple, and a device for cooling the circulating metal with water, air, etc. The liquid is made to flow through the indicator by a special small pump or by the

pressure difference in the system.

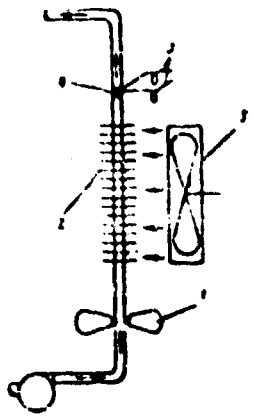

Fig. 207. Bottleneck indicator of oxides in sodium.

(1) Flow meter; (2) Condenser; (3) Thermocouple;

(4) Collar; (5) Fan.

The amount of oxygen is determined in the following way. The condenser located in front of the inlet of the liquid into the zone of contraction of the stream (collar) is turned on. The condenser gradually cools the sodium down to a temperature corresponding to the limit of solubility of the oxide in it. When this temperature is reached, sodium oxide begins to precipitate out of the solution and forms a bottleneck in the narrowest cross section of the pipe, i.e., in the collar. This bottleneck is indicated on the flow meter. If the temperature at which the bottleneck begins to form is known, the amount of oxygen in the metal can be determined from the solubility curve of the oxide (Fig. 50).

The bottleneck indicator described in report [90] was installed on the main duct, $d = 6_{mm}$. Local contraction was created by a steel plate with eight openings 2.3 mm in diameter. The indicator enabled the amount of oxygen to be determined within limits of 0.0006-0.02% in Na and Na-K (56% K), when $t = 100$-$370°C$. A total of about 300 determinations were made, yielding results agreeing with the data from

a chemical analysis to within ± 0.001%.

The indicator should be cooled at a rate not exceeding 3°C/min. Cooling should be continued until the flow of sodium is decreased by one-half and it is certain that the decrease in circulation is not due to accidental factors. The circulation of the liquid metal through the indicator should not be permitted to stop completely, since the oxide bottleneck forming may be refractory. 10-15 min after heating of the indicator starts, the flow is fully restored. A curve illustrating the decrease in flow with decrease in temperature for one type of indicator is shown in Fig. 208 [90]. In addition to simplicity of design, convenience, and reliability during operation, the advantage of the bottleneck indicator is the comparatively short time needed for analysis (about a half-hour).

Since there may be other substances of low solubility (e.g., calcium) in the sodium besides the oxides, the effect of a concentration of these substances in the metal on the operation of the bottleneck indicator should be taken into account. In practice it was not possible to detect such an effect. This may be due to the comparatively high degree of purity of the metal being analyzed.

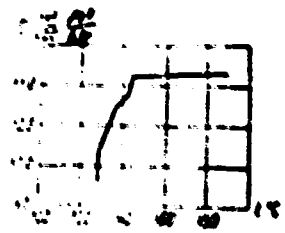

Fig. 208. The effect of cooling on the reduction of the flow of sodium through a bottleneck indicator.

Potassium. If it is known beforehand whether the Na-K alloy is hypoeutectic or hypereutectic, the relative concentration of potassium in the alloy may be determined to the nearest 1% at the freezing point of the alloy. Otherwise an analysis of the shape of the cooling curve of the alloy may indicate which of the components of the alloy predominates. Actually, recooling of the alloy near the freezing point occurs only in alloys rich in sodium. Obviously this is due to the formation of the chemical compound Na_2K.

The chemical methods for detecting potassium mentioned below are more accurate.

1. The Na-K alloy is removed in a special ampoule, is weighed, and is treated with alcohol. Then the products of the reaction are titrated with acid, using methyl orange as an indicator. The error of the method is $\pm 0.1\%$ K.

2. The Na-K alloy is treated in this way in order to obtain a mixture of chloride salts of Na and K, the relative concentration of which in the mixture can be found with the aid of silver nitrate. This method is almost as accurate as the first.

The spectrometric method of analysis is a highly sensitive one, but an accurate determination of one of the alkali metals in the presence of great quantities of the other is difficult because of mutual interference. The accuracy of the analysis can be increased by separating the sodium and potassium salts by the ion-exchange method followed by photometric determination of the relative concentration of the salts.

Calcium. For concentrations ranging from 0.005 to 0.1% calcium is detected by titrating the sample with a solution of ethylenediaminotetraacetic acid (Versene solution). Reduction of the accuracy of the analysis due to the presence of a number of metals (Ni, Co, Fe, Cu, Mn) in the sodium can be avoided. Very small quantities of calcium (1 mg in several kilograms of sodium) can be detected by precipitating it out of the sample with hydroxyquinoline followed by precipitation

of the oxalate and titration of the permanganate precipitate.

The spectrographic method and a method based on the measurement of neutron activity may also be used when analyzing for calcium.

Carbon. Carbon in sodium is usually detected in the following way. The sample is heated up to $t = 950^{\circ}C$ in an oxygen atmosphere, so that all the carbon is converted into carbon dioxide, which is then collected and weighed. The error of the method is ±1%.

The second method of analysis is based on the conversion of sodium into sodium sulfate, which is burned together with liquid Van Slyke fuel in a special device. The quantity of CO_2 formed is determined by the volumetric method. The accuracy of the analysis is ± 0.004% C, when the amount of carbon in the metal is about 0.01%.

The third method of analysis consists in converting sodium into sodium hydroxide (NaOH) by treating it with moist nitrogen and then burning the residue.

Hydrogen. Hydrogen, a component of several of the impurities in the sodium (NaOH, NaH, etc.), is detected by heating the sample up to 450°C in a hermetically sealed iron capsule in a vacuum. The volume of the hydrogen diffusing through the wall of the capsule is measured. The error of the analysis is ±0.2%.

Application of this method to a sodium-potassium alloy did not give satisfactory results because of the incomplete conversion of KOH into potassium oxide during heating.

It is theoretically possible to determine the amount of sodium hydride in sodium with the aid of a device similar to the Bottlebrook oxide indicator, since the limit of solubility of the hydride in the metal is known (Fig. 51). The accuracy of the analysis may be affected by an admixture of sodium oxide in the system.

Metals. The preparation for analyzing sodium or potassium for metallic impurities consists of the following: The metal removed from the system is treated with alcohol (ethyl, methyl), as a result of which sodium (or potassium) alcoholate is formed. This operation takes place at room temperature, preferably in a shield of

of the oxalate and titration of the permanganate precipitate.

The spectrographic method and a method based on the measurement of neutron activity may also be used when analyzing for calcium.

Carbon. Carbon in sodium is usually detected in the following way. The sample is heated up to $t = 950^{\circ}C$ in an oxygen atmosphere, so that all the carbon is converted into carbon dioxide, which is then collected and weighed. The error of the method is ±4%.

The second method of analysis is based on the conversion of sodium into sodium sulfate, which is burned together with liquid Van Slyke fuel in a special device. The quantity of CO_2 formed is determined by the volumetric method. The accuracy of the analysis is ± 0.00[illegible]% C, when the amount of carbon in the metal is about 0.01%.

The third method of analysis consists in converting sodium into sodium hydroxide (NaOH) by treating it with moist nitrogen and then burning the residue.

Hydrogen. Hydrogen, a component of several of the impurities in the sodium (NaOH, NaH, etc.), is detected by heating the sample up to 450°C in a hermetically sealed iron capsule in a vacuum. The volume of the hydrogen diffusing through the wall of the capsule is measured. The error of the analysis is ±0.2%.

Application of this method to a sodium-potassium alloy did not give satisfactory results because of the incomplete conversion of KOH into potassium oxide during heating.

It is theoretically possible to determine the amount of sodium hydride in sodium with the aid of a device similar to the bottleneck oxide indicator, since the limit of solubility of the hydride in the metal is known (Fig. 51). The accuracy of the analysis may be effected by an admixture of sodium oxide in the system.

Metals. The preparation for analyzing sodium or potassium for metallic impurities consists of the following: The metal removed from the system is treated with alcohol (ethyl, methyl), as a result of which sodium (or potassium) alcoholate is formed. This operation takes place at room temperature, preferably in a shield of

inert gas (nitrogen), since the presence of peroxides of alkali metals (especially potassium) in the sample may render the reaction explosive. It is essential to prevent intense evaporation of the alcohol and removal of part of the sample together with the alcohol vapors. For this purpose the sample metal is frozen, cut into small pieces, and added gradually to a mixture of alcohol and dry ice. When the temperature is increased to room temperature, a certain quantity of acid is formed in addition to the other products of the reaction. The reaction may be slowed down by placing the sodium under a layer of mineral oil in a beaker and slowly pouring alcohol into the beaker in an inert gas medium. The preparation of the sample for analysis is completed by dissolving the alcoholate thus prepared in water.

The most convenient and accurate method of analysis for metallic impurities in sodium or potassium is the spectrographic method, which may be used in a wide range of concentrations of the elements to be detected (Table 54).

Table 54

Sensitivity of the Spectrographic Method of Detecting Certain Elements in Alkali Metals

Element	Quantities detected, %	
	From	To
Aluminum	0.0025	0.025
Barium	0.0005	0.012
Calcium	0.0120	1.250
Copper	0.0025	0.125
Iron	0.0025	0.125
Potassium	0.0250	1.250
Magnesium	0.0025	0.050
Nickel	0.0120	0.125
Silicon	0.0050	0.125
Strontium	0.0005	0.012

The content of certain metallic impurities may be found by radiochemical analysis. This method may be used to study the solubility in sodium of elements contained in structural steels as basic components or as impurities, e.g., Fe, Co, Cr, Ta, Mn, Ag, Zn, Cd, Sb, Sn, and Cs. The great sensitivity of radiochemical analysis (Table 55) makes it the only possible method of quantitatively detecting impurities in a number of cases. The error of the method is approximately ±10% of the amount to be detected.

Table 55

Sensitivity of Radiochemical Analysis to Certain Elements of the Periodic Table

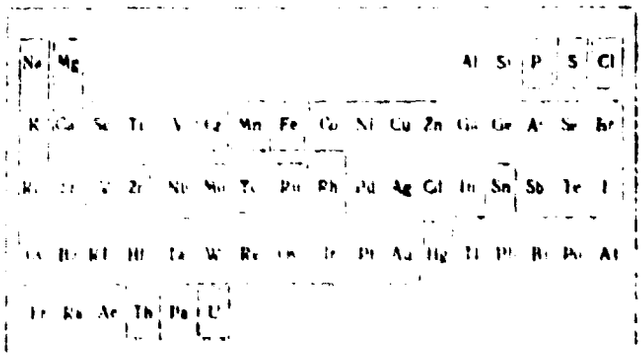

Designations: ---- - poor sensitivity (the quantity of the element needed to conduct an accurate analysis amounts to 0.1-10 micrograms);

▭ - good sensitivity (the necessary quantity of the element amounts to 10^{-5}-0.1 micrograms).

RE - rare-earth elements.

In the case of certain metals the results of analysis obtained by methods of neutron activity and ordinary chemical methods differ greatly from each other. For example, the amount of iron in sodium removed from the process circuit according to radiochemical analysis is usually 100-1,000 times less than it is according to ordinary

chemical analysis conducted, for example, according to the colorimetric method.

Before conducting a chemical analysis for metal content, the sample is treated with concentrated hydrochloric acid, after which the precipitate is filtered, thus partially separating the impurities remaining in the filtrate from the base metal. Chemical methods of analyzing sodium and potassium are usually used to detect the following impurities: chlorides, nitrogen, phosphates, sulfates, heavy metals, and iron.

The detection of mercury in sodium and sodium in mercury is of special interest, since mercury is used in liquid-metal heat-exchangers for filling the space separating the tube systems of the heat-exchangers, direct contact between which is forbidden (e.g., water and sodium). Large quantities of mercury in an alkali metal may be determined by extracting the sodium from the sample and then weighing the residue. To detect small quantities of mercury, it is best to use the spectrographic method.

When the concentration of mercury in sodium or potassium is about 5×10^{-5}%, the sample is treated so that the mercury is in a solution of alkali metal salts, from which it is then extracted by amalgamation of copper powder in an acidified solution of chlorides.

46. Purification of Sodium and Na-K Alloy

If the alkali metals are not cleansed of oxides periodically or continuously, in the course of time the main ducts of the system become completely clogged up. The formation of oxide bottlenecks in the pipes is more characteristic of sodium circuits than of sodium-potassium circuits because of the lower amount of oxygen in Na-K than in sodium, since the sodium in the alloy is oxidized selectively (see Chapter 11). The maximum concentration of oxygen in Na in the form of weighed particles of oxides is 0.04-0.06% (by weight), while in Na-K alloys it amounts to 0.02-0.03%.

Filtration. Filtration is a good method of cleansing sodium of insoluble impurities. Porous stainless-steel or glass strainers are mainly used as the filtering material, and metal sieves to a lesser degree. The use of filters with glass strainers is limited to laboratory experiments conducted at comparatively low temperatures. Filters made by sintering stainless-steel powder have pores the average size of which is 10 microns.

A liquid-metal circuit, as a rule, is equipped with a filter installed on the charging duct. During operation of the apparatus oxides and other insoluble impurities gradually accumulate in the filter. As a result the pressure drop needed for a given flow of liquid through the charging line increases as the time of operation of the apparatus increases.

It may be assumed that in the case of a filter with pores whose average size is 5 microns, a flow of sodium through the filter of $\sim 4{,}000$ kg/m^2·hr corresponds to a pressure drop of 1 atmospheres, if the temperature of the metal is 120-150°. These data are corroborated by experiment.

The difficulties arising from the constant clogging up of the filters can be lessened, if they are constructed in such a way as to permit periodic cleaning or washing.

The efficiency of a filter with a porous metallic strainer, i.e., the ratio between the amount of oxide collected by it to the total quantity of oxide in the metal passing through the strainer, varies from 60 to 95% depending on the conditions of filtration. The efficiency increases as the quantity of oxide in the initial metal increases. Filters with porous stainless steel strainers collect particles as small as 1-2 microns [195].

The use of filters enables sodium to be cleansed not only of oxides, but also of other insoluble impurities, e.g., filings, shavings, and slag falling into the circuit during its assembling and dismantling.

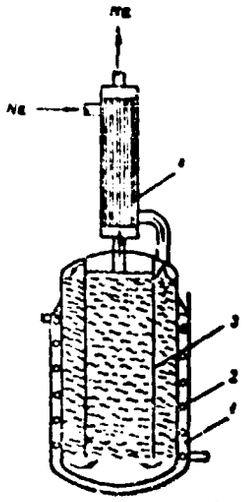

Fig. 210. Cold trap with forced circulation of sodium.

(1) layer (liquid); (2) coil; (3) filler;

(4) economizer.

Let us turn now to a description of cold traps with continuous forced circulation of metal. Such purification devices are most suitable for large installations.

Figure 210 schematically shows a cold trap together with a heat-exchanger - economizer. The trap is installed parallel to the main duct of the system, and the metal is made to circulate through it either by the pressure difference in the main duct or by a special pump. The installation of a heat-exchanger - economizer together with a cold trap is not mandatory, but is desirable, since it keeps the temperature of the liquid at the outlet of the purification device equal to the temperature of the liquid at the inlet. Water, oil, Dowtherm, and toluene may be used as cooling media for cold traps. The cooling temperature of the sodium is usually chosen equal to 150°C, although it is sometimes reduced to 130-140°C. The internal filler is made primarily of pressed steel wire. The traps are designed for an optimum flow of liquid varying from 5 to 100 liter/min. The metal must remain in

Purification in Cold Traps. The simplest cold trap is a certain region, in which the circulating metal is cooled down to a temperature corresponding to the limit of solubility of some impurity (such as an oxide) in the metal, as a result of which the impurity is precipitated in the trap.

There are two types of cold traps: a) settling tanks in which precipitation of impurities takes place by diffusing the impurities from the main stream into a region of comparatively low temperatures (diffusion traps); b) traps with forced circulation of the metal, in which the sodium is cooled as it moves.

The first type of trap is shown in Fig. 209. The settling tank connected to the main duct of the system is cooled by convection of the surrounding air. The casing of the settling tank must be long enough to enable the temperature in its lower part to be decreased to 120-150°C. As was shown by experiment, when the temperature of the sodium in the main duct is equal to 500-600°C, this length is 250-300 mm. A diffusion trap is used mainly to cleanse sodium of oxides. The concentration of oxide in the metal in the settling tank after prolonged operation of the trap may amount to as much as 20% or more. A case has been described, where in a pipe 12 mm long, used as a diffusion trap, the concentration of Na_2O amounted to 70% of the entire contents of the pipe.

The settling tanks being used at present cannot be regarded as perfected. The most widely used traps are those in the form of a cylindrical container connected to the system by a tube of the same diameter as that of the main duct. In this case the ratio between the volume of the settling tank and the volume of the whole system is 0.01-0.03.

It is not of great importance where a diffusion trap is installed in the system, although from the point of view of intensity of purification it is preferable that the trap be installed in the hot section of the circuit, where the temperature difference between the upper and lower parts of the settling tank is a maximum. At the same time, it is desirable that the heat losses caused by the trap

not be great. In a case where these losses must be a minimum, it is preferable to install the settling tank in the cold section of the circuit.

Diffusion-type traps are used to precipitate certain metallic impurities of sodium, e.g., iron, cobalt, and nickel. It was even noted that the presence of settling tanks in the system intensified the aggressive action of sodium on stainless steel. In this case certain substances contained in the steel (Fe, Cr, Ni) gradually accumulated in the trap after being transported from the hotter sections of the circuit. The transport mechanism is not clear, although it may be assumed that it is accompanied by a reaction between the element being transported and the sodium and the oxygen contained in the sodium, since great transport intensity usually accompanies a larger concentration of oxide in the system. It should be noted that the substances transported to the settling tank may be gradually returned to the system, if the cold trap is heated up to the temperature of the circulating sodium.

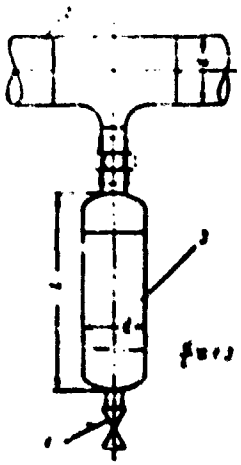

Fig. 209. A diffusion-type cold trap.

(1) drainage valve; (2) main duct; (3) settling tank for oxides.

them for not less than three minutes. The cross sections of the internal channels of the heat-exchanger - economizer, as well as the cross sections of the inlet and outlet connecting tubes, must be chosen as large as possible, in order to prevent them from becoming clogged with oxides. The cooling system must maintain an even reduction in the temperature of the metal while it is flowing. Otherwise, local accumulations of oxides may form within the filler. A successfully designed trap can reduce the concentration of oxygen in sodium to 0.001%.

Fig. 211. Reduction in temperature at the start of precipitation of oxides in sodium passing through a cold trap n times.

It is desirable that the metal be purified continuously during operation of the installation. If at the initial moment of time there are no oxides in an undissolved state in the system, the relationship between time and the total amount of oxygen in the system may be expressed by the following equation:

(101)

where x_0 is the initial concentration of O_2 in %;

x_c is the concentration of O_2 corresponding to the limit of solubility of the oxides at the temperature of the cold trap in %;

x is the concentration of O_2 at a given moment of time in %;

Q is the volumetric flow of the liquid through the trap in m^3/hr;

W is the total volume of the system in m^3;

τ is the length of operation of the trap in hours.

In order to reduce the concentration of O_2 in the system to the value x_c, it is necessary to pass all the metal through the trap about three times (Fig. 211).

The total quantity of oxide precipiteted in the trap after one operating cycle (before washing), is not less than 10% (by weight) of the Na_2O in the entire quantity of sodium which the trap can contain.

Cold traps make it possible for the installations to operate for a long time without becoming contaminated with oxides. For example, Hall and Crofts noted that without a cold trap their apparatus operated only several hundred hours, after which the experiments were halted because of the excessive accumulation of oxides in the system. After installation of a cold trap the circuit operated for 10,000 hours without becoming contaminated with oxides.

Chemical Purification. Chemical removal of oxygen from Na is done by adding to the system substances which reduce sodium oxide. Such substances may be chosen by comparing the thermochemical characteristics of oxidation reactions of different elements. The given substances may not always be effective. For example, beryllium oxide has greater free formation energy than sodium oxide. However, under actual existing conditions beryllium does not reduce Na_2O.

Reducing agents can be divided into two classes. To the first belong elements which themselves dissolve readily in liquid metal, but form oxides which are not readily soluble. A typical example of such an element is calcium, which in practice was added to Na in quantities of not less that one percent. It was found that in a majority of cases an addition of calcium intensifies the aggressive action of the liquid metal on stainless steel, although, on the other hand, evidence of decrease in corrosion in the presence of calcium was noted. Obviously the decrease in corrosion results from the reduction of the sodium oxide aggressively acting on a number of materials (see Chapter IV). To this class of substances belong lithium, magnesium, and barium, which, in contrast to calcium, do not reduce the corrosion resistance of the steel.

Insoluble oxides of reducing agents are removed from the system by filtration or are precipitated in a cold trap, if there is one in the circuit. Simultaneous

use of reducing agents and cold traps is not mandatory.

The collection of insoluble oxides of magnesium, lithium, and barium in cold traps has never been described.

To the second class belong substances, which themselves are insoluble in sodium and form insoluble oxides, e.g., uranium, titanium, and zirconium.

If need be, chemical methods may be used to remove Na from K and K from Na. Sodium is removed from potassium by adding oxygen to the metal and then removing the Na_2O by filtration or by precipitation in cold traps. A small amount of potassium may be removed from sodium by heating the metal to 300°C with graphite and then filtering it. By so doing the concentration of potassium is reduced to ~0.005%.

Similar methods are theoretically possible for removing Ca from Na and Na from Ca.

During actual operation of liquid-metal power plants chemical methods were mainly used for removing oxygen from sodium. Chemical purification of Na was also used when testing materials for corrosion resistance. When testing specimens of zirconium, sodium was chemically cleansed of nitrides, hydrides, and alkali.

When adding reducing agents to a nuclear reactor system, their nuclear properties must be taken into account. For this reason elements with a large neutron-capture cross section should not be used. Nor should elements be used, if the products of their irradiation have a long half-life in the reactor or if they are sources of high-energy radiation.

Distillation. In the first stages of utilization of liquid metals as coolants distillation was used to remove oxygen from sodium. Then it was found that cold traps ensure purification of no less high quality than that attainable with distillation equipment. At the same time they are cheaper to produce and more convenient to operate. However, through distillation alkalis and alkali-earth elements can be removed from Na, and a superfine purification of the latter can be achieved.

Thus through vacuum distillation Na can be made 99.9995% pure.

47. Prevention of Accidents and Fires When Working with Alkali Metals

Alkali metals require special consideration from the point of view of accident and fire prevention because of their great activity in comparison with other substances. Since experience in prolonged operation of liquid metal installations was acquired mainly through working with sodium and a sodium-potassium alloy, the information given below concerning accident prevention relates almost exclusively to these metals. It may be assumed that accident prevention measures for working with lithium are similar.

Observation of the proper precautionary measures ensures safety of operation with alkali metals even at high temperatures and pressures, and these precautions are no greater than those required when working with other hot and potentially explosive materials, many tons of which are produced every day. As was shown by experimental operation of alkali-metal power plants in the Knolls Atomic Energy Laboratory (USA), the power plant can be operated safely for an uninterrupted period of tens of thousands of hours, if safety measures are observed.

Properties of Alkali Metals Injurious to Health. The properties of Na, K, and their alloys, from the point of view of their danger to health and the danger of their causing fires, are similar. However:

1) in contrast to Na and K, their alloys used as coolants are liquid at room temperature;

2) in contrast to sodium, potassium, when reacting with oxygen in the air, forms peroxides, which react explosively with certain organic substances.

Sodium and sodium-potassium spontaneously ignite in air at a temperature of about 120°C. The combustion temperature depends on the magnitude of the relative surface of the metal (degree of pulverization) and the humidity of the air. During combustion the temperature of the hot mass rises rapidly to 800-900°C. Sodium

cannot burn in an atmosphere containing less than 5% oxygen.

The oxide liberated (in the form of smoke), when the sodium burns, acts into the circulatory passages and causes serious irritation, but does not cause permanent damage.

Alkali metals react violently with water and generate a sufficient amount of heat to burn the hydrogen forming in the air. If the reaction occurs in a closed container, the liberation of hydrogen causes a sharp increase in the pressure in the container.

Molten alkali metals falling on human skin are dangerous, since the thermal and chemical action of the metal can cause burns. Such burns take a much longer time to heal than ordinary burns.

Many cases are known where violent explosions occurred when peroxides of alkali metals were mixed with hydrocarbons. Sodium can oxidize to a peroxide in air, only at temperatures above 250°C, while potassium yields a peroxide at room temperature. Both potassium peroxide and sodium peroxide are reduced to an oxide after prolonged contact with a liquid metal. Therefore, in a liquid metal shielded with a cushion of inert gas, the formation of peroxides is impossible. However, in every case where hydrocarbons are used in sodium-potassium circuits (for washing, etc.) special precautions must be taken.

Safety Measures Observed during Operation of the Circuit. The system should be constructed in such a way that the liquid metal can be drained out rapidly. The drainage pipes must always be kept at a temperature exceeding the temperature of the coldest section of the circuit, in order to avoid precipitation of relatively insoluble impurities in the drainage pipes. It is important to ensure good ventilation of the inert-gas system by linking all the gas cavities together.

Even when measures are taken to ensure rapid drainage, part of the metal still manages to leak out, and measures must be taken to decontaminate it. Leaking sodium and sodium-potassium alloy usually catch fire immediately, but burn

relatively quietly. Personnel equipped with gas masks may approach the fire, if there is no danger of a reaction with water causing the hot metal to spatter. In order to prevent hot sodium - Na-K alloy from falling on the concrete floor, metal pans must be used, since the heat generated during burning causes the concrete to crack.

Methods of Protecting Personnel From Alkali-metal Fires. When the pressure in the system is low, the protection afforded by the heat insulation of the equipment is fully adequate. Under high pressures special protection is necessary. Frequently the dangerous area is partitioned off with metal sheets, and metal pans are placed on the floor. In order to reduce spattering of the metal, when a leak occurs, the pressure in the system must be reduced rapidly.

Ventilation of the premises is a good way to protect personnel from the action of sodium oxide or potassium oxide during a fire.

Personnel directly servicing liquid-metal power plants wear protective clothing different from those required for fire-fighting.

In order to select materials for protecting personnel working with molten-alkali metals, special tests were conducted. The results of these tests are shown in Table 56. As can be seen from the table, at the same temperature, e.g., at 350°C, the action of the Na-K alloy is sometimes more aggressive than the action of sodium. This is due to the fact that sodium hardens after contact with the protective material, while the alloy remains liquid.

For protecting the eyes, glasses fitting tightly against the face are used. Shields made of noninflammable material are used in addition to these glasses, but not as a substitute for them. For protecting the head, a felt hat with wide brims is fully adequate, and for protecting hands and feet, leather mittens and boots are used. Persons working with alkali metals must be dressed in loose-fitting overalls, or if possible, in suits made of fire-resistant material. Special protection of the respiratory passages is not required for this category of personnel.

Protective Clothing for Fire[illegible]ting. Since the personnel who are to extinguish sodium or sodium-potassium fires are equipped with respirators (gas masks), special protection for the eyes is not necessary. For protection of the head, a wide hood made of asbestos is used in addition to a felt hat. To protect the feet, special boots made of leather or asbestos are used. These boots are worn over the regular working boots. The hands are protected in a similar fashion. To protect the body from spattering metal and fire, asbestos suits are used. In certain cases portable metal shields may be used. To protect the respiratory organs from the action of sodium oxide fumes, filter-type respirators are used. Respirators of the self-purifying type, good for any concentration of smoke, are to be preferred. All types of respirators (gas masks) must fully cover the face.

Table 54

Protective ability of certain materials with respect to the action of liquid Na and Na-K alloy.

Material	Temperature in °C				
	150	350		550	
	Na-K	Na	Na-K	Na	Na-K
	Protection				
Glass for ordinary goggles	-	-	-	Good	Good
Glass for welder's goggles	-	-	-	Good	Good
Leather (chrome)	Good	Good	Good	Good	Good
Sheet bakelite	Good	Good	Good	Good	Good
Rubber (for gloves)	Good	Good	Poor	Poor	Poor
Cellulose acetate (for protection of the face and eyes)	Good	Good	Poor	Poor	Poor
Cloth	Satisfactory	Poor	Poor	Poor	Poor
Cotton	Poor	Poor	Poor	Poor	Poor

First Aid during All Li-metal Fires. Burned portions of the skin may be washed with water. At the same time the alkali which forms may be neutralized with a weak solution of acetic acid (from 3 to 5%). The acid solution must not be used to wash the eyes. In the case of burns of the eyes, the burnt portion must first be washed for 10-15 min with a spray of pure water under low pressure and then washed with a weak solution of boric acid.

It is especially dangerous when spattering sodium or sodium-potassium alloy falls on clothing or on the skin at the same time as kerosene. In such a case the best technique is to wash the burned portion with a spray of water.

Some people are of the opinion that it is better to wash the skin with mineral oil and at the same time remove the particles of metal with tweezers. This method of washing is definitely safer than the first (i.e., washing with water and acid). However, it does not neutralize the alkali, which has penetrated deep into the skin.

Fire-Fighting. In order to extinguish a sodium or sodium-potassium alloy fire, it is necessary to cut off the access of oxygen to the fire. Water, carbon tetrachloride, carbon dioxide, and sodium bicarbonate (bicarbonate of soda) must not be used to extinguish the fire. The oxygen may be cut off by covering the burning sodium or Na-K alloy with dry alkali-metal chlorides, graphite, powdered anhydrous soda (Na_2CO_3), or sand. In so doing the danger that the sodium might burst into flame and start the fire going again is not fully eliminated.

An effective method of fire-fighting is to reduce the concentration of oxygen in the dangerous spots. Experiments showed that in an atmosphere containing 2.75% oxygen, 0.6 kg out of sodium burns of a total of 27 kg (initial temperature of the metal 450°C), whereas when the oxygen content is 7%, 2.9 kg of Na burns out of a total of 27 kg (at the same temperature).

In order to extinguish alkali metal fires, certain laboratories in the USA use Met-L-X powder, which is specially treated sodium chloride, highly friable and insensitive to changes in the humidity of the air. Fire-extinguishers filled with

this powder are available in 9, 15, 70, or 155 kg sizes. Met-L-X powder, when heated, has the valuable property of forming a solid crust on the surface of the burning sodium which isolates the molten metal from the oxygen in the air. The formation of the crust is facilitated if the metal burns on a smooth, horizontal surface.

Brand G-1 Pyrene powder, which consists mainly of graphite, is also used to extinguish alkali-metal fires.

In every case metal pans should be placed in the region of the fire to catch drippings of the burning metal. The pan may be covered on the top with a perforated iron sheet, through the openings of which the metal flows into the pan. At the same time access of oxygen to the surface of the metal is limited. The perforated sheet may in addition be covered with a layer of Met-L-X powder.

Lithium fires are best extinguished with G-1 powder. Standard fire-extinguishers, even those of the carbon-dioxide type, are ineffective, and their use may be dangerous, since Li reacts with carbon dioxide.

Removal of alkali metal residue after extinguishing the fire is as dangerous as extinguishing the fire itself. The residue of the metal must be carefully mixed with dry ice and then burned.

During a fire it is necessary to ensure maximum ventilation of the premises, since the oxide fumes being given off from the fire not only hamper breathing, but also sharply reduce visibility.

Specific Accident-prevention Requirements When Working with Radio ..ire Sodium. As a result of the capture by sodium of neutrons in the active zone of the reactor, the radioactive isotope Na^{24} is formed. Calculations show that the activity level of Na^{24} in a power reactor with a capacity of about 50,000 kw ranges from 10^4 to 10^7 curies. Na^{24} is a powerful emitter of β and γ particles, which have a maximum energy of ~1.4 Mev and 2.76 Mev, respectively. Its half-life is 14.8 hours.

Almost all the Na^{24} entering the human organism through the alimentary tract or through the respiratory passages is rapidly and uniformly distributed throughout it by the circulation of the blood. According to the standards of the USA the maximum total quantity of isotope Na^{24} permissible in the organism is 15 microcuries. The comparatively large dose permitted is explained by the fact that the rate of biological elimination of Na^{24} is fairly high.

Obviously the most serious danger to health may arise during a leak of radioactive sodium in any system with subsequent combustion of the sodium.

The maximum permissible concentration of Na^{24} isotope in air according to the standards of the USA is $2 \cdot 10^{-6}$ microcuries/ml.

Protective clothing for working with radioactive alkali metals must satisfy all the requirements relating to work with nonradioactive metals plus the requirements relating to work with radioactive isotopes. The premises where the sodium circuit is installed must be equipped with devices indicating the activity level in the area and must also be equipped with appropriate signaling devices.

When radioactive sodium falls on clothing, the latter must immediately be removed from the victim, and the burned portions of the skin must be washed with a strong spray of water.

Fires caused by leakage of radioactive sodium must, as a rule, be extinguished by remote control by preventing air from entering the area where the fire is taking place, while at the same time feeding inert gas into this area. In the latter case it is necessary to discharge the contaminated gaseous combustion products into the atmosphere or into a special area set aside for this purpose. Sometimes the fire may be extinguished with Met-L-X powder fed to the fire by a system of special pipes.

If it is known that the sodium does not contain long-lived radioactive-isotope impurities, the residue of sodium may be destroyed by ordinary means after being kept for two or three weeks.

48. Accident Prevention When Working with Mercury, Lead, Tin, and Bismuth

Mercury. The toxicity of mercury is very great. Therefore, special measures must be taken to ensure the safety of personnel servicing mercury power plants. According to the standards of the USA, the maximum concentration of mercury permissible in the air is 0.1 mg per cubic meter of air[1]. According to Hill's data, at 20°C the saturated mercury vapor pressure is 0.00182 mm Hg. Hence it may be assumed that under normal conditions (p = 760 mm Hg, t = 20°C) a concentration of 199 mg/m^3 of mercury in the atmosphere corresponds to saturation of the air with mercury vapor; i.e., the concentration is much higher than the permissible limit.

When mercury spills on a floor, table, etc., it evaporates more readily. In addition dust and dirt prevent individual drops of metal from sticking, and this also facilitates evaporation.

In order to determine the concentration of mercury vapor in the air, a device is used which is based on the absorption by mercury vapor of ultraviolet rays of definite wave length corresponding to the mercury line in the spectrum. The intensity of absorption is measured by a sensitive photoelectric cell.

The presence of mercury vapor in the air may be shown by the blackening of a sheet of paper coated with a layer of selenium sulfide (SeS).

When the concentration of mercury vapor rises above the permissible limit, the premises must be carefully cleansed of mercury by using ammonia or polysulfides dissolved in water.

Premises where mercury is being processed must be equipped with sufficiently powerful ventilation.

Lead. Lead is a very dangerous substance for the human organism. It is

---

[1] The health standards of the USSR permit a concentration of 0.01 mg/m^3. (Editor)

especially dangerous to health to inhale or swallow lead vapor or fine lead dust. The danger of lead poisoning increases as the size of the particles of the metal decreases, in which case it is more dangerous to inhale the particles than to swallow them. Lead first enters the bloodstream of the victim. Then part of the metal, together with its precipitates, is eliminated from the organism, but part remains and settles in the bones. If the victim ceases to be subjected to the harmful action of lead, the quantity of the metal already in his blood begins to decrease gradually. At the same time, a new outbreak of the sickness is possible, since the lead accumulated in the bones may pass back into the bloodstream again.

Premises where lead is being processed must be kept scrupulously clean and be equipped with powerful ventilation. Personnel working with lead must undergo a periodic physical examination (not less than once in six months).

Tin and Bismuth. The toxicity of tin and bismuth is not so great as the toxicity of mercury and lead. However, it is mandatory that premises where these metals are being processed be ventilated, so as to prevent the vapors of the metal from accumulating in the air.

References

1. Ageykin, D. I. and Dessorova, A. A.: Electromagnetic Flowmeter (Elektromagnitnyy raskhodomer), Avtomatika i telemekhanika, XVII, No. 12, 1123-1126 (1956).

2. Amorzi, A., Donnen, A., and Wagner, G.: Experimental Fast-neutron Breeder-reactor (Opytnyy reaktor-razmnozhitel' na bystrykh neytronakh). Symp. Materialy Mezhdunarodnoy konferentsii v Zheneve po mirnomu ispol'zovaniyu atomnoy energii, vol. 3, P/491, Cosenergoizdat, 1958.

3. Barns, A., Koch, L., Monson, G., and Smith, F.: Technical Project E.R.B. II, model of a power plant with a fast reactor. (Tekhnicheskiy proyekt E.R.B. II, prototip energeticheskoy ustanovki s reaktorom na bystrykh neytronakh). Materialy Mezhdunarodnoy konferentsii v Zheneve po mirnomu ispol'zovaniyu atomnoy energii, vol. 3, P/501, Cosenergoizdat, 1958.

4. Belyayev and Firsanova: Reaction of Carbon Materials with Sodium at High Temperatures (Vzaimodeystviye uglerodistykh materialov s natriyem pri vysokikh temperaturakh). Trudy Moskovskogo instituta tsvetmetnolota im. M. I. Kalinina, No. 25, p. 162-171.

5. Borishanskiy, V. M. and Kutateladze, S. S., Energomashinostroyeniye, 1957, No. 6.

6. Bos, Bogard, Grand, et al.: Solubility of Structural Steels in Sodium (Rastvorimost' konstruktsionnykh staley v natrii). Materialy Mezhdunarodnoy konferentsii v Zheneve po mirnomu ispol'zovaniyu atomnoy energii, vol. 8, P/124, Metallurgizdat, 1958.

7. Gel'man, L. L.: Heat Exchange During the Condensation of Mercury Vapor (Teploobmen pri kondensatsii rtutnogo para), Teploenergetika, No. 3, 1958.

8. Gudtsov, N. T. and Gavze, M. N.: Effect of Mercury as a Heat-transport Agent on Steel in Power Plants (Vozdeystviye rtuti kak teplonositelya na stal' v energeticheskikh ustanovkakh), Izd. AN SSSR, 1956.

9. [illegible], V.: Fast-neutron Power Reactors (Energeticheskiye reaktory na bystrykh neytronakh). Materialy Mezhdunarodnoy konferentsii v Zheneve po mirnomu ispol'zovaniyu atomnoy energii, vol. 3, P/814, Gosenergoizdat, 1958.

10. Fruzhilin, G. N.: Izvestiya AN SSSR, OTN, 5, 1949.

11. Kanayev, A. A.: Zhurnal tekhnicheskoy fiziki, 1953, vol. XXIII, issue 2.

12. Kanayev, A. A.: Sovetskoye kotloturbostroyeniye, 1953, No. 2.

13. Kendell, J. and Frey, T.: Fast-neutron Reactor Project in Dounreay (Proyekt reaktora na bystrykh neytronakh v Daunri). Materialy Mezhdunarodnoy konferentsii v Zheneve po mirnomu ispol'zovaniyu atomnoy energii, vol. 3, P/405, Gosenergoizdat, 1958.

14. Clark, F. M.: Mechanical Liquid-metal Pumps (Mekhanicheskiye nasosy dlya zhidkogo metalla). Prikladnaya mekhanika i mashinostroyeniye, No. 3, 1954.

15. Kontorovich, L. M. and Rappoport, F. M.: Fine Purification of Gases of Oxygen (Tonkaya ochistka gazov ot kisloroda), Zavodskaya laboratoriya, XVII, No. 5, p. 632-33, 1951.

16. Kornayev, M. I.: Teploenergetika No. 4, No. 7, 1955.

17. Kriver, F. Ye., Bridshmen, U. Kh., and Troki, T.: Utilization of Sodium and Sodium-Potassium Alloy as a Heat-transfer Agent (Ispol'zovaniye natriya i natriyevo-kaliyevogo splava v kachestve teplonositelya). Materialy Mezhdunarodnoy konferentsii v Zheneve po mirnomu ispol'zovaniyu atomnoy energii, vol. 8, P/123, Metallurgizdat, 1958.

18. Lozhkin, A. N. and Kanayev, A. A.: Sovetskoye kotloturbostroyeniye, 1939, No. 4.

19. Lozhkin, A. N. and Kanayev, A. A.: Independent cycle plants (Binarnyye ustanovki), Mashgiz, 1946.

20. Lozhkin, A. N., Kanayev, A. A., and Siryy, P. O.: Sovetskoye kotloturbostroyeniye, No. 8-9, 1938.

21. Mikheyev, M. A., Baum, V. A., Voskresenskiy, K. D., and Yedynskiy, O. S.: Heat Transfer of Molten Metals (Teplootdacha rasplavlennykh metallov). Doklad na Mezhdunarodnoy konferentsii po mirnomu ispol'zovaniyu atomnoy energii, Zheneva, 1955.

22. Novikov, I. I., Solov'yev, A. N., Khabakhpasheva, Ye. M., Gruzdev, V. A., Pridantsev, A. I., and Vasenina, M. A.: Atomnaya energiya, No. 4, 1956.

23. Parkins, V.: Experimental Sodium Reactor (Eksperimental'nyy natriyevyy reaktor). Materialy Mezhdunarodnoy konferentsii v Zheneve po mirnomu ispol'zovaniyu atomnoy energii, vol. 3, P/499, Gosenergoizdat, 1958.

24. Pugachevich, P. P.: Experimental Study of the Surface Tension of Metals and Solutions (Eksperimental'noye izucheniye poverkhnostnogo natyazheniya metallov i rastvorov). Zhurnal fizicheskoy khimii, XXV, p. 1365, 1951.

25. Semenchenko, V. K.: Surface Phenomena in Metals and Alloys, Metallurgizdat, 1957.

26. Sidzhel, S., Parker, R., Bauman, N., and Kheyvordish, R.: Engineering Principles of Sodium Reactors (Osnovy tekhnologii natriyevogo reaktora). Materialy Mezhdunarodnoy konferentsii v Zheneve po mirnomu ispol'zovaniyu atomnoy energii, vol. 8, P/829, Metallurgizdat, 1958.

27. Styrikovich, M. A., Sorin, A. R., and Semenovker, I. Ye.: Sovetskoye kotloturbostroyeniye, No. 9-10, 1940.

28. Trudy Instituta fiziki, VIII, Izdatel'stvo AN Latv. SSR, Riga, 1956. Prikladnaya magnitogidrodinamika.

29. Pastovskiy, V. G. and Rovinskiy, A. Ye.: Laboratory Device for Producing and Analyzing Pure Argon (Laboratornaya ustanovka dlya polucheniya i analiza chistogo argona). Zavodskaya laboratoriya, XVII, No. 5, p. 531-541, 1951.

30. Tsuprun, L. I. and Tarytina, M. N.: Study of the Behavior of 1Kh18N9T Stainless Steel in Contact with Liquid Lead, Bismuth, and their Eutectic Alloy at a Temperature of 500-600°C (Issledovaniye povedeniya nerzhaveyushchey stali 1Kh18N9T v kontakte s zhidkim svintsom, vismutom i ikh evtekticheskim splavom pri temperature 500-600°C), Moscow, 1956.

31. Shvab, V. A.: Theoretical Formula of Heat Exchange in a Tube with Turbulent Flow of Liquids (Teoreticheskaya formula teploobmena v trube pri turbulentnom techenii zhidkostey), TsKTI, 1938.

32. Shvidkovskiy, Ye. G.: Certain Questions on the Viscosity of Molten Metals (Nekotoryye voprosy vyazkosti rasplavlennykh metallov). Gos. izd. tekhniko-teoreticheskoy literatury, Moscow, 1955.

33. Shikhtenberger, T., Talgott, Rainyu, V., and Novik, M.: Operational Experiences and Experimental Results Obtained from the Operation of a Fast Sodium-potassium Reactor (Opyt raboty i eksperimental'nyye rezul'taty, poluchennyye pri ekspluatatsii reaktora na bystrykh neytronakh s natriyevo-kaliyevym okhlazhdeniyem). Materialy Mezhdunarodnoy konferentsii v Zheneve po mirnomu ispol'zovaniye atomnoy energii, vol. 3, P/613, Gosenergoizdat, 1958.

34. Nuclear Reactors (Yadernyye reaktory), vol. II (Nuclear Reactor Equipment) Tekhnika yadernykh reaktorov . Materialy Komissii po atomnoy energii (USA) SShA , 1957, vol. III (Materialy dlya yadernykh reaktorov), 1956.

35. Addison, C., Addison, W., and Kerridge, R.: 'J. Chem. Soc.', p. 3047-3050 (September, 1955). Liquid Metals. Part III. Influence of Oxide Film on the Surface Tension of Liquid Sodium (Vliyaniye plenki okisi na poverkhnostnoye natyazheniye zhidkogo natriya).

36. 'Atomics', 7, V, No. 5, p. 175-177 (1956). Pumps for Liquid Metals (Nasosy dlya zhidkikh metallov).

37. Barnes, A.: 'Nucleonics', January, 1953, p. 16. Electromagnetic A-C Pumps (Elektromagnitnyye nasosy peremennogo toka).

38. Barnes: Symp. "Progr. Nucl. Energy", Ser. 4, 1, 1956, p. 165-176. Moving Liquid Metals (Perekachivaniye zhidkikh metallov).

39. Bauer, S. G.: "AERE", No. X/R 1381, 1954. Liquid Metals as Effective Heat-transfer Agents at High Temperatures (Zhidkiye metally v kacheatve effektivnykh teplonositeley pri vysokikh temperaturakh).

40. Bauer, S. G.: "Chem. Engng. Progr.", 52, No. 2, p. 75-76, 1956. Technology of Working with Liquid Metals (Tekhnika raboty s zhidkimi metallami).

41. Bauer, S. G.: Symp. "Progr. Nucl. Energy", Ser. 4, Techn. a. Engng., 1956, p. 135-145. Handling of Liquid Metals (Obrashcheniye s zhidkimi metallami).

42. Blake, L.: "Engineer", 202 (5256), p. 541-544, 1956. "Engineer", 202 (5257), p. 573-575, 1956. Conduction A-C and D-C Pumps for Liquid Metals (Konduktsionnyye nasosy postoyannogo i peremennogo toka dlya zhidkikh metallov).

43. Blake, L.: "Proceedings of Institution of Electrical Engineers", vol. 104, part A, no. 13, 1957, p. 49-67. Electromagnetic Pumps for Liquid Metals (Elektromagnitnyye nasosy dlya zhidkikh metallov).

44. Cowdle, C.: "Atomics and Nuclear Energy", vol. 8, No. 2, 1957, p. 41-45. Liquid Metals and Nuclear Energy (Zhidkiye metally i yadernaya energiya).

45. Bowman, F. and Cubicciotti, D.: Symp. "Problems in Nuclear Engineering", Edited by Hughes, D., Mc. Lain, S., and Williams, C., vol. 1, 1957. Application of Zirconium in Sodium Circuits (Primeneniye tsirkoniya v natriyevykh kontурakh).

46. Brill, E.: "Mechanical Engineering", vol. 75, No. 5, 1953, p. 369-373. Pumps for Moving Liquid Metals (Nasosy dlya perekachivaniye zhidkikh metallov).

47. Brooks, K. and Rosenblatt, A.: "Mechanical Engineering", vol. 75, No. 5, May, 1953, p. 363-368. Design and Testing of Heat-exchangers and Steam Generators Operating on Liquid Metals (Proyektirovaniye i ispytaniye teploobmennikov i parogeneratorov na zhidkikh metallakh).

/11

48. Brown, H., Amstead, B., and Short, B.: "Trans. of the ASME", vol. 79, No. 2, 1957, p. 279-285. Distribution of Temperatures and Velocities and Heat Transfer in Liquid Metals (Raspredeleniye temperatur i skorostey i teploot-dacha v zhidkikh metallakh).

49. Bruggeman, W. H.: "Am. Inst. Chem. Engrs", 2, VI, No. 2, p. 153-156, 1956. Purity Check of the Sodium Heat-transfer Agent in Reactor Systems (Kontrol' chistoty natriyevogo teplonositelya v reaktornykh sistemakh).

50. Brush, E.: "Corrosion", vol. 11, No. 7, 1955, p. 299-303. Structural Materials for Operation in a Liquid Sodium Medium (Konstruktsionnyye materialy dlya raboty v srede zhidkogo natriya).

51. Brusch and Koenig: Symp. "Nucl. Metallurgy", 1956, p. 21-32. Behavior of Materials in Liquid Metals (Povedeniye materialov v zhidkikh metallakh).

52. "R. W. K.," 7, No. 4, 1955, "V. D. I.", 95, No. 5, p. 663-640, 1953, 96, No. 19, 1954. Electromagnetic Flowmeters (Elektromagnitnyye raskhodomery).

53. Case, J.: "Mechanical Engineering", May, 1955, p. 369. Electromagnetic Pumps for Operation at High Temperatures (Elektromagnitnyye nasosy dlya raboty pri vysokikh temperaturakh).

54. Cothcart, J. and Manly, W.: "Corrosion", vol. 10, 1954, p. 432-434. Methods of Corrosion Testing in a Liquid Lead Medium (Metodika korrozionnykh ispytaniy v srede zhidkogo svintsa).

55. "Chem. and Engng News", 32, No. 30, p. 2966, 1954. Design of a Sodium-Graphite Power Reactor (Proyekt natriyevo-grafitovogo energeticheskogo reaktora).

56. "Chem. Engng News", 32, No. 47, p. 4706, 1954. Electromagnetic Pump for Liquid Metals (Elektromagnitnyy nasos dlya zhidkikh metallov).

57. "Chem. Engng. News", 33, VIII, No. 33, p. 3199-3201, 1955. Hermetically sealed Pumps (Germetichnyye nasosy).

58. 'Chem. Engng' (Tokyo), 19, No. 5, p. 283-289, 1955. The theory of the Analogy of Heat Transfer and Resistance in the Movement of a Liquid in a Tube and Heat Transfer When Using Molten Metal (Teoriya analogii teploot-dachi i soprotivleniya pri dvizhenii zhidkosti v trube i teplootdacha v sluchaye ispol'zovaniya rasplavlennogo metalla).

59. 'Chem. Engng', 63, VIII, No. 7, p. 215, 1956. Valves for Liquid Metals (Ventili dlya zhidkikh metallov).

60. Clark, P.: 'Mechanical Engineering', vol. 75, No. 8, 1953, p. 615-618. Mechanical Pumps for Liquid Metals (Mekhanicheskiye nasosy dlya zhidkikh metallov).

61. Codegone, C.: 'Termotecnica', 10, No. 10, p. 449-457, 1956. Heat-transfer Agents in Power Nuclear Reactors (Teplonositeli v energeticheskikh yadernykh reaktorakh).

62. Cope, W.: General Discussion on Heat Transfer. Inst. Mech. Eng. and ASME, 1951, p. 453-458. Heat Transfer to Mercury (Teplootdacha k rtuti).

63. Cottrell, W. and Mann, L.: 'Nucleonics', vol. 12, No. 12, Dec. 1954, p. 22-25. Materials for Use in a Medium of Sodium and Sodium-Potassium (Materialy dlya raboty v srede natriya i natriy-kaliya).

64. Cygan, R. and Stelle, A.: 'Chemical Engineering Progress', vol. 52, No. 4, 1956, p. 157-159. Designs and Performance of Pumps and Valves with Frozen Seals (Konstruktsii i rabota nasosov i ventiley s zamorazhivayushchimsya uplotneniyem).

65. Donohue, D.: 'Industrial and Engineering Chemistry', vol. 41, 1949, p. 2499-2511. Heat Transfer and Resistance in Heat Exchangers (Teloperedacha i soprotivleniye v teploobmennikakh).

66. Doody, T. and Younger, A.: Preprints of papers presented at meeting of Am. Inst. Chem. Eng., Atlantic City (New Jersey), Dec. 5, 1951, p. 77-88. Heat Transfer to Pure Mercury and to Mercury Containing Sodium Admixtures (Teplootdacha k chistoy rtuti i k rtuti, soderzhashchey dobavki natriya).

67. Douglas, T.: Specific heats of liquid metals and liquid salts. Symp. 'Problems in Nuclear Engineering', vol. I, ed. by D. Hughes, S. Mcbain, C. Williams, 1957, p. 191-199.

68. Dubsek, F.: Strojirenstvi, 5, No. 11, p. 819-824, 1955. Use of Sodium as an Intermediary Heat-transfer Agent in Nuclear Power Plants (Ispol'zovaniye natriya v kachestve promezhutochnogo teplonositelya na atomnykh elektrostantsiyakh).

69. Dunn, W. E., Monilla, C. F., Forsterberg, C., and Gross, B. J.: 'Am. Inst. Chem. Engrs', 2, No. 2, p. 184-189, 1956. Mass Transport in Liquid Metals (Massoobmen v zhidkikh metallakh).

70. Dwyer, O.: 'Nucleonics', vol. 12, No. 6, 1951. Heat Transfer in Liquid-metal Fuel Reactors (Teploobmen v reaktorakh na zhidkometallicheskom toplive).

71. 'Electr. J.', 36, No. 3, p. 53, 1956; 'Electr. Rev.', 158, No. 11, p. 404, 1956; 'Process Control a. Automat.', 3, No. 3, p. 112, 1956. Liquid-metal Pumps for Nuclear Power Plants (Zhidkometallicheskiye nasosy dlya atomnykh elektricheskikh stantsiy).

72. 'Electr. J.', 161, No. 8, p. 536, 1956. Experimental Reactor Cooled by a Sodium Coolant (Eksperimental'nyy reaktor, okhlazhdayemyy natriyevym teplonositelem).

73. 'Electr. Times', 129, No. 3353, p. 190, 1956. Liquid-metal Pump (Nasos dlya zhidkogo metalla).

74. 'Electr. Times', 130, No. 3390, p. 666-667, 1956. Liquid-metal Pumps (Nasosy dlya zhidkikh metallov).

75. Ehred, K. and Fouss, R.: 'Transactions of the ASME', vol. 74, No. 4, 1952. Calculation of Electromagnetic Flowmeters (Raschet elektromagnitnykh rashkhodomerov).

76. "Engineer". 201, No. 5231, p. 409, 1956; "Metallurgia", 53, VI, No. 320, p. 277, 1956. Electromagnetic Pumps for Liquid Metals (Elektromagnitnyye nasosy dlya zhidkikh metallov).

77. English, D. and Barret, T.: General Discussion on Heat Transfer, Inst. Mech. Eng. and ASME, 1951, p. 458-460. Heat Transfer Properties of Mercury (Teploperedayushchiye svoystva rtuti).

78. Ewing, C., Grand, J., and Miller, R.: "The Journal of Physical Chemistry", vol. 58, No. 12, Dec., 1954, p. 1086-1088. Viscosity of Sodium-Potassium Alloys (Vyazkost' splavov natriy-kaliy).

79. Ewing, C., Seelold, E., Grand, J., and Miller, R.: "The Journal of Physical Chemistry", vol. 59, June, 1955, No. 6, p. 524-526. Heat Conductivity of Mercury and Two Sodium-Potassium Alloys (Teploprovodnost' rtuti i dvukh splavov natriy-kaliy).

80. "Fluid Handling", No. 68, 240-246, 1955. Liquid Metals and the Designing of Nuclear Power Plants. Review. (Zhidkiye metally i proyektirovaniye atomnykh elektrostantsiy. Obzornaya stat'ya).

81. "Fluid Handling", No. 70, p. 319-322, 324, 1956. Liquid Metals and the Layout of a Nuclear Power Plant. Review. (Zhidkiye metally i konstruksiya atomnoy energeticheskoy ustanovki. Obzornaya stat'ya).

82. Ford, G. W.: "Engineering", 182, No. 4735, p. 727-730, 1956. Comparison of Power Reactors Cooled by Water under Pressure and Reactors with Graphite Moderators Cooled by Sodium Coolants (Sravneniye energeticheskikh reaktorov, okhlazhdayemykh vodoy pod davleniyem, i reaktorov s grafitovym zamedlitelem, okhlazhdayemykh natriyem teplonositelem).

83. Ford, G. W.: Symp. "Progr. Nucl. Energy", Ser. 4, 1, 1956, p. 177-193. Mechanical Pumps for Coolants in Power Reactors (Mekhanicheskiye nasosy dlya teplonositeley v energeticheskikh reaktorakh).

84. Fortescue, P.: J. "Nuclear Energy". 1954. vol. I, p. 1-23. Designing of Absolutely Leaktight Mechanical Pumps for Liquid Sodium (Proyektirovaniye absolutno germetichnykh mekhanicheskikh nasosov dlya zhidkogo natriya).

85. Frost, B.: "Atomics and Nuclear Energy", vol. 8, No. 10, Oct. 1957, p. 387-390. Wetting Solids with Liquid Metals (Smachivaniye tverdykh tel zhidkimi metallami).

86. Frost, B.: "Nuclear Engineering", No. 8, Nov., 1956, p. 334-339 (Part I); No. 9, Dec., 1956, p. 373-377 (Part II). Problems of Reactors with Liquid-metal Fuel (Problemy reaktorov s zhidkometallicheskim toplivom).

87. Gangler, J.: "Journal American Ceramic Society", vol. 37, No. 7, 1954, p. 312-316. Resistance of Heat-resistant Materials to the Effect of Bismuth-Lead Alloy (Soprotivleniye zharoprochnykh materialov vozdeystviya splava vismut-svinets).

88. "Gas, Wasser, Wärme", 7, No. 1, p. 21, 1953. Gallium as a Heat-transfer Agent in the Generation of Nuclear Energy (Galliy kak teplonositel' pri proizvodstve yadernoy energii).

89. Gilliland, E., Musser, R., and Page, W.: General Discussion on Heat Transfer, Inst. Mech. Eng. and ASME, 1951, p. 402-404. Heat Transfer to Mercury (Teplootdacha k rtuti).

90. Gray, J., Neal, R., and Gerhens, B.: "Nucleonics", vol. 14, No. 10, Oct., 1956, p. 34-37. Simple Method of Checking Oxygen Content in Liquid Sodium (Prostoy metod kontrolya s derzhaniya kislorada v zhidkom natrii).

91. Greenwood, G. W. and Charpe, R.: "J. Nucl. Energy", 3, No. 1/2, p. 1-6, 1956. Effect of Heat Flux in Metal-cooled Reactors (Vliyaniye teplovykh nagruzok v reaktorakh s metallicheskim teplonositelem).

92. Gurinsky: "Nucleonics Metallurgy", 1956, p. 5-20. Behavior of Materials in Liquid Metals (Povedeniye materialov v zhidkikh metallakh).

93. Haag, F.: "Nucleonics", vol. 15, No. 2, 1957, p. 58-63. Radioactivity Transport in Sodium Circuits (Perenos radioaktivnosti v natriyevykh konturakh).

94. Hackett, E.: "Transactions of the ASME", vol. 64, p. 647, 1942. Application of Mercury in Power Engineering (Primeneniye rtuti v energetike).

95. Hall, W. B. and Crofts, T. J.: "Engineer", 201, No. 5218, p. 128-130, 1956; "Chart. Mec. Engng", 3, No. 1, p. 40-41, 1956; "J. Brit. Nucl. Energy Conf.", 1, No. 2, p. 76-92, 1956. Application of Sodium and Sodium-Potassium Alloys as Coolants (Primeneniye natriya i natriyevo-kaliyevykh splavov v kachestve teplonositeley).

96. Hall, W. B. and Crofts, T. J.: "Fluid Handling", No. 73, p. 45-48, 1956. Application of Sodium and Sodium-Potassium Alloys as Coolants (Primeneniye natriya i natriyevo-kaliyevykh splavov v kachestve teplonositeley).

97. Hall, W. and Jenkins, A.: "Journal of Nuclear Energy", vol. I, 1955, p. 244-263. Experiments Regarding Heat Transfer to Sodium and Sodium-potassium Alloy (Opyty po teplootdache k natriyu i splavu natriy-kaliy).

98. Harrison, W. and Menke, J.: "Trans. ASME", vol. 71, No. 7, Oct., 1949, p. 797-803. Heat Transfer to Liquid Metals. Flow in Asymmetrically-Heated Ducts (Teplootdacha k zhidkim metallam. Techeniye v asimmetrichno obogrevayemykh kanalakh).

99. "Heating, Pip. a. Air Condit.", 25, No. 7, p. 112-113, 1953. Liquid Metal Pipeline (Truboprovod dlya zhidkogo metalla).

100. Hines, E., Gemont, A., and Kelley, J.: "Nucleonics", 14, No. 10, p. 38-41, 1956. Experimental Determination of the Peak Pressure and Temperature to which the Housing of the Reactor can be Subjected in the Event of a Reaction Between Sodium and Air (Eksperimental'noye opredeleniye maksimal'nykh znacheniy davleniya i temperatury, kotorym mozhet byt' podvergnut korpus reaktora v sluchaye reaktsii mezhdu natriyem i vozdukhom).

101. Hoe, R., Dropkin, D., and Dwyer, O.: "Transactions of the ASME", vol. 79, May, No. 4, 1957, p. 899-907. Heat Transfer to Mercury Transversely Washing Checkerboard Tube Clusters (Teplootdacha k rtuti, omyvayushchey v poperechnom napravlenii shakhmatnyy puchok trub).

102. Hoffman, E. and Manly, W.: Symp. "Problems in Nuclear Engineering", v. 1, ed. by Hughes, D., Mc Lain, S., Williams, C., 1957, p. 128-137. Comparison of Sodium, Lithium, and Lead by Their Corrosion Effect on Structural Materials (Sravneniye natriya, litiya i svintsa po ikh korrozionnomu vozdeystviyu na konstruktsionnyye materialy).

103. Hughes, D., Mc Lain, S., and Williams, C.: Symp. "Problems in Nuclear Engineering", vol. 1, 1957. Problems of Nuclear Engineering (Problemy yadernoy tekhniki).

104. Hurst, R. and Mc Lain, S.: (ed.). Symp. "Progress in Nuclear Energy", Series IV, Technology and Engineering, vol. I, London, 1956. Questions of Nuclear Engineering (Voprosy yadernoy tekhniki).

105. Isakoff, S. and Drew, T.: General Discussion on Heat Transfer, Inst. Mech. Eng. and. ASME, 1951, p. 405-409. Transfer of Heat and Quantity of Motion in a Turbulent Flow of Mercury (Perenos tepla i kolichestva dvizheniya v turbulentnom potoke rtuti).

106. Jackson, B.: (ed.). Liquid-Metals Handbook, Sodium (NaK) supplement, June, 1955. Handbook of Liquid Metals (Spravochnik po zhidkim metallam).

107. "J. Amer. Ceram. Soc.", 37, No. 3, p. 146-153, 1954. Stability of Heat-resistant Materials in Molten Metals (Ustoychivost' zharoupornykh materialov v rasplavlennykh metallakh).

108. Jay, T. C.: "Radio Electronic", 26, No. 11, p. 60, 1955. Magnetic Flowmeter (Magnitnyy raskhodomer).

109. Johnson, H., Clabaugh, W., and Hartnett, J.: "Trans. of the ASME", vol. 76, 1954, p. 505-511. Heat Transfer to Mercury With Turbulent Flow in Tubes (Teplootdacha k rtuti pri turbulentnom techenii v trube).

110. Johnson, H., Hartnett, J., and Clabaugh, W.: "Trans. of the ASME", vol. 75, No. 6, Aug. 1953, p. 1191-1198. Heat Transfer to the Molten Eutectic Bismuth-Lead With Turbulent Flow in Tubes (Teplootdacha k rasplavlennoy evtektike vismut-svinets pri turbulentnom techenii v trube).

111. Johnson, H., Hartnett, and Clabaugh, W.: "Trans. ASME", vo. 76, No. 4, p. 513-517, 1954. Heat Transfer to a Liquid Alloy of Bismuth with Lead and to Mercury With Laminar and Transient Flow in Tubes (Teplootdacha k zhidkomu splavu vismuta so svintsom i rtuti pri laminarnom i perekhodnom potokakh v trubakh).

112. Johnson, H., Hartnett, J., Clabaugh, W., and Fried, L.: "Trans. of the ASME", vol. 79, No. 5, July, 1957, p. 1079-1084. Coefficient of the Expenditure of Choke Discs and the Coefficient of Resistance With Turbulent Flow of Eutectic Lead-Bismuth in Tubes (Koeffitsiyent raskhoda drossel'nykh shayb i koeffitsiyent soprotivleniya pri turbulentnom techenii evtektiki svinets-vismut v trube).

113. Klein, H. Z.: "Metallkunde", X, 44, No. 10, p. 450-456, 1953. Heat Transfer With Free Convection in Molten Metal (Teplootdacha pri svobodnoy konvektsii v rasplavlennom metalle).

114. Koenig, R. and Brush, E.: "Materials and Methods", vol. 42, No. 6, 1955, p. 110-114. Structural Materials for Liquid-Sodium System (Konstruktsionnyye materialy dlya sistem s zhidkim natriyem).

115. Lee, J. F.: "Nucleonics", 12, No. 4, p. 74, 76-77, 1954. Thermodynamic Properties of Liquid Sodium (Termodinamicheskiye svoystva zhidkogo natriya).

116. Lehnert, B.: "Phys. Review", 94, No. 4, 1954. Magnetohydrodynamic Waves in Liquid Sodium (Magnitogidrodinamicheskiye volny v zhidkom natrii).

117. Lehnert, B.: "Proc. Roy. Soc.," Ser. A. 233, XII, p. 1194-1195, 1955. Instability of a Laminar Flow of Mercury Caused by an External Magnetic Field (Nestabil'nost' laminarnogo potoka rtuti, vyzvannaya vneshnim magnitnym polem).

118. Lewis, J. B.: "Discovery", 17, No. 11, p. 469-471, 1956. Application of Liquid Metals in Nuclear Reactors (Primeneniye zhidkikh metallov v yadernykh reaktorakh).

119. Lubarsky, B. and Kaufman, S.: "NACA", Report 1270, 1956. Review of Experimental Research on Heat Transfer in Liquid Metals (Obzor eksperimental'nykh issledovaniy po teplootdache v zhidkikh metallakh).

120. Lyon, R.: (ed.), Liquid-Metals Handbook, Atomic Energy Comm., Dept. Navy, First ed., June, 1950, Second ed., June, 1952. Handbook of Liquid Metals (Spravochnik po zhidkim metallam).

121. Lyon, R. N.: Symp. "Progr. Nucl. Energy", Ser. 4, 1, 1956, p. 245-252. Calculation of Heat Transfer to Liquid Metal (Raschet teplootdachi k zhidkomu metallu).

122. Lyon, R.: "Transactions of Am. Inst. Chem. Engrs.", vol. 47, 1951, p. 75-79. Heat Transfer in Liquid Metals (Teplootdacha v zhidkikh metallakh).

123. McIntosh, A. B. and Begley, K. G.: "J. Inst. Metals", 84, No. 7, p. 251-270, 1955-1956. Selection of a Material for Casings of Nuclear Reactors Cooled by Sodium (Potassium) and Carbon Dioxide (Vybor materiala dlya obolochek atomnykh reaktorov, okhlazhdayemykh natriyem [kaliyem] i uglekislotoy).

126. Mack, G., Jr., Jarvis, J., and Bartell, F.: "Journal of Physical Chemistry", vol. 56, 1952. Surface Tension of Gallium (Poverkhnostnoye natyazheniye galliya).

127. Makansi, M., Mundel, C., and Melton, W.: "The Journal of Physical Chemistry", vol. 59, No. 1, January, 1955, p. 40-42. Determining the Sodium Vapor Pressure (Opredeleniye upругosti parov natriya).

128. Manly, W. D.: "Corrosion", 12, No. 7, p. 44-52, 1956. Corrosion of Liquid Metals (Korrozionnoye deystviye zhidkikh metallov).

129. Martinelli, R.: "Trans. of ASME", vol. 69, No. 8, Nov. 1947, p. 947-959. Heat Transfer to Molten Metals (Teplootdacha k rasplavlennym metallam).

130. Martin, J. W. and Smith, G. C.: "Metallurgia", 54, No. 325, p. 227-232, 1956. Preliminary Investigation of the Fatigue of Metals Functioning in a Liquid Metal Medium (Predvaritel'noye issledovaniye ustalosti materialov, rabotayushchikh v srede zhidkogo metalla).

131. "Mech. Engng", 77, VI, No. 6, p. 488, 1955. Hermetically sealed Pumps with Electric Drive (Germetichnyye nasosy s elektroprivodom).

132. Meyer, W. and Ehemen, W.: "Journal of Applied Physics", vol. 25, No. 3, March, 1954. Measurement of Thermal Resistance on the Surface of Separation of Sodium and Stainless Steel (Izmereniye termicheskogo soprotivleniya na poverkhnosti razdela natriy-- nerzhaveyushchaya stal').

133. Munch, R.: "Industrial and Engineering Chemistry", vol. 44, No. 1, 1952. Electromagnetic Flowmeter (Elektromagnitnyy raskhodomer).

134. Murgatroyd, W.: "Phil. Mag.", Series 7, vol. 44, p. 1348, Dec., 1953. Experiments on the Magnetohydrodynamics of Flow in Ducts (Opyty po magnitogidrodinamike techeniya v kanalakh).

Best Available Copy

134. Naiman, K. A.: "Phys. Chem.", 2, No. 3-4, p. 215-228, 1954. Vaporization Coefficient of Liquid Potassium (Koeffitsiyent isparemiya zhidkogo kaliya).

135. Northfield, H. J.: "Engineering", 182, No. 4722, p. 293-295, 1956. On the Effectiveness of Electromagnetic Liquid-Metal Pumps (Ob effektivnosti elektromagnitnykh nasosov dlya zhidkikh metallov).

136. "Nuclear Power", vol. 1, No. 3, July, 1956, p. 131. Porous Stainless Steel Filters with Pores from 1 to 2 Microns (Poristyye fil'try iz nerzhaveyushchey stali s razmerom por do 1-2 mikron).

137. "Nuclear Power", vol. 2, No. 16, Aug., 1957, p. 338. Heat Insulation of a Sodium Circuit of the Reactor in Dounreay (Termoizolyatsiya natriyevogo kontura reaktora v Daunri).

138. "Nucl. Engng.", 1, No. 6, p. 238-240, 1956. Application of Liquid Metals as Heat-transfer Agents in Chemical Engineering (Primeneniye zhidkikh metallov v kachestve teplonositeley v protsessakh khimicheskoy tekhnologii).

139. "Nucleonics", 13, No. 2, p. 70, 1955. Testing of Heat-transfer and Corrosion Properties of the Material "Globeiron" for Shells of Heat-generating Elements in a Fast-neutron Sodium-cooled Breeder-reactor (Ispytaniye teplootmennykh i korrozionnykh svoystv materiala "globayron" dlya obolochek teplovydelyayushchikh elementov v reaktore-razmnozhitele na bystrykh neytronakh s natriyevym teplonositelem).

139. Olson, R. L.: "Nucleonics", 13, No. 6, p. 70-72, 1955. Design of an Experimental Sodium-Cooled Reactor (Konstruktsiya eksperimental'nogo reaktora s natriyevym okhlazhdeniyem).

140. Perkins, J. E.: Rep. Proc. Liquid Met. Utillis. Confer., AERE, No. X/R. 1981, 1954. Investigation into the Performance of a Steam-generator on Liquid Sodium (Issledovaniye raboty parogeneratora na zhidkom natrii).

141. Perkins, W.: Symp. 'Problems in Nuclear Engineering', vol. 1, ed. by Hughes, D., McLain, S., Williams, C., 1957, p. 191-199. Equipment for an Experimental Sodium Reactor (Oborudovaniye dlya eksperimental'nogo natriyevogo reaktora).

142. Pulsford, D. W.: 'J. Sci. Instr. Phys.', 32, No. 9, p. 362-363, 1955. Measurement of Liquid Sodium Level in Stainless Steel Tubes by the Induction Method (Izmereniye urovnya zhidkogo natriya v trubakh iz nerzhaveyushchey stali induktsionnym metodom).

143. Reed, E.: 'J. of American Ceramic Society', vol. 37, No. 3, 1954, p. 146-153. Stability of Heat-resistant Materials in Liquid Metals (Stoykost' zharoprochnykh materialov v zhidkikh metallakh).

144. Risk, A. E.: 'Mod. Pow. Engng', 49, No. 9, p. 102-103; No. 12, p. 116-117, 1955. Pumping Equipment and Heat Removal in Nuclear Reactors (Nasosnoye oborudovaniye i teplos'yem v yadernykh reaktorakh).

145. Savage, H. and Cobb, W.: 'Chemical Engineering Progress', vol. 50, No. 9, Sept., 1954. Centrifugal Liquid-metal Pumps Working at High Temperature (Tsentrobezhnyye nasosy dlya zhidkikh metallov, rabotayushchiye pri vysokoy temperature).

146. Seban, R. and Casey, D. F.: 'Trans. of ASME', vol. 79, No. 7, t., 1957, p. 1514-1517. Heat Transport at Turbulent Flow of Lead-bismuth Alloy in Annular Ducts (Teplootdacha pri turbulentnom techenii splava svinets-vismut v kol'tsevom kanale).

147. Seban, R.: 'Trans. ASME', vol. 72, No. 6, Aug., 1950, p. 783-785. Heat Transfer to Turbulent Flow of Liquid Flowing Between Parallel Walls with Asymmetric Distribution of Temperatures (Teplootdacha k turbulentnomu potoku zhidkosti, tekushchey mezhdu parallel'nymi stenkami s asimmetrichnym raspredeleniyem temperatur).

148. Seban, R. and Shimazaki, T.: "Trans. of the ASME", vol. 73, 1951, p. 803-807. Heat Transfer to Turbulent Flow of Liquid Flowing in a Tube at Constant Temperature of the Wall (Teplootdacha k turbulentnomu potoku zhidkosti, tekushchey v trubke pri postoyannoy temperature stenki).

149. Serra, F.: "Termotecnica", 9, No. 9, p. 442-451, 1955. Liquid Heat-transfer Agents (Zhidkiye teplonositeli).

150. Shercliff, T. A.: "Proc. Roy. Soc.", Ser. H., 233, XII, p. 1194, 1955. Some Engineering Applications of Magnetic Hydrodynamics (Nekotoryye inzhenernyye prilozheniya magnitnoy gidrodinamiki).

151. Sittig, M.: Sodium; its manufacture, properties and uses, Reinhold, 1956. Sodium, Its Production, Properties, and Application (Natriy, yego proizvodstvo, svoystva i ispol'zovaniye).

152. Sleicher, C. and Tribus, M.: "Trans. of the ASME", vol. 79, 1957, p. 789-797. Heat Transfer during Turbulent Flow of Liquid in Tubes with Arbitrary Distribution of Wall Temperatures (Teplootdacha pri turbulentnom techenii zhidkosti v trube s proizvol'nym raspredeleniyem temperatury stenki).

153. Speed, F.: "Nuclear Power", vol. 2, No. 15, July, 1957, p. 277-284.

154. Starr, C.: "Electr. World", 14, 5, No. 13, p. 44, 1956. Utilization of a Sodium-to-Graphite Reactor for Electric Power Generation (Ispol'zovaniye natriy-grafitovogo reaktora dlya proizvodstva elektro-energii).

155. Starr, C.: "Power", 99, No. 7, p. 152, 154, 1955. Electric Power Plant with a Sodium-to-Graphite Reactor (Elektrostantsiya s natriyevo-grafitovym reaktorom).

156. Starr, C.: Symp. "Progr. Nucl. Energy", Ser. 2, Reactors, 1956, 1, p. 389-434. Graphite-moderated Sodium-cooled Reactor: Its Description, Characteristics, and Application Prospects (Reaktor s grafitovym zamedlitelem, okhlazhdayemyy natriyevym teplonositelem, yego opisaniye, kharakteristiki i perspektivy primeneniya).

157. Strachan, J. F. and Harris, N. J.: "J. Inst. Metals", 3, No. 1, p. 17-24, 1956. Liquid-mercury Corrosion of Metals Which are not Subjected to Mechanical Stress (Raz"yedeniye zhidkoy rtut'yu metallov, ne podvergayushchikhsya mekhanicheskim napryazheniyam).

158. "Strojirenstvi", 5, No. 9, p. 664-670, 1955. Liquid Metals: Heat-transfer Agents of the Future (Zhidkiye metally-- teplonositeli budushchego).

159. Taylor, J. M.: "Research", 8, No. 3, p. 102-105, 1955. Importance of Liquid Metals in Designing Nuclear Reactors (Znacheniye zhidkikh metallov dlya razrabotki konstruktsiy yadernykh reaktorov).

160. Taylor, J.: "Phil. Mag.", vol. 46, p. 867, 1955. Surface Energy of Alkali Metals (Poverkhnostnaya energiya shchelochnykh metallov).

161. Taylor, J. W.: "J. Nucl. Energy", 2, No. 1, p. 15-30, 1955. On the Significance of Liquid-metal wetting Phenomena for Processes in Nuclear Reactors (Znacheniy yavleniy smachivaniya zhidkimi metallami dlya protsessov v yadernykh reaktorakh).

162. Tidhall, R.: Preprints of papers for heat transfer symposium at forty-fourth annual meeting, the American Institute of Chemical Engineers, Dec. 5, 1951, p. 99-122. Performance of Small Laboratory-type Liquid-metal Heat Exchangers (Rabota nebol'shikh zhidkometallicheskikh teploobmennikov laboratornogo tipa).

163. Threlfall, L.: General Discussion on Heat Transfer, Inst. Mech. Engs. and ASME, 1951, p. 436-438. Heat Transfer to Liquid Metals During Flow in Round Tubes and Annular Ducts (Teplootdacha k zhidkim metallam pri techenii v kruglykh trubakh i kol'tsevykh kanalakh).

164. Trocki, T., Bruggemann, W., and Crewer, F.: Symp. "Progr. Nucl. Energy", Ser. 4, "Techn. a. Engng", 1956, I, p. 146-162. Problems on Outfitting Reactors Employing Sodium or a Sodium-potassium Alloy as Heat Transfer Agents (Problemy oborudovaniya reaktorov s natriyem ili splavom natriy-kaliy v kachestve teplonositelya).

165. Trocki, T. and Nelson, D.: "Mechanical Engineering", vol. 75, No. 6, 1953, p. 472-476. Outfitting a Semi-industrial Liquid-metal Circuit (Oborudovaniye polupromyshlennogo zhidkometallicheskogo kontura).

166. Watt, D.: "Engineering", vol. 181, No. 1703, April 27, 1956. Liquid-metal Electromagnetic Pumps (for Moving Coolants and Nuclear Reactor Fuel) (Elektromagnitnyye nasosy dlya zhidkikh metallov perekachivaniye teplonositeley i topliva yadernykh reaktorov).

167. Webber, H., Goldstein, D., and Fellinger, R.: "Trans. ASME", II, 77, No. 2, p. 97-102, 1955. Determination of the Heat Conductivity of Molten Lithium (Opredeleniye teploprovodnosti rasplavlennogo litiya).

168. Weeks, J. R.: Symp. "Progr. Nucl. Energy", Ser. 4, No. 1, p. 378-408, 1956. Metallurgic Research of Liquid Bismuth and Its Alloys as a Heat-transfer Agent and as Composite Part of Liquid-metal Fuel in Nuclear Reactors (Metallurgicheskoye issledovaniye zhidkogo vismuta i yego splavov v kachestve teplonositelya i sostavnoy chasti zhidkometallicheskogo topliva yadernykh reaktorov).

169. "Westinghouse Eng.", 16, VIII, No. 4, 127, 1956. New Mechanical Liquid-metal Pump (Novyy mekhanicheskiy nasos dlya zhidkikh metallov).

170. Woodrow, J.: 'AERE', No. F/R, 452, 1954. Electromagnetic and Induction Pumps for Nuclear Reactors (Elektromagnitnyye i induktsionnyye nasosy dlya yadernykh reaktorov).

171. Woolen, W.: 'Nuclear Power', vol. 2, No. 15, July, 1957, p. 267-276. Electromagnetic Pumps (Elektromagnitnyye nasosy).

PART THREE

SOVIET STUDIES OF LIQUID-METAL HEAT TRANSFER MEDIA

In this section a few results of Soviet studies of liquid-metal heat transfer media are considered in condensed form.

We shall consider the results of studies of heat transfer and hydraulics of liquid metals, of determinations of their thermophysical constants, the selection of structural materials for liquid-metal systems, obtaining the necessary purity of certain metals, the designing and construction of pumps, fittings, and measuring instruments for liquid metals.

Mercury was the first of the liquid metal heat-transfer media to undergo fairly thorough thermophysical studies (as early as the prewar years). These studies were organized at the Central Boiler and Turbine Institute in 1935-1936 in a specially created laboratory. The main intention was to study heat transfer during the flow of boiling and nonboiling mercury through tubes, and to study the process of condensation of mercury vapor and the hydrodynamics of mercury flow.

These studies were initiated as a result of a need to obtain reliable theoretical data, since mercury differs greatly from water and other previously studied liquids with respect to thermophysical properties. Among the specific properties of mercury are: great thermal conductivity, low heat capacity and viscosity of the liquid and vapor phases, great surface tension, which makes pipe surfaces nonwettable by mercury. The properties of other liquid metals also differ greatly from those of water.

49. Heat Transfer and Hydraulic Resistance during Flow of Liquid Metals in Pipes.

Heat transfer without boiling. The first studies of heat transfer during the flow of mercury in a tube were carried out in 1936-1938 [20]. Studies were made both of installations with electrically generated radiant heating where the section being heated was 0.97 — 1.5 m high with a diameter of 16 mm, as well as for mercury flow through an annular channel with an equivalent diameter of 14.6 and 30.4 mm. The heat flux varied from 45,000 to 120,000 kcal/m^2 hr, the temperature of the mercury from 360 to 450°C, and the Reynolds number from 50,000 to 220,000.

Comparison of the experimental data obtained at the Central Scientific Research Institute for Boilers and Turbines with calculations according to empirical formulas of the Kraussol'd, Cox, and other types ($Nu = ARe^m Pr^n$) and according to the theoretical Prandtl-Karman formulas showed that the experimental points lie significantly above those calculated according to Prandtl-Karman and significantly below those calculated according to Kraussol'd.

In plotting functions of the type $Nu = f(Re, Pr)$ certain allowances were permitted, in particular those caused by the absence of reliable data concerning the heat capacity of liquid mercury at temperatures higher than 100-150° C. Analysis of the experimental data was also hindered by the instability of the heat transfer coefficients being measured during experiments with tubes made of carbon steel and alloy steel. Carbon steel tubes had great relative roughness, and oxide films formed and were destroyed more quickly on them. In comparing the experimental data with those calculated according to the empirical formulas $Nu = f(Re, Pr)$, it was assumed that these formulas were obtained in experiments with liquids where Pr = 0.008 to 0.009.

In 1939-1940 in the same laboratory of the Central Scientific Research Institute for Boilers and Turbines more detailed studies of heat transfer were made in the case of nonboiling mercury [27]. The experiments were performed on

[illegible] up to 2.7 m [illegible] with diameters
[illegible] from [illegible] to 15,000 kcal/m^2 hr,
[illegible] to [illegible], and Re$_f$ [illegible] number from 100,000
[illegible] heat transfer coefficients found in the experiments
[illegible], particularly as a result of utilizing only tubes made of alloy
[illegible] the parameters(temperature and velocity)was wider in
[illegible] than in the first experiments previously described. The results of the
[illegible] were plotted in Nu=f(Re) coordinates and in this form are recommended for practical calculations.

[illegible] of the Central Scientific Research Institute for [illegible] the following conclusions were reached:

1. [illegible] during the flow of mercury through a pipe cannot be calculated by any known theoretical or empirical formulas. For the calculations the graphic functions obtained, $\alpha = f(Re)$ or $Nu = f(Re)$ may be used.

2. A possible reduction in the value of the heat transfer coefficient as a result of the formation of the oxide film on the heat-exchange surface, especially in the case of carbon-steel tubes, must be taken into account.

3. Under the conditions of the experiments the relationship between the heat transfer coefficient and the heat load was not ascertained.

In 1941 the experiments were stopped. After 1946 an additional series of experiments based on heat transfer in nonboiling mercury was performed. These experiments dealt in particular with the movement of mercury through a spiral pipe under forced circulation. It was noted that artificial agitation of the mercury flow (by means of a spiral trajectory) somewhat increased the efficiency of heat transfer. It is possible that this effect is a result of the destruction of the oxide film. The same was also observed in the former experiments, when a more strong agitation of the mercury flow was introduced into the pipe being heated.

Best Available Copy

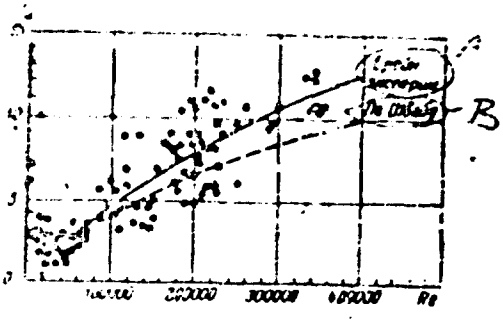

Fig. 212. Heat transfer in liquid mercury.

(a) average of experiment

(b) according to Shvab

The first empirical formula for calculating heat transfer when a liquid metal is flowing in a heated tube was proposed by A. A. Kanayev in 1951 after processing of the pre-and postwar experiments with mercury [12].

In dimensionless quantities this formula had the form $Nu = f(Re) = f(Re, Pr)$. Since the temperature of the mercury was close to 500°C in a majority of cases, it was not possible to separate the effects of Re and Pr on the value of Nu. During the processing of the experimental data Pr was taken to be constant. The empirical formula had the form:

$$Nu = A Re^{n} \qquad (102)$$

As can be seen from Fig. 212, the results of calculations according to Formula (102) are close to the results of the calculations according to V. A. Shvab's theoretical formula [31]. However, when $Re = 2 \cdot 10^5$ to $4 \cdot 10^5$, the calculated values of Nu are 15 to 25% lower than the experimental values.

The numerical coefficient A in Formula (102) equals 0.0009 to 0.001. The exponent n = 0.74 to 0.75

The [illegible] calculation formula is

[illegible] (103)

In this [illegible] the formula is convenient for engineering calculations with a slide rule.

In Fig. 213 the calculated data based on Formula (103) are compared with the most foreign experimental data obtained in the postwar years, those of [illegible] (USA) and Elser (Switzerland). The data of Muser and Page closely [illegible] with the data of the Central Scientific Research Institute for Boilers and Turbines. Elser's experimental values are 3-4 times lower than the Soviet and American values. Apparently Elser did not succeed in calculating the heat balance correctly, and thus the accuracy of his experiments was inadequate.

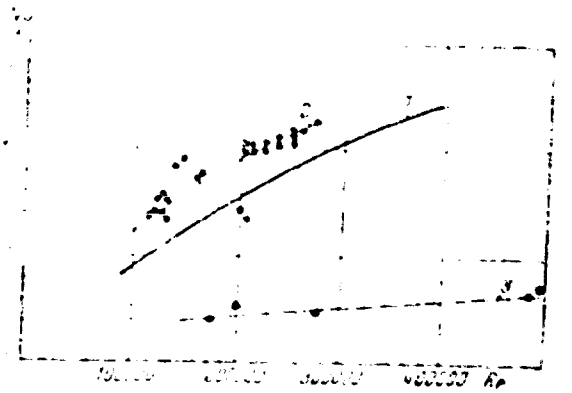

Fig. 213. Heat transfer in liquid mercury (according to Formula 103).
(1) according to A. A. Kenayev's formula.

(2) according to Muser and Page.

(3) according to Elser.

More recent studies of heat transfer during flow of mercury and amalgams through tubes were carried out in the Central Scientific Research Institute for Boilers and Turbines by M. I. Kornoyev [16]. The results of these studies were close to the results of the preceding experiments.

Fundamental studies of heat transfer during flow of liquid metals through a tube were carried out in the postwar years at the Institute of Power Engineering of the Academy of Sciences of the USSR, in the laboratory of Academician M. A. Mikheyev. The results of these studies were reported in August, 1955 at the International Conference on Peaceful Utilization of Atomic Energy, at Geneva [21]. Heat transfer with mercury, tin, lead, bismuth, sodium, bismuth-lead alloys, and sodium-potassium alloys was studied, and the values Pr = $4 \cdot 10^{-3}$ to $3 \cdot 2 \cdot 10^{-2}$ and Pe = $1 \cdot 10^{4}$ to $6 \cdot 5 \cdot 10^{5}$ were thus obtained. The heat flux varied from $2 \cdot 10^{4}$ to $1 \cdot 10^{6}$ kcal/m^2 hr.

An emperical formula was obtained for calculating heat transfer during turbulent flow of molten metals through tubes:

$$Nu = 4.5 + 0.0142 Re\,Pr^{0.8}.* \qquad (104)$$

---

* Instead of formula (104) the following simplified formula may be recommended for practical calculations:

$$Nu = 4 + 0.025\,Pe^{0.8} \quad (Pe > 300).$$

As in the case of the experiments at the Central Scientific Research Institute for Boilers and Turbines, the effect of wettability of the heating surface on the heat exchanged was noted. It was suggested that oxides form on the tube wall because it is not wetted by liquid metals, and that the thermal resistance increases as a result. The following formula was obtained for the transfer of heat from a liquid metal to an oxidized heating surface:

$$Nu = 3 + 0.011 (Re\,Pr)^{0.8}. \qquad (105)$$

Equations (104) and (105) are correct for long tubes, when $\frac{l}{d} \gg 30$. When the ratio $\frac{l}{d}$ is lower, a correction factor $1.72 \cdot \left(\frac{d}{l}\right)^{0.16}$ must be introduced into the formula.

Formulas (104) and (105) may be recommended for calculation of heat transfer during the flow of liquid metals through commercially smooth pipes.

The experimental values in the experiments of the Institute of Power Engineering of the Academy of Sciences of the USSR are lower than the values obtained from Lyon's and Seban's analytical solutions and agree relatively well (within 10 to 20%) with the data derived from Dwyer's formula: $Nu = 4.9 + 0.018\,(Re\,Pr)^{0.8}$ obtained for heavy liquid metals and also agree with Johnson's experimental data.

In this report a generalized formula was obtained for metallic and non-metallic heat transfer media differing by four orders with respect to the value of Pr:

$$Nu = (3.2 + 0.021\,Re^{0.8} Pr^{0.8})\,K \qquad (106)$$

For liquids and gases having low thermal conductivity n = 0.43; for molten metals n = 0.9. The coefficient K represents the effect of the direction of the heat flow and the effect of temperature difference. In the case of molten metals K = 1. The last equation is universally applicable to heat transfer calculations for turbulent flow of any heat transfer medium through long tubes.

To calculate heat transfer in the presence of natural convection of any heat transfer medium, including liquid metals, the following formula is recommended:

$$Nu = c\,Gr^m\,Pr^n; \qquad (107)$$

when $Gr = 10^3 \ldots 10^8$, $c = 0.52$ и $m = 0.25$,
$Gr = 10^9 \ldots 10^{13}$, $c = 0.105$ и $m = 1/3$

when

The exponent $$n = 0.3 + \frac{0.02}{Pr^{1/3}}.$$

Thus the studies carried out under the direction of M. A. Mikheyev, in comparison with all other Soviet and foreign studies of liquid metals, provided the most profound physical analysis of the processes of heat transfer and the most widely applicable and accurate calculation formulas.

In 1956 the results of experimental studies of heat transfer during the flow of liquid sodium through tubes were published. These studies were carried out under the direction of I. I. Novikov [22]. The experiments were conducted on copper, nickel, and stainless steel tubes. The measurement section was 400 mm long with an internal diameter of 8.6 mm. The determining parameters varied within the following limits

$$Re = 1.5 \cdot 10^4 \div 2.1 \cdot 10^5;$$
$$Pr = (5 \div 9)\,10^{-3};$$
$$Pe = 100 \div 1400.$$

These experiments confirmed the conclusion reached in the prewar studies of the Central Scientific Research Institute for Boilers and Turbines as to the influence of an oxide film in pipes on the efficiency of heat transfer.

I. I. Novikov and others obtained the following empirical formula for the interval Pe = 200 to 1,400:

$$Nu = 5{,}9 + 0{,}015\,Pe^{0{,}8} \qquad (108)$$

Formula (108) gives results close to M. A. Mikheyev's Formula (104). For the range where Pe < 200 an empirical formula could not be obtained, since the number of experimental points was insufficient.

In 1957 the results of S. S. Kutateladze's and V. M. Borishanskiy's experiments on heat transfer and resistance in liquid metals[5] performed at the Central Scientific Research Institute for Boilers and Turbines were published. This was a study of heat transfer when lead-bismuth eutectics and sodium are flowing through round tubes 4 to 35 mm in diameter, where Pr = 0.005 to 0.035, the heat flux $q = 3 \cdot 10^4$ to $1.3 \cdot 10^6$ kcal/m^2 hr, Pe = 170 to 11,000.

When Pe = 300 to 11,000 and $\frac{l}{d} > 30$, the experimental points for the bismuth lead alloy and for sodium yielded a common function in Nu-Pe coordinates, expressed by the equation

$$Nu = 5 + 0{,}0021\,Pe. \qquad (109)$$

When Pe = 50 to 300, the values obtained for Nu were less in comparison with the theoretical solution for a laminar flow. For the given Pe region the following approximate formula was recommended

$$Nu = 0{,}7\,Pe^{\frac{1}{3}}. \qquad (110)$$

A reliable function Nu = (Pe) for this range of values of Pe may be obtained by accumulating a greater number of experimental points.

The results of foreign studies (published from 1951 to 1956) of heat transfer in liquid metals coincide fairly well with the functions obtained at the Institute of Power Engineering.

The reprocessed experimental data of the Central Scientific Research Institute for Boilers and Turbines concerning heat transfer in liquid mercury and magnesium amalgam (utilizing the physical constants of mercury obtained by the Institute of Power Engineering (see Appendix VII) also agreed closely with the functions of the Institute of Power Engineering.

Hydraulic Resistance. In 1935 the hydraulic resistance of a smooth glass tube was studied for mercury flowing in the region Re = $11 \cdot 10^3$ to $35 \cdot 10^3$. The data obtained agreed with Blasius's law:

$$\xi = 0.316\,\mathrm{Re}^{-0.25}. \qquad (111)$$

In 1938-1939 A. R. Sorin and I. Ye. Semenovker of the Central Scientific Research Institute for Boilers and Turbines measured the hydraulic resistance of steel tubes when mercury is flowing through them. When $Re > 5 \cdot 10^4$, a square-law resistance was noted, but the scattering of the points was great. A. A. Konayev and L. I. Gel'man conducted more precise experiments on carbon and alloy-steel tubes with measurement sections 10, 16, and 20.5 mm in diameter and Re = $10 \cdot 10^3$ to $4 \cdot 10^5$. These experiments were repeated in the postwar years [13]. In the case of used carbon-steel tubes, the following formula was obtained for the square-law resistance region (Fig. 214):

$$\xi = \frac{2g}{\quad} \quad 0.0$$

An equivalent roughness of K = 0.06 to 0.08 mm corresponds to this value of the resistance coefficient.

In the case of carbon-steel tubes and alloy-steel tubes $\xi = 0.02$ and K = 0.02 to 0.04 mm.

In the postwar years the Central Scientific Research Institute for Boilers and Turbines studied the hydraulic resistance of tubes when magnesium amalgam was flowing through them. The resistance coefficients obtained fell on the curve in Fig. 214, with an equivalent roughness of 0.0 mm.

Best Available Copy

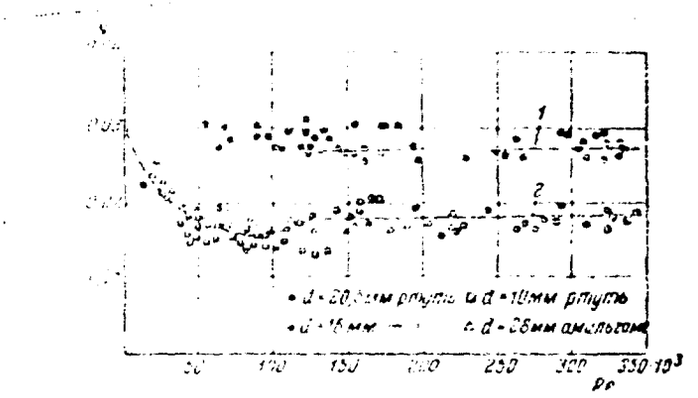

Fig. 214. Coefficient of friction for flow of mercury and amalgams through steel tubes.

(a) mm Hg (b) mm (c) mm amalgam

(1) used carbon steel tubes.

(2) new carbon steel tubes and alloy-steel tubes.

In a previously mentioned study [5] the hydraulic resistance during isothermal and nonisothermal flow of molten bismuth and bismuth-lead eutectics through tubes were investigated. The experiments were performed on tubing of steel 20 with a diameter of 10 mm and for values of Re up to $180 \cdot 10^3$. The effect of the magnitude of the heat flux on the hydraulic resistance was not ascertained. In the region of square-law resistance the experimental points for liquid metals and water fall on a common curve. The numerical values of the resistance coefficient for liquid metals were of the same order as those in ref. [12].

Heat transfer during boiling. Of the greatest practical interest at the present time is the study of heat transfer in boiling mercury, which may be used in the cooling circuit of boiling fast-neutron reactors or in the secondary

[illegible] sodium-cooled.

[illegible] already, the fact that steel tubes are not wettable by [illegible] heat transfer than the mercury is not boiling. When the mercury is boiling, the effect of nonwettability on heat transfer is greater. When the contact angle of wetting by mercury exceeds 90°, the bubbles of mercury vapor are not disk-shaped, but ball-shaped, which causes their diameter and disengagement period to be larger. On a vertical heating surface a bubble of mercury vapor does not rise into the center of the stream but slides along the wall, since, in the absence of wetting, this requires less work than does penetration of the liquid layer. As was shown by observations of a heated glass tube, layers of mercury vapor form along the tube wall, while liquid mercury is moving in the most of the interior portion of the cross-section.

The vapor layer along the perimeter of the tube is an additional heat resistance with worsens heat transfer in boiling mercury in comparison with liquids wetting the heating surface. In the case of wetting liquids under moderate heat fluxes, bubble boiling occurs and only under very high fluxes does the transition to film boiling with impaired heat transfer occur. As was already mentioned, in the case of nonwetting metals similar to mercury film boiling occurs.

The first studies of heat transfer during boiling of a nonwetting liquid (mercury) were carried out at the Central Scientific Research Institute for Boilers and Turbines in 1936-1937 [20]. It was found that the efficiency of heat transfer in the case of boiling nonwetting liquids is considerably less than in the case of liquids which wet the heating surface. Impairment of heat transfer begins long before the moment when the mercury stream reaches the boiling temperature corresponding to the pressure at a given point of the vaporizing element. The experiments were conducted during the vaporizing of mercury in an annular channel. These experiments were continued in 1938-1939 on a loop-circulation circuit, where both the characteristics of heat transfer during boiling and the

Best Available Copy

circulation characteristics were measured. In 1939 studies of heat transfer in mercury in a vertical pipe over a wider range of velocities, pressures, and heat fluxes were carried out at the Central Scientific Research Institute for Boilers and Turbines on a circulation circuit with a measurement section of greater height [27]. As a result of these studies, experimental data were obtained which made it possible to calculate the circulation in mercury steam-generator circuits.

It was not possible to express the results of the experiments in terms of generalized dimensionless formulas, since even in the case of heat transfer during boiling of fairly well-known wetting liquids (water and others) there were no theoretical or empirical equations available at that time. The mechanism of boiling of nonwetting liquids was even less amenable to theoretical analysis.

Additional experiments were carried out for the purpose of studying the boiling mechanism of nonwetting liquids. A series of experiments, performed on glass and steel vaporizing elements, clearly indicated film boiling of mercury and bubble boiling of water. These experiments indicated the possibility of considerably improving heat transfer with boiling mercury by adding amalgams of magnesium, titanium, and certain other metals. It was also shown that heat transfer in the presence of boiling mercury may be intensified mechanically, by agitating the current with spiral inserts in the vaporizing elements.

In 1939 the phenomenon of separation of a vapor-liquid emulsion into a vapor and liquid phase in the horizontal tubes of a mercury steam generator was established at the Central Scientific Research Institute for Boilers and Turbines. This phenomenon caused great deterioration in the conditions of heat transfer [10].

In postwar experiments at the Central Scientific Research Institute for Boilers and Turbines (M. I. Kornayev), dealing with heat transfer in the presence of free convection of boiling mercury and magnesium amalgam and also during natural circulation in tubes, new data were obtained [3].

In the case of a large volume of boiling mercury the following equation was obtained:

$$\alpha = 2.76\, q^{1.5} \cdot 10^{-6}$$ kcal/m² · sec · °C.

In the case of a large volume of boiling magnesium amalgam with a concentration by weight of 0.01-0.04% the following equation was obtained:

$$\alpha = 5.25\, q^{0.67}$$ kcal/m² · sec · °C.

In the case of boiling magnesium amalgam in vertical tubes this equation takes the form:

$$\alpha = 7.3\, q^{0.67}$$ kcal/m² · sec · °C.

The same equation was obtained in the case of amalgam boiling in horizontal tubes, where measurements are taken along the lower generatrix of the tubes. On the upper generatrix of a tube, as a result of the separation of the mercury and mercury vapor phases in the mixture, the exponent of q varies from 0, when the entrance velocity of the mercury is equal to 0.02 m/sec, to 0.67, when the entrance velocity equals 0.3 m/sec.

M. I. Kornayev's experiments showed that G. N. Kruzhilin's theoretical equations [10] for free-convection and natural-circulation conditions correctly describe the boiling process of magnesium amalgams.

In 1941, heat transfer in the boiling region, when the circulation rate was low (up to one inclusive), was studied at the Central Scientific Research Institute for Boilers and Turbines using a mercury steam generator with forced circulation. It was found that in cross sections of the tube with high vapor content (up to 100%) the heat transfer coefficient remained high, whereas in the case of natural circulation even with a vapor content of only 3% intolerable overheating of the tube occurred. The experiments were repeated in 1946. With a heat flux of 50,000-55 kcal/m² hr the heat transfer coefficient for the boiling mercury at the exit turns of the coil reached 5,500-6,000 kcal/m² hr °C. When the coil was replaced by a straight pipe with fluxes up to 200,000 kcal/m² hr

the heat transfer coefficient was still very high (1,500 kcal/m^2 hr°C). Apparently in the case of forced circulation the mercury stream is divided into very fine drops, which are carried by the vapor current in the form of a suspension and intensively cool the heating surface. This theory may be corroborated visually by observing a flow of mercury-air mixture in a glass tube. It is possible to choose the entrance velocities of the gas and liquid phases in such a way that the two-phase stream becomes homogeneous and all the mercury will be in the form of very fine drops suspended in the air current.

If the results of the laboratory experiments are corroborated on a semi-industrial scale, then it will be possible to achieve great heat fluxes by using mercury as a cooling medium in reactors or in secondary heat exchangers [19].

50. Heat Transfer during Condensation

The efficiency of heat transfer during the condensation of vapor varies greatly depending on the type of condensation (film or drop). In the case of nonwetting liquids the cohesive forces of the particles of the liquid are greater than the adhesive forces of the particles of a liquid on a solid surface. Thus in the case of nonwetting liquids the drop form of vapor condensation is predetermined.

From 1937 to 1941 A. A. Kanayev, A. N. Lobkin, P. I. Starostin, and L. I. Gel'man of the Central Scientific Research Institute for Boilers and Turbines studied the condensation of mercury vapor. The drop form of condensation was established both visually and with the aid of a motion-picture camera. With a heat flux of 100,000-150,000 kcal/m^2 hr and a temperature difference of 20-25°C between the mercury vapor and water vapor, the heat transfer coefficient in the condenser-vaporizer was 3,500-4,000 kcal/m^2 hr °C. The relationship between the temperature difference and the over-all heat transfer coefficient during condensation of mercury vapor with vaporized-water cooling is shown in Fig. 215.

In the postwar years additional studies of the condensation of mercury vapor were carried out. The relationship between the heat transfer coefficient and the steam condensing on the wall was analyzed. This relationship is expressed by the following formula:

$$\alpha = \frac{1}{\Delta t^{0.5}} \cdot 10^{4} \ \frac{\text{kcal}}{\text{m}^2 \cdot \text{hr} \cdot {}^{\circ}\text{C}}.$$

The above formula is correct, when $\Delta t \leq 25^{\circ}$ C. The efficient temperature difference for power plants lies between 15-20°C.

The studies of heat transmission during condensation of mercury vapor were continued later by L. I. Gel'man [7].

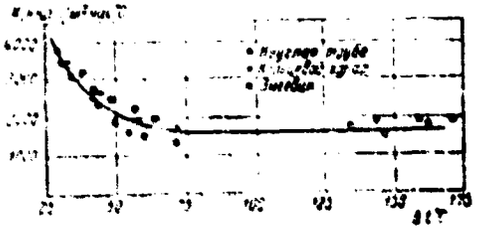

Fig. 215. The relationship between the temperature difference and the heat transfer coefficient during condensation of mercury vapor.
(a) circular pipe (b) annular channel (c) coil
(d) K, kcal/m^2 hr °C

The experimental data were plotted in the following coordinates:

$$\left[\frac{\alpha}{\quad}\right] = f(\Delta t)$$

The following function was obtained for the case where air is not present in the mercury vapor:

$$\alpha = 17.10 \frac{P^{\frac{1}{3}}}{\Delta t} \left[1 - (1'V')^{\frac{1}{3}}\right] \frac{\text{kcal}}{\text{m}^2 \cdot \text{hr} \cdot {}^\circ\text{C}}$$

The following function was obtained for the case where air is present in the condensing mercury vapor:

$$\alpha = 17.10 \frac{P^{\frac{1}{3}}}{\Delta t} \left[1 - \left(\frac{P_{\text{air}}}{P}\right)^{\frac{1}{3}}\right]$$

Designations used:

α — heat transfer coefficient during condensation;

P — vapor pressure in the condenser;

Δt — difference in temperature between the mercury vapor and the cooling surface;

V'' — average velocity of the vapor in the condenser;

γ'' — specific gravity of the vapor;

$V_{v.m}$ — average velocity of the vapor-air mixture

$\gamma_{v.m}$ — specific gravity of the vapor-air mixture

c — concentration by weight of air in the vapor-air mixture

51. Friction Losses of a Disk in Liquid Metals

In designing the working wheels of centrifugal pumps for liquid metals, it is necessary to determine the power lost through friction between the face surfaces of a working wheel (and its rim) and the liquid.

Because of the absence of experimental data concerning friction of a disk rotating in liquids whose properties differ from those of water, in 1938-1939 A. A. Ivanov of the Central Scientific Research Institute for Boilers and Turbines carried out experiments to determine the power lost through friction of a disk in liquids differing greatly in density and viscosity: water, kerosene, turbine oil, and mercury. Steel disks 200 to 300 mm in diameter were studied, both smoothly finished and artificially roughened (using sand with grains of

NCL-55

0.1-0.45 mm bonded with lacquer). The experiments were conducted with Reynolds numbers ranging from 10^2 to 10^7.

From the results of the experiments with mercury an empirical formula for the value of the losses through friction was obtained:

$$N_1 = 2^{0.6} \pi^{2.8} 0.4 \cdot 10^{-7} \rho \nu^2 n^{2.8} D^5, \qquad (112)$$

where D is the diameter of the disk, in m;

n is the number of rotations, in rpm;

ν is the kinematic viscosity of mercury, in m^2 sec;

ρ is the specific gravity of mercury, in kg/m^3.

It was found that Karman's theoretical solution for a rotating disk did not agree satisfactorily with the experiment.

A general solution has been given to the problem of the friction of a disk in a liquid, taking the thickness of the disk into account [11].

A ring-shaped element of radius r and width dr on the face of the disk has a two-sided surface:

$$dF = 2\pi r\, dr.$$

To this surface element there corresponds a friction force:

$$dT = \frac{C}{2g} \gamma w^2 dF = \frac{1}{g} \gamma w^2 r\, dr,$$

where C is the resistance coefficient;

γ is the specific gravity;

w is the velocity of motion of the liquid relative to the surface of the ring element.

The moment $dM = r\, dT$,

and power $dN = \frac{\omega dM}{75}$.

corresponds to the friction force dF

If c_f is determined from experiments with a rotating disk, then $u = \omega r$.

By integrating the element-of-work equation from 0 to r_H (the outside radius of the disk) we obtain

$$N_1 = \frac{c_f \pi \omega^3}{75.5\, g}\, \gamma r_H^5 \text{ h.p.} \tag{119}$$

This equation gives the loss of power through friction of both face surfaces of a disk rotating in the liquid.

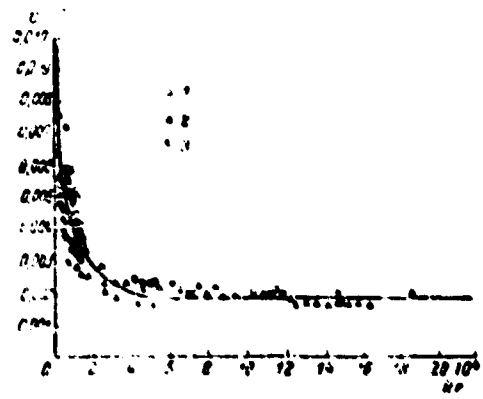

Fig. 216. Relation between the resistance coefficient and Reynolds number. (1) kerosene (2) water (3) mercury

The energy lost through friction by the rim of a disk rotating in a liquid is:

$$N_2 = c_f \frac{\pi}{75} \cdot \frac{1}{g} \gamma b r_H^4 \omega^3 \text{ h.p.}$$

where b is the width of the rim of the disk.

The total energy lost through friction by the rim and the faces of a disk rotating in a liquid is:

$$N = N_1 + N_2 = 0.5 \cdot 10^{-3} \gamma \omega^3 r^5 (0.4 c_1 + c_2) \ldots \quad (115)$$

The resistance coefficient c depends on the Reynolds number $Re = \frac{\omega r^2}{\nu}$ and on the roughness of the surface of the disk, K. The results of experiments with smoothly finished disks rotating in water, kerosene, and mercury fell on a common curve (Fig. 216).

The effect of roughness on the value of the resistance coefficient is obvious from the following figures:

Commercially smooth disk		$Re = 4 \cdot 10^5$; $C = 0.006$
Sand roughness	$K = 0.25$ mm;	$Re = 4 \cdot 10^5$; $C = 0.014$
Sand roughness	$K = 0.45$ mm;	$Re = 4 \cdot 10^5$; $C = 0.02$

The roughness of the cast surfaces was about to 0.2 mm, and the roughness of the treated surface was approximately 0.1 mm.

Figure 216 gives the resistance coefficients for treated disks.

59. Thermophysical Constants of Certain Liquid Metals

Mercury. Kh. Khalilov, a scientist at the All-Union Heat and Power Engineering Institute, carried out experiments to determine the viscosity of liquid mercury for temperatures ranging from 20 to 600°C and the viscosity of mercury vapor for temperatures ranging from 350 to 600°C. The results of the experiments are given in Table 57.

TABLE 57

(A)

Results of Measurements of Viscosity

(D) Temperature t, °C	(B) Viscosity of liquid mercury		(C) Viscosity of mercury vapor	
	(E) Dynamic, μ, kg sec/m^2 X 10^6	(F) Kinematic, ν, m^2/sec X 10^8	(G) Dynamic, μ, kg sec/m^2 X 10^6	(H) Kinematic, ν, m^2/sec X 10^7

(A)

Таблица 57

Результаты измерений вязкости

(D) Температура t, C	(B) Вязкость жидкой ртути		(C) Вязкость ртутного пара	
	(E) динамическая μ, кг сек/м^2 X 10^6	(F) кинематическая ν, м^2/сек X 10^8	(G) динамическая μ, кг сек/м^2 10^6	(H) кинематическая ν, м^2/сек X 10^7
20	157	11,4	-	—
50	143	10,4		
100	127	9,77	-	
150	116	8,57	-	--
200	105	7,97	--	--
250	98,8	7,48		—
300	92,8	7,07	-	--
350	89,0	6,77	5,53	150
400	84,5	6,55	5,8	80,1
450	81,5	6,38	6,75	50,0
[illegible]	79,0	6,25	7,84	33,4
550	76,9	6,15	9,33	23,0
600	75,3	6,08	10,4	13,0

1. The solubility of iron and alloying elements in mercury at various temperatures.

2. The solubility of mercury in steel at high temperatures and pressures.

3. The penetration of mercury along the steel grain boundaries which occurs at high temperatures under stress.

4. The wettability of the steel surface by mercury at high temperatures.

5. The interaction of mercury and steel at high temperatures in the presence of oxygen.

It was found that an 'amalgam' of iron is not a true amalgam, but a suspension of iron or of oxides of iron in mercury.

When there was no oxygen in the mercury the amount of iron dissolved under ordinary conditions did not exceed 0.0002%. In the presence of small quantities of oxygen, the amount of iron dissolved in the mercury increased to 0.03%, i.e., it increased by approximately 100 times. The effect of the temperature of mercury on the solubility of iron in it was not ascertained.

The experiments showed that mercury was not soluble in iron at high temperatures and pressures. The penetration of mercury along the steel grain boundaries at high temperatures in stressed steel specimen was also not ascertained.

Thus it was found that in the absence of oxygen mercury does not affect steel. Steel specimens tested in a medium of saturated and superheated mercury vapor at temperatures from 500 to 700°C did not show signs of aggressive action on the part of the mercury vapor.

Mercury containing oxygen can have a considerable effect on steel. During the operation of the mercury steam generator at the Central Scientific Research Institute for Boilers and Turbines, the formation of an oxide film on the walls of the boiler tubes and the deposition of oxide in the collectors was noted. A large quantity of oxygen in mercury can cause the tubes of the steam generator

V. K. Semenchenko, P. P. Bering, and N. L. Pokrovskiy [25] experimentally studied the surface tension of amalgams of barium, lithium, sodium, potassium, rubidium, and other metals. It was found that the experimental values closely coincided with values calculated according to a more precise version of Shishkovskiy's formula developed by the authors of the study.

Methods of preparing amalgams of surface-active metals were devised by V. K. Semenchenko.

P. P. Pugachevich's study [24] was devoted to an investigation of the surface tension of mercury and other metals.

Sodium, Potassium, and Lithium. I. I. Novikov, A. N. Solov'yev, Ye. M. Khabakhpasheva, and V. A. Grusdev [22] measured the viscosity, thermal conductivity, and density of sodium, potassium, lithium, and a sodium potassium eutectic. In the report written by these scientists the values for the kinematic viscosity, thermal conductivity, and density of sodium, potassium, their eutectic, and lithium were given in graphic form for temperatures ranging from 100 to 700°C.

In Ye. O. Shvidkovskiy's monograph [3] problems in the theory of torsion-vibration measurement of the viscosity of liquids (in particular, mercury, tin, lead, bismuth, and a lead-bismuth alloy) are considered. Values for viscosity calculated according to this method closely coincide with values determined according to the capillary method.

For certain liquid metals the experimentally determined values for viscosity coincide fairly well with the values obtained theoretically according to A. I. Bachinskiy's formula:

$$\eta = \frac{a}{(V - b)^2},$$

where a and b are constants and V is the specific volume.

The divergences from Bachinskiy's formula were greatest in the case of mercury and gallium.

53. Purification of Liquid Metals

Soviet scientists were the first to develop effective methods of removing impurities from such metals as mercury, sodium, tin, lead, and bismuth. Even in the prewar years Professor M. P. Slavinskiy and others at the Leningrad Polytechnic Institute had developed a method for purifying nonferrous metals by filtration.

The requirements for purity of nonferrous metals are determined by GOST (All-Union State Standard). In the appendix the GOST (classification and technical specifications) are given for mercury, lead, tin, and sodium.

It was possible to obtain high-quality sodium by filtering technical-grade sodium through porous plates or through very fine sieves. A bronze sieve or a stainless steel sieve combined with a nickel sieve is a reliable filter for obtaining sodium of stable purity. Pressed and sintered plates of powdered iron are also good filtering material.

54. The Behavior of Steels in a Liquid-metal Medium

The Effect of Mercury on Steel. The first studies of the effect of mercury in the liquid and vapor phases on steel were carried out in 1938-1940 at the Central Scientific Research Institute for Boilers and Turbines. At temperatures up to 500-550° C carbon-steel specimens were stable in a mercury medium in the absence of a load. When the specimens were loaded, an effect of mercury and mercury vapor was observed. It took the form of a change in the structure of the surface layers of the carbon steel.

M. T. Oudtsov and M. M. Orlov [8] of the Metallurgical Institute of the Academy of Sciences of the USSR conducted special studies of the effect of mercury on alloyed and carbon steel. The authors of this report describe the interaction between steel and mercury in terms of the following indices:

to become clogged with sediment as a result of the large quantities of iron dissolved by the mercury. As a result of oxidation of the surface of the steel tubes, scale forms, through which mercury can diffuse, thus causing further precipitation of scale. When the pipe surfaces are cleaned, they are again subject to oxidation.

The mercury can be prevented from affecting steel by alloying the steel or by adding to the mercury elements having a greater affinity for oxygen than iron has.

The following steels displayed the greatest stability in a mercury medium:

(A)

Chemical Composition, %

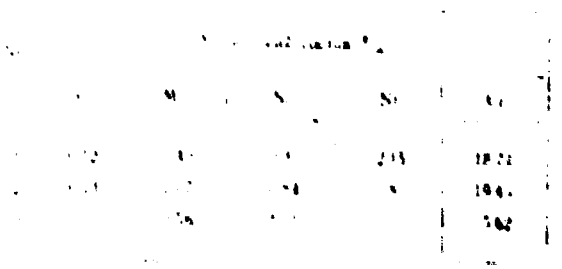

Chromium-nickel steel (2) performed well during operation of the mercury steam generator.

Chromium-silicon-manganese steel (3) is distinguished by a finely dispersed structure of scale particles acting in similar fashion to surface-active materials and thus causing the mercury to wet the steel.

Chromium-nickel-manganese-silicon steel (1) forms a scale composed of flakes and powder floating on the surface of the mercury, thus enabling the sediment to be removed in a separator. This steel is resistant to corrosion by sulfur.

The addition of inhibitors (titanium, magnesium) to mercury prevents or decreases the action of mercury on steel even at very high temperatures. The experiments showed that titanium is the best inhibitor, since it forms a reliable protective film on the surface of the steel. Magnesium absorbs oxygen and nitrogen, thus supporting titanium in the active state. An addition of 10 parts of titanium per million parts of mercury is sufficient to prevent interaction with steel at a temperature of 650°C. At this temperature an addition of 20 parts of magnesium is sufficient to effectively bind the free oxygen.

Sodium and zirconium are less effective than magnesium. Additions of magnesium and titanium to mercury not only decrease the effect of the latter on steel, but cause a wetting effect, which contributes to improving heat transfer when boiling mercury is used.

The Effect of Lead, Bismuth, and their Eutectic Alloy on Steel. In 1955, at the International Conference on Peaceful utilization of Atomic Energy, L. I. Tsuprun and M. I. Tarytina reported on a study of the effect of liquid lead, bismuth, and their eutectic alloy on stainless chromium-nickel steel [30].

The interaction between 1Kh18N9T steel and these liquid metals was studied at 500° and 600°C. The chemical composition of this steel in weight percent is:

Cu	Ti	Cr	Ni	Si	Mn	S
0.09	0.51	17.67	10.45	0.54	1.27	0.023

Prolonged heating of steel in an argon atmosphere up to a temperature of 500°C did not cause significant changes in the mechanical properties or structure of the metal. As a result of prolonged soaking at 600°C, the relative elongation of the steel decreased by 15% and the tensile strength increased slightly. The grain size and hardness of the steel did not change.

In a medium of liquid lead, bismuth, and their eutectic alloy at temperatures of 500 - 600°C a deterioration in the mechanical properties of 1Kh18N9T steel (a decrease in relative elongation and tensile strength) was noted. The effect of the lead-bismuth eutectic on this steel causes "leaching" of the nickel through selective dissolution of the surface layer. The structure of the steel changes from austenitic to magnetic.

The solubility of nickel in lead at 327°C is approximately 0.2%, while its solubility in bismuth at 600°C reaches 6%. Iron is practically insoluble in either lead or bismuth. The solubility of chromium in lead is 1%, while its solubility in bismuth is insignificant. Adding 0.1-0.3% calcium or barium to the lead-bismuth eutectic creating an oxide film on the alloy surface cuts the aggressive action of the alloy on steel approximately in half.

Best Available Copy

Adding 0.7% nickel to the lead-bismuth alloy reduces corrosion of the steel at 500-600°C to one-half or one-third without changing the tensile strength, while the relative elongation decreases negligibly (5 or 6%). Thus nickel is a good inhibitor and decreases the aggressive action of the lead-bismuth alloy on type 18-8 stainless steel at temperatures of 500-600°C. At temperatures up to 500°C this steel may be effected by prolonged action of the lead-bismuth alloy even without an inhibitor.

55. Pumps, Fittings, and Measuring Devices for Liquid Metals.

The first attempts to make the above-mentioned equipment in the USSR for liquid metals were conducted in 1937-1940 at the Central Scientific Research Institute for Boilers and Turbines [19].

A single-stage centrifugal mercury pump with a vertical shaft was designed and manufactured. This pump was intended for a mercury output of 70 m^3/hr at a pressure of 7 kg/cm^2 and a temperature of 250-300°C. A unique and reliable shaft packing was used in the pump, which prevented leakage of mercury into the outer medium. The mercury is fed into the annular space between the sleeve of the shaft and the shaft itself from a pressure pipe and is precooled in a contact condenser. Passing through the annular cooled-off space, the mercury returns through the throttle valve to the suction pipe.

The bearing of the shaft is cooled by a water jacket. Cool water from the jacket flows into the hollow around the pump shaft and condenses the mercury vapor, if it should penetrate from the sealed space. The pump has operated for many thousands of hours, and at this time is still in good working order.

This principle of construction is also used in pumps for transferring other liquid metals.

Glandless shut-off valves for mercury and mercury vapor were manufactured.

Best Available Copy